2021

Characterizing Inflammatory Mechanisms in Hidradenitis Suppurativa

Kristina Navrazhina

CHARACTERIZING INFLAMMATORY MECHANISMS IN HIDRADENITIS SUPPURATIVA

A Thesis Presented to the Faculty of
The Rockefeller University
in Partial Fulfillment of the Requirements for
the degree of Doctor of Philosophy

by
Kristina Navrazhina
June 2021

CHARACTERIZING INFLAMMATORY MECHANISMS IN HIDRADENITIS SUPPURATIVA

Kristina Navrazhina, Ph.D.
The Rockefeller University 2021

Hidradenitis suppurativa (HS) is an inflammatory skin disease manifesting in painful nodules and abscesses, and malodorous draining tunnels in more advanced disease. Effective treatment options remain limited, with Tumor Necrosis Factor inhibitor adalimumab remaining the only approved biologic despite its limited efficacy. The development of novel therapeutics is impeded by our lack of understanding of disease pathogenesis and an absence of standardized approaches to study HS.

In this thesis, we establish a translational approach to characterize HS by examining nonlesional, perilesional and lesional HS skin in comparison to site-matched control skin from healthy volunteers. We demonstrate that relatively healthy-appearing perilesional skin (2cm away from the target nodule) has the same inflammatory profile as the visibly inflamed lesional skin (target nodule) and is marked by an increase of Th17 and neutrophil-related signatures.

Given that inflammation in HS extends beyond visible nodules to perilesional skin, we asked if dermal inflammation also contributes to disease pathogenesis. Dermal tunnels, also known as tracts or sinuses, are structures unique to HS and have been considered an end-stage feature of the disease. By examining biopsies of dermal tunnels, we show that tunnels recapitulate features of the overlying epidermis and are associated with increased infiltration of T cells, dendritic cells and neutrophils, formation of neutrophil extracellular traps, and increased production of epithelium-derived inflammatory cytokines. Our work demonstrates that dermal tunnels are active contributors to the inflammatory burden of HS.

To address whether tunnels are associated with a unique HS subtype, we assessed serum biomarkers in HS compared to healthy controls. Patients with tunnels had higher levels of IL-17 regulated neutrophil gelatinase-associated lipocalin (LCN2), and serum level of this biomarker correlated with clinical severity. These data demonstrate that HS tunnels are associated with a unique inflammatory profile in the skin and blood, suggesting a novel HS endotype.

Data from our clinical trial of brodalumab, a human anti-IL-17 receptor A (IL-17RA) monoclonal antibody, provides the first molecular characterization of IL-17 pathway blockade in HS. We demonstrate that treatment with brodalumab reduces several pathogenic inflammatory axes in HS skin and serum. We also establish that perilesional skin provides a more robust assessment of treatment response. To further support HS stratification in the context of therapeutic antagonism, we demonstrate that patients with high expression of LCN2 in skin and IL-17A in serum had a superior molecular response in the skin as measured by a greater decrease of known inflammatory mediators of HS. Furthermore, we validate that dermal tunnels are therapeutically targetable, exhibiting decrease of tunnel wall and lumen diameter, as well as a decrease in clinical drainage.

Taken together, this work provides novel insight into HS pathogenesis. Given the equally high inflammation present in lesional and perilesional HS skin, our data suggests there is a large field of inflammation beyond visible lesions. HS can be subdivided into unique subtypes, potentially introducing the concept of disease endotypes in this highly heterogeneous disease. This has direct applicability towards stratification of patients who may be better responders in the context of targeted therapy in HS.

Dedicated to my Parents for their unconditional love, ongoing support and endless sacrifice

ACKNOWLEDGMENTS

No words can adequately express the gratitude that I feel for the people who supported and encouraged me throughout my graduate training.

I would first like to thank my advisor Dr. Jim Krueger for the extraordinary opportunity to get involved in translational research. I am grateful for Dr. Krueger's mentorship, contagious excitement for the scientific process, insightfulness into the pathogenesis of skin disease, and above all his dedication to training future physician-scientists. It has been truly inspiring to be a part of a laboratory whose research has improved the lives of many patients suffering from systemic skin disease. I would also like to thank past and present members of the Krueger laboratory. In particular, I thank Dr. Sandra Garcet for teaching me to perform biostatistical analysis and for our vibrant discussions about the latest data. I also thank Dr. John Frew for setting up the clinical HS studies. I thank Polina Bulkina, Sandy Coats, Inna Cueto, Tali Czarnowicki, Daniel Gareau, Patricia Gilleaudeau, Juana Gonzalez, David Grand, Nick Gulati, Jason Hawkes, Hong Hur, Jaehwan Kim, Norma Kunjravia, Jongmi Lee, Xuan Li, Shunsuke Miura, Darshna Rambhia, Charissa Salud, Yael Renert-Yuval, Mary Sullivan-Whalen, Samuel Williams, Kazuhiko Yamamura and Mika Yamamura. I would also like to thank all our collaborators as well as the nurses and staff at the Rockefeller University Hospital. I am grateful to Dr. Emma Guttman-Yassky who generously provided scientific expertise, advice and mentorship. I would also like to thank my clinical mentor Dr. Kira Minkis for her encouragement, support and positivity throughout my PhD journey.

I thank Dr. Olaf Andersen, Dr. Catharine Boothroyd, Dr. Jochen Buck, Dr. Mark Pecker, Dr. Ruth Gotian, Renee Horton, Hanna Silvast and Benjamin Levitt at the Weill Cornell/Rockefeller/Sloan Kettering Tri-Institutional MD-PhD Program and the Dean's office at the Rockefeller University for providing a superb training environment. I am particularly grateful to Dr. Andersen and Dr. Boothroyd for their support, advice and overall leadership. I also thank my committee members Dr. Sohail Tavazoie, Dr. Olaf Andersen, Dr. Paul Cohen, and my external examiner Dr. John Carucci for their expertise, constructive feedback and guidance on both my research and career development. I thank Dr. Tavazoie who first inspired me to pursue the physician-scientist path and has remained my role model and mentor for many years.

This translational work would not have been possible without our patients. Patients continue to be my inspiration for research, and I hope that the work presented in this thesis will lead to improvement of therapeutic options for HS patients.

I am grateful for my friends who always keep me laughing. Above all, I thank my parents who have immigrated to this country for a better life, and who have taught me the value of hard work and determination.

TABLE OF CONTENTS

LIST OF FIGURES

LIST OF TABLES

LIST OF ABBREVIATIONS

AA	Alopecia Areata
AD	Atopic Dermatitis
BMI	Body Mass Index
DAMP	Damage-Associated Molecular Pattern
DC	Dendritic Cell
DEGs	Differentially expressed genes
DEPs	Differentially Expressed Protein
FCH	Fold Change
FDA	Food Drug Administration
FDR	False discovery rate
GSVA	Gene Set Variation Analysis
H&E	Hematoxylin and eosin
HiSCR	Hidradenitis Suppurativa Clinical Response
HIV	Human Immunodeficiency Virus
HGF	Hepatocyte growth factor
HS	Hidradenitis Suppurativa
HSTR	Hidradenitis Suppurativa Transcriptome
IBD	Inflammatory Bowel Disease
IFNγ	Interferon gamma
IHC	Immunohistochemistry
IHS4	International Hidradenitis Suppurativa Severity Score System
IL	Interleukin
IL-17RA	IL-17 Receptor A
IPA	Ingenuity Pathway Analysis
K16	Keratin 16
LCN2	Lipocalin 2
LS	Lesional skin
MAD3	Meta-analysis derived psoriasis dataset
MMP	Matrix metalloproteinase
NL	Nonlesional skin
NE	Neutrophil Elastase
NETs	Neutrophil extracellular traps
PASI	Psoriasis Area and Severity Index
PCA	Principal component analysis
PL	Perilesional skin
RNA-seq	RNA-sequencing
RT	Room temperature
QoL	Quality of Life
SEM	Standard error of mean
T_H	T helper cell
TNF	Tumor necrosis factor
WBC	White Blood Cell Count
XGR	eXploring Genomic Relations Tool

CHAPTER 1:

Introduction

CHAPTER 1. Introduction

1.1 Background

Hidradenitis suppurativa (HS), also known as acne inversa, is a chronic, debilitating inflammatory skin disease with a reported prevalence of 1-2% [1-3]. Patients present with painful inflamed nodules and abscesses, as well as malodorous pus-draining tunnels (also referred to as fistulae or sinus tracts). The disease typically affects intertriginous areas including the axillary, inguinal, inframammary, gluteal and anogenital regions. HS has an average onset in patients in their twenties, with earlier onset linked to family history and a higher number of body sites involved[4]. HS is also associated with a substantial increase in mortality.[5]

Due to the severe pain, fibrosis-associated movement restrictions and the malodorous purulent secretions, HS has a negative impact on the quality of life (QoL) [6]. HS has a greater QoL impairment than other systemic skin diseases including psoriasis, atopic dermatitis (AD), alopecia areata (AA), acne vulgaris and chronic urticaria[7, 8]. HS-associated impairment also affects patients' professional lives and may negatively alter their economic situation[7, 9].

The aetiology of HS remains multifactorial, with reported genetic, environmental, lifestyle and hormonal factors as well as interactions with microbiota as contributing causes. Appropriately 30% of HS patients have a family history of the disease, suggesting a genetic predisposition[10, 11]. Mutations impairing γ-secretase activity, a protease complex responsible for cleaving transmembrane proteins including the Notch receptor, have been implicated in HS[12]. The attenuated γ-secretase activity may reduce the stability of the hair follicle, which may favor rupture of the hair follicle as an early step of HS pathogenesis[12-14]. Furthermore, both obesity and tobacco smoking have been implicated as lifestyle risk factors for HS development. Near 90% of HS patients are current or former smokers[15]. Nicotine smoking induces epidermal hyperplasia, intracellular cAMP levels in monocytes and increases production of IL-10, all known pathogenic factors in HS [16-18]. Approximately 60% of HS patients are obese, and 40% have metabolic syndrome (a combination of conditions including hyperglycemia, dyslipidemia, hypertension and/or obesity), establishing a link between lifestyle factors and HS onset. [15, 19-21]. Obesity also influences response to treatment, as obese patients have a near 4.5 fold increase in recurrence following HS surgical excision compared to non-obese patients[22]. Hormonal involvement in HS may also play a role, as androgen receptor pathway activation has been observed in HS skin[23].

1.2 Clinical diagnosis and management of HS

HS is a clinical diagnosis based on localization of skin lesions and course of disease. HS morphology is extremely heterogenous, ranging from papules, pustules, nodules (inflammatory, noninflammatory, eroded), plaques, ulcers, comedos (double comedo, interconnected comedones), abscesses and dermal tracts/tunnels (draining and nondraining tunnels, fistulae). Early lesions mimic other disorders, and HS is frequently misdiagnosed. The differential diagnoses of HS are extensive and range from bacterial infections (folliculitis, nocardiosis, granuloma inguinale), to deep fungal infections (blastomycosis, sporotrichosis, chromoblastomycosis, mycetoma), cysts (pilonidal, epidermoid, Bartholin's) and other conditions including but not limited to giant comedones, acne keloidalis nuchae, pyoderma gangrenosum and cutaneous Crohn's disease [1]. There are currently no HS associated biomarkers, further complicating disease diagnosis. These factors likely contribute to the average diagnostic delay of 7 years [24].

Patients commonly present with several lesional morphologies simultaneously and thus a total body skin examination is critical for proper diagnosis and staging. Hurley staging, introduced in 1989, was the first severity score for HS, however, its role in assessment of response in therapeutic trials remains limited due to its static nature [1]. Other grading rubrics including the Sartorius Scale, physician global assessment tool, and the HS Clinical Response (HiSCR) tool have all been validated but are limited and focus primary on target lesions rather than the surrounding inflammation (such as tunnels) [25-27]. A recently developed tool, International Hidradenitis Suppurativa Severity Score System (IHS4), which assigns a weighted value on HS manifestations including nodules, abscesses and draining tunnels. The IHS4 tool holds promise for monitoring of treatment response in therapeutic trials as it allows for a dynamic assessment during clinical trials and integrates non-nodular inflammation into the clinical grading[28].

Owing to a diagnostic delay and a lack of curative treatments, patients have a high unmet medical need. HS patients are initially treated with topical and systemic interventions, including antibiotics (tetracycline, clindamycin, rifampicin) and retinoids[29-31]. Surgery is a plausible option in certain cases; however, HS has a high rate of post-surgical recurrence. Approved in 2015, Tumor Necrosis Factor (TNF) inhibitor adalimumab remains the only U.S. FDA-approved biologic for HS treatment. However, clinical trials have shown an efficacy of only 50% [29, 32].

1.3 Pathogenesis

HS pathogenesis is complex and remains incomplete understood. HS was originally considered a disease of follicular occlusion. Perivascular and perifollicular immune cell infiltration, hyperkeratosis and hyperplasia of the infundibular epithelium are some of the earliest detectable events in HS [15, 33-37]. However, it remains unclear if the infundibular alterations or the immune infiltration are the primary event [38]. Follicular plugging and stasis may promote resident bacteria growth, leading to dilatation of the hair follicle and eventual rupture[39]. The bacterial components including the danger-associated molecular patterns (DAMP) activate macrophages, which produce pro-inflammatory IL-1β and TNF[40]. Studies have also shown an elevation of Toll-like receptor 2 and the NLRP3 inflammasome component, both of which may further help in release of TNF and IL-1β[41-43].

Cytokines IL-1β and TNF are pleiotropic mediators, and promote several pro-inflammatory pathways revolving activation of endothelial cells and the induction of chemokine production within local tissues [38]. IL-1β leads to production of neutrophilic chemokines (including CXCL1, CXCL6 and CXCL8) and matrix metalloproteinase (MMPs, MMP1, MMP3, MMP10) while TNF induces a range of cytokines that attract neutrophils (CXCL8), T cells and monocytes towards the skin[15]. Macrophages hyperactivate the 5-lipoxygenase pathway, leading to increased production of leukotriene B4 which promotes neutrophilic granulocyte influx [38, 44]. Consistent with this, HS lesions exhibit heavy immune infiltration of monocytes, neutrophils, macrophages and dendritic cells (DCs). The increased production of extracellular matrix-degrading proteases including MMPs may play a role in skin destruction and tunnel formation [15].

Recent work has identified broad inflammatory circuits in HS beyond innate immunity [45-47]. HS lesions are enriched in cytokines produced by T-cells, including interferon-γ (IFNγ) and IL-17 levels, consistent with the observed enrichment of CD4+ T cells[29, 48, 49]. Th1 family IFNγ

promotes secretion of other Th1-attracting chemokines (CXCL10) and leads to increased infiltration of inflammatory milieu from the bloodstream [50]. Amongst its pleotropic functions, IL-17 secreted by Th17 cells induces the production of neutrophil-attracting chemokines CXCL1 and CXCL8[15]. IL-12 and IL-23 are also elevated in HS lesions, and maintain Th1 and Th17 cells[15]. The IL-36 family of cytokines, which plays a role in induction of neutrophil-attracting chemokines, is also increased in HS lesions. An increased Th17 signature predominating from T helper 17 type lymphocytes has been observed in HS [42, 48, 51, 52].

It has been hypothesized that the increased inflammatory pathways participate in feed-forward loops, leading to more inflammation in the tissue as is observed in psoriasis[53]. The combination of the massive inflammatory flux and the inflammatory byproducts such as the MMPs lead to the clinically visible formation of nodules and abscesses. This leads to the destruction of skin architecture, upregulation of processes involved in wound healing and ultimately fibrotic scar formation, including the macrophage dependent chronic WNT activity which promotes fibrotic skin healing and scarring[15, 54].

While the pathogenesis of HS is clearly multifactorial, there is growing evidence for the role of the neutrophil axis in the disease. Neutrophils form neutrophil extracellular traps (NETs), web-like structures which are composed of decondensed chromatin. In HS, NETosis has been shown to be associated with autoantibodies[55, 56]. Neutrophil gelatinase-associated lipocalin, also known as lipocalin-2 (LCN2), is produced by neutrophils and activated keratinocytes in HS, and also to increased neutrophil recruitment to the tissues. This evidence suggests that neutrophils not only contribute to pus formation but are directly involved in the feed-forward HS inflammation [57, 58]. Whether the processes responsible for disintegration of tissue are involved in formation of dermal tunnels is currently unknown.

Based on the identification of these pathways, recent clinical trials have explored other biologic therapies including infliximab (TNF inhibitor), ustekinumab and guselkumab (both anti IL-12/IL-23 therapies), anakinra and bermekimab (IL-1 alpha inhibitors) as well as secukinumab, bimekizumab and brodalumab (IL-17 receptor A (IL17-RA) inhibitor)) [32, 59-72].

1.4 Systemic co-morbidities

Inflammation in HS extends beyond skin and has a systemic component affecting several other organs. While HS is associated with the metabolic syndrome, and Inflammatory Bowel Disease (Crohn's disease and ulcerative colitis), it is currently unknown whether the systemic or cutaneous manifestations occur first [15]. It has been reported that up to 25% of patients with IBD develop HS, suggesting a biologic link of underlying inflammatory pathogenesis[73]. Patients with HS are at a higher risk factor for metabolic syndrome, atherosclerosis, and depression [15]. It also remains unknown whether HS is an individual risk factor for cardiovascular-related mortality, or if the combination of smoking and the presence of the metabolic syndrome predisposes patients to the cardiovascular-related events. A recent study demonstrated that patients with HS have a significantly higher mean Charlson Comorbidity Index, which predicts mortality risk, compared to age-, sex-, and race-matched healthy control patients[74]. HS patients have an overall increased mortality (mean incidence ratio of 1.35) mainly due to cardiovascular events (mean incidence ratio of 1.95)[1, 5].

On a molecular level, HS blood has increased levels of IL-1β and IL-6 cytokines, both of which have been shown to be atherogenic, as well as increase in LCN2, known to play a role in metabolic syndrome [41, 58, 75-77]. A large-scale comparison of cytokine levels in blood and lesional HS skin, as well as the interactions between these cytokines in blood and skin is currently undefined.

1.5 Thesis aims

The overarching aim of this thesis is to characterize the cutaneous and systemic inflammation in HS. We first established a novel approach to study dermal inflammation in HS which relies on ultrasound-guided biopsies of HS as well as demographic and site matched healthy control skin **(Chapter 2)**. We then evaluated whether the inflammation from HS lesions extends to perilesional and nonlesional skin **(Chapter 3).** In **Chapter 4,** we focused specifically on dermal tunnels, a unique feature of HS, and asked whether tunnels are end-stage fibrotic features of disease as has been accepted in the field or whether these tunnels contribute to the overall disease pathogenesis. In **Chapter 5**, we expanded our work to address whether unique HS manifestations (specifically the tunnels) influence the overall systemic inflammation in HS by characterizing biomarkers in HS blood. Lastly, in **Chapter 6,** we report the clinical and molecular response to our clinical trial of IL-17RA blockade in HS.

CHAPTER 2:

Developing a standardized approach to study hidradenitis suppurativa

CHAPTER 2. Developing a standardized approach to study hidradenitis suppurativa

2.1 Introduction

The differences in the structure and the inflammatory milieu of human and murine skin must be considered while selecting appropriate models to study HS. Human skin is over 100mm and adheres to underlying tissues whereas murine skin is less than 25mm and loose [78]. This makes it challenging to model deep dermal tunnels, which are frequently found 1-1.5cm underneath the epidermis, in mouse skin. Neutrophil defensins, rete ridges and eccrine sweat glands, all features described in HS, are absent from murine skin[78]. Furthermore, on a systemic level, humans have a neutrophil predominance (50-70%) whereas murine blood has a lymphocytic predominance (75-90%) [79]. Given the prominent role of these cellular subsets in HS pathogenesis, and the potential role of dermal tunnels, it is challenging to rely on mouse models to accurate recapitulate HS pathogenesis. We thus undertook a translational approach to study the disease pathogenesis where we studied skin biopsy and blood samples from HS patients enrolled at the Rockefeller University (please see Section 8.1 for more information regarding subject enrollment).

Many of translational studies rely on comparison of diseased skin with healthy control skin without consideration of the anatomic sites. However, intertriginous and pilosebaceous-apocrine unit rich areas of skin (which are primary affected by HS) have a unique inflammatory environment marked by an increased non-inflammatory IL-17 milieu as well as distinct barrier properties[80-82]. Apocrine gland rich skin areas also demonstrate an increase of T cell and Dendritic Cell (DC) infiltration[80]. Furthermore, the intertriginous body areas are subject to mechanical stress, which may produce microinjuries causing the release of cellular damage molecules including DAMPs, which in turn stimulate local macrophages, DCs, and keratinocytes [38, 83, 84]. Studies have suggested that these topographical variations specific to apocrine gland rich skin may predispose the areas to Il-17 type inflammatory disease, ultimately leading to the subclinical inflammation and eventual progression to the IL-17/IFNγ type inflammation observed in HS [80]. The bacterial environment surrounding the intertriginous skin is thought to contribute to either initiation or propagation of disease pathogenesis[15].

Taken together, these data highlight the need for site-matched comparison of skin specimens. Given the topographical inflammatory variation, we elected to utilize site-matched healthy control samples in order to prevent overestimation of the IL-17 inflammatory response.

2.2 Results

2.2.1 Consensus of biopsy sites for molecular analysis of HS skin

Unlike other systemic skin diseases, HS lesions are morphologically diverse, with presentations ranging from nodules, abscesses, dermal tunnels and fibrotic tracts, as well as permutations of these morphologies. As such, a 'lesional' site in one patient varies greater from the 'lesional' site in another patient, complicating both severity assessment and translational studies. There have been only two high-quality studies with a priori definitions of biopsy sites defining lesional skin at an edge of an active inflammatory lesion and unaffected skin as ≥10 cm away on normal appearing skin [42, 85]. However, this is complicated by the presence of dermal tunnels or deep abscesses is often not visualized easily and may be difficult to appreciate clinically with careful palpation. This can lead to a biopsy of an 'unaffected' skin with dermal tunnels or abscesses. As such, we used ultrasound imaging as a noninvasive approach to diagnose dermal

tunnels and abscess prior to biopsying and prevent the inadvertent biopsying of a lesion in a control sample.

As part of a joint taskforce, we have recently put forward expert recommendations to establish consensus for studying HS skin specimens (Figure 1) [86]. We recommend that lesional skin is biopsied at an edge of an active inflammatory lesion (such as a nodule), and perilesional and nonlesional skin is biopsied on healthy/normal appearing skin within the same or contralateral region. These recommendations become critical in the context of clinical trials and assessment of molecular response and have been used for work performed in this thesis.

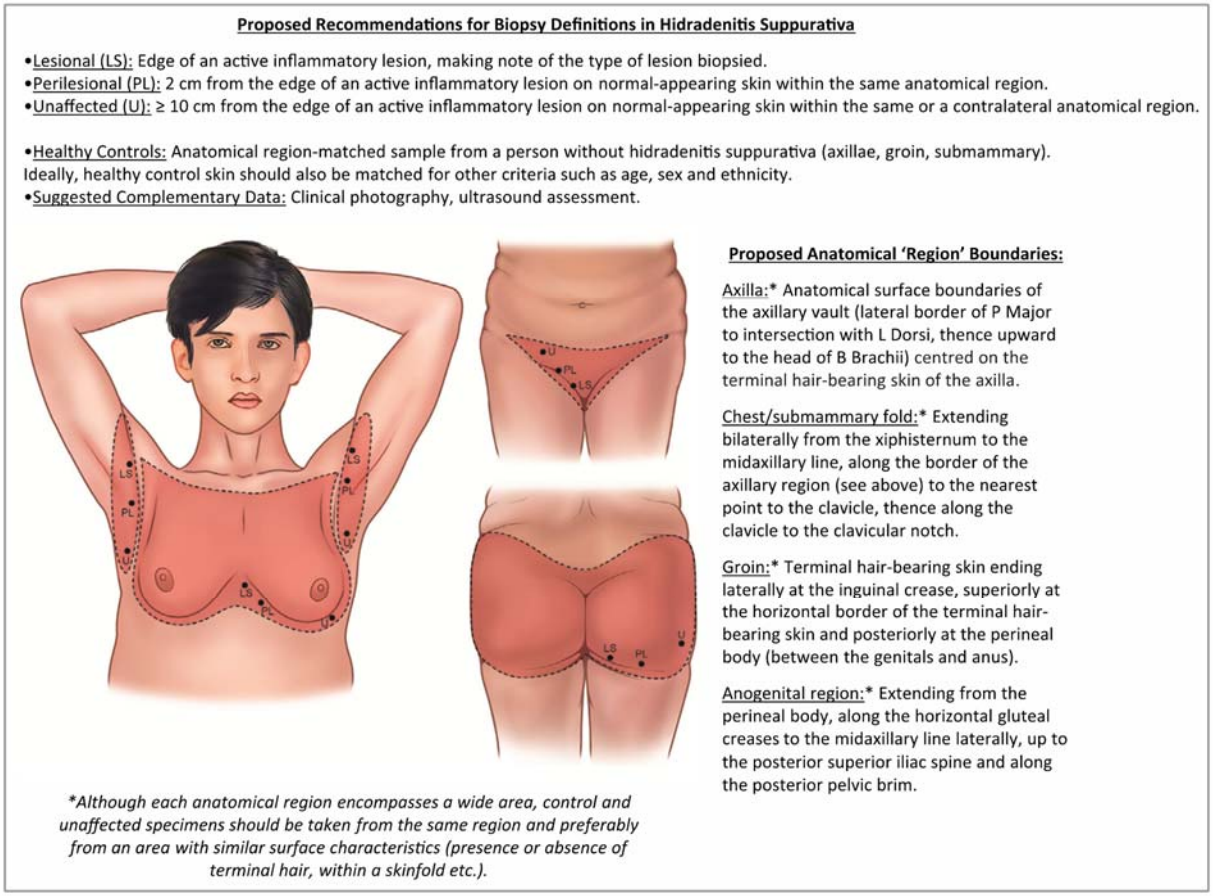

Figure 1: Biopsy definition recommendations for molecular characterization of Hidradenitis Suppurativa (HS).
Recommendations for biopsying nonlesional, perilesional and lesional skin with comparison to site-matched healthy control skin [86].

2.2.2 Ultrasound assessment is a valid approach to study HS

Ultrasound is a safe and relatively affordable modality that has been utilized in a number of inflammatory and fibrotic skin diseases[87, 88]. While ultrasonographic findings have been reported in HS, a correlation between clinical, histological and immunological characteristics and

ultrasonographical parameter have not been performed [87-92]. We therefore sought to examine the clinical validity of ultrasound using histological biomarkers[93]. In total 22 individuals with untreated moderate-to-severe HS and 10 healthy controls were recruited for this study. All participants were not on active treatment and had a washout period of at least five half-lives prior to study enrollment. In total 65 cutaneous sites underwent matched clinical assessment, ultrasound and skin biopsy.

Ultrasound of HS lesional skin identified a prominent hyperechoic linear band with adjacent hypoechogenicity: the entry signal–entrance echo and surface reflection, corresponding areas of psoriasiform epidermal hyperplasia on histology (Figure 2A). This degree of hyperechogenicity and adjacent hypoechogenicity was not seen in healthy controls (Figure 2A). As previously described in psoriasis and HS, the thickness of the entry signal correlates with the maximum thickness of the rete ridges of the epidermis, and referred to as 'epidermal thickness' hereinafter [94] . Statistically significant differences between HS lesional skin and skin of site-matched healthy controls were seen in both histological and sonographic measurements of epidermal thickness (Figure 2B-C). A strong correlation was noted between histological and sonographic measurements of epidermal thickness (Figure 2D), indicating a high level of analytical validity. Sonographic epidermal thickness was consistently greater than histological epidermal thickness. Sonographic epidermal thickness displayed moderate correlation with quantitative $CD3^+$ cell counts, and only fair-to-poor correlation was observed with $CD11c^+$ and NE^+ quantitative cell counts (Figure 2E-G).

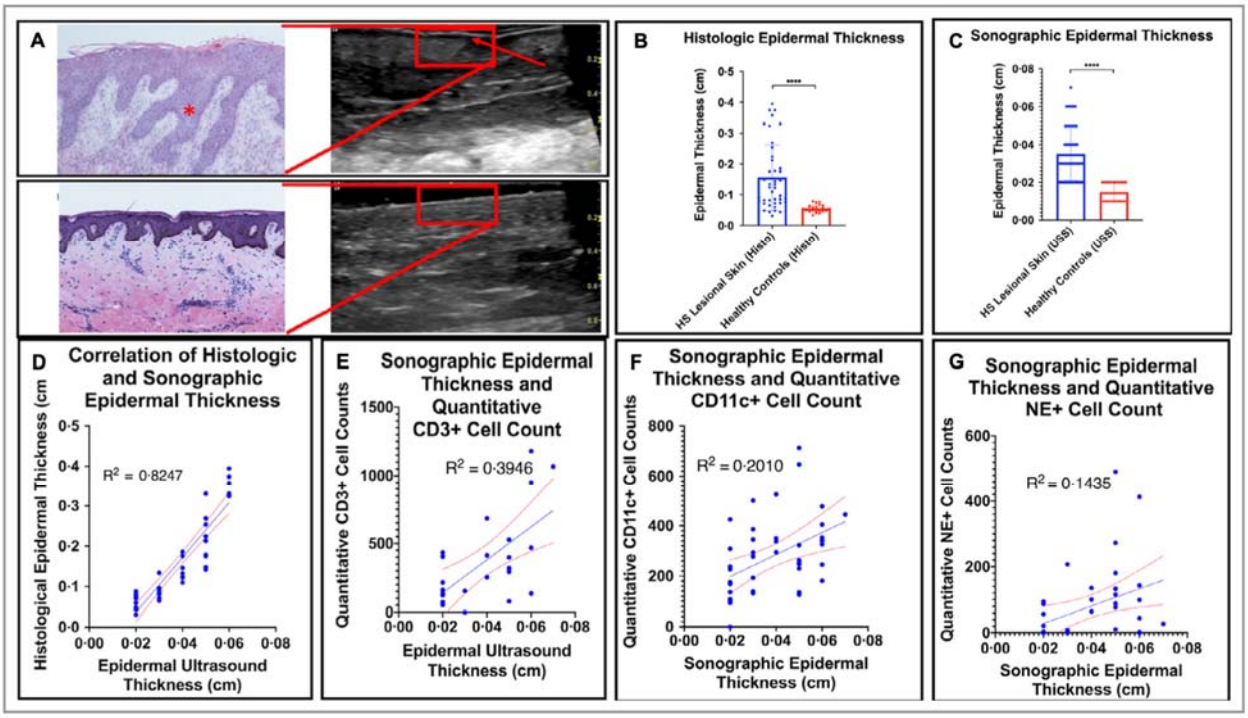

Figure 2: Ultrasound analysis of HS skin displays a correlation with histological properties. **A)** Psoriasiform epidermal hyperplasia (*) correlated with prominent hyperechoic thickening on ultrasound (red arrow) compared to healthy control skin. **B-C)** Histologic and sonographic epidermal thickness was significantly different between HS lesional skin and controls. **** $p < 0.0001$. **D)** A high degree of correlation is observed in measures of epidermal thickness by ultrasound and epidermal thickness by validated methods in histopathology. **E)** Sonographic epidermal thickness correlated moderately with $CD3^+$ cell counts **F)** and $CD11c^+$ cell counts **G)** but not with neutrophil elastase $(NE)^+$ cell counts (g)[93].

Dermal tunnels were detected in 36 of 44 lesional and perilesional sites. They were represented sonographically by hypoechoic–anechoic bands bordered by hyperechoic strips corresponding to epithelialized tunnels seen on histology (Figure 3A-C). The hyperechoic strips of keratinized tunnels had greater echogenicity and less branching than surrounding areas of fibrosis, which can also appear as linear hyperechoic bands on ultrasound. Tunnel diameter as measured by ultrasound had a very high level of correlation with histological tunnel diameter (Figure 3D). Stratification by draining and nondraining tunnels suggested a higher correlation with draining as opposed to nondraining tunnels (Figure 3E-F). Visual differences in echogenicity of linear bands and power Doppler intensities were observed between draining and nondraining tunnels (Figure 3G-J). Statistically significant differences in both histological and sonographic tunnel diameter were observed between draining and nondraining tunnels (Figure 3K-I).

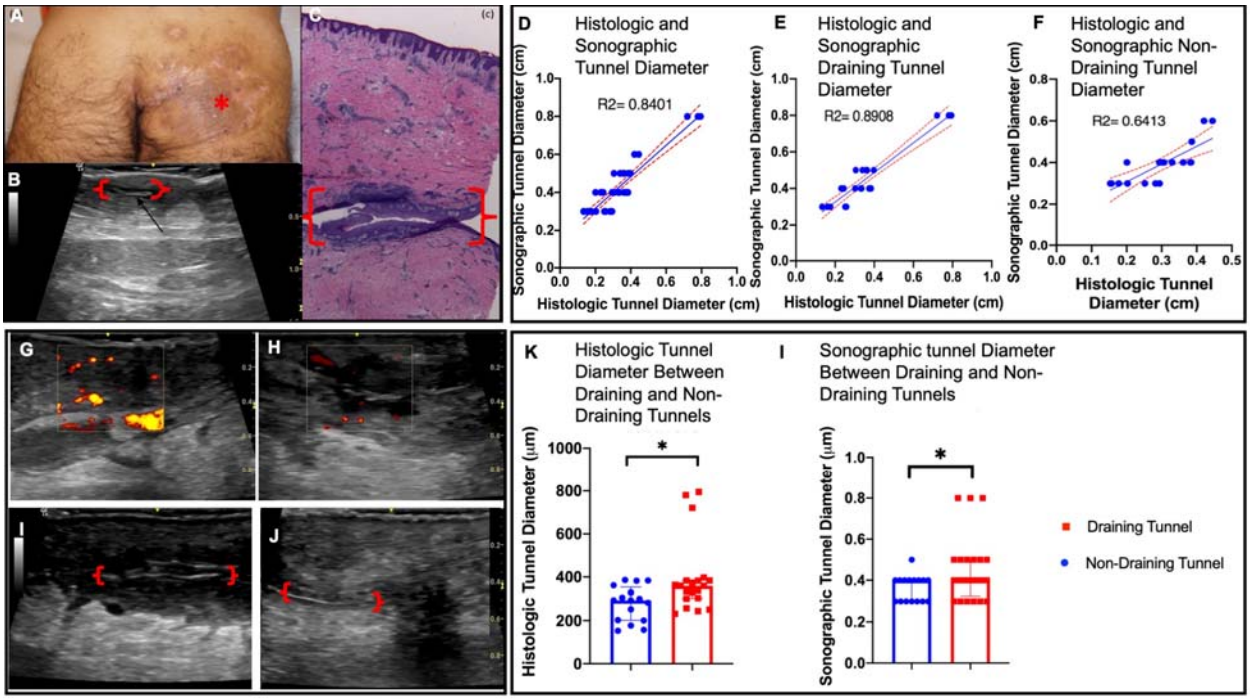

Figure 3: Doppler ultrasound can be used to identify dermal HS tunnels.
A) The clinical presentation of dermal tunnels correlates with **B)** ultrasound findings highlighting hyperechoic keratinized dermal tunnels (black arrow and red brackets) and **C)** histology specimen. **D)** Correlation between the diameter of tunnels based on ultrasound and histological measurements, with variation in correlation in the presence of **E)** draining and **F)** nondraining tunnels. Comparison of Doppler ultrasound findings between draining **G-I)** and nondraining **H-J)** tunnels. Significant differences in the diameter of tunnels are seen on **K)** histological and **I)** sonographical assessment when stratified by the drainage of tunnels. *$p < 0.05$ [93].

Semiquantitative power Doppler intensity was able to measure and localize inflammation in a variety of clinical presentations of HS. The degree and location of power Doppler intensity signaling was more superficial in lesions such as nodules (Figure 4A), and deeper in deeper lesions such as abscesses and tunnels (Figure 4B-D). The intensity of the power Doppler signal also correlated with the degree of neutrophil infiltration, as indicated by NE^+ immunohistochemical staining (Figure 4I-L). Quantitative dermal $CD3^+$ cell counts had the highest correlation with semiquantitative power Doppler intensity (Figure 4M), followed by $CD11c^+$ dermal cell counts (Figure 4N), with quantitative NE^+ immunohistochemistry demonstrating the lowest correlation (Figure 4O).

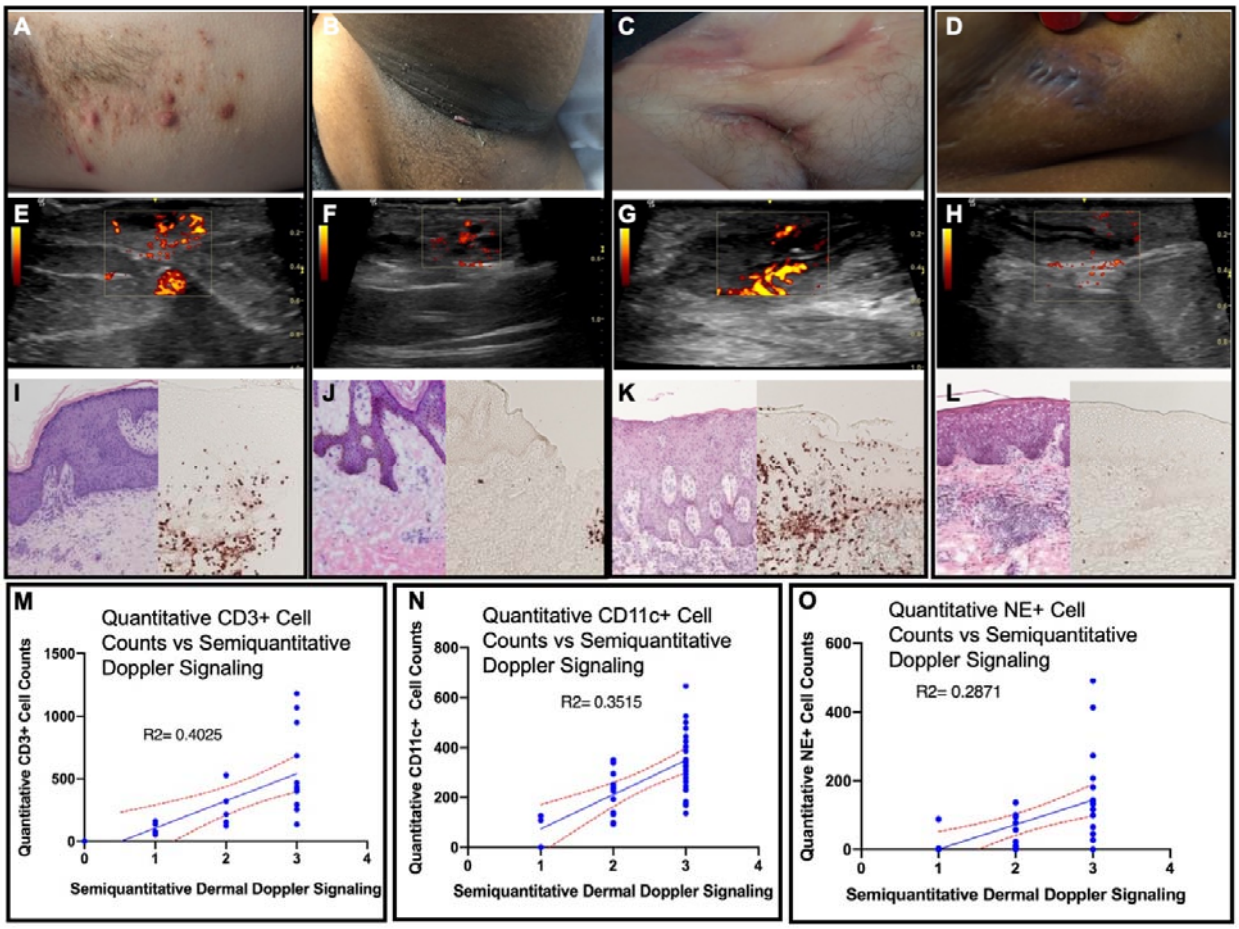

Figure 4: Doppler ultrasound has validity across different HS manifestations.
Clinical and ultrasound correlations of **A)** nodules, **B)** deep abscesses, **C)** draining tunnels and **D)** nondraining tunnels demonstrate localization and intensity of power Doppler flow consistent with clinical manifestations and **I-L)** histological hematoxylin and eosin (H&E) and NE staining. **M)** Semiquantitative scoring of power Doppler intensity has moderate correlation with $CD3^+$ dermal cell counts, **N)** $CD11c^+$ dermal cell counts and **O)** NE^+ dermal cell counts. [93]

2.3 Discussion

We present quantitative data to explore the analytical and clinical validity of ultrasound-based biomarkers in HS. The overall level of analytical validity was high regarding epidermal thickness, tunnel diameter and power Doppler intensity, suggesting that ultrasound-based measures can be a potential surrogate measurement for histology-based outcomes in HS. The ability for ultrasound to identify tunnels in HS is of vital importance, particularly as the extent of tunnels is difficult to appreciate with clinical examination alone [90].

The high analytical validity of tunnel diameter and epidermal thickness suggests that these are potential biomarkers for longitudinal change in disease activity over time and in the setting of pharmacological interventions. This also emphasizes the utility of ultrasound in the selection of biopsy sites, given the high inflammatory activity surrounding tunnels. Inadvertent biopsy of a perilesional or nonlesional site with an underlying tunnel may introduce errors in measurement of inflammatory mediators[15]. Therefore, prebiopsy assessment of sites with ultrasound has high utility in assessment for occult tunnels, and the high degree of analytical validity presented by our data supports this notion.

In conclusion, sonographic epidermal thickness and dermal tunnel diameter have acceptable levels of analytical validity in the assessment of HS lesions compared with histological correlates. Power Doppler signaling demonstrates acceptable levels of both clinical and analytical validity, suggesting it is a valid imaging-based biomarker in HS. Future work is necessary to assess the response of these biomarkers to established therapeutic interventions, and assessment of the utility of image- based biomarkers as diagnostic and predictive tools for directing and optimizing patient care and outcomes.

CHAPTER 3:
Characterizing the inflammatory profile of hidradenitis suppurativa

CHAPTER 3. Characterizing the inflammatory profile of hidradenitis suppurativa skin

3.1 Introduction

The pathogenesis of HS remains incompletely understood [95], limiting the ability to identify and implement novel therapeutic strategies. Despite histological similarities of HS epidermis to psoriasis vulgaris [96, 97], HS has deep dermal inflammation that is absent from psoriasis [98, 99]. Previous studies have identified multiple inflammatory pathways involved in HS, including Th17 immune axis [51, 85, 97, 100], B and plasma cells [56, 101-104], dendritic cells [101, 102], anti-Saccharomyces cerevisiae antibodies [105] and antibodies to citrullinated peptides [56]. The role of neutrophil activation and trafficking, and neutrophil extracellular trap development has also been established [56, 98, 101]; IL-1 production in keratinocytes, fibroblasts and other inflammatory leukocytes [41, 102] and the potential role of complement and tissue-microbiome interactions have also been described [104, 106-108]. HS and psoriasis share mutual pathophysiology marked by dysregulation of keratinocytes, up-regulation of type I interferon signature, tumor necrosis factor (TNF) and IL-1 signaling, as well as hyperactivation of the Th17 and IL-12/IL-23 axis [40, 42, 48, 49, 97, 109-111]. The discovery of these pathways in HS has stimulated numerous ongoing trials studying psoriasis-approved therapeutics in HS, including TNF inhibitors (adalimumab, infliximab), and anti IL-17 (brodalumab, secukinumab, ixekizumab, bimekizumab), IL-12/IL-23 (guselkumab, rizakizumab, ustekinumab) and IL-1 therapies (anakinra, bermekimab) [32, 59-71]. While adalimumab is the only FDA-approved biologic for HS, 50% of patients either fail to respond or lose response efficacy overtime [112].

Many of the current transcriptomic studies in HS have focused on the comparison between HS lesional skin and nonlesional skin (frequently from surgical discard) [104, 113]. However, non-lesional HS skin is known to be inflamed [42, 97]. Hence, comparisons to only non-lesional tissue may mask transcripts which can potentially inform us about mechanisms associated with predisposition to the disease. Furthermore, it has been shown that there is an immunological heterogeneity between topographic locations of the skin, with apocrine gland-rich skin having an enhanced Th17 signature compared to apocrine gland-poor skin [80, 114]. Therefore, comparison with site-matched healthy control skin (rather than surgical discard from other anatomic locations) is necessary. Given the recent development of standardized biopsy definitions in HS, the molecular profiles of lesional, perilesional and nonlesional tissue remain incompletely characterized [86]. Furthermore, majority of studies in HS have thus far focused on transcriptomic profiling but have not examined the proteomic profile of skin, and therefore have not demonstrated whether the mRNA is actively translated into functional protein on a proteomic level [42, 109, 115].

We thus sought to characterize the inflammatory transcriptomic and proteomic profile in HS skin and correlate these biomarkers with clinical severity in HS (Table 1).

3.2 Results

3.2.1 HS skin has a differing transcriptomic profile compared to healthy control skin.

We biopsied HS lesional (LS), perilesional (PL) and nonlesional (NL) skin as previously defined [86, 116]. In summary, lesional biopsy was taken at an edge of an inflammatory nodule, perilesional biopsy was taken from healthy-appearing skin 2cm away from the edge of the

inflammatory nodule and nonlesional biopsy was taken from healthy-appearing skin 10cm away in the same anatomic region either on the same side or on the contralateral side of the body (Figure 5A). Healthy control skin was obtained from site-matched anatomic region of healthy volunteers. Principal Component Analysis (PCA) and phylogenetic tree clustering demonstrated that HS skin clustered separately from healthy volunteers (HV), with perilesional and lesional HS skin clustering away from nonlesional skin (Figure 5B-D).

We defined differentially expressed genes (DEGs) using the criteria of fold change (FCH) of FCH≥ |1.5|, and FDR ≤ 0.05. The top DEGs in our HS samples were dominated by a strong polyclonal immunoglobulin signature. There was an enrichment of pathways involving complement activation and B cell signaling, consistent with recent reports of the strong B and plasma cell signature in HS [101, 102]. Since the prominent immunoglobulin signature may mask the presence of other pathways in HS, immunoglobulin transcripts were redacted from our larger transcriptomic analysis in order to identify additional pathways involved in HS. Pathway enrichment analysis of perilesional and lesional samples identified similar enrichment of genes involved in neutrophil degranulation, immune response and extracellular matrix organization (Figure 6) whereas enrichment analysis of genes in nonlesional skin showed enrichment of genes involved in early epidermal development/reprogramming.

Table 1: Characteristics of study participants.

	Healthy Control	**Hidradenitis Suppurativa (HS)**
Number of participants	10	22
Age, years, mean (SD)	64.10 (8.48)	37.41 (13.27)
Gender, n (%) Male Female	 2 (20.00%) 8 (8.00%)	 10 (45.45) 12 (54.55)
BMI, kg/m^2, mean (SD)	32.07 (6.57)	31.63 (8.32)
Smoking Status, n (%) Yes No	 5 (50.00%) 5 (50.00%)	 14 (63.64%) 8 (36.36%)
Biopsy Location, n (%) Axilla Buttock/groin/inguinal Neck Submammary	 9 (90.00%) 1 (10.00%) 0 (0.00%) 0 (0.00%)	 14 (63.64%) 6 (27.27%) 1 (4.55%) 1 (4.55%)
Hurley Stage II, n (%) Hurley Stage III, n(%)	N/A	15 (68.18%) 7 (31.82%)
IHS4, average (SD)	N/A	40.82 (65.80)

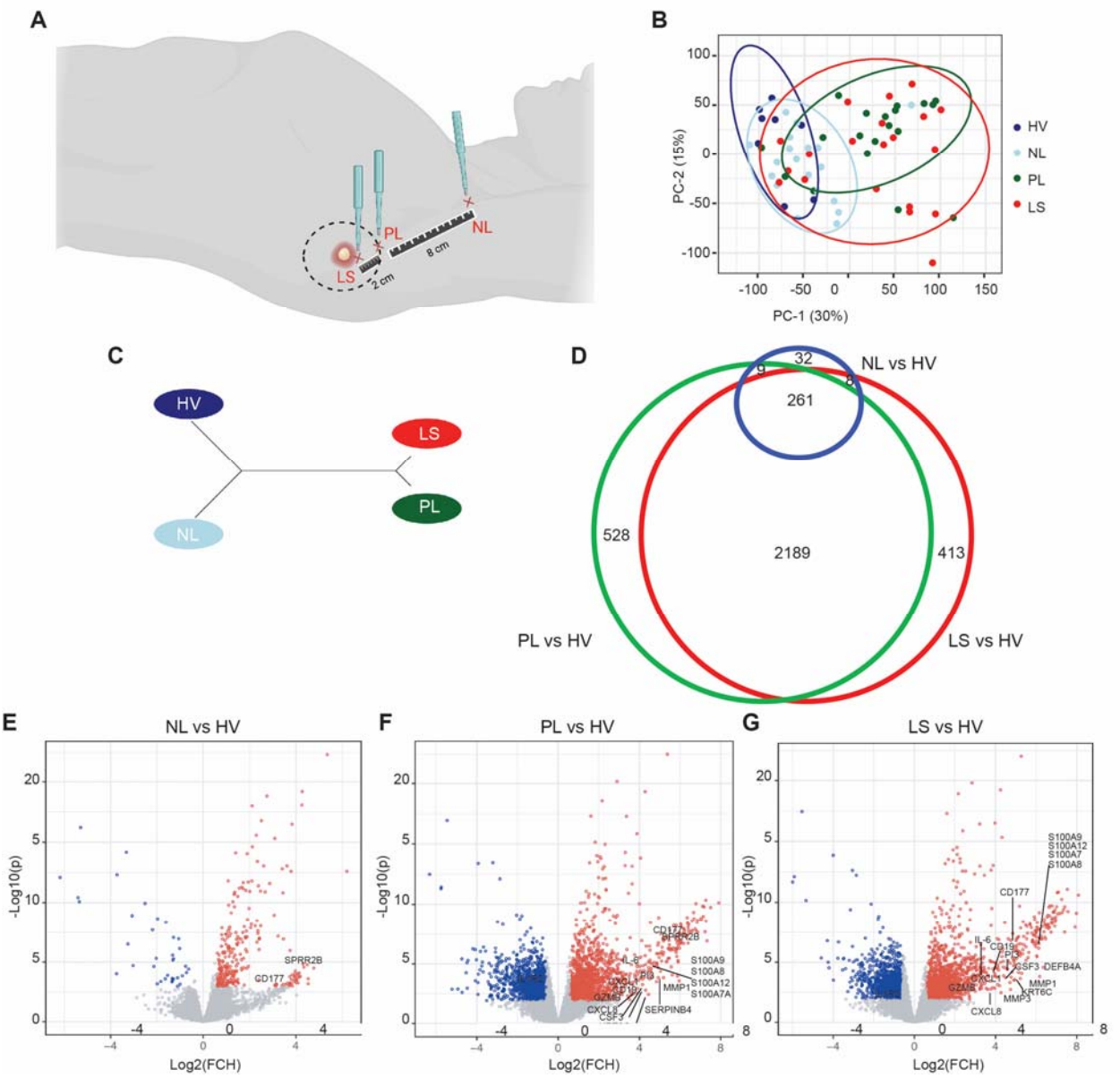

Figure 5: HS lesional and perilesional skin is molecularly distinct from both nonlesional HS and site-matched healthy control skin.

A) Schematic representation of lesional (LS), perilesional (PL) and nonlesional (NL) HS skin biopsies. Lesional skin was biopsied at an edge of an inflammatory lesion, perilesional skin was biopsied 2cm away on healthy appearing skin and nonlesional skin was biopsied 10cm away from the inflammatory lesion on healthy appearing skin on the same or contralateral skin. **B-C)** Principal Component Analysis (PCA) and phylogenetic tree clustering shows that healthy control skin clusters away from lesional and perilesional HS skin, with nonlesional HS skin clustering away from healthy volunteers (HV). **D)** Venn diagram comparing all of the genes between HS (NL, PL and LS) relative to healthy volunteer (HV) control skin. Volcano plot analysis of all genes between **E)** NL, **F)** PL and **G)** LS skin compared to HV.

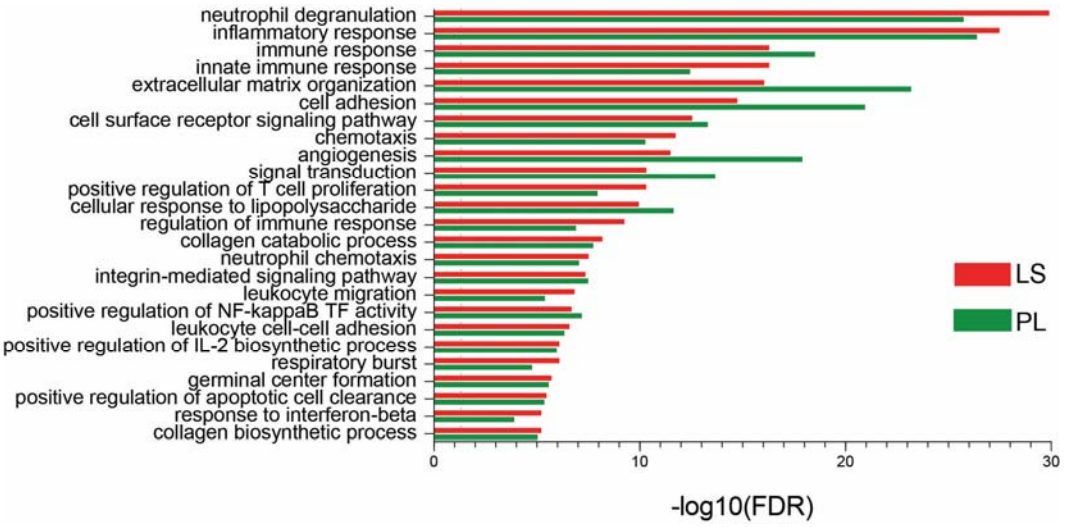

Figure 6: Comparable enrichment of immune-related pathways in perilesional and lesional HS skin.
Enrichment for GO-biological processes pathways of differentially expressed genes (DEGs) in LS (red) and PL (green) HS skin relative to healthy controls excluding the immunoglobulins. Dashed vertical line indicates a false discovery rate (FDR) of 0.05.

To identify the major immune cell infiltrates in HS, we applied the xCELL scoring tool to our transcriptome data [117]. There was increased infiltration of granulocyte-monocyte progenitor cells, myeloid dendritic cells, B cells (B cell, B cell memory and B cell plasma cells), macrophages (macrophages, M1 macrophages and M2 macrophages) as well as T cell $CD4^+$ cells (naïve and effector) in the perilesional and lesional skin (Figure 7), consistent with enriched pathways of complement activation and B cell receptor signaling which were uniquely found in HS (Figure 8).

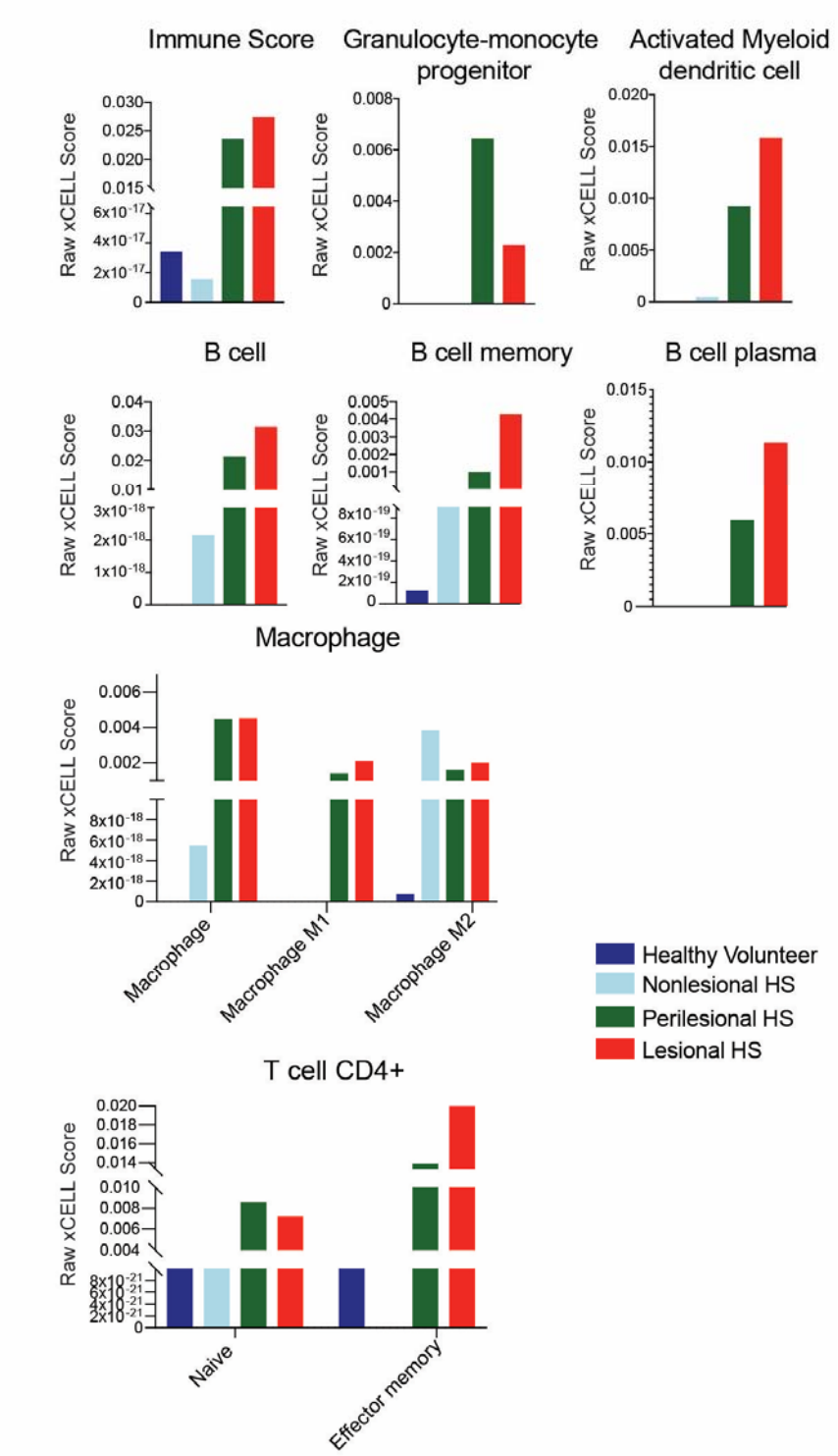

Figure 7: Diverse immune infiltration in nonlesional, perilesional and lesional HS skin. xCell scores with predicted enrichment of different cell population in the RNA-seq transcriptomic data in healthy volunteer, and nonlesional, perilesional and lesional HS skin.

3.2.2 Inflammation in lesional skin extends to healthy-appearing perilesional area.

We observed a comparable and statistically significant up-regulation of genes within several immune axis including Th1(CXCL8, IL2RA, IL12RB1), Th2 (IL4R, OX40), IL-12/IL-23 (IL6, CXCL1, CCL2, IL2RA, EBI3), Th17 (CXCL1) and Th22 (S100A9, S100A12) [118, 119]. There was a comparable upregulation of neutrophil related (CD177, CXCL1, CXCL8, SERPINB4, CSF3, DEFB4A) as well as psoriasis related (PI3, S100A family) genes. Consistent with this, there was a comparable and significant enrichment of genes involved in neutrophil chemotaxis (IL1B, CXCL1-3, CXCL5-6, CXCL8, ITGB2, CXCR1), neutrophil migration (MDK, RAC2, CXCL8) and neutrophil extravasation (MDK, CD177) in both perilesional and lesional skin compared to healthy controls. This suggests that there is neutrophilic infiltration in perilesional skin despite appearing visually normal on clinical examination. This data suggests that healthy-appearing perilesional skin has similar transcriptomic profile as lesional skin, suggesting that there are molecular changes occurring either or without development of visible lesions.

To globally assess whether inflammation from lesional skin extends to the surrounding perilesional skin (2cm away from the edge of a nodule), we compared the transcriptomic profile of lesional and perilesional HS skin. There were no DEGs between perilesional and lesional skin, further highlighting that comparable inflammation extends beyond visibly affected skin (Figure 9A). Lesional and perilesional skin had an upregulation of select canonical pathways including leukocyte extravasation signaling, complement system, Th2 and Th1 pathways and IL-8 signaling (Figure 9B). Consistent with previously published reports, we observed IFNγ, TNF, and IL-1β as upstream regulators whereas the immunomodulatory IL10RA were reduced [102, 120]. We demonstrate that the same upstream regulators involved in HS lesional skin govern the inflammation in perilesional skin (Figure 9C).

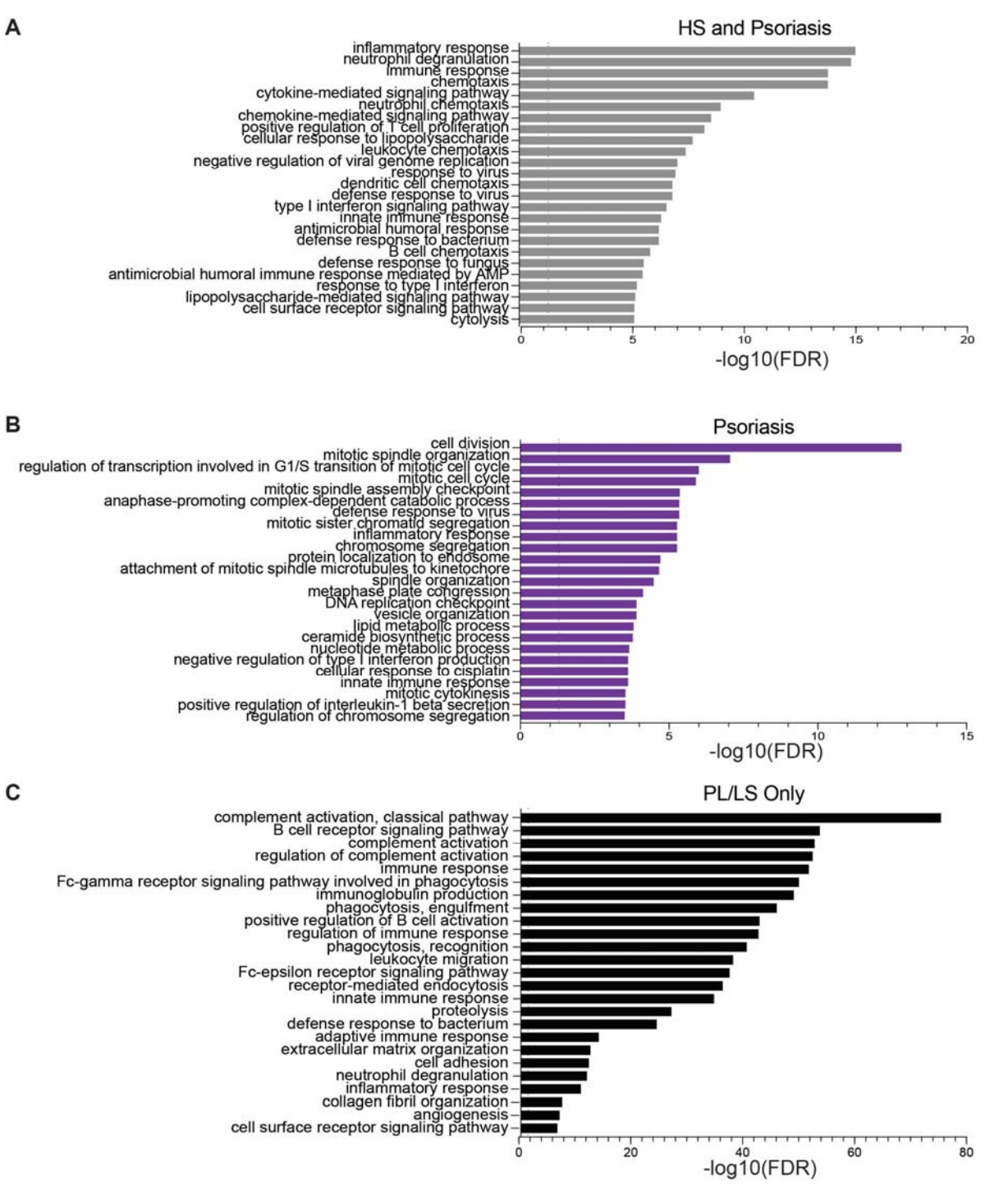

Figure 8: HS skin has an upregulation of B-cell related pathways.
Enrichment for GO-biological processes in **A)** overlapping transcripts between HS and Psoriasis **B)** transcripts unique to psoriasis and **C)** transcripts unique to HS skin.

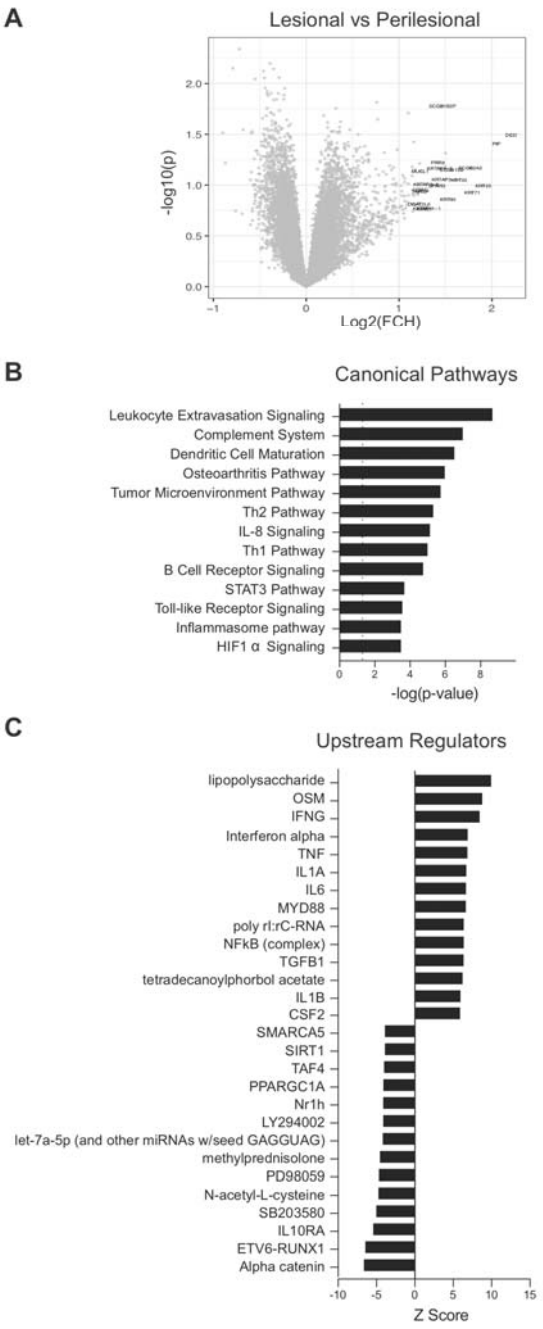

Figure 9: There are no differentially expressed genes between lesional and perilesional HS skin.
A) Volcano plot of genes in lesional versus perilesional HS skin demonstrates no differentially expressed genes. **B)** Select canonical pathways upregulated in both lesional and perilesional tissue compared to healthy controls as assessed by Ingenuity Pathway Analysis (IPA) ($p<0.05$) **C)** IPA analysis of upstream regulators in HS perilesional and lesional skin compared to healthy controls ($p<0.05$).

We next performed immunohistochemistry on healthy control skin, nonlesional, perilesional and lesional HS skin. We observed a thickened epidermis with robust keratin 16 positivity in the suprabasal keratinocytes, consistent with psoriasiform hyperplasia (Figure 10A-B). The psoriasiform hyperplasia was comparable between perilesional and lesional skin. There were no significant differences in leukocytic infiltration of CD3+, CD11c+ and NE+ cells between perilesional and lesional skin, with both having a significantly higher infiltration compared to healthy control skin (Figure 10C-D).

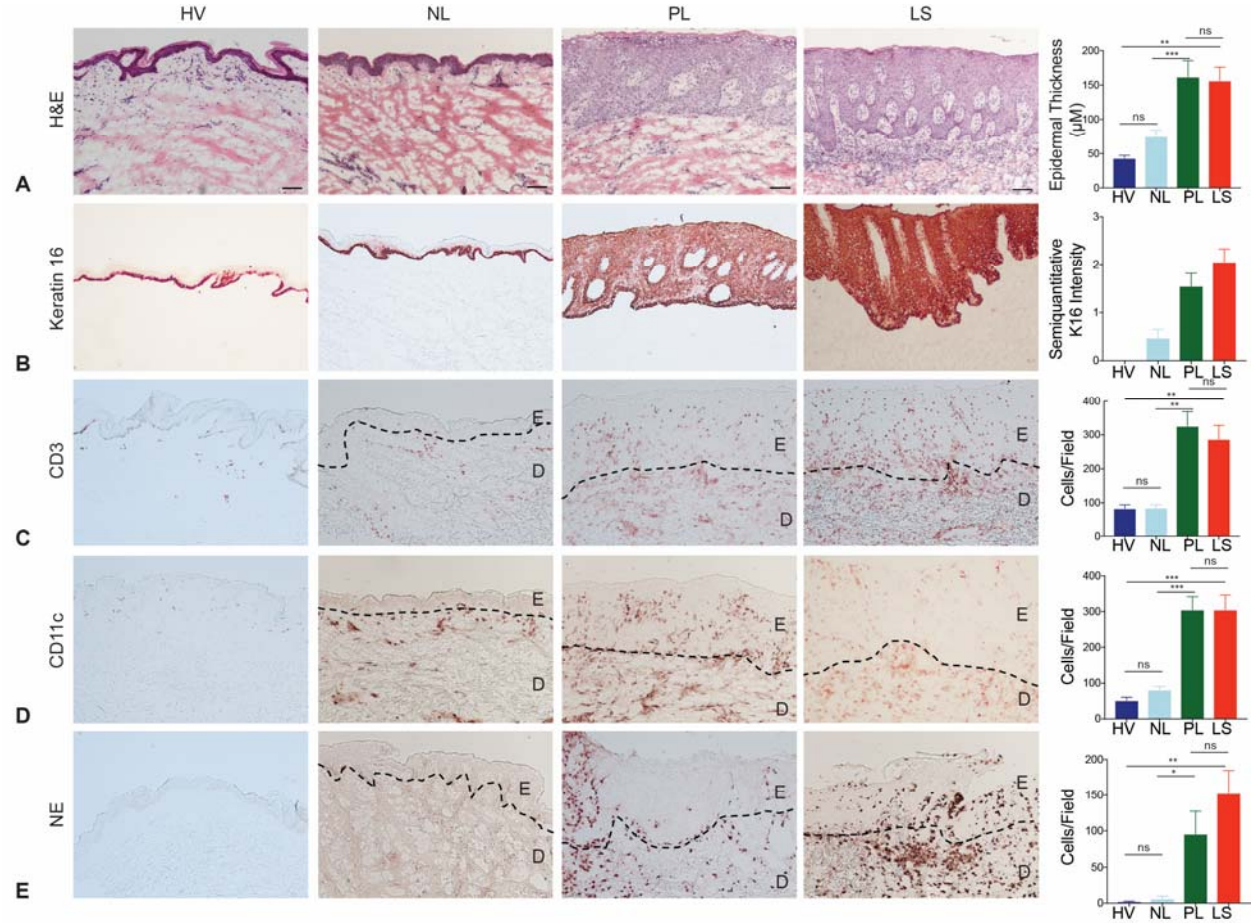

Figure 10: HS lesional and perilesional skin has a similar histological profile.
A) H&E stain of healthy volunteer, nonlesional, perilesional and lesional HS skin. Scale Bar, 100μm **B)** Keratin 16 (K16) staining and semiquantitative quantification of K16 intensity. Immunohistochemical analysis of **C)** $CD3^+$ **D)** $CD11c^+$ **E)** NE^+ cellular infiltration and quantification across multiple patients. E denotes epidermis and D denotes dermis. Mean ± standard error of mean (SEM) is shown with *p<0.05, **p<0.01, ***p<0.001.

3.2.3 HS perilesional skin has a comparable activation of IL-17 pathway as lesional skin

Given HS and psoriasis share features of psoriasiform epidermal hyperplasia, that psoriasis is governed by the IL-17 axis, and the comparable transcriptomic profile between lesional and perilesional skin, we asked whether HS perilesional skin also has an activation of the IL-17 pathway. There was a comparable upregulation of genes involved in the IL-17 pathway (as defined by Gene Ontology (GO)) in HS perilesional and lesional samples (Figure 11A). We then performed a gene set variation analysis (GSVA) of published IL-17 signatures relating to psoriasis and observed a consistent activation of these pathways in both perilesional and lesional skin (Figure 11B) [121, 122]. Notably, there was detectable activation of IL-17 signature even in nonlesional skin (Figure 11B). There were 214 differentially expressed transcripts shared between HS and psoriasis (MAD3) (Figure 11C), with the top enriched pathways involving neutrophil degranulation. Pathways unique to psoriasis related to proliferation, including cell division, mitotic spindle organization and regulation of transcription. Pathways enriched in HS lesional and perilesional skin were related to complement activation and B cell signaling. Taken together, this data suggests that both HS and psoriasis share an activation of IL-17 pathways and a neutrophilic signature, with HS exhibiting an activation of the IL-17 pathway even in healthy-appearing perilesional skin. Uniquely, HS has an enrichment of pathways relating to complement, B cell signaling and immunoglobulin production whereas psoriasis has an enrichment of a proliferative signature, likely due to keratinocyte hyperplasia as a dominant cellular feature (Figure 8A-B).

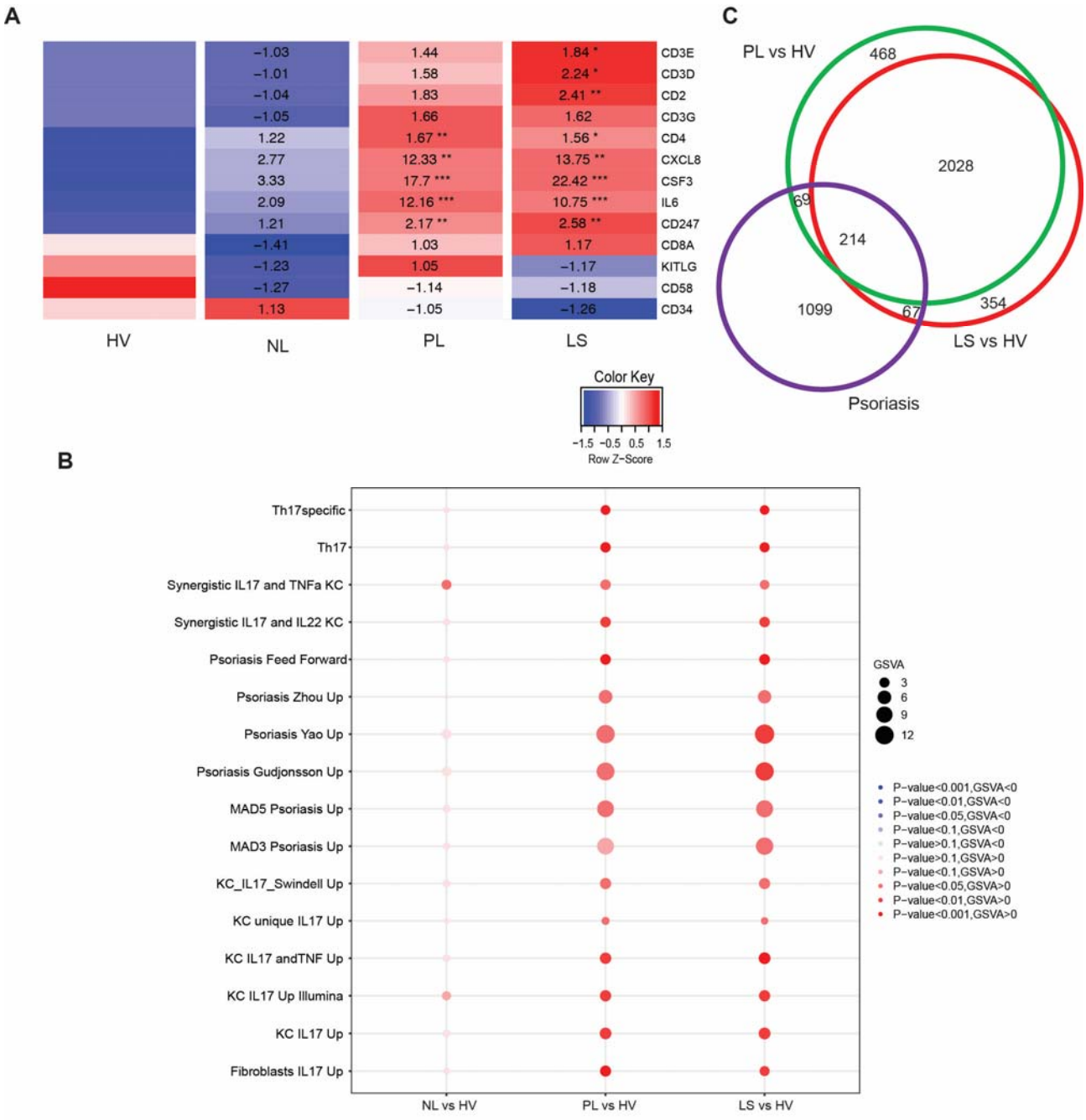

Figure 11: Activation of the IL-17 pathway in both perilesional and lesional HS skin. **A)** Heatmap of all differentially expressed genes in the curated BioCarta IL-17 Pathway gene list. Fold Changes (FCHs) relative to HV are shown with *p<0.05, **p<0.01, ***p<0.001. **B)** Bubble plot with Gene Set Variation Analysis (GSVA) scores across NL, PL, and LS HS skin samples for known Th17 pathways. The diameter of the bubble is proportionate to the log FCH of the GSVA score of HS skin relative to healthy control skin. KC is keratinocyte. **C)** Comparison of PL and LS skin with Meta-Analysis Derived (MAD3) psoriasis transcriptome.

3.2.4 HS skin has increased expression of IL-17C

Interleukin 17C (IL-17C) is a cytokine produced by epithelial cells, including keratinocytes, in response to multiple stimuli such as IL-17A, IL-17F, TNF-α, bacterial stimuli and toll-like receptor agonists [123].When produced in keratinocytes, IL-17C mediates the production of inflammatory molecules, including IL-1β, IL-8, CXCL1, and IL-36γ. In addition, IL-17C induces further elevation in IL-17A and IL-17F in Th17 cells in a pro-inflammatory positive amplification loop [124, 125]. These mechanisms contribute to the feed-forward inflammatory cascade described in psoriasis and AD [124]. Elevated levels of IL-17A and IL-17F have been identified in HS lesional tissue and is thought to be associated with epidermal psoriasiform patterning[41].We thus questioned whether epithelial derived cytokines (such as IL-17C) are also produced in HS lesional tissue, given the existing commonalities in IL-17A and IL-17F signaling and psoriasiform epidermal patterning between the three disorders.

We observed a significant elevation of IL-17C expression in all HS samples including in lesional, perilesional and unaffected tissue compared to site-matched healthy controls (Figure 12A-B). These changes were comparable to the elevations seen in psoriasis, wherein the role of IL-17C has been well defined. IHC localized IL-17C to the supra-basal epidermis with particular accentuation of the stratum corneum and stratum granulosum, a visible gradient toward the stratum corneum, as well as diffuse dermal staining (Figure 12A). Semi-quantitative visual scoring identified a significant difference between basal epidermal staining in unaffected tissue and lesional/perilesional tissue, with supra-basal staining increasing from unaffected to perilesional and lesional tissue (Figure 12C). However, in some patients with pronounced epidermal acanthosis, pan-epidermal staining for IL-17C was present (not shown) in a similar pattern to psoriasis vulgaris. mRNA levels of IL-17C in lesional, perilesional and unaffected HS tissues were not significantly different from one another. Significant differences were only seen when compared with healthy controls ($p<0.05$) (Figure 12B).

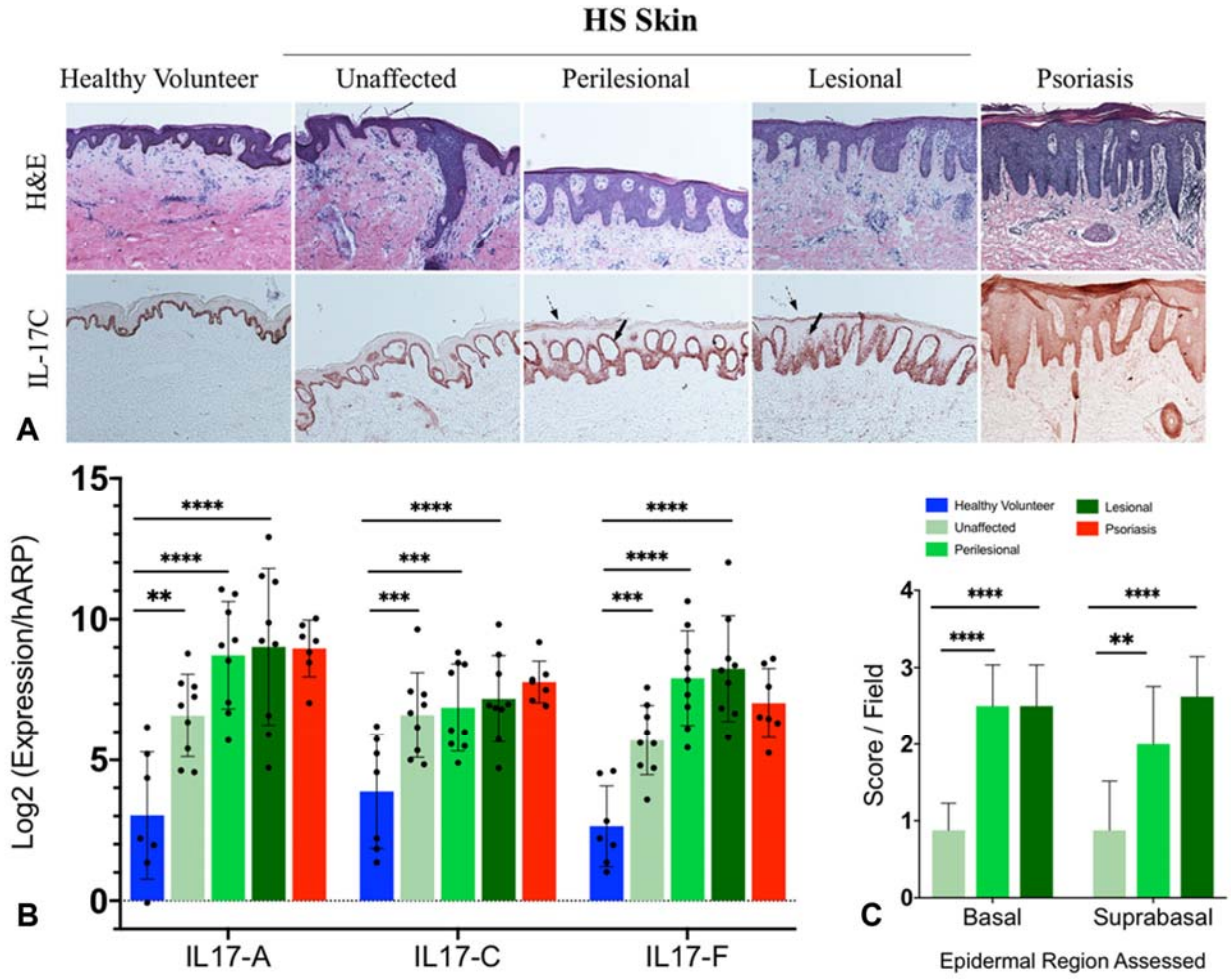

Figure 12: IL-17C is elevated in HS skin.
A) IL-17C localizes to the keratinocytes of psoriasiform epidermal hyperplasia in Hidradenitis Suppurativa by immunohistochemistry with increased IL-17C in suprabasal and granular layer of HS lesional skin. Diffuse dermal and epidermal staining is indicative of IL-17C protein diffusing into the surrounding dermis and epidermis at levels comparable with psoriasis. **B)** mRNA levels of IL-17C are significantly elevated in lesional, perilesional and unaffected skin compared with healthy controls and comparable to the levels seen in psoriasis skin. mRNA elevations of IL-17A and IL-17F are provided for comparison. **C)** Semiquantitative scoring of IL-17C IHC staining identifies statistically significant elevation in perilesional and lesional tissue compared to unaffected tissue. Key: *= $p>0.05$; **= $p<0.01$; ***=$p<0.001$; ****= $p<0.0001$ [97].

3.2.5 LCN2 expression categorizes HS into two subtypes

Since HS has a high heterogeneity in both clinical manifestations and molecular pathways, we sought to identify a biomarker that could cluster HS into molecular subtypes. Given that IL-17 and neutrophilic signature in prominent in HS, we asked whether can use an IL-17-regulated neutrophilic marker to subdivide HS samples into subtypes. A recent study identified increased expression of such marker, Lipocalin-2 (LCN2), in blood and skin of HS patients, with activated granulocytes and to a lesser degree keratinocytes as being the source of LCN2 expression[58]. LCN2 is also as a known biomarker for inflammatory bowel disease, which shares similar pathogenic mechanisms with HS [126, 127]. Given the strong neutrophilic signature in our HS skin samples, we asked if we could use LCN2 expression to identify differing inflammatory subtypes of HS. Unsupervised hierarchical clustering demonstrated that samples cluster based on the level of LCN2 expression in the skin. Lesional and perilesional samples with high LCN2 expression (higher expression than the median) clustered separately and away from lesional and perilesional samples with low LCN2 expression (Figure 13A-D). We validated that samples with high LCN2 mRNA had increased levels of LCN2 protein using immunohistochemistry (Figure 13E). In order to assess whether LCN2 is a unique classifier or a reflection of a more general inflammatory state, we correlated LCN2 levels in lesional skin with clinical markers. There was no significant correlation between lesional tissue LCN2 levels and known markers of clinical inflammation including absolute granulocyte, lymphocyte and neutrophil counts, nodule count, BMI or IHS4 (Figure 14).

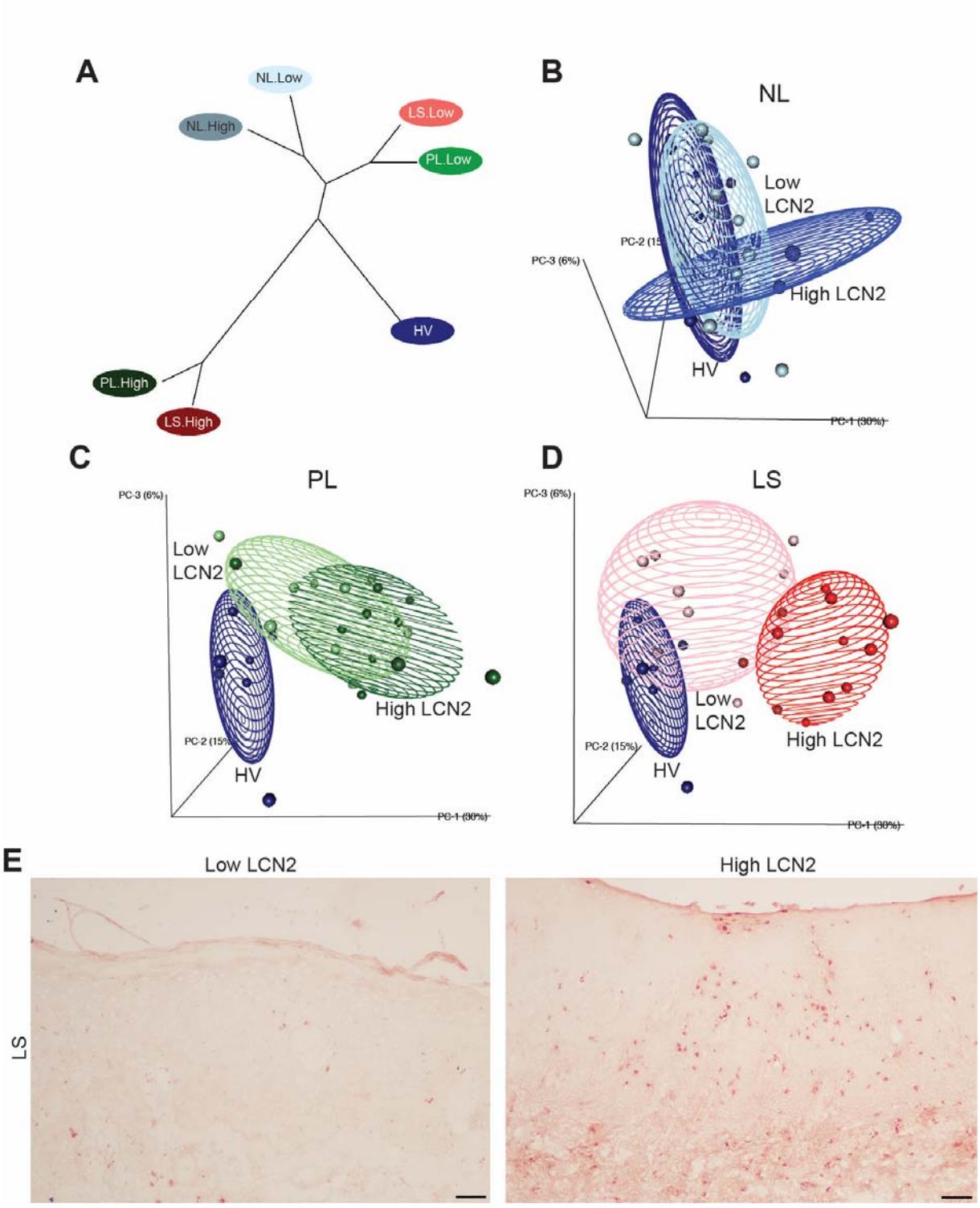

Figure 13: Stratification of HS samples identifies LCN2 high and LCN2 low subgroups. **A)** Unsupervised hierarchical tree clustering demonstrates that samples cluster based on high and low LCN2 levels. PCA demonstrating that HS **B)** nonlesional **C)** perilesional and **D)** lesional skin clusters based on low and high LCN2 levels **E)** validation of LCN2 protein levels in lesional skin by immunohistochemistry. Scale Bar, 100µm.

We then performed a pathway enrichment analysis of the top 50 genes upregulated in LCN2-high samples and identified an enrichment of genes in pathways relating to epidermal biology (keratinocyte differentiation, cornification, epidermis development) and neutrophilic inflammation (antimicrobial humoral immune response mediated by AMP, neutrophil chemotaxis) (Figure 15A-B). In contrast, LCN2-low samples did not have an upregulation of genes involved in these pathways (Figure 15B). Consistent with this, LCN2-high samples showed a higher activation of the IL-17 pathway compared to LCN-2 low samples (Figure 15C). Previous studies have reported IL-17 activation in both HS skin and blood, and LCN2 is an IL-17 regulated factor [42, 97, 128]. We thus asked if there was a correlation between LCN2 expression in skin and IL-17A expression in serum and identified a significant correlation (Figure 16).

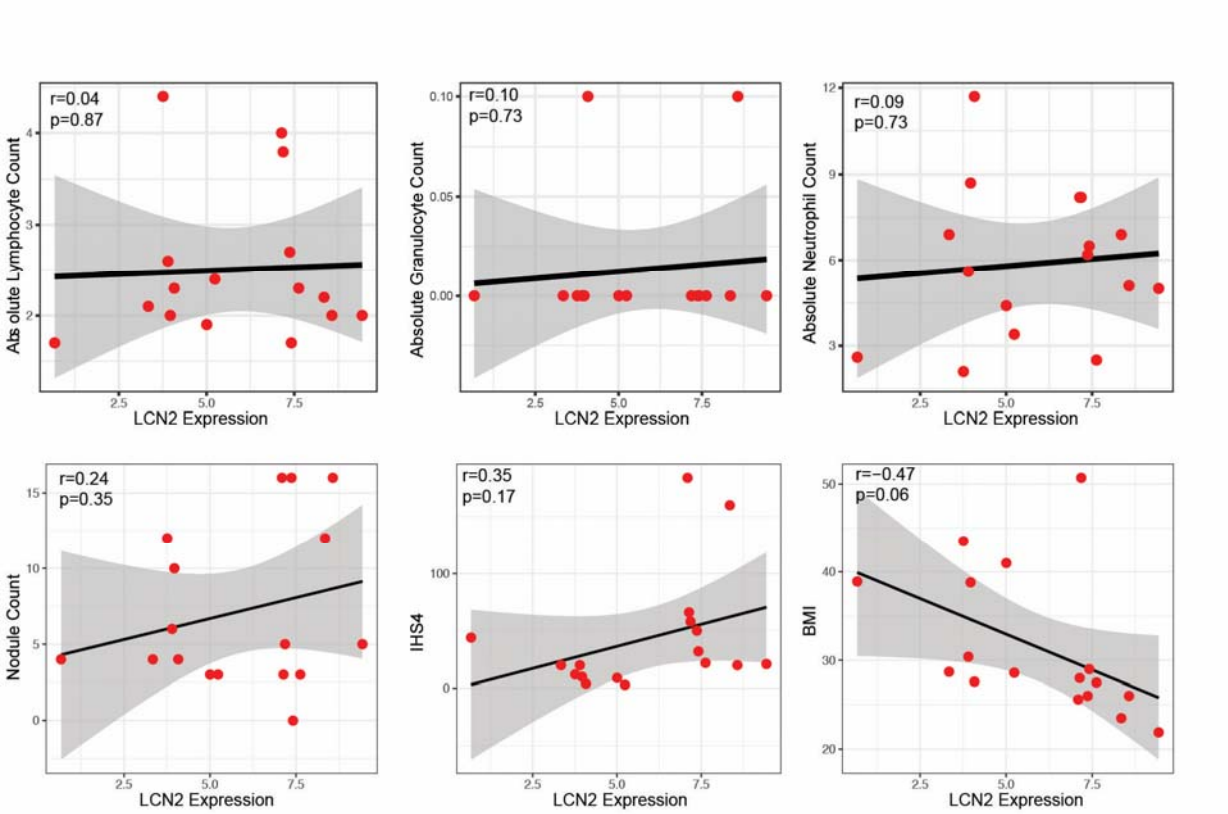

Figure 14: Expression of LCN2 in the skin does not correlate with general inflammation. Correlation of known clinical parameters in skin and blood with lesional skin expression of LCN2. r is Pearson correlation.

Figure 15: IL-17 signaling is enriched in LCN2 high samples.
A) Enrichment for GO-biological processes in the top 50 upregulated genes in LCN2 high samples **B)** Heat map of the top 50 upregulated genes in LCN2 high samples demonstrating clustering of samples based on low and high LCN2 levels. FCH is shown relative to HV **C)** Bubble plot with GSVA scores for known Th-17 pathways demonstrates an activation of the IL-17 pathway in LCN2 high samples. Bubble diameter is proportionate to log FCH of the GSVA score. KC is keratinocyte.

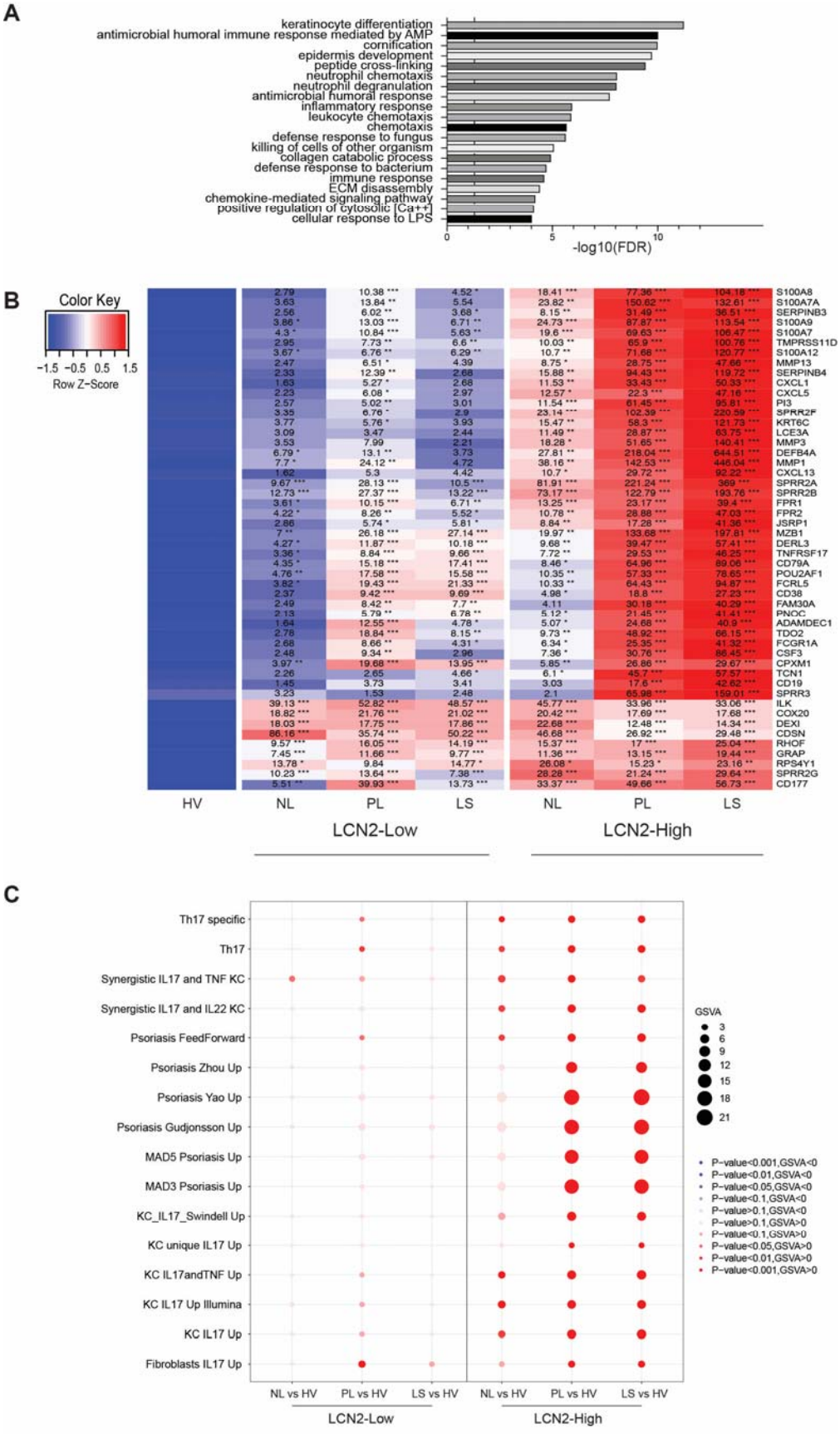
A
keratinocyte differentiation
antimicrobial humoral immune response mediated by AMP
cornification
epidermis development
peptide cross-linking
neutrophil chemotaxis
neutrophil degranulation
antimicrobial humoral response
inflammatory response
leukocyte chemotaxis
chemotaxis
defense response to fungus
killing of cells of other organism
collagen catabolic process
defense response to bacterium
immune response
ECM disassembly
chemokine-mediated signaling pathway
positive regulation of cytosolic [Ca++]
cellular response to LPS
0
5
10
-log10(FDR)
B
Color Key
−1.5 −0.5 0.5 1.5
Row Z-Score
S100A8
S100A7A
SERPINB3
S100A9
S100A7
TMPRSS11D
S100A12
MMP13
SERPINB4
CXCL1
CXCL5
PI3
SPRR2F
KRT6C
LCE3A
MMP3
DEFB4A
MMP1
CXCL13
SPRR2A
SPRR2B
FPR1
FPR2
JSRP1
MZB1
DERL3
TNFRSF17
CD79A
POU2AF1
FCRL5
CD38
FAM30A
PNOC
ADAMDEC1
TDO2
FCGR1A
CSF3
CPXM1
TCN1
CD19
SPRR3
ILK
COX20
DEXI
CDSN
RHOF
GRAP
RPS4Y1
SPRR2G
CD177
HV
NL
PL
LS
NL
PL
LS
LCN2-Low
LCN2-High
C
Th17 specific
Th17
Synergistic IL17 and TNF KC
Synergistic IL17 and IL22 KC
Psoriasis FeedForward
Psoriasis Zhou Up
Psoriasis Yao Up
Psoriasis Gudjonsson Up
MAD5 Psoriasis Up
MAD3 Psoriasis Up
KC_IL17_Swindell Up
KC unique IL17 Up
KC IL17andTNF Up
KC IL17 Up Illumina
KC IL17 Up
Fibroblasts IL17 Up
NL vs HV
PL vs HV
LS vs HV
NL vs HV
PL vs HV
LS vs HV
LCN2-Low
LCN2-High
GSVA
3
6
9
12
15
18
21
P−value<0.001,GSVA<0
P−value<0.01,GSVA<0
P−value<0.05,GSVA<0
P−value<0.1,GSVA<0
P−value>0.1,GSVA<0
P−value>0.1,GSVA>0
P−value<0.1,GSVA>0
P−value<0.05,GSVA>0
P−value<0.01,GSVA>0
P−value<0.001,GSVA>0

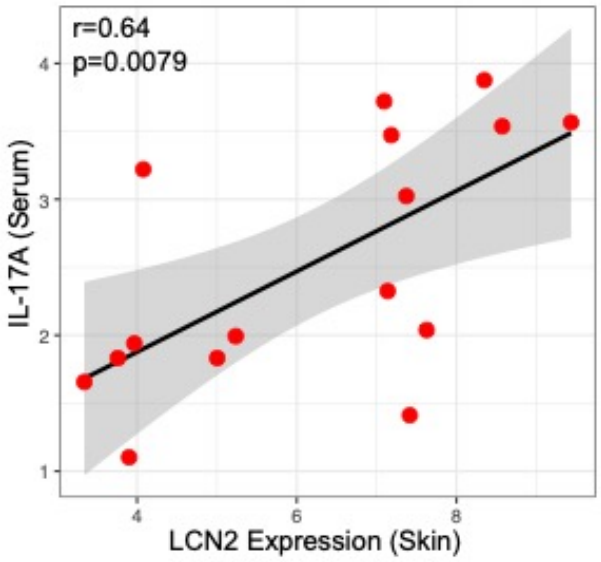

Figure 16: Correlation between LCN2 in skin and IL-17A in serum.
mRNA LCN2 expression (RNA-sequencing) in lesional skin is correlated with LCN2 protein expression (Olink proteomics) in serum. r is Pearson correlation.

3.2.6 Higher LCN2 expression in skin distinguishes a highly inflammatory HS subtype

Genes involved in neutrophil chemotaxis were upregulated in LCN2-high samples compared to LCN2-low samples (Figure 17A). We validated these findings by RT-PCR and found significant differences in neutrophil-related genes (CXCL1, CXCL8, CSF3, NCF2 and DEFB4B) between LCN2-high and low samples. We also identified IL-36 isoforms as more highly expressed in LCN2-high samples. Other markers of inflammation not directly related to neutrophils were also increased in LCN2-high samples. Specifically, markers of general inflammation (INFγ, IL-6, ICOS) were higher in LCN2-high compared to LCN2-low samples. We also found a higher expression of stem cell and cartilage differentiation products (THY1, CILP2) in LCN2-high samples (Figure 17B). Expression of LCN2 in lesional HS skin correlated with expression of other molecular regulators of inflammation and neutrophil biology including IL1B, IL36G, TNF and granulocyte colony-stimulating factor CSF3 (Figure 18).

Figure 17: Differences in inflammatory profiles within HS subtypes.
A) Heatmap of genes involved in the curated GO neutrophilic chemotaxis gene-set between lesional samples with low and high LCN2 levels. FCH relative to HV control skin is shown. *p<0.05, **p<0.01, ***p<0.001 Real-Time PCR of HV, and perilesional/lesional skin with low and high LCN2 levels. Figure error bars show mean ± SEM is shown with *p<0.05, **p<0.01, ***p<0.001 assessing **B)** genes implicated in neutrophilic inflammation, **C)** IL-36 family cytokines, **D)** general inflammation, **E)** keratinocyte and fibroblast markers.

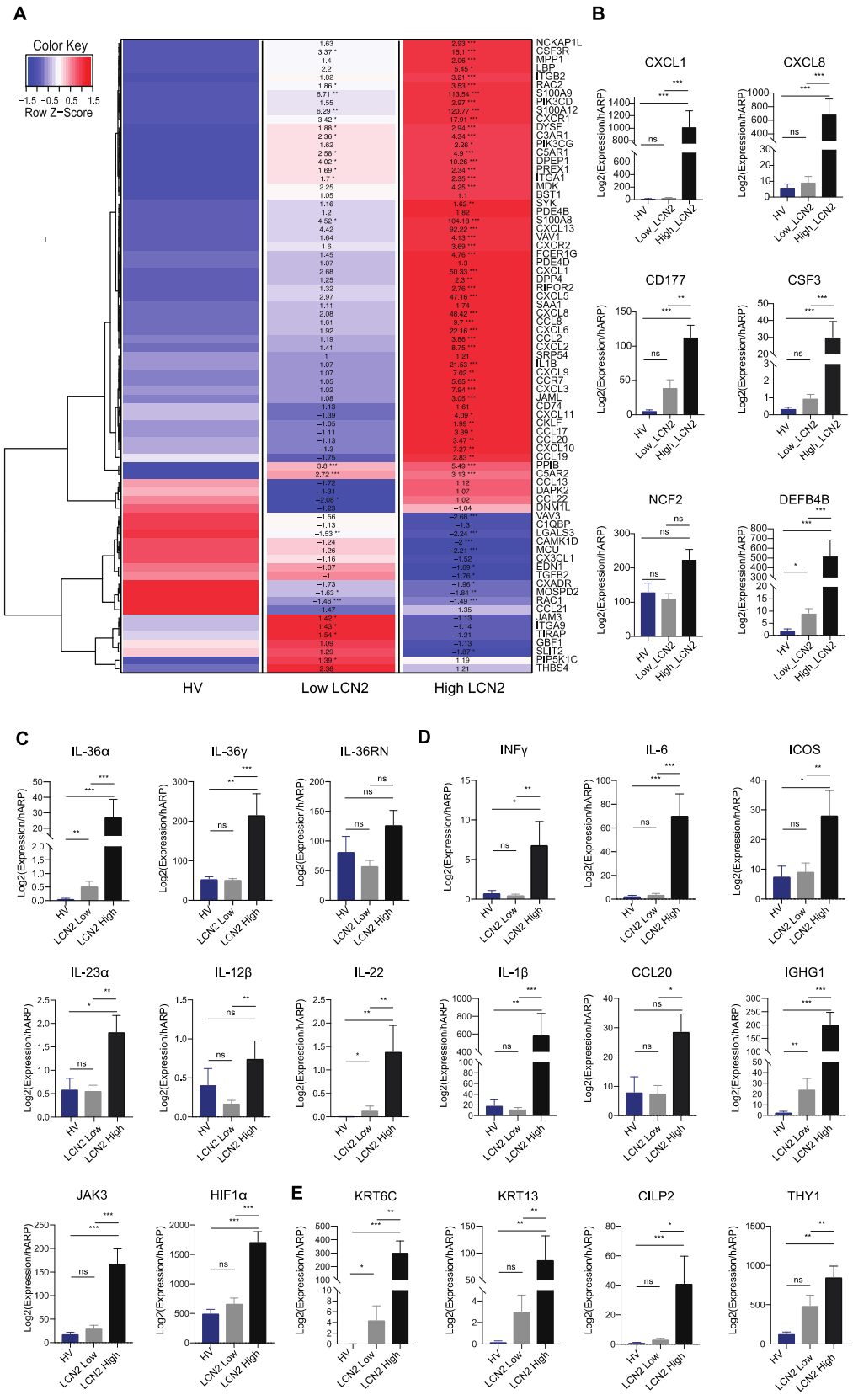
A
Color Key
−1.5 −0.5 0.5 1.5
Row Z−Score
HV
Low LCN2
High LCN2
B
CXCL1
CXCL8
CD177
CSF3
NCF2
DEFB4B
Log2(Expression/hARP)
HV
Low_LCN2
High_LCN2
C
IL-36α
IL-36γ
IL-36RN
IL-23α
IL-12β
IL-22
JAK3
HIF1α
D
INFγ
IL-6
ICOS
IL-1β
CCL20
IGHG1
E
KRT6C
KRT13
CILP2
THY1
HV
LCN2 Low
LCN2 High

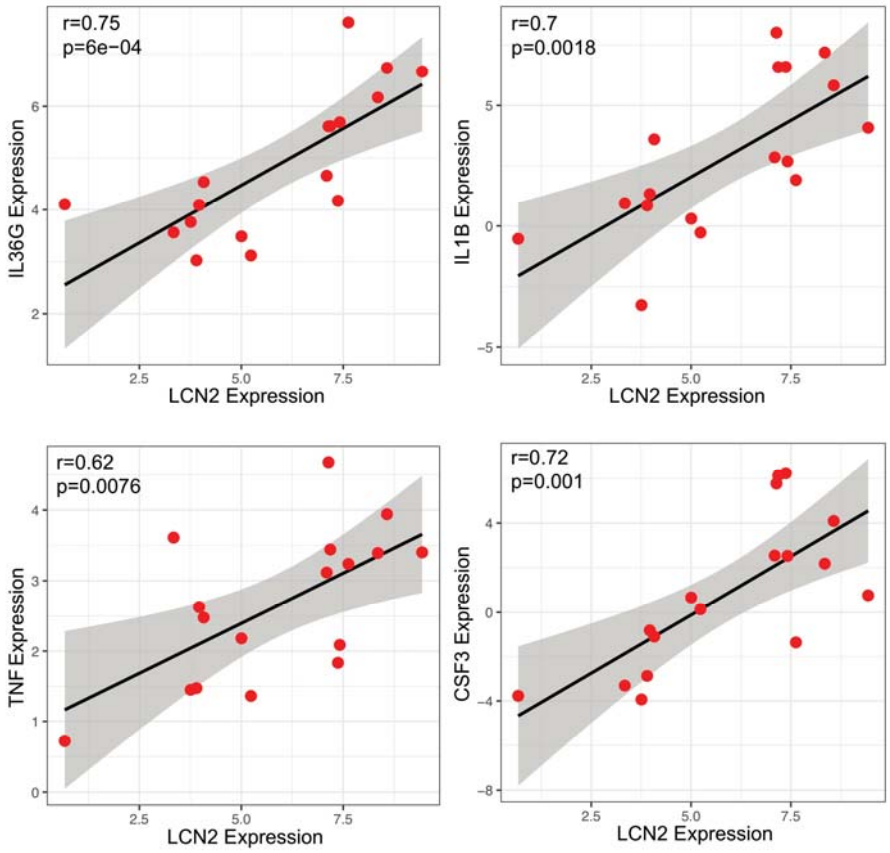

Figure 18: There is significant correlation of LCN2 expression with expression of other inflammatory regulators in HS skin.
Expression of LCN2 in lesional skin versus expression of other inflammatory regulators in lesional skin. r is Pearson correlation.

3.2.7 The proteomic profile of HS and psoriasis skin has an increased inflammatory tone

Whether mRNA transcripts are actively translated into protein in the context of a highly neutrophilic environment has not been evaluated. We thus performed a comparison of the biomarkers in HS skin compared to matched healthy controls and psoriasis samples. Principal component analysis demonstrated that lesional skin in HS and psoriasis clustered separately from nonlesional skin and healthy controls (Figure 19). An overall narrower inflammatory tone was observed in psoriasis compared to HS. Using a criterion of $|FCH| \geq 1.2$ and $p \leq 0.05$, we identified 57 differentially expressed proteins (DEPs) in lesional psoriasis skin and 64 DEPs in lesional HS skin, compared to healthy controls (Figure 20). Lesional skin in both dermatoses showed a significant upregulation of Th1(IL-8, CCL3, CCL4, CXCL9, CXCL10, CXCL11), IL-12/IL-23 (CCL3, CXCL9, TNF, IL-17A, IL12-B), Th17 (CXCL1, CCL20, IL-17A), neutrophil-related (CXCL6, CXCL1, IL-8) and cardiovascular-related (EN-RAGE, OSM, TNF, MMP-1, IL-8) proteins compared to healthy controls. Anti-inflammatory cytokine IL-10, which prevents excessive Th1 response and limits the production of multiple inflammatory cytokines including TNF, IL-6 and IL-1α/β, was significantly decreased in both diseases [129]. Consistent with this, GSVA demonstrated a comparable up-regulation of Th1 and IL-12/IL-23 pathways but higher Th17 and known psoriasis-signatures in psoriasis (Figure 21).

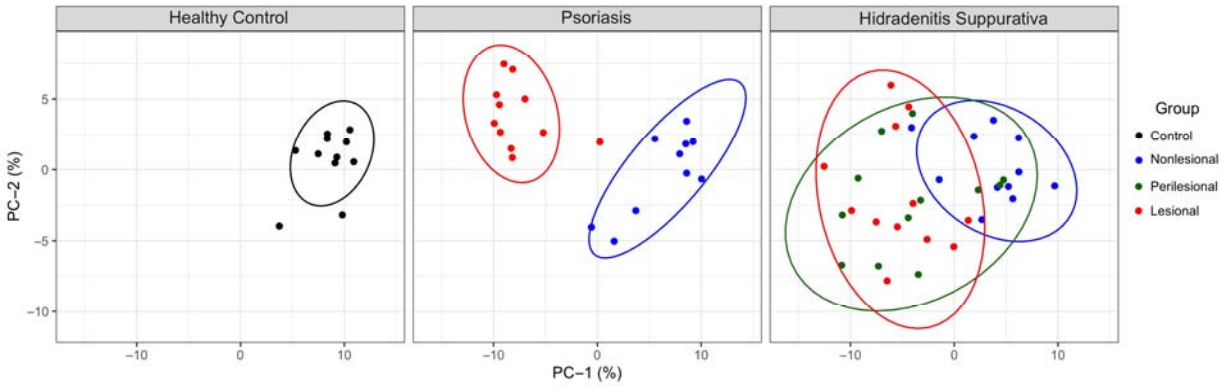

Figure 19: Unique proteome profile of HS and psoriasis skin.
Principal component analysis of psoriasis and Hidradenitis Suppurativa skin compared to healthy controls.

Among proteins uniquely up-regulated in HS were mesenchymal-cell produced Hepatocyte Growth Factor (HGF), which has been shown to play a role in hair follicle growth, re-epithelialization during skin wound healing and induction of epithelial cell migration, and CXCL5, a neutrophil chemoattractant activated by both IL-1 and TNF [130-133]. Both Artemin (ARTN), a member of the glial cell line-derived neutrophilic factor related family which has been reported to be elevated in deep epidermis and dermis and involved in neuropathic and inflammatory pain, and Neutrophin-3 (NT-3), involved in the neuro-immune interface of allergic skin disease and diabetic polyneuropathy skin, were elevated in HS [134, 135 136, 137]. Proteins involved in continued T cell development and activation (CD6), eosinophil recruitment (CCL11) and monocyte recruitment (MCP-1) were also upregulated in HS [138-140].

To better understand how HS inflammation compares to psoriasis, we directly compared HS to psoriasis lesional skin and identified an upregulation of 18 DEPs. In addition to CXCL5 and HGF, we observed a significant upregulation of IL-6 and IL-6 family cytokine Leukemia Inhibitory Factor (LIF). HS had an upregulation of TNF superfamily TNFSF14/LIGHT expressed on immature dendritic cells (DCs), and TWEAK, which has been implicated in chronic inflammation [141-143]. IL-24, expressed by keratinocytes during wound healing, was also elevated in HS. [144, 145]. Psoriasis, on the other hand, showed upregulation of 14 proteins compared to HS, including IL-17 cytokines (IL-17A/C and CCL20), CXCL1, IL-8, IL-12B and IL-20. HS perilesional and lesional skin shared a highly similar proteomic profile. In a direct comparison of lesional to perilesional skin, lesional HS skin had only 1 significantly up- (CXCL1) and 1 down-regulated (TNFSF14) protein.

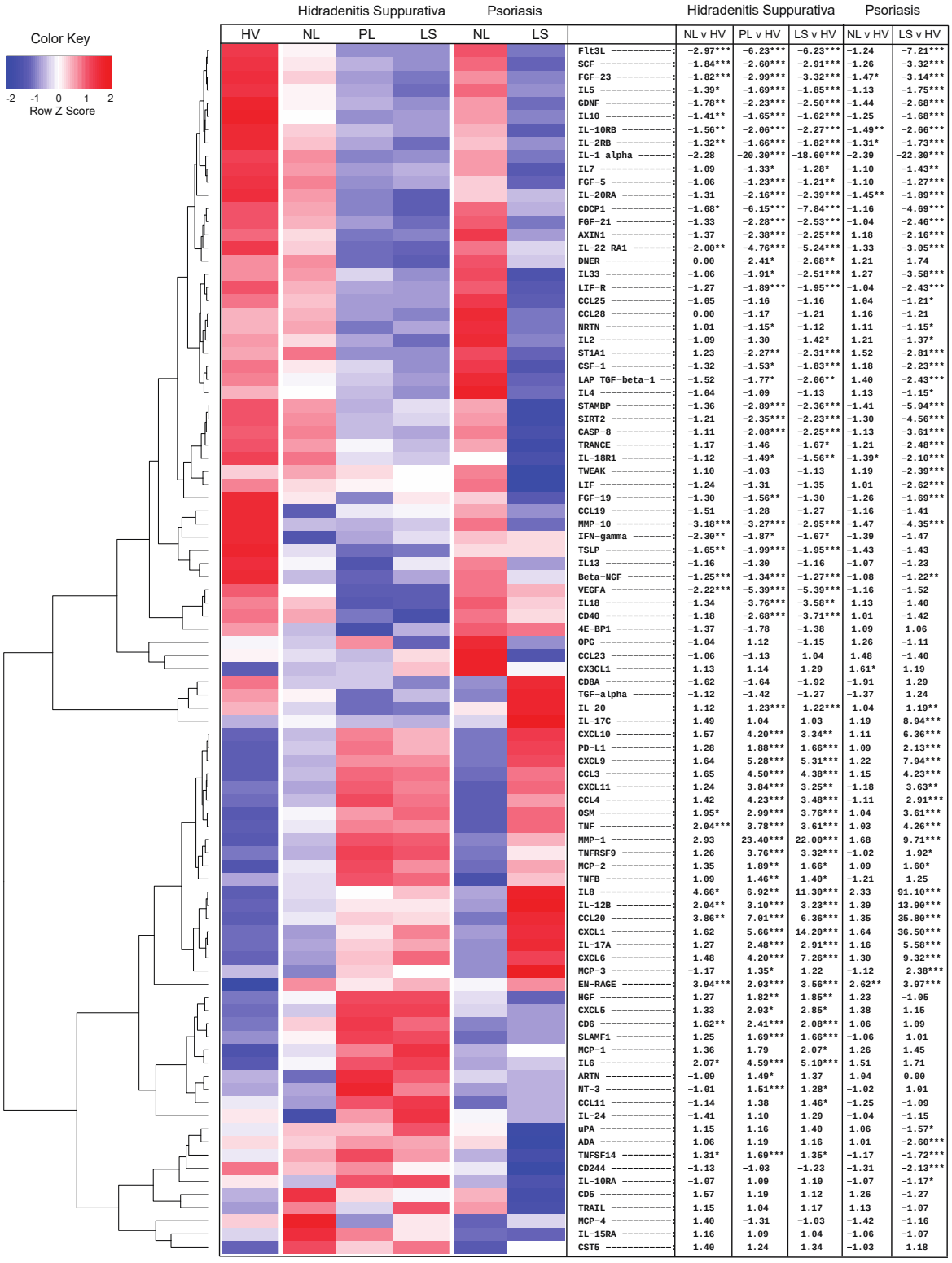

	Hidradenitis Suppurativa			Psoriasis	
	NL v HV	PL v HV	LS v HV	NL v HV	LS v HV
Flt3L	-2.97***	-6.23***	-6.23***	-1.24	-7.21***
SCF	-1.84***	-2.60***	-2.91***	-1.26	-3.32***
FGF-23	-1.82***	-2.99***	-3.32***	-1.47*	-3.14***
IL5	-1.39*	-1.69***	-1.85***	-1.13	-1.75***
GDNF	-1.78**	-2.23***	-2.50***	-1.44	-2.68***
IL10	-1.41**	-1.65***	-1.62***	-1.25	-1.68***
IL-10RB	-1.56**	-2.06***	-2.27***	-1.49**	-2.66***
IL-2RB	-1.32**	-1.66***	-1.82***	-1.31*	-1.73***
IL-1 alpha	-2.28	-20.30***	-18.60***	-2.39	-22.30***
IL7	-1.09	-1.33*	-1.28*	-1.10	-1.43**
FGF-5	-1.06	-1.23***	-1.21**	-1.10	-1.27***
IL-20RA	-1.31	-2.16***	-2.39***	-1.45**	-1.89***
CDCP1	-1.68*	-6.15***	-7.84***	-1.16	-4.69***
FGF-21	-1.33	-2.28***	-2.53***	-1.04	-2.46***
AXIN1	-1.37	-2.38***	-2.25***	1.18	-2.16***
IL-22 RA1	-2.00**	-4.76***	-5.24***	-1.33	-3.05***
DNER	0.00	-2.41*	-2.68**	1.21	-1.74
IL33	-1.06	-1.91*	-2.51***	1.27	-3.58***
LIF-R	-1.27	-1.89***	-1.95***	-1.04	-2.43***
CCL25	-1.05	-1.16	-1.16	1.04	-1.21*
CCL28	0.00	-1.17	-1.21	1.16	-1.21
NRTN	1.01	-1.15*	-1.12	1.11	-1.15*
IL2	-1.09	-1.30	-1.42*	1.21	-1.37*
ST1A1	1.23	-2.27**	-2.31***	1.52	-2.81***
CSF-1	-1.32	-1.53*	-1.83***	1.18	-2.23***
LAP TGF-beta-1	-1.52	-1.77*	-2.06**	1.40	-2.43***
IL4	-1.04	-1.09	-1.13	1.13	-1.15*
STAMBP	-1.36	-2.89***	-2.36***	-1.41	-5.94***
SIRT2	-1.21	-2.35***	-2.23***	-1.30	-4.56***
CASP-8	-1.11	-2.08***	-2.25***	-1.13	-3.61***
TRANCE	-1.17	-1.46	-1.67*	-1.21	-2.48***
IL-18R1	-1.12	-1.49*	-1.56**	-1.39*	-2.10***
TWEAK	1.10	-1.03	-1.13	1.19	-2.39***
LIF	-1.24	-1.31	-1.35	1.01	-2.62***
FGF-19	-1.30	-1.56**	-1.30	-1.26	-1.69***
CCL19	-1.51	-1.28	-1.27	-1.16	-1.41
MMP-10	-3.18***	-3.27***	-2.95***	-1.47	-4.35***
IFN-gamma	-2.30**	-1.87*	-1.67*	-1.39	-1.47
TSLP	-1.65**	-1.99***	-1.95***	-1.43	-1.43
IL13	-1.16	-1.30	-1.16	-1.07	-1.23
Beta-NGF	-1.25***	-1.34***	-1.27***	-1.08	-1.22**
VEGFA	-2.22***	-5.39***	-5.39***	-1.16	-1.52
IL18	-1.34	-3.76***	-3.58**	1.13	-1.40
CD40	-1.18	-2.68***	-3.71***	1.01	-1.42
4E-BP1	-1.37	-1.78	-1.38	1.09	1.06
OPG	-1.04	1.12	-1.15	1.26	-1.11
CCL23	-1.06	-1.13	1.04	1.48	-1.40
CX3CL1	1.13	1.14	1.29	1.61*	1.19
CD8A	-1.62	-1.64	-1.92	-1.91	1.29
TGF-alpha	-1.12	-1.42	-1.27	-1.37	1.24
IL-20	-1.12	-1.23***	-1.22***	-1.04	1.19**
IL-17C	1.49	1.04	1.03	1.19	8.94***
CXCL10	1.57	4.20***	3.34**	1.11	6.36***
PD-L1	1.28	1.88***	1.66***	1.09	2.13***
CXCL9	1.64	5.28***	5.31***	1.22	7.94***
CCL3	1.65	4.50***	4.38***	1.15	4.23***
CXCL11	1.24	3.84***	3.25**	-1.18	3.63**
CCL4	1.42	4.23***	3.48***	-1.11	2.91***
OSM	1.95*	2.99***	3.76***	1.04	3.61***
TNF	2.04***	3.78***	3.61***	1.03	4.26***
MMP-1	2.93	23.40***	22.00***	1.68	9.71***
TNFRSF9	1.26	3.76***	3.32***	-1.02	1.92*
MCP-2	1.35	1.89**	1.66*	1.09	1.60*
TNFB	1.09	1.46**	1.40*	-1.21	1.25
IL8	4.66*	6.92**	11.30***	2.33	91.10***
IL-12B	2.04**	3.10***	3.23***	1.39	13.90***
CCL20	3.86**	7.01***	6.36***	1.35	35.80***
CXCL1	1.62	5.66***	14.20***	1.64	36.50***
IL-17A	1.27	2.48***	2.91***	1.16	5.58***
CXCL6	1.48	4.20***	7.26***	1.30	9.32***
MCP-3	-1.17	1.35*	1.22	-1.12	2.38***
EN-RAGE	3.94***	2.93***	3.56***	2.62**	3.97***
HGF	1.27	1.82**	1.85**	1.23	-1.05
CXCL5	1.33	2.93*	2.85*	1.38	1.15
CD6	1.62**	2.41***	2.08***	1.06	1.09
SLAMF1	1.25	1.69***	1.66***	-1.06	1.01
MCP-1	1.36	1.79	2.07*	1.26	1.45
IL6	2.07*	4.59***	5.10***	1.51	1.71
ARTN	-1.09	1.49*	1.37	1.04	0.00
NT-3	-1.01	1.51***	1.28*	-1.02	1.01
CCL11	-1.14	1.38	1.46*	-1.25	-1.09
IL-24	-1.41	1.10	1.29	-1.04	-1.15
uPA	1.15	1.16	1.40	1.06	-1.57*
ADA	1.06	1.19	1.16	1.01	-2.60***
TNFSF14	1.31*	1.69***	1.35*	-1.17	-1.72***
CD244	-1.13	-1.03	-1.23	-1.31	-2.13***
IL-10RA	-1.07	1.09	1.10	-1.07	-1.17*
CD5	1.57	1.19	1.12	1.26	-1.27
TRAIL	1.15	1.04	1.17	1.13	-1.07
MCP-4	1.40	-1.31	-1.03	-1.42	-1.16
IL-15RA	1.16	1.09	1.04	-1.06	-1.07
CST5	1.40	1.24	1.34	-1.03	1.18

Figure 20: HS skin has an increased inflammatory tone.
Heatmap and corresponding table showing FCH of NL, PL, LS relative to HV skin * ≤0.05 ** ≤0.01 ***≤0.001.

3.2.8 Nonlesional HS skin is more inflamed than nonlesional psoriasis skin

We next compared the proteomic profile of nonlesional skin in HS and psoriasis [146, 147]. Compared to healthy control skin, HS and psoriasis had 25 and 7 DEPs, respectively. Unlike psoriasis nonlesional skin, HS had a significant upregulation of TNF, CCL20, IL-6, IL-8 and IL-12B cytokines. GSVA analysis demonstrated a higher dysregulation of Th17 and IL-12/IL-23 pathways in HS versus psoriasis nonlesional skin (Figure 21).

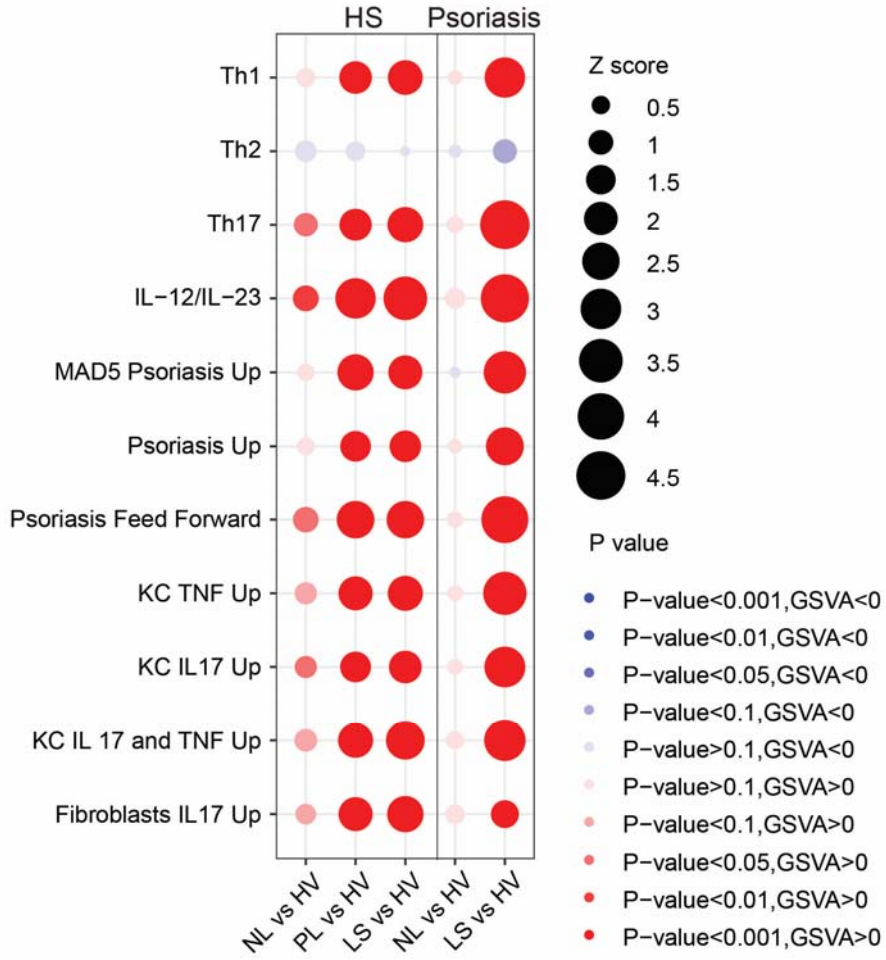

Figure 21: Enrichment of pathways in psoriasis and HS skin.
Bubble plot comparing Gene Set Variation Analysis (GSVA) scores between HS and Psoriasis skin relative to healthy controls. Bubble diameter is proportional to the Z score while the color of the bubble reflects the significance (p value).

3.2.9 mRNA expression and protein levels in HS skin are significantly correlated

Majority of previous studies have focused on the transcriptomic analysis of HS skin however whether these transcripts are actively translated into protein products has not been determined. We therefore assessed whether there was a correlation between mRNA levels and the protein levels in the skin. We first limited the RNA-sequencing (RNA-seq) analysis to only those transcripts that overlapped with the Olink inflammation panel. There was a significant correlation between mRNA and protein levels within lesional skin and perilesional as compared to healthy control skin ($r=0.78$, $p<0.01$, and $r=0.76$, $p<0.01$, respectively) (Figure 22). The correlation between nonlesional skin was also significant but less pronounced ($r=0.58$, $p<0.01$). We note that in both perilesional and lesional HS skin several neutrophil-associated proteins (MMP1, CXCL1, CXCL5, CXCL6, IL-8, S100A12) had a higher mRNA expression compared to protein levels, both relative to healthy controls.

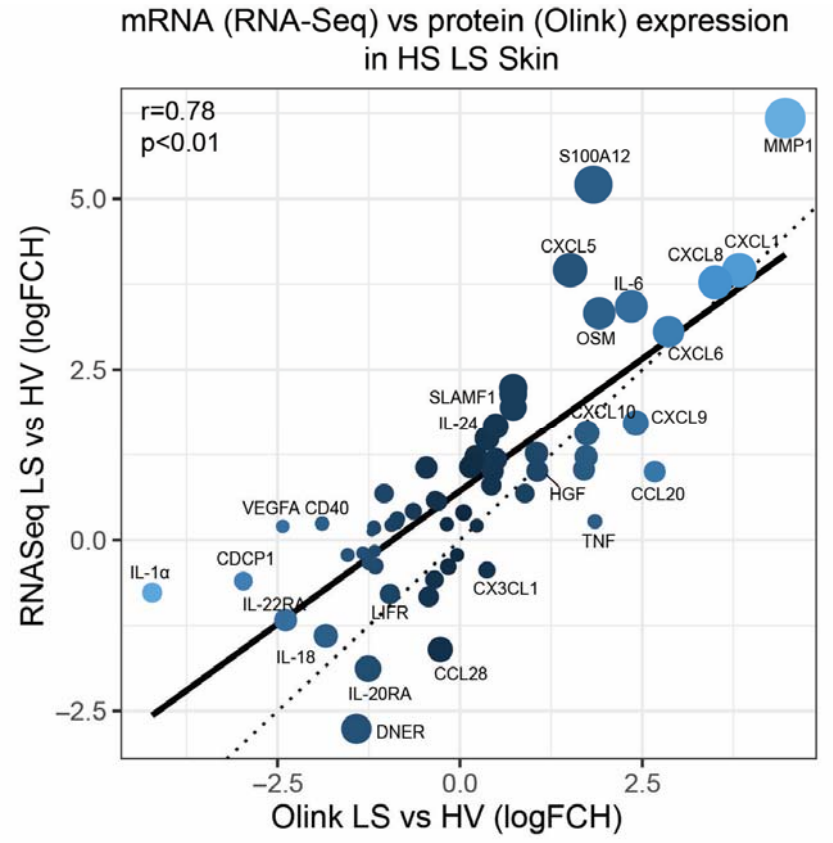

Figure 22: Correlation of mRNA and protein expression in HS lesional skin.
Protein levels (NPX units, Olink) versus gene expression (mRNA, RNA-sequencing) in HS LS compared to HV control skin. The size of the circle depicts the difference in log FCH between HS and HV skin by Olink and RNA-seq. R is Pearson correlation.

3.2.10 Protein expression in the skin is correlated with clinical parameters

We then correlated clinical parameters (absolute granulocyte, lymphocyte, neutrophil counts and IHS4) with protein biomarkers in the skin (Pearson correlation (r) ≥ 0.5 and p value of ≤ 0.1). Lcn2 is not part of the inflammation Olink panel, therefore, we focused on TNF. TNF protein levels in nonlesional (r=0.75, p=0.01), perilesional (r=0.60, p=0.04) and lesional skin (r=0.64, p=0.02) significantly correlated with IHS4 score (Figure 23). TNF levels were not correlated with BMI or other clinical parameters (absolute granulocyte, lymphocyte and neutrophil counts), suggesting that the correlation is specific to clinical severity of HS. In perilesional HS skin, levels of 9 proteins (CXCL10, CXCL11, FGF23, IFNγ, IL-10, SLAMF1, ST1A1, TNF, and TRANCE) correlated with IHS4 score. None of these proteins in the skin correlated with BMI or absolute lymphocyte count. In nonlesional skin, expression of 20 proteins correlated with IHS4. Among these, members of Th1 family (CXCL9, CXCL10 and CXCL11), TNF and IL-17A had a positive correlation with IHS4. In lesional HS skin, only protein levels of TNF had a significant correlation with IHS4 score, likely due to the highly neutrophilic environment and protease associated degradation, which may affect the stability of proteins.

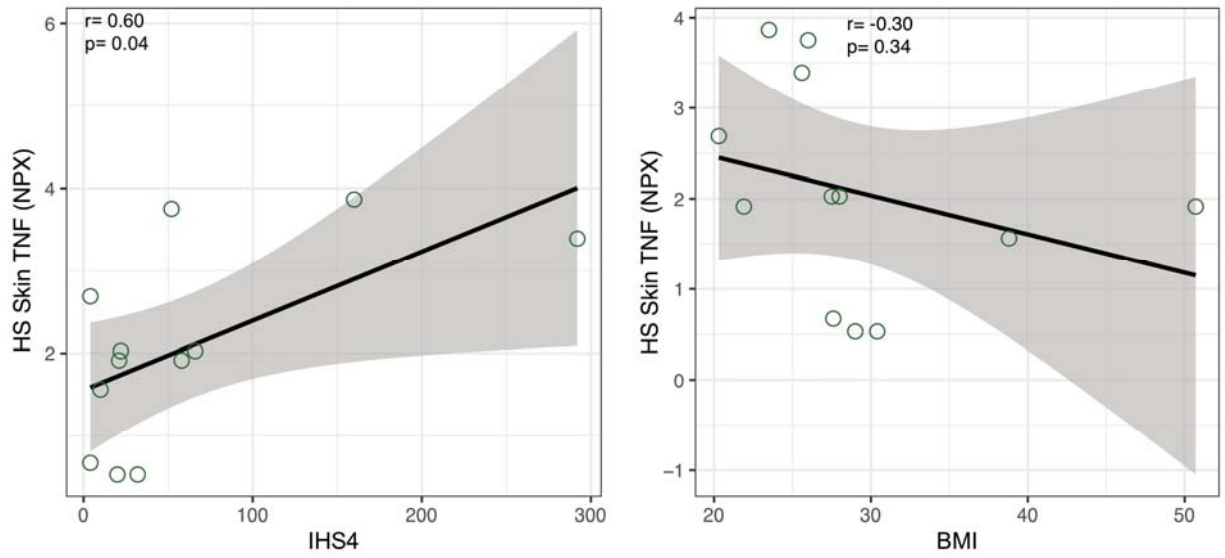

Figure 23: Correlation of clinical parameters with the TNF expression in HS skin.
Correlation of clinical parameters (IHS4 and BMI) and protein expression of TNF in perilesional HS skin. r is Pearson correlation.

3.3 Discussion

The complex pathophysiology of HS remains incompletely understood and is limited by a lack of standardized approaches to study the disease. Recently, we published a consensus report that recommended that molecular studies focus on three anatomical subregions of skin areas affected by HS – lesional, perilesional (2cm distant) and non-lesional (10 cm distant) [86]. Two previous studies have compared lesional and perilesional skin via a series of cellular markers using immunohistochemical approaches, but detailed molecular profiling of these regions has not been compared in paired biopsies [96, 98]. In our study, we assessed lesional, perilesional and non-lesional biopsies from twenty-two active HS patients and compared the molecular profiles in the matched biopsy sets to ten site-matched healthy volunteer controls.

Two other studies have provided extensive disease-associated transcriptomic gene sets in lesional HS biopsies in comparison to either normal skin [101] or non-lesional HS skin [102]. Our analysis of HS lesions is largely consistent with the multi-axis inflammatory pathways identified in the previous transcriptomic studies [101, 102, 104]. How these identified pathways may extend to the larger field of skin around HS lesions is currently unknown. The comparison of gene expression between lesional and perilesional skin is important for understanding pathogenesis and potential treatment targets in HS. Furthermore, characterizing perilesional skin is also relevant to the selection of scoring tools that assess pathological features other than nodules [26 28]. We found extremely high inflammatory profiles in perilesional skin that could not be distinguished from gene expression in lesional skin, with no differentially expressed genes between perilesional and lesional skin, and no significant differences between inflammatory infiltration on histological assessment. This is despite perilesional skin appearing less inflamed (visually healthy appearing) than lesional skin by visual examination. Interestingly, psoriasiform hyperplasia was similarly present in perilesional and lesional skin but a surface appearance did not suggest the presence of psoriasis vulgaris, perhaps due to diffuse disease or occlusion of skin in these regions. Our analysis of perilesional skin demonstrates that there is a large inflammatory area around lesions that extends a large inflammatory burden.

Based on the results of our profiling study, both lesional and perilesional regions have comparable, high-level inflammatory signatures. Consistent with previous reports, we observed increased expression of IFNγ [41, 111], IL-17A and IL-17F [41, 98, 148] , and IL-22 [41] in HS skin. Interesting, lesional and perilesional skin had comparable upregulation of these cytokines, suggesting presence and activation of Type 1, Type 17, and Type 22 T-cell subsets in both lesional and perilesional regions, along with a strong activation of innate cytokine/neutrophilic response axis.

It is understood that apocrine gland rich skin (such as axillary, inguinal and sub-mammary tissues which have predilections to the development of HS) has an increased Th17 signal compared to other body sites[80]. Our use of site matched control skin accounts for this immuno-topographical variation in Th17 activity and highlights the significant elevation of IL-17C even in clinically "unaffected" tissue. IHC staining illustrates the development of a trans-epithelial IL-17C gradient in perilesional and lesional HS tissues compared with unaffected tissues. The presence of such a transepithelial gradient is documented as a potent neutrophil chemoattractant in other conditions including pustular psoriasis [80, 149]. Our results suggest that the supra-basal localization of IL-17C and establishment of a trans-epithelial gradient may be functionally important in the development of clinical disease, as opposed to absolute IL-17C levels in HS tissues; particularly as C/EBP β and

C/EBP σ transcription factors that mediate signaling of IL-17A,C and F isoforms are more concentrated in differentiated keratinocytes of the spinous and granular layers[150].

We present the first identification of IL-17C in HS. Extrapolating from known mechanistic pathways in psoriasis and AD, IL-17C may contribute to the upregulation of other keratinocyte derived cytokines and inflammatory mediators including IL-36y, IL-32, CXCL1, CXCL8 and LCN2. IL-36y is elevated in HS and is highly upregulated in other pustular disorders including generalized pustular psoriasis (GPP)[41, 149].Interactions between IL-17C and IL-36γ are central to the pathogenesis of disease given effect of keratinocyte-derived factors in promoting trans-epithelial neutrophil migration.

Prior work has identified major up-regulation of IL-36 cytokines in lesional HS skin [41, 151, 152]. As shown in our manuscript, the major upregulation of IL-36α and Il-36γ also extends to perilesional regions. These IL-36 cytokines are also highly expressed in psoriasis vulgaris [153, 154] and pustular variants of psoriasis and have been shown to be pathogenic in generalized pustular psoriasis [149, 155]. We speculate that IL-36 isoforms may be essential for neutrophilic inflammation in HS, where IL-36 may be induced through combined actions of IL-1β(upregulated >6 fold) and IL-17A or IL-17F, which are both strongly upregulated in lesional and perilesional HS skin. In turn, activation of IL-36 and IL-17C in keratinocytes [97] likely drive the strong upregulation of CXCL1 and CXCL8 chemokines that promote neutrophil chemotaxis. Of note, we note that IL-17A/F and TNF or IL-1 cytokines also induce these CXCL chemokines and can synergize in this induction [156, 157]. Psoriasiform patterning of the epidermis, first reported in HS lesional skin [37, 96, 158], clearly extends to the perilesional skin area, along with increased proliferation of epidermal keratinocytes, keratin 16 expression and up-regulation of IL-19 and CCL20 cytokines which are also upregulated in psoriasis [159-161]. Another factor that may promote neutrophilic inflammation is CSF3/G-CSF (>17-fold upregulation), which would increase granulopoiesis in the bone marrow. It has been suggested that IL-17 may promote granulopoiesis through CSF3 induction, further contributing to the IL-17/CSF3/LCN2 axis [162-167].

These results highlight the abnormal inflammatory milieu in clinically healthy-appearing perilesional tissue surround HS inflammatory nodules. If perilesional skin is defined as a ring around a lesion (2cm radius), the total surface area affected is >10-times that of lesional skin and thus the total production of cytokines and other inflammatory mediators would dominate in perilesional skin. Biopsy of active lesions in the setting of clinical trials may interfere with quantification of active nodules/abscesses, whereas a biopsy of perilesional skin should not interfere with this measurement. While the main measure of HS severity has been focused on inflammatory nodules (HiSCR), it has been shown that characteristics of HS skin outside of nodular lesions (i.e., tunnels) impacts the therapeutic success with adalimumab, the only approved biologic therapy for HS. [168, 169]. Demonstrating that perilesional biopsies 2cm adjacent to active lesions exhibit no significant difference relative to lesional samples will allow for translational and mechanistic studies to be undertaken in the clinical trial setting without concerns regarding iatrogenic elevation of clinical response rates. Therefore, in the context of biomarker studies in clinical trials of new therapeutics, a biopsy of a perilesional region would provide nearly identical molecular/cellular information to a biopsy of a lesion, but with the advantage that the biopsy would not risk draining a nodule/lesion that is being used to grade disease activity during a treatment phase.

HS is diverse both in its clinical manifestations and molecular heterogeneity marked by upregulation of several inflammatory axes. The stratification of a complex and heterogeneous disease such as HS into discreet disease subtype or endotypes has implications for therapeutic targeting. In this study, LCN2 expression clearly identifies a subtype that is associated with higher cytokine expression and neutrophilic infiltration. To the extent that LCN2 expression is related to high expression of CSF3, higher expression of cytokine and chemokine pathways in both skin and blood, and the further association with increased infiltration of neutrophils into skin, LCN2 expression appears to identify a related neutrophil response axis that might be considered a disease endotype. A key cytokine in the serum correlated with LCN2 expression is IL-17A, suggesting that therapeutic targeting with IL17 antagonists may be best suited for patients with higher LCN2 expression. Furthermore, the LCN2 high subset is correlated with increased expression of CSF3, which is known to stimulate the production and release of granulocytes from the bone marrow and has previously been shown to be elevated in HS skin and might thus explain neutrophilic increases observed in the blood of HS patients[167]. Increases in JAK3 expression is also associated with the LCN2-high subtype, suggesting a possible use of JAK inhibitors in this higher inflammatory phenotype. While our findings suggest a potential HS endotype, further validation in many cohorts is necessary. However, our results provide preliminary insights into the differential inflammatory (and wider transcriptomic) profiles of tissue with varying LCN2 levels in the setting of HS.

Additionally, this is the first study comparing the proteomic profile of nonlesional, perilesional, and lesional HS skin versus psoriasis and healthy controls. One previous study identified 17 proteins upregulated in HS, 14 of which overlapped with the 64 DEPs we identified in our study [170]. However, that study did not detect TNF, or neutrophil-associated (CXCL1, IL-8) proteins that were detected in our analysis. In our study, we extracted proteins directly from frozen tissue and were able to quantify all 92 analytes within the Olink inflammation panel whereas only 75/92 proteins were detected after *ex vivo* tissue culture [170-172]. Other studies of select proteins reported an increased expression of IL-1β, IL-17A, TNF, IL-8, CXCL16 and RANTES in HS skin, consistent with our findings [40, 148, 173, 174].

We demonstrate significant skewing towards Th1 (IL-8, CXCL9, CXCL10, CXCL11) and Th17 (IL-17A, CCL20, CXCL1) in HS, as well as an increase of TNF previously reported by transcriptomic analysis [85, 104, 109, 115]. We also detect neutrophil-related proteins (CXCL5, CXCL6, CXCL1, IL-8). While HS and psoriasis share epidermal features, HS has discernable dermal inflammation and the presence of immunologically active dermal tunnels [99]. We identify novel proteins previously not reported in HS which may reflect tunnel biology. Artemin (ARTN), whose elevated expression in skin has been associated with hyperalgesia and Neutrophin-3 (NT-3), whose levels are increased in skin of patients with diabetic neuropathy, are both elevated in HS [137, 175, 176]. This suggests neuroinflammation might contribute to pain common in HS patients [134, 135 136, 137, 177, 178]. Tunnels are inflammatory-active, epithelialized structures unique to HS, and their development is not well understood [99]. Hepatocyte Growth Factor (HGF) and epithelial-derived IL-24, both elevated in HS skin, are growth factors that might influence formation of epithelialized dermal tunnels [144, 145, 179, 180].

We show that expression of TNF in the skin is significantly correlated with IHS4. The role of TNF as a disease driver is firmly established through antagonism in clinical studies [32, 67, 85, 110, 115]. Previous work has shown that elevations of TNF in HS skin may be correlated with Hurley

staging [40, 85, 115]. We found that TNF protein levels in both skin and blood were significantly correlated with IHS4 but were not correlated with other clinical parameters (BMI, absolute granulocyte, lymphocyte, or neutrophil counts), establishing a direct association with disease activity. While TNF could originate either from innate inflammatory pathways or activated T cells, our data presents evidence that activated polar T cell subsets including Th1 (CXCL9, CXCL10, CXCL11, IFNγ) and Th17 (IL-17A, CXCL1) correlate with disease activity in perilesional and nonlesional skin.

Our findings that inflammation extends to perilesional and nonlesional skin have importance for conceptualizing HS pathogenesis and for adopting scoring systems that incorporate measures beyond inflammatory nodules (currently considered the main "lesion" in affected HS regions). In previous work, we found that perilesional skin may contain deep dermal tunnels with active inflammation despite appearing visually healthy on the surface [181]. This is coupled with intense production of inflammatory transcripts in deep dermis of HS skin, especially skin with tunnels [99]. Therapeutic modulation of dermal inflammation has been demonstrated by Doppler ultrasound and by reduced drainage from surface ostia that are termini of dermal tunnels at the epidermis [62, 99, 181]. The differences in inflammatory gene expression in nonlesional HS skin compared to healthy controls also supports the view of HS pathology as not discreetly localized within the affected regions of the skin. Accordingly, HS might be better characterized as a 'field' disease rather than focused only on localized nodules. This view is reflected in alternative scoring systems such as the IHS4, which considers both inflammatory nodules and draining tunnels/fistulae. Measurement approaches that do not integrate perilesional involvement may provide a limited measurement of disease.

Taken together, we provide data as to the transcriptomic and proteomic characteristics of lesional, perilesional and nonlesional HS skin compared with site-matched healthy controls. In-depth transcriptomic profiling of HS tissue identifies no significant difference between lesional and perilesional tissue, suggesting that the large inflammatory burden extends beyond visible nodule, and directly having implications for tissue sampling in clinical trials. Further investigation into the role of discrete inflammatory endotypes of disease that may identify associations with therapeutic efficacy area are warranted.

CHAPTER 4:
Epithelialized tunnels contribute to inflammation in hidradenitis suppurativa

CHAPTER 4. Epithelialized tunnels contribute to inflammation in hidradenitis suppurativa

4.1 Introduction

Dermal tunnels (also known as sinus tracts or fistulae) are structures unique to HS, and have not been identified in any other inflammatory systemic skin disease [182] . Tunnels cause significant pain and morbidity [1, 183] via chronic, malodorous discharge, and are predictors of poor response to existing medical therapies including Adalimumab [1, 32]. Furthermore, it has been suggested that the presence of tunnels is associated with a more aggressive course of Hurley Stage 3 disease [184] . Tunnels have traditionally been considered an end-stage fibrotic product of dermal inflammation with no known contributions to inflammation in HS [95, 182, 185, 186]. This is despite existing evidence of stratified squamous tunnel epithelium similar to the overlying epidermis [187] and the active inflammatory characteristics of the tunnel-associated Infiltrative Proliferative Gelatinous Mass (IPGM) [188, 189] . The IPGM is an opaque white, reddish or violaceous jelly- like material found in the lumen of HS tunnels, which contains a mixed population of $CD45^+$ inflammatory cells, neutrophils, macrophages and T-helper cells as well as elevations of IL8, IL-16, IL-1α and IL1-β [189] . These features mirror the inflammatory characteristics of the dermal compartment in HS lesions [45] [41] suggesting a role for tunnels as active mediators of inflammation. However, the precise mechanism of IPGM formation, as well as the cellular and molecular characteristics of HS tunnels remain incompletely described and their potential contributions to inflammation in the disease unclear.

Here, we analyze specimens from HS patients with and without tunnels, and report that dermal tunnels contribute to inflammation, and are not just an inactive end-stage feature of the disease. We demonstrate that HS tunnels are associated with increased levels of inflammatory infiltration and proinflammatory cytokines compared to samples without tunnels, and healthy controls. We establish the potential role of tunnels in HS clinical pathology by blocking IL-17 signaling with IL-17RA antagonist, Brodalumab, and demonstrating a decrease in tunnel diameter and drainage.

4.2 Results

4.2.1 Dermal HS tunnels can be clearly identified sonographically and histologically

A total of 22 patients were included in this study, and 9 site-matched healthy volunteer controls. HS lesional skin was examined. Visual assessment of the clinical appearance of tunnels in the gluteal (Figure 24A), axillary (Figure 24B-D) and submammary (Figure 24C) regions; with more severe (Hurley Stage 3 disease: Figure 24B,D) demonstrated hypertrophic scarring and dermal retraction of the superficial skin into linear cords (Figure 24D). Clinically, however, dermal tunnels in HS could only be detected by their superficial ostia in areas of active disease, posing challenges in locating tunnels (white arrows, Figure 24A-D). We therefore elected to utilize sonographic assessment to identify clinically appearing tunnels for biopsies. Under sonographic assessment, parallel hyper echoic linear bands were identified (Figure 24E-H). These appear similar to the hyperechoic linear band of the overlying epidermis and correlate on histology to the presence of stratified squamous epithelial structures in the deep dermis (Figure 24I-L). Histopathologic analysis of affected skin samples by H&E staining demonstrated the presence of deep dermal tunnels (Figure 24I-L).

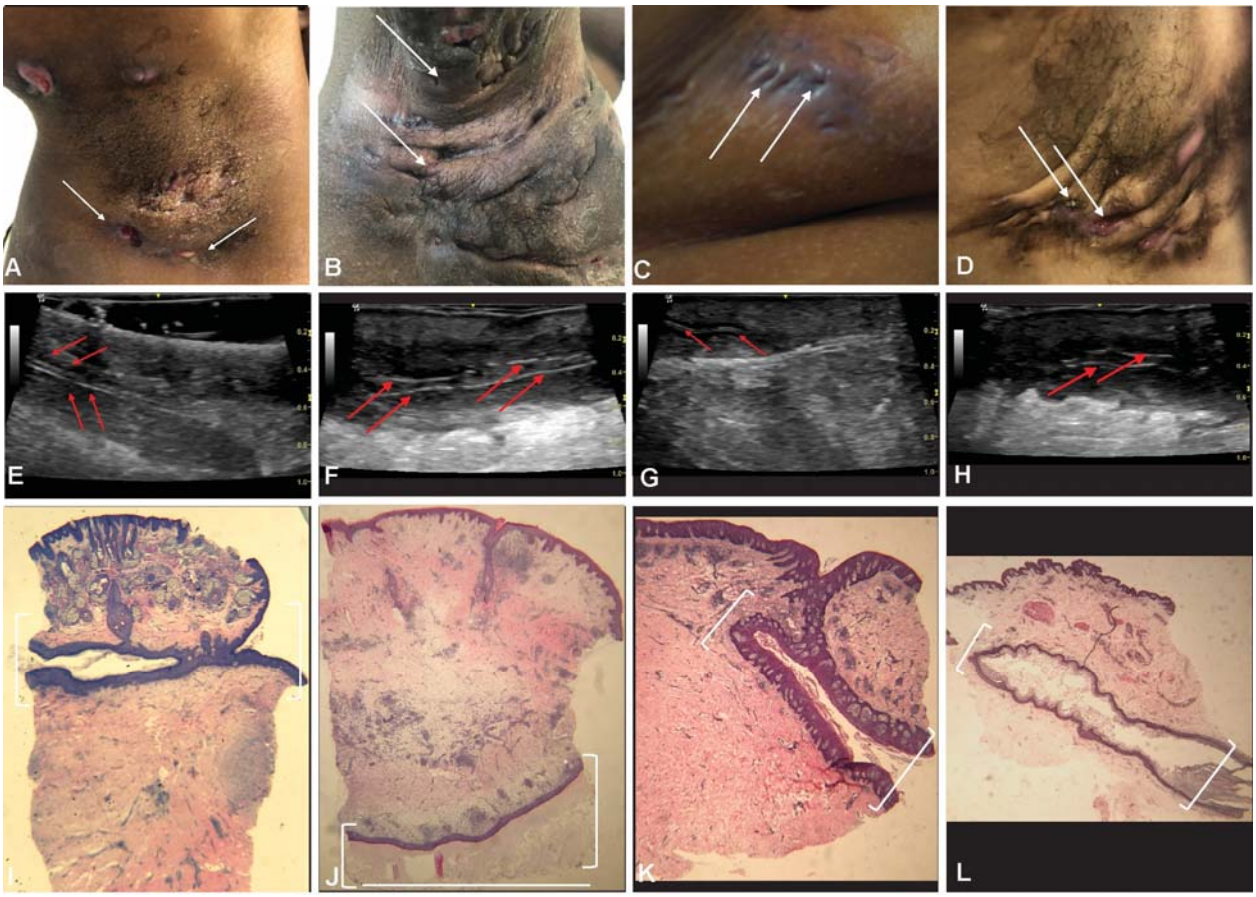

Figure 24: Ultrasonography identifies deep dermal tunnels in HS.
Clinical assessment of tunnels marked by superficial ostia (white arrows) **A)** Axilla **B)** Axilla **C)** Breast **D)** Axilla. **E-H)** Corresponding ultrasound images of tunnels detected by clinical examination. Red arrows highlight the hyperechoic border of the tunnel on ultrasound. **E-H)** Light microscopy of the tunnel (1.2X magnification). White brackets outline the tunnel[99].

4.2.2 The epithelium of dermal tunnels recapitulates the structure of the overlying epidermis.

HS epidermis has been previously characterized histologically by epidermal hyperplasia [37, 45, 97, 158]. Consistent with this, we observed a thickened epithelium with epidermal psoriasiform hyperplasia in HS lesional skin (Figure 25A). Previous studies have shown that tunnels may be lined by squamous epithelium (23). Histological analysis of HS tunnels by H&E staining demonstrated that tunnels are characterized by a contiguous interconnected cylinder of keratinocytes with a central lumen (Figure 25A, "L" denotes Lumen). The more basal portions of the tunnel demonstrate interconnected rete ridges with features similar to the overlying psoriasiform epidermis. Intermittent loss of nuclear hemotoxin staining and the development of a glassy appearance along with an eosin-staining hyperkeratosis was seen in the luminal portions of the epithelium. These features were all suggestive of a keratinocyte-based epithelial structure with progressive differentiation in line with what is seen in the epidermis.

Given that histologically the epidermis of HS samples displayed psoriasiform-like hyperplasia, and that tunnels are epithelial in nature, we compared the immunohistochemical staining of the tunnel epithelium to markers of known positivity in the psoriasiform epidermis and hair follicle keratinocytes (Figure 25). Within the tunnels, basal and suprabasal keratinocytes were discernible but no equivalent of the stratum granulosum or stratum spinosum was evident. Comparison to healthy unaffected skin demonstrated a significant elevation in S100A7 across the luminal third portion of the epidermis comparable to the intense granular layer staining in the overlying psoriasiform epidermis (Figure 25B). Keratin 16 staining was identified throughout the entirety of the tunnel epithelium whereas normal and psoriasiform epidermis had concentration in the basal (and less so suprabasal) keratinocytes (Figure 25C). This indication of ongoing keratinocyte hyperplasia was corroborated by increased Ki67 positive staining in the basal layer of the tunnel epithelia comparable with the overlying psoriasiform epidermis (Figure 25D). Taken together, positive staining to S100A7 (Figure 25B), Keratin 16 (Figure 25C) and Ki67 (Figure 25D) confirmed the epithelial structures to be composed of actively proliferating keratinocytes.

Filaggrin and loricrin, both essential components of the cornification of the epidermis, demonstrated different staining patterns in tunnels compared to overlying epidermis or healthy controls. Filaggrin staining (Figure 25E) was inconsistent but localized to the luminal epithelium with slightly less intensity whereas loricrin staining was in line with staining in the overlying psoriasiform epidermis. (Figure 25F). This suggests an intact keratinocyte differentiation program consistent with differentiation in the overlying epidermis.

We then asked whether tunnels contained other cellular components of skin. Trichohyalin was absent from healthy controls and overlying epidermal keratinocytes but was intermittently positive in the tunnel epithelia (Figure 25G). No evidence of follicular morphology was evident across the sections examined. Melanocytes were identified in the basal layer of HS tunnels by Melan A (Figure 25H) and c-Kit (Figure 25I) as well as dermal mast cells c-Kit (Figure 25H). Intraepithelial melanocyte cell populations were of comparable density to that seen in the overlying psoriasiform epidermis (Figure 25H). Tunnels had increased staining of Lipocalin-2, previously associated as a marker of IL-17 activated keratinocytes (Figure 25J) [58]. These results indicate that the morphological structure of dermal tunnels recapitulate the structure of the overlying psoriasiform epidermis, with the exception of intermittent trichohyalin staining and incomplete intermittent staining of components of the cornified envelope. We termed the morphological characteristics of the tunnels as demonstrating a “pseudo-psoriasiform” pattern reflecting the similarities in the overlying epidermis.

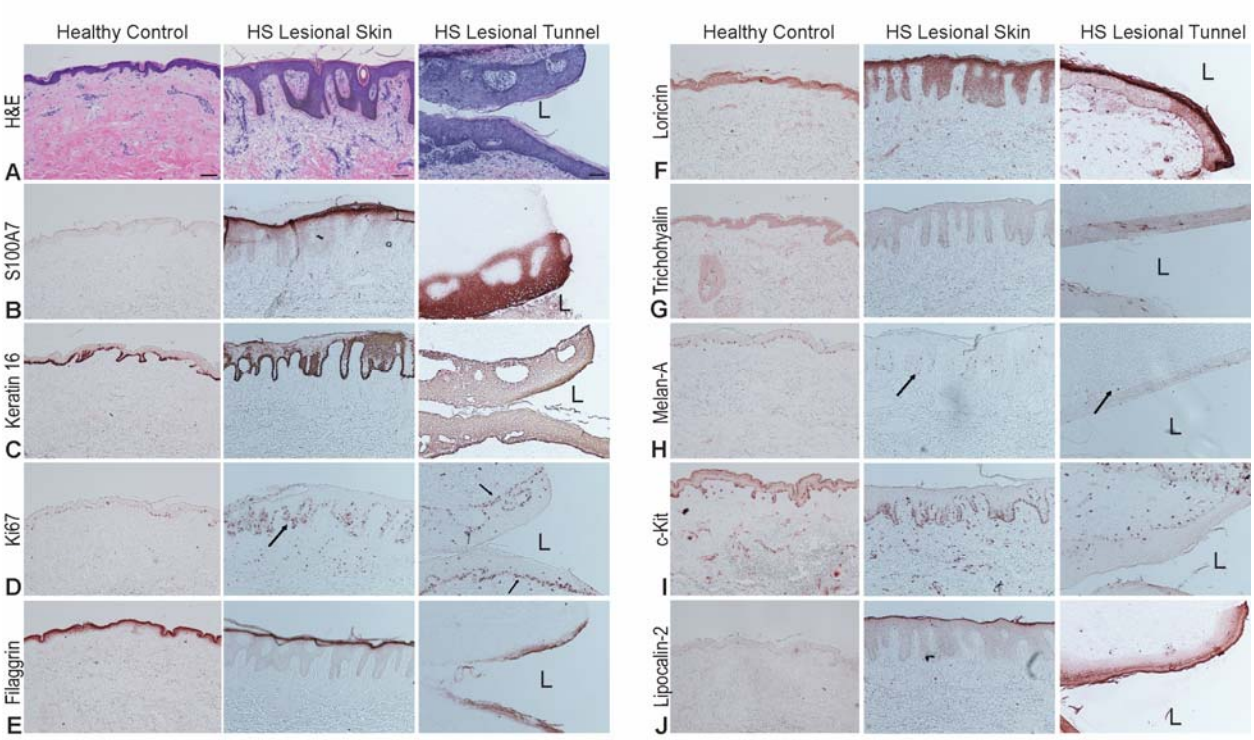

Figure 25: HS tunnels recapitulate the structural properties of the overlying epidermis. Representative biopsies from HS patients and site-matched healthy volunteers stained with **A)** H&E demonstrating prominent psoriasiform lengthening of the rete ridges, thinning of the suprapapillary plate, hyper and parakeratosies as well as reduction of the granular layer in the HS epidermis compared to healthy controls. HS tunnels contain a thick stratified squamous epithelium with increasing differentiation towards the lumen (L). Scale Bar, 100μm **B)** S100A7 positivity **C)** Keratin-16 and **D)** Ki67 identify this epithelium as composed of dividing keratinocytes with increasing differentiation towards the luminal layer compared to the more basal cells (D, black arrows). Differentiation is indicated by filaggrin **E)** and loricrin **F)** staining. Intermittent positive trichohyalin staining **G)** is also observed. Other cell types within the tunnel include melanocytes **H)** with **I)** c-Kit identifying dermal mast cells. **J)** Lipocalin-2 staining is also increased in intensity in the luminal layers of the tunnel epithelium compared to superficial HS epithelium[99].

4.2.3 HS tunnels have increased inflammatory infiltration compared to the overlying epidermis.

Given that histologically, the tunnels recapitulate the structure of the overlying epidermis of HS skin, we asked whether tunnels are also immunologically active. First, we inquired as to whether the normal pro-inflammatory functions of epithelial keratinocytes are also intact in HS tunnels. IL-36γ tract staining was highly positive in the dermal tracts (Figure 26). We then evaluated the potential for inflammatory leukocyte signaling and migration toward epithelialized tunnels in HS. Immunohistochemical analysis demonstrated an increased T cell ($CD3^+$), Dendritic Cell ($CD11c^+$) and Neutrophil (NE^+) infiltration in HS samples compared to site-matched healthy controls (Figure 27A). Clusters of $CD3^+$, $CD11C^+$ and NE^+ cells were evident surrounding dermal cells (Figure 27A). When HS samples were subdivided by the presence or absence of dermal

tunnels (Figure 27B), a significantly greater number of $CD3^+$, $CD11c^+$ and NE^+ cells were present in samples containing tunnels compared to samples without tunnels ($p<0.001$ for $CD3^+$ and $CD11c^+$, and $P<0.05$ for NE^+ cells). We then asked which region of the skin was contributing to the differences in inflammatory infiltration. There was no difference in density of inflammatory infiltrates in the epidermis and superficial dermis, however, there was a statistically significant difference in the density of inflammatory infiltration between the deep dermis and the tunnel ($P<0.001$) (Figure 27C). Staining with CD177 (a neutrophil activation marker) demonstrated recruitment and transmigration of neutrophils towards the tunnel lumen (Figure 26D, width of black triangle depicting gradient). A variable CXCL1 gradient with increasing CXCL1 levels towards the tunnel lumen was observed (width of black triangle indicating the gradient) (Figure 26E). CXCL8 was also positive throughout the tunnel epithelium although the gradient was less well-defined (Figure 26F). It was previously shown that neutrophils are able to form web-like neutrophil extracellular traps (NETs) following exposure to microbes [56, 190-192], and that neutrophils in HS are primed to form NETs [56]. Within the epithelialized tracts, nests of neutrophils were observed, with a dense concentration at the epithelial border of the lumen (Fig. 3D). Consistent with this, we observed a strong infiltration of neutrophils in the tunnel lumen with formation of NETs, marked by strong NE staining (Figure 28). Taken together, these data suggest that the ancillary nidus of inflammatory tissue surrounding the epithelized tunnel has at least an equal inflammatory infiltration than the superficial dermis, which has traditionally been considered the center of inflammation in the disease.

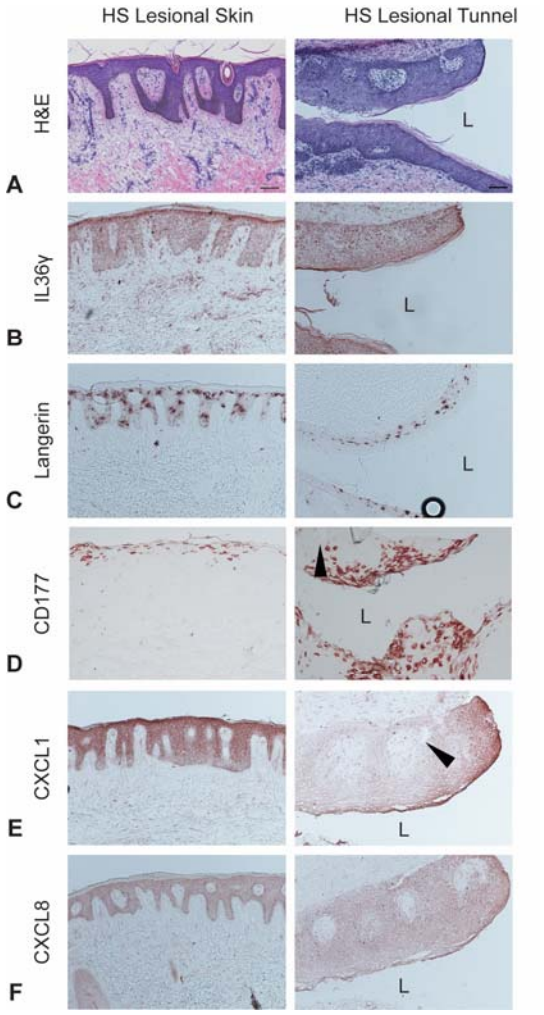

Figure 26: Tunnels recapitulate the inflammatory profile of the overlying epidermis. Representative immunohistochemistry images of HS skin and tunnel **A)** H&E staining shows psoriasiform hyperplasia with elongated bridging retention ridges, hyperkeratosis, parakeratosis and inflammatory infiltrate. "L" denotes lumen. Scale Bar, 10μm **B)** IL-36 γ staining indicates staining the psoriasiform hyperplasia of the epidermis and the epithelium of tunnels with a gradient towards the granular layer of the superficial epidermis. **C)** Increased staining is appreciable at the luminal portion of the tunnel epithelium. Langerin staining highlights the presence of Langerhans cells in the superficial epidermis as well as throughout the tunnel epithelium. **D)** CD177 staining identifies activated neutrophils in the epidermis and surrounding the tunnel. CXCL1 **E)** and CXCL8 **F)** both demonstrate staining in the epidermis and tunnel epithelium with a gradient increasing towards the stratum corner of the epidermis and the luminal portion of the tunnel epithelium. These chemokine gradients support the proposed mechanism of trans epithelial migration of neutrophils across the epidermis-epithelium in HS. Black arrow indicates the gradient of CD177 and CXCL1 positive staining towards the tunnel lumen, with wide end depicting increased positivity [99].

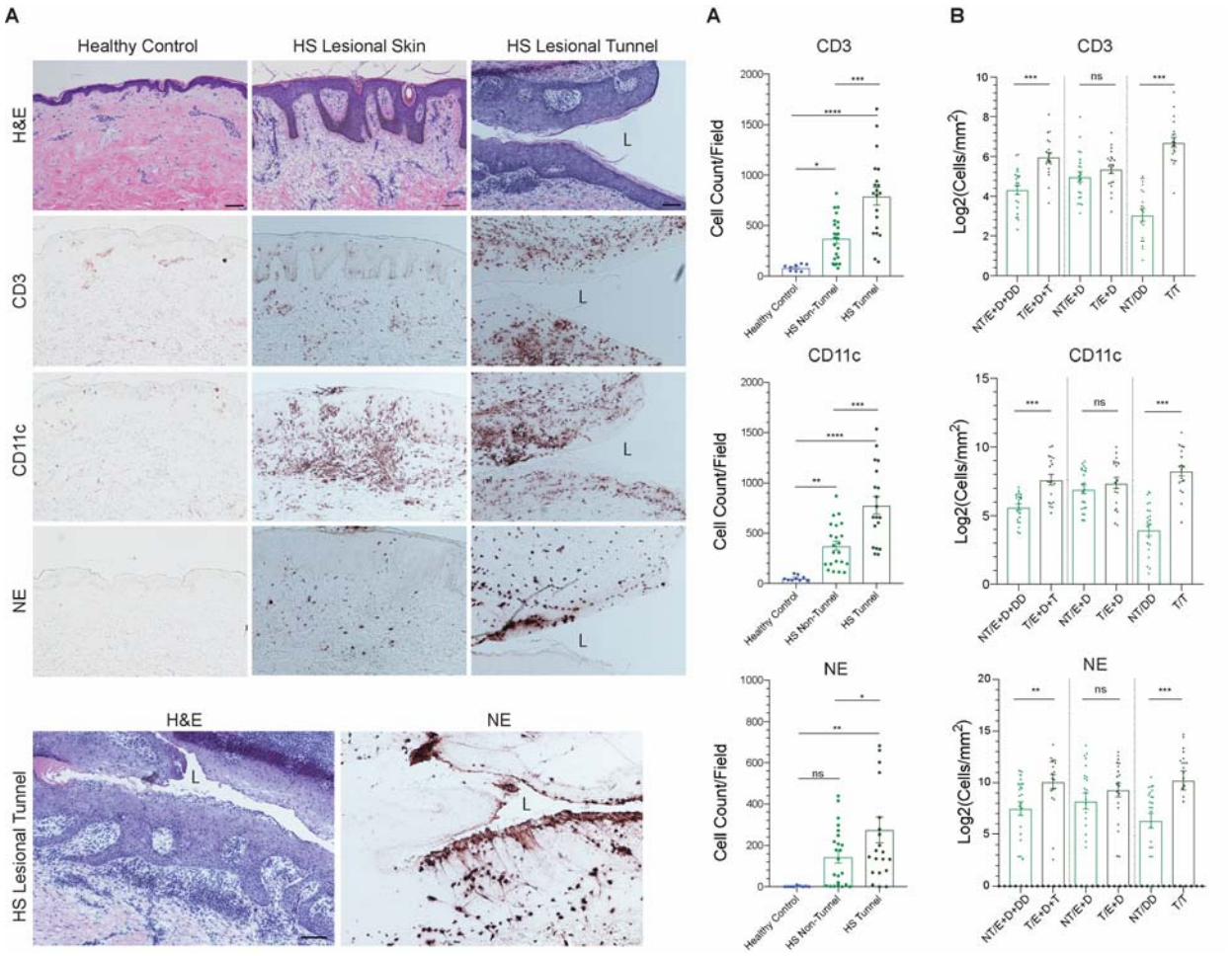

Figure 27: Tunnels are immunologically active.
A) Immunohistochemistry demonstrates increased infiltration of CD3, CD11c, and NE positive cells in HS compared to site-matched healthy controls. Epidermotropism and transepithelial migration towards the tunnels are also observed. Scale Bar, 100μm. "L" denotes lumen. **B)** Quantitative $CD3^+$, $CD11c^+$ and NE^+ cell counts highlight a significant difference in CD3, CD11c and NE positive cells between HS samples with and without tunnels. **C)** Density of CD3, CD11c, and NE positive cellular infiltrate was analyzed within non-tunnel (NT) and tunnel (T) HS specimens stratified by location of cells within the biopsy (E=Epidermis; D=Dermis; T=Tunnel and depth-matched DD=Deep Dermis). There is a significant increase in inflammatory infiltration between tunnel and non-tunnel specimens when the deep dermal component of biopsies is taken into account. No significant elevation of CD3+ CD11c+ and NE+ cell density was seen between the epidermis and the superficial dermis in tunnel and non-tunnel specimens. Results are the mean ± SEM *p<0.05, **p<0.01, ***p<0.001 **D)** Dense clusters of neutrophils undergoing NETosis in the tunnel epithelium adjacent to the lumen (L) [99].

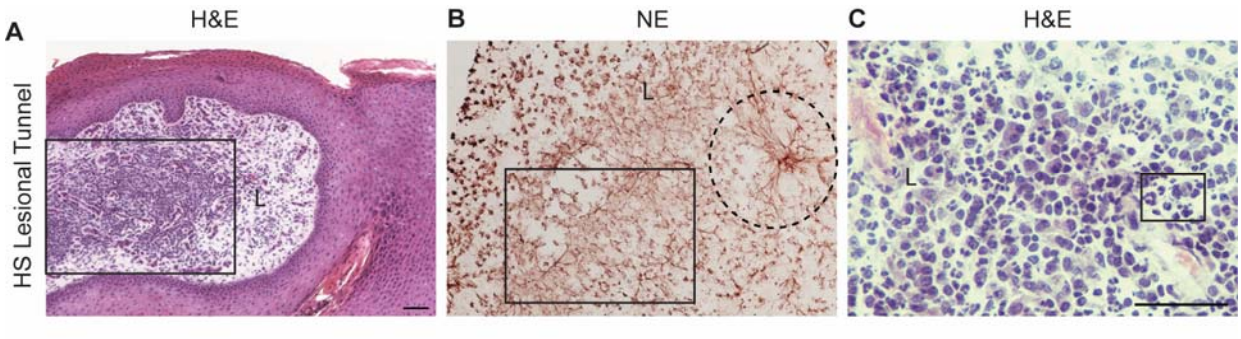

Figure 28: Prominent neutrophilic infiltration in tunnel lumen.
A) Representative H&E staining of HS tunnel and lumen. L denotes lumen. Scale Bar, 100μm. **B)** Neutrophil elastase staining of tunnel lumen demonstrates infiltration of neutrophils with formation of neutrophil NETs (dashed circle). **C)** The infiltration of tunnel lumen contains is predominantly multilobed neutrophils. Scale Bar, 100μm[99].

4.2.4 HS skin clusters based on the presence or absence of dermal tunnels

Having established the pro-inflammatory associations of epithelialized tunnels, we sought to explore the molecular profile of HS tissue by TaqMan Low Density Array (TLDA) analysis. Unsupervised hierarchical clustering demonstrated that HS lesional skin clustered away from HS non-lesional skin, and lesional skin clustered separately based on the presence or absence of epithelialized tunnels on histological sections (Figure 29A). Results are shown as a heatmap, with fold changes (FCH) relative to nonlesional skin (NL) (Figure 29B). Multiple pro-inflammatory factors were upregulated in both tunnel and non-tunnel specimens when compared to non-lesional skin, however the degree of elevation was much more pronounced in tunnel samples then non-tunnel samples (Figure 29B).

Genes that demonstrated a greater upregulation in tunnel compared to non-tunnel samples included keratinocyte-derived factors (S100A7, S100A8, S100A9, LCN2); antimicrobial factors (DEFB4, IL-26); cytokines and chemokines promoting neutrophil chemotaxis (CXCL1, CXCL8), pro inflammatory cytokines (IL1β, GZMB, TNFRSF4, IL6, IL12B, IL36α), neutrophil associated factors (NCF1C, CD177) and B-cell associated cytokines and chemokines (CD79A, TNFRSF13B, IL20). The elevation of keratinocyte derived factors is consistent with the epithelized nature of the tunnels. Anti-inflammatory mediators including IL37, and MIF were downregulated in tunnel specimens compared to non-tunnel specimens. Increased expression of CD38, CD79A, GZMA, HLADOB, IL26, JCHAIN, LCK, S100A9, and TNFRS17 with decreased expression levels of CCL17 and IL37 mRNA were observed as statistically significant between samples with and without tunnels. Taken together, there was a trend towards a greater upregulation of pro-inflammatory genes and decreased expression of anti-inflammatory genes in tunnel specimens compared to non-tunnel specimens. The neutrophilic signature in TLDA associated with tunnel samples was confirmed using RT-PCR on lesional HS tissue (Figure 29C). There was a statistically significant increase in epithelial-derived CXCL1 (40.01-fold) and CXCL8 (46.75-fold), CD177 (activated neutrophil marker, 3.78-fold), CSF3 (driver of increased production of neutrophils, 19.61-fold) (38), DEFB4B (a neutrophil-associated defensin peptide, 33.82-fold), IL-36α (64.09-fold) as well as Keratin 6C (44.54-fold) and Keratin-13 (33.82-fold) in samples with tunnels compared to samples without tunnels (Figure 29C). This data suggests that samples with epithelialized tunnels have a unique inflammatory profile compared to samples without tunnels.

Figure 29: HS samples cluster based on presence of tunnels.
A) Unsupervised hierarchical clustering analysis of TLDA data based on the histological presence of tunnels demonstrates distinct clustering of tunnel and non-tunnel biopsy specimens compared to non lesional tissue **B)** Heatmap of differential gene expression of HS-associated genes in HS Non-Lesional (NL) specimens (n=7), HS samples without tunnels (n=10) and HS samples containing tunnels (n=6), all confirmed by histological presence of tunnel. Results indicate FCH *p<0.05, **p<0.01, ***p<0.001. **C)** Confirmatory RT-PCR of healthy controls (n=4), and actively inflamed HS lesional samples without (n=3), and with tunnels (n=5). Results are the mean ± SEM, FCH is shown. *p<0.05, **p<0.01, ***p<0.001 [99].

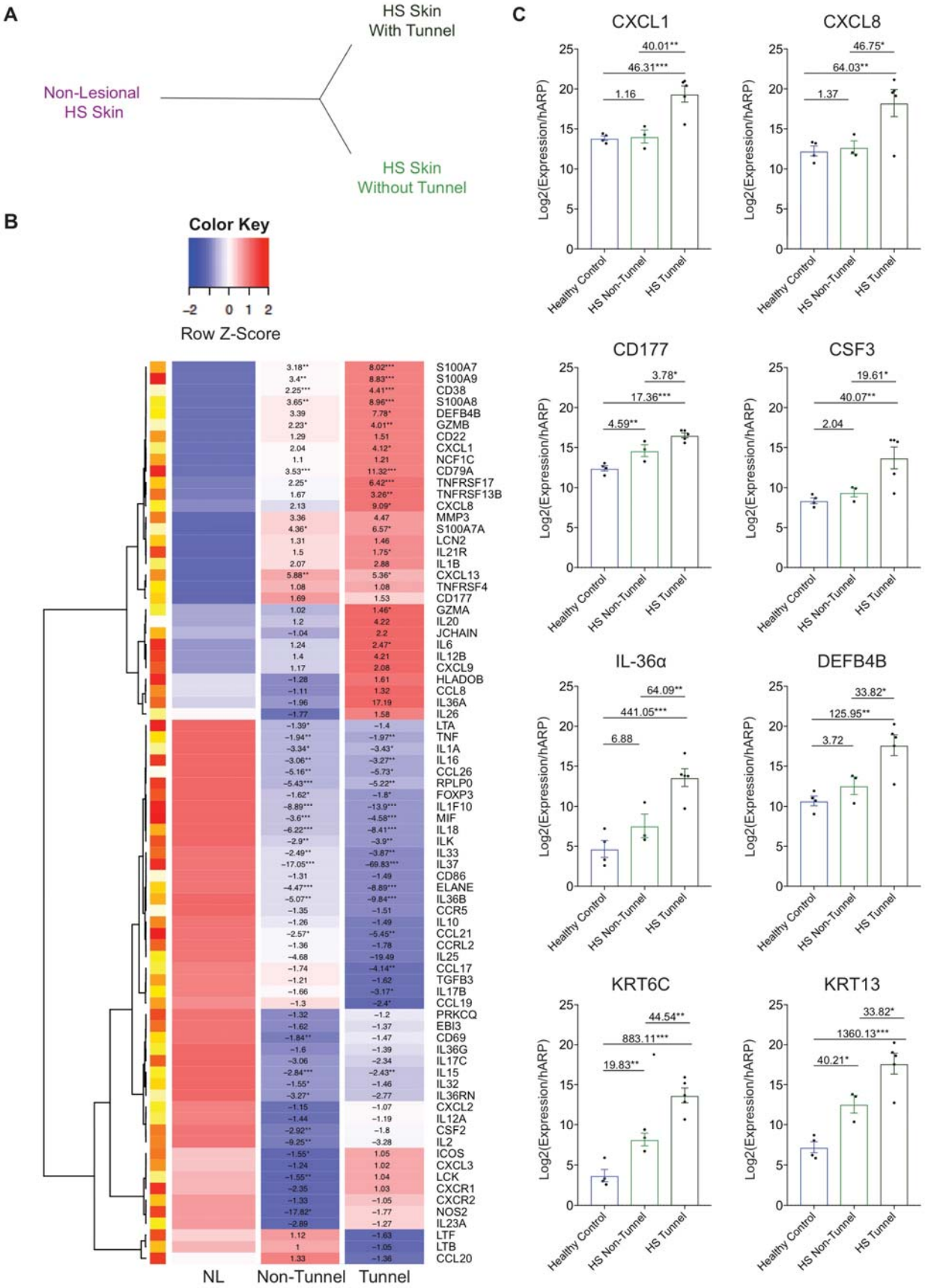
A
HS Skin
With Tunnel
Non-Lesional
HS Skin
HS Skin
Without Tunnel
B
Color Key
−2 0 1 2
Row Z-Score
S100A7
S100A9
CD38
S100A8
DEFB4B
GZMB
CD22
CXCL1
NCF1C
CD79A
TNFRSF17
TNFRSF13B
CXCL8
MMP3
S100A7A
LCN2
IL21R
IL1B
CXCL13
TNFRSF4
CD177
GZMA
IL20
JCHAIN
IL6
IL12B
CXCL9
HLADOB
CCL8
IL36A
IL26
LTA
TNF
IL1A
IL16
CCL26
RPLP0
FOXP3
IL1F10
MIF
IL18
ILK
IL33
IL37
CD86
ELANE
IL36B
CCR5
IL10
CCL21
CCRL2
IL25
CCL17
TGFB3
IL17B
CCL19
PRKCQ
EBI3
CD69
IL36G
IL17C
IL15
IL32
IL36RN
CXCL2
IL12A
CSF2
IL2
ICOS
CXCL3
LCK
CXCR1
CXCR2
NOS2
IL23A
LTF
LTB
CCL20
NL
Non-Tunnel
Tunnel
C
CXCL1
CXCL8
CD177
CSF3
IL-36α
DEFB4B
KRT6C
KRT13
Log2(Expression/hARP)
Healthy Control
HS Non-Tunnel
HS Tunnel

4.2.5 Epithelialized tunnels produce high levels of pro-inflammatory cytokine mRNA

Based on whole-tissue analysis, it is challenging to discern whether the increase in inflammatory profile of samples with tunnels is due direct inflammatory contribution of tunnels, or an indirect pathway of tunnels stimulating the overlying epidermis. To address the relative contributions of epithelialized tunnels and superficial epidermis/dermis towards inflammation in HS tissue, we bisected HS specimens containing tunnels (confirmed histologically) to isolate the superficial epidermis and superficial dermis from the deep dermis and epithelialized tunnels. RT-PCR of HS epidermis (and superficial dermis) and HS Dermis (containing epithelialized tunnels) was performed to assess HS-associated inflammatory cytokines, demonstrating higher levels keratinocyte-derived pro-inflammatory mRNA in HS samples with tunnels compared to healthy controls (Figure 30A). Given the different sizes of tunnels (as evident in Figure 24I-L), we normalized expression values relative to the amount of total RNA extracted (Figure 30B). We detected significant elevations of CXCL8 (27.66-fold), IL-36α (7.4-fold), IL-17A (8.83-fold), IL-17C (4.57-fold), IL-17F (7.93-fold) in HS dermis with tunnels compared to the overlying epidermis (Figure 30B-D). Elevations of IL-17C in both the epidermis and tunnel were confirmed by immunohistochemistry. (Figure 30C). The high levels of inflammatory and epithelial-derived cytokine mRNA detected in both the epidermis and dermal tunnels, as well as increased expression of pro-inflammatory cytokine mRNA in tunnels relative to the epidermis, suggests that tunnels may contribute to inflammation in HS.

Figure 30: Tunnels are active mediators of inflammation in HS.
A) Heatmap of supervised clustering of pro-inflammatory mediators in bisected specimens of HS skin containing healthy controls (n=6), epidermis/superficial dermis (n=8) or deep dermis containing epithelialized tunnels (n=8). Known pro-inflammatory mediators are highest in dermal (tunnel) specimens compared to epidermis/superficial dermis and normal healthy controls. FCH is shown with *p<0.05, **p<0.01, ***p<0.001 relative to healthy controls **B)** RT-PCR demonstrates elevated expression of targetable cytokines in HS dermal tunnels (HS Dermis) compared to the overlying epidermis and healthy controls, relative to the total amount of RNA recovered. There is a significant elevation of cytokines in HS tunnels compared to the overlying epidermis. FCH is shown. **C)** Healthy control epidermis illustrates IL-17C expression only in the basal keratinocytes. The gradient of IL-17C expression (black arrow) in epithelialized dermal tunnels also recapitulates the gradient seen in psoriasiform epithelium, with greatest expression in the basal layer with reduction of expression towards the lumen of tunnels (L). Scale Bar, 100μm. Arrow indicates direction of IL-17C gradient. **D)** Tunnels in HS dermis express IL-17 family cytokines [99].

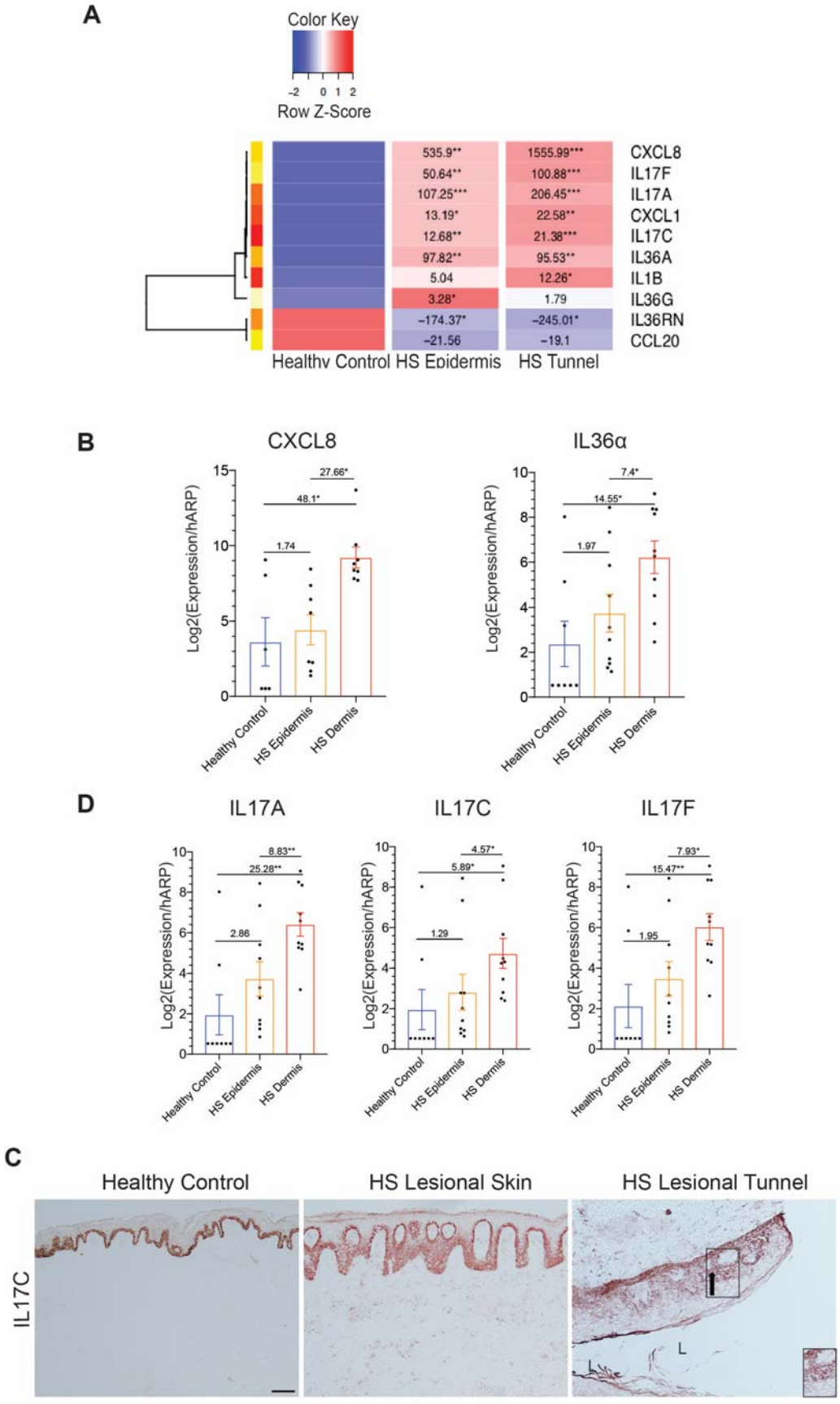
A
Color Key
−2 0 1 2
Row Z-Score
535.9**
50.64**
107.25***
13.19*
12.68**
97.82**
5.04
3.28*
−174.37*
−21.56
1555.99***
100.88***
206.45***
22.58**
21.38***
95.53**
12.26*
1.79
−245.01*
−19.1
CXCL8
IL17F
IL17A
CXCL1
IL17C
IL36A
IL1B
IL36G
IL36RN
CCL20
Healthy Control
HS Epidermis
HS Tunnel
B
CXCL8
IL36α
Log2(Expression/hARP)
27.66*
48.1*
1.74
7.4*
14.55*
1.97
Healthy Control
HS Epidermis
HS Dermis
D
IL17A
IL17C
IL17F
8.83**
25.28**
2.86
4.57*
5.89*
1.29
7.93*
15.47**
1.95
C
Healthy Control
HS Lesional Skin
HS Lesional Tunnel
IL17C
L

4.3 Discussion

Dermal tunnels are structures unique to HS, however, whether they are merely an end-stage feature of the disease or are an active inflammatory component has remained unanswered. We characterize and report that dermal HS tunnels recapitulate the structure of the overlying epidermis. Tunnels are immunologically active and contribute to inflammation in HS. HS samples with tunnels have a distinct molecular profile compared to HS samples without tunnels. By isolating tunnels from the overlying epidermis by microdissection, we demonstrate significantly higher levels of epithelial-derived and pro-inflammatory cytokine mRNA in HS tunnels compared to the overlying epidermis and healthy controls. Furthermore, we show that the HS tunnels are at least in part dependent on IL-17 signaling, with tunnel diameter and drainage clinically decreasing in patients treated with IL17-Receptor A (IL-17RA) antagonist brodalumab.

HS is mediated by a complex milieu of inflammatory pathways and the precise pathogenesis of disease is not understood. The Th17 axis (including IL-17 isoforms) is considered a central feature of inflammation in the disease and has been previously characterized in HS tissues [51, 97]. Cutaneous IL-17 signaling recruits neutrophils and enables their survival as well as producing a myriad of IL-17-induced inflammatory mediators including CXCL chemokines, Lipocalin-2 and cathelicidin [193, 194] (Fig. 2J, Fig. S2D-E). Furthermore, IL-17-derived IL-22 mediates proinflammatory effects upon keratinocytes, leading to epidermal acanthosis and hyperproliferation - features seen in both psoriasis and HS[195].Additionally, apocrine-gland-rich skin, which is a common predilection site for HS, has an enhanced non-inflammatory IL-17 signature, which may partially explain the disease predilection in these anatomical regions[80]. We recently published the first report of IL-17C in HS tissue samples[97]. In this manuscript, demonstrate that epithelialized tunnels also express IL-17C. We show that the abundance of IL-17C and IL-36 in tunnel keratinocytes likely leads to increased expression of proinflammatory cytokines and chemokines including CXCL1 and CXCL8, which are potent neutrophil chemoattractants. The increasing CD177 gradient towards the lumen of the tunnels as well as formation of NETs within tunnel lumen and tunnel wall epithelium further suggests that neutrophils are activated in tunnels and are being actively recruited with transmigration towards the lumen of the tunnels. Furthermore, granulocyte colony-stimulating factor (CSF3) mRNA, a cytokine involved in neutrophil production and release[166], is elevated in tunnel compared to non-tunnel samples, further giving credence to the role of neutrophilic activity in HS tunnel pathogenesis. Given the high levels of IL-17C in pustular psoriasis, and the neutrophilic nature of HS, parallels between the two diseases need to be explored in the future.

Quantitative immunohistochemistry allowed us to assess the association of the mixed inflammatory cellular infiltrates with epithelialized tunnels as compared to the overlying epidermis. HS samples with tunnels demonstrated greater numbers and densities of $CD3^+$ $CD11c^+$ and NE^+ cells with the greatest change in density surrounding the epithelialized tunnels during the process of transepithelial migration. Active NETosis was also seen surrounding these tunnels to a greater degree than the overlying epidermis. The histone scaffolds associated with NETs have been identified as components of the IPGM and thought to be due to the presence of bacterial biofilms in tunnel lumen[56, 189]. Our immunohistochemical findings provide observational evidence to support epithelialized tunnels as the source of the IPGM. The CXCL1 and CXCL8 trans-epithelial gradient in tunnel epithelium may drive the migration of activated neutrophils into the tunnel lumen (Fig. S2D-E, Fig. 5C, Fig. S3-4). This is further supported by neutrophil activation and

transmigration marker, CD177 (Fig. S2D). Additionally, CXCL8 can induce the process of NETosis [56].This trans-epithelial trafficking may occur either in the presence (or absence) of a co-existing luminal biofilm. These results provide a potential mechanism for IPGM development independent of microbial biofilms [196].

Unsupervised hierarchical clustering demonstrated that samples with tunnels clustered separately from samples without tunnels and non-lesional tissue. The molecular signature of tunnels was significantly enhanced for keratinocyte derived inflammatory mediators previously implicated in the pathogenesis of HS including CXCL1, CXCL8, DEFB4B. Additionally, B cell associated factors, (IL-20, JCHAIN) were only significantly upregulated in tunnel biopsies and not non-tunnel biopsies. This supports the results of Byrd *et al* [56] regarding the role of B cells in the disease but identifies that strong B cells signals may only be associated in severe, tunnel-associated disease (which was the subset of disease which Byrd *et al* examined). This differential immunological profile based upon the presence or absence of tunnels in HS may explain the wide variability in tissue cytokine levels seen in the disease [45], as stratification by disease severity and/or morphological structures has not routinely been performed [86].

Our investigations have characterized the structural and immunological characteristics of epithelialized tunnels in HS lesions. Contrary to the previous pathogenic paradigm of the disease, tunnels are not merely inert, fibrotic, end-stage results of chronic inflammation [95] . We have illustrated that epithelialized tunnels recapitulate the structure of the overlying epidermis, containing not only keratinocytes but also melanocytes and Langerhans cells (Fig. 2). Additionally, tunnel epithelium demonstrates pseudo-psoriasiform hyperplasia and presence of a keratinocyte differentiation program similar to that seen in the overlying epidermis (Fig. 2). Positive intermittent trichohyalin staining was one discrepancy seen, which is consistent with previous data of alteration in epithelial and follicular keratinocyte differentiation identified in transcriptomic data [95]. Trichohyalin staining may also be an indicator of the origin of these tunnels given the extruding keratinocyte response seen on the outer root sheath of intact hair follicles [37, 158]. However, other epithelial sources such as eccrine and apocrine glands and ducts would also have the potential to switch cell fate in the same way as cells of the follicular outer root sheath [197-199]. Additionally, it is unclear whether epithelial- mesenchymal transition mechanisms may be involved as part of an aberrant wound healing mechanisms as suggested in transcriptomics data of HS lesions [200]. Further mechanistic enquiry would be necessary in order to faithfully ascertain the source of the cells comprising the tunnel epithelium to answer this question.

The strong Th17 inflammatory signature seen in specimens with epithelialized tunnels (and in the microdissected specimens containing epithelialized tunnels) suggests that tunnels may be involved in a Th17-mediated inflammation in a similar way to superficial epithelium in HS [41, 97] and Psoriasis Vulgaris [201]. This is further supported by the strong CXCL8 signatures in bisected specimens. Although CXCL8 is produced by mononuclear phagocytic cells, as well as fibroblasts and epithelial cells, confirmatory CXCL8 staining identified a positive staining associated with the tunnel epithelium rather than dermal inflammatory cell infiltrates. Importantly, our data demonstrates that HS tunnels may be therapeutically targetable inflammatory structures. Treatment with IL-17RA antagonist Brodalumab, which effectively blocks the activity of all IL-17 isoforms, reduced the draining (as measured by Doppler intensity), wall thickness, and the tunnel diameter in our clinical trial. HS research is hindered by the lack of animal models of HS

and the limitations to *in vitro* approaches to modeling disease [202]. While the limitation of our data is that it cannot discern whether blockade of IL-17 signaling pathway has a direct or an indirect effect on tunnels, this data provides the first insight that tunnels are associated with IL-17 signaling.

Redefining tunnels as immunologically active structures has direct clinical relevance. Here, we demonstrate that that patient samples with dermal tunnels demonstrate significantly greater inflammatory burden than those without dermal tunnels. In a given volume of a biopsy specimen, the epithelialized tunnels produced at least the same amount of pro-inflammatory mediators as the superficial epidermis. Therefore, the presence of tunnels will effectively double the level of inflammation within a defined volume of skin tissue. The presence of tunnels has been recently associated with a significantly decreased odds of achieving clinical response in a re-analysis of the Phase 3 clinical trials of Adalimumab in HS [168]. Our presented data provides a molecular explanation behind this clinical observation of decreased odds of clinical response in the setting of tunnels. Standard dosing of HS therapies may successfully suppress epidermal inflammation (in the absence of tunnels) but may be insufficient for the significantly increased level of inflammation associated with tunnels [168]. Additionally, the Th17 feed-forward inflammatory loop driven by epithelium (both superficial and tunnel-associated) may reduce the likelihood of adequate inflammatory suppression with TNFα blockade alone. It is possible that the response of the subcutaneous nodules to TNFα blockade and not the tunnels suggests that the cellular migration to and across tunnel epithelium is more dependent on IL-17 signaling rather than TNF-a signaling. Changes in inflammation and thickness of the tunnel wall demonstrate that IL-17 pathway blockade may mediate tunnel activity. We previously reported a decrease in the number of total number of nodules and abscesses in response to IL-17RA blockade, suggesting the role of IL-17 signaling in multiple HS manifestations [203]. As surface drainage of pus secretions from tunnel ostia is significantly ablated by Brodalumab treatment [203], this suggests that cellular trafficking into the lumen of dermal tunnels may be a potential mechanism promoting purulent drainage. However, it is unknown whether these tunnels are able to be completely resolved by medical therapy alone. Currently- the opinion is that only surgery can remove these structures due to their epithelialized nature. Given that surgery has a high recurrence rates in HS patients and tends to be disfiguring thus leading to lower quality of life, novel therapies for HS are urgently needed. Furthermore, it has been suggested that HS is a progressive disease, with a diagnostic delay leading to an increased severity at presentation. Our study uncovers a novel avenue for exploring the role of biologic therapy at an earlier stage of disease in order to prevent the progression to a more advanced stage and prior to formation of tunnels [39]. Thus, future clinical trials including HS patients with tunnels are warranted to determine if tunnels are potentially reversible structures.

Our study was limited by the number of patients included (n=22) although this was comparable to other studies in this disease [56]. The study only included clinically advanced HS (Hurley Stage 2 and 3), limiting the results to this patient group. The presented data is unable to answer the question of the origin of the tunnels in HS. Whilst the tunnels recapitulate the structure of the epidermis, including the ability to display psoriasiform hyperplasia, the expression of trichohyalin could suggest a follicular origin. We provide the first evidence of the associated role of IL-17 signaling in tunnel biology, and further studies are necessary to ascertain the role of IL-17 in tunnel development and function.

Taken together, our data demonstrates that the previously uncharacterized dermal tunnels in HS are active mediators of disease pathogenesis. Unsuccessful therapeutic targeting of tunnels may explain the poor response rates to therapy in HS. Blockade of IL-17RA with Brodalumab leads to a clinical decrease in inflammation and size of HS tunnels, suggesting that tunnels may be associated with the IL-17 pathway. Taken together, these data demonstrate a novel avenue for development of therapeutics for this devastating disease.

CHAPTER 5:
Systemic inflammation in hidradenitis suppurativa

CHAPTER 5. Systemic inflammation in hidradenitis suppurativa

5.1 Introduction

Current treatment options for HS have limited efficacy [204], and are hindered by a lack of blood and serum biomarkers for assessment of inflammatory activity and therapeutic response. Several studies have examined the serum proteome to identify potential disease biomarkers, with varying results regarding the abundance of these cytokines and proteins compared to healthy controls [58, 75, 174, 205]. A study assessing the in-depth proteomic profile of HS serum in order to identify biomarkers of disease is lacking.

Multiple studies have utilized the Olink broad proteomic panels to gain molecular insight into disease activity in the serum of inflammatory dermatoses including AD [206, 207], alopecia areata [118] and psoriasis vulgaris, as well as for biomarkers of therapeutic response in psoriasis [208]. In addition to an increase in inflammatory proteins, these studies have identified alterations in cardiovascular biomarkers, consistent with systemic inflammation associated with these disorders. In this study, we aimed to evaluate protein expression in HS serum. A large-scale proteomic study directly comparing systemic alterations in HS and psoriasis has not been performed. We also aimed to broaden the current knowledge by evaluating a comprehensive panel of biomarkers in serum from moderate-to-severe psoriasis and HS patients and healthy controls, utilizing a novel extended Olink platform assessing 1,536 biomarkers.

5.2 Results

5.2.1 The proteomic profile of HS serum is molecularly distinct from healthy controls and other systemic inflammatory dermatoses

Using the Olink proteomic platform, we first assessed the serum proteome of patients with untreated Hurley II and III HS (n=22) and BMI-matched healthy control individuals (n=9) using the inflammation (92 biomarkers), cardiometabolic (92 biomarkers), cardiovascular II (92 biomarkers) and cardiovascular III (92 biomarkers) panels. Principal component analysis (PCA) demonstrated that HS samples clustered separately from healthy volunteers (Figure 31A). Unsupervised two-dimensional hierarchical clustering algorithm was used to group the samples based on differentially expressed proteins (DEPs, defined as FCH $\geq |1.2|$ and $p \leq 0.05$) (Figure 31B). HS serum had a significant increase in neutrophil-related proteins (IL-17A, CXCL1, Cathepsin D), mediators of atherosclerosis (HGF), chemotactic cytokines and receptors (CCL5, IL-4RA) and growth factors (TGF-α, HGF, HB-EGF) (Figure 31B) [209]. HS exhibited elevations of ST2 protein, a biomarker for cardiovascular stress and fibrosis that is a potential predictor for outcomes in patients with heart failure [210]. This finding is consistent with increased risk of cardiovascular complications in patients with HS [211, 212].

Figure 31: HS serum is molecularly distinct from other skin diseases.
A) PCA and **B)** unsupervised hierarchical clustering of all differentially expressed proteins FCH≥|1.2|, and p≤0.05) between HS and HV controls. FCH relative to healthy controls are shown; * $p \leq 0.05$, ** $p \leq 0.01$, *** $p \leq 0.001$. c-Kit-ligand is found in both inflammation and cardiovascular panel. **C)** GO biological process pathway enrichment analysis of differentially expressed proteins in HS relative to HV using the XGR tool. Vertical line is FDR=0.05[213].

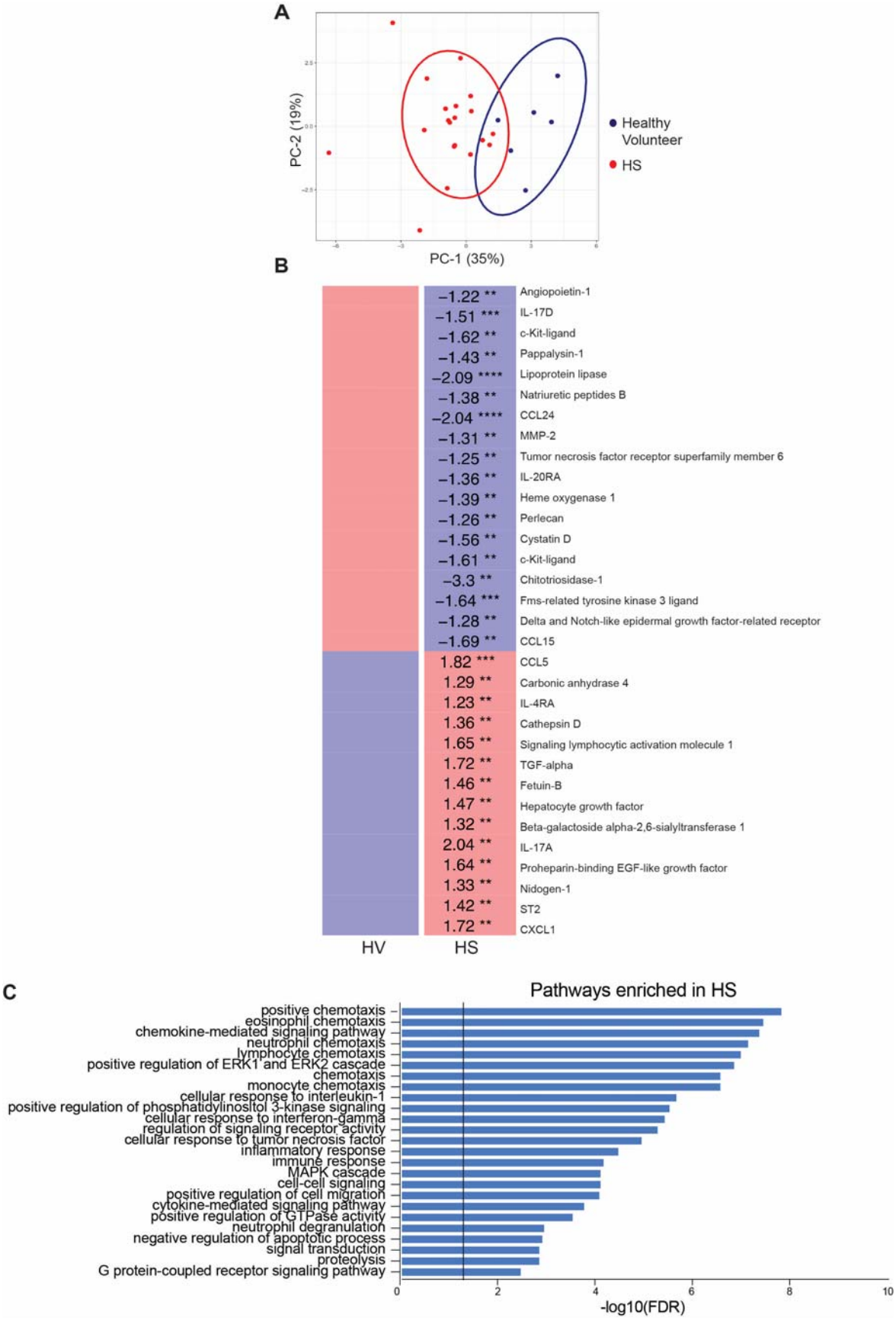
A
PC-2 (19%)
PC-1 (35%)
Healthy Volunteer
HS
B
−1.22 ** Angiopoietin-1
−1.51 *** IL-17D
−1.62 ** c-Kit-ligand
−1.43 ** Pappalysin-1
−2.09 **** Lipoprotein lipase
−1.38 ** Natriuretic peptides B
−2.04 **** CCL24
−1.31 ** MMP-2
−1.25 ** Tumor necrosis factor receptor superfamily member 6
−1.36 ** IL-20RA
−1.39 ** Heme oxygenase 1
−1.26 ** Perlecan
−1.56 ** Cystatin D
−1.61 ** c-Kit-ligand
−3.3 ** Chitotriosidase-1
−1.64 *** Fms-related tyrosine kinase 3 ligand
−1.28 ** Delta and Notch-like epidermal growth factor-related receptor
−1.69 ** CCL15
1.82 *** CCL5
1.29 ** Carbonic anhydrase 4
1.23 ** IL-4RA
1.36 ** Cathepsin D
1.65 ** Signaling lymphocytic activation molecule 1
1.72 ** TGF-alpha
1.46 ** Fetuin-B
1.47 ** Hepatocyte growth factor
1.32 ** Beta-galactoside alpha-2,6-sialyltransferase 1
2.04 ** IL-17A
1.64 ** Proheparin-binding EGF-like growth factor
1.33 ** Nidogen-1
1.42 ** ST2
1.72 ** CXCL1
HV
HS
C
Pathways enriched in HS
positive chemotaxis
eosinophil chemotaxis
chemokine-mediated signaling pathway
neutrophil chemotaxis
lymphocyte chemotaxis
positive regulation of ERK1 and ERK2 cascade
chemotaxis
monocyte chemotaxis
cellular response to interleukin-1
positive regulation of phosphatidylinositol 3-kinase signaling
cellular response to interferon-gamma
regulation of signaling receptor activity
cellular response to tumor necrosis factor
inflammatory response
immune response
MAPK cascade
cell-cell signaling
positive regulation of cell migration
cytokine-mediated signaling pathway
positive regulation of GTPase activity
neutrophil degranulation
negative regulation of apoptotic process
signal transduction
proteolysis
G protein-coupled receptor signaling pathway
0
2
4
6
8
10
-log10(FDR)

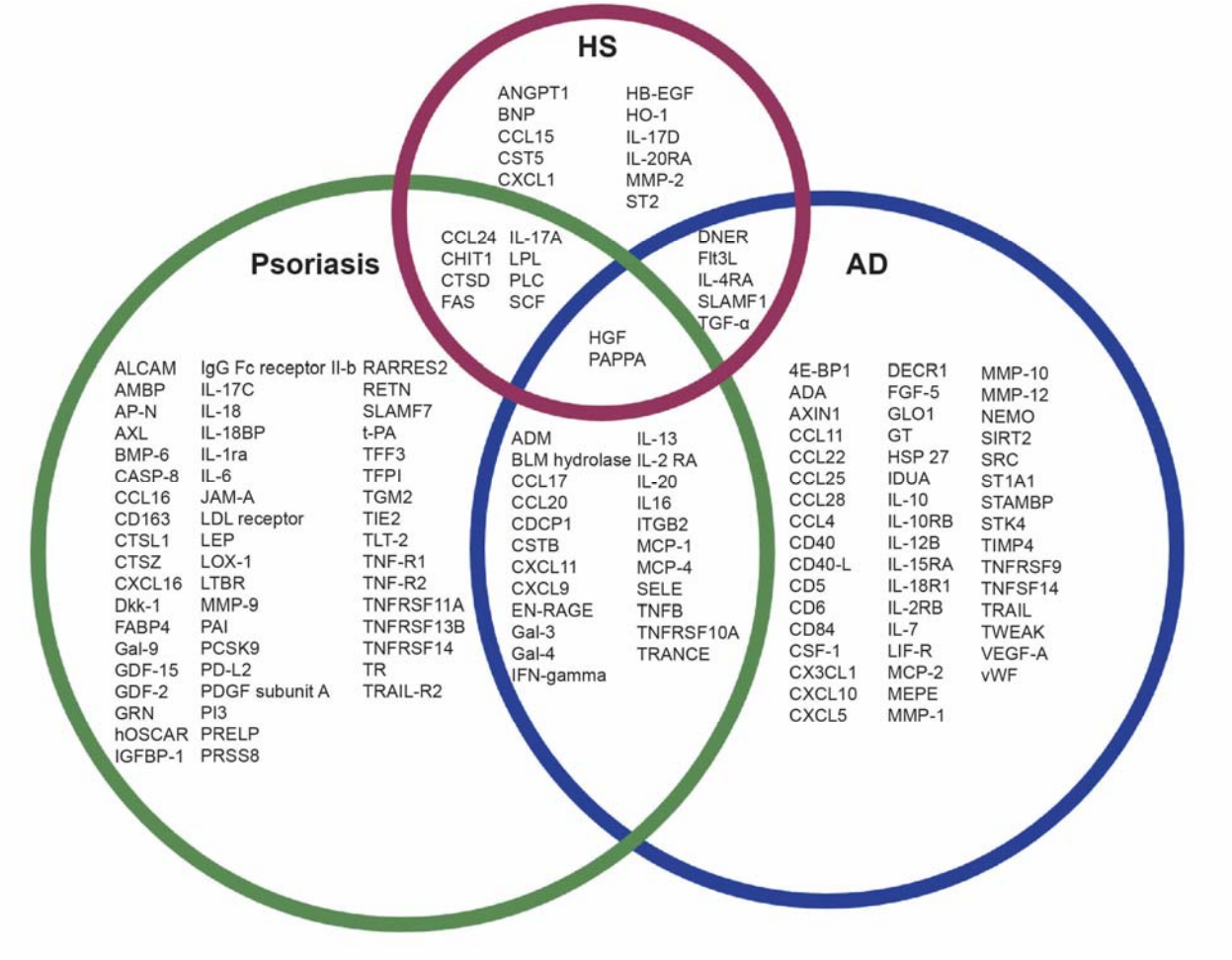

Figure 32: Comparison of serum proteome in HS, psoriasis and AD.
Venn diagram of DEPs (|FCH|≥1.2, p≤0.05) between HS, psoriasis and AD sera [213].

We then conducted an enrichment analysis of DEPs for Gene Ontology (GO) biological processes terms. Pathways that were significantly enriched in the serum of HS patients relative to healthy volunteers are shown in Figure 31C, with the vertical line demonstrating a false discovery rate (FDR) of 0.05. The most significantly enriched pathways were related to general immune response (positive chemotaxis, chemokine-mediated signaling pathway, lymphocyte chemotaxis, immune response, regulation of signaling receptor activity, inflammatory response, signal transduction) and neutrophil-mediated inflammation (neutrophil chemotaxis, neutrophil degranulation). Since the serum contains secreted proteins, we assessed the cellular structures in which the DEPs are localized to function. Protein Analysis Through Evolutionary Relationships (PANTHER) statistical overrepresentation test for GO cellular component terms identified the tertiary granule lumen (p=3.95E-05), specific granule lumen (neutrophil-associated) (p=5.57E-05), and extracellular space (p=9.42E-13) as the cellular locations in which HS-specific proteins functioned [214]. Given that smoking may be associated with HS, we performed a sensitivity analysis to account for smoking status. There were 7 proteins differentially expressed between HS smokers

and nonsmokers (SLAMF7, QPCT, CHIL1, SELE, NCAM1, MB, and SERPINA7). None of these proteins were differentially expressed between HS and healthy control patients regardless of the smoking status.

Since we observed systemic inflammation in HS serum, we compared the HS serum proteome to previously published Olink cardiovascular and inflammation panels in atopic dermatitis (AD) and psoriasis vulgaris [206] using FCH $\geq |1.2|$, and P-value of ≤ 0.05 (Figure 32). All three dermatoses had an up-regulation of mediators involved in atherosclerosis (HGF) [209]. Compared to AD and psoriasis, HS only had 11 unique DEPs. HS was characterized by a significant upregulation of proteins related to neutrophil chemotaxis (CXCL1) and biomarkers of cardiovascular disease (ST2), with downregulation of IL-17D. HS was more akin to psoriasis, with an up-regulation of Th17 pathway (IL-17A), neutrophil-related proteins (IL-17A, Cathepsin D, CCL24). Both HS and AD had an upregulation of growth factors (TGFα) and IL-4 immune signaling (IL4-RA, SLAMF1).

5.2.2 Serum LCN2 expression distinguishes HS subtypes

Lipocalin-2 (LCN2), also known as neutrophil gelatinase-associated lipocalin, has been suggested as a potential biomarker in HS, with reports demonstrating elevated levels of LCN2 in serum of patients with HS and palmoplantar pustular psoriasis (PPP) [57, 58]. LCN2 is a potent chemoattractant for neutrophils, promoting adhesion and extravasation of granulocytes [215]. LCN2 can also be used to measure of inflammation in the context of inflammatory bowel disease [126, 127]. Given the neutrophilic signature of HS serum and the applicability of LCN2 as a biomarker of inflammatory disease, we asked whether LCN2 is elevated in our HS cohort. Unsupervised two-dimensional hierarchical clustering of all samples arranged by LCN2 levels identified two HS subgroups: subset of HS patients with high LCN2 levels and a subset of HS patients with low LCN2 levels which clustered more closely to the controls (Figure 33A). We identified a node of the dendrogram which was associated with increasing levels of LCN2 (black box, Figure 33A). This cluster identifies proteins directly proportional to LCN2 levels in serum, including neutrophil-related proteins (AZU1, MPO, EN-RAGE, DEFA1, CEACAM8, MMP-9, CXCL8) (Figure 33B-C). Phylogenetic tree clustering of all the samples demonstrated two distinct subtypes of HS based on high or low LCN2 levels in the serum (Figure 33D). We then evaluated the clinical and histological parameters associated with the patients in each subgroup. The majority of the patients in the LCN2-high subgroup had histologically diagnosed dermal HS tunnels (based on ultrasound examination of HS skin as well as the presence of a visible tunnel on the histological assessment of the biopsy), compared to the LCN2-low subgroup, in which patients did not have histologically diagnosed tunnels. Since the criteria of histologically confirmed dermal tunnels was used, it is plausible that a patient may have had a tunnel that was missed by the punch biopsy, thus explaining the two outliers in the cohort (Figure 33D).

Figure 33: Serum LCN2 levels differentiate HS into two subgroups.
A) Unsupervised hierarchical clustering of all proteins in HS and HV control serum arranged by increasing levels of LCN2 in the serum. Red indicates upregulated and blue indicates downregulated protein expression levels. Blue circle demonstrates node of interest on the dendrogram with black box identifying a cluster of proteins that are directly proportional with LCN2 levels **b)** Magnification of the LCN2-related cluster of proteins identifies a clear demarcation of two HS sub-groups based on protein level of LCN2 in serum **c)** Pearson's correlation between LCN2 protein levels and levels of other neutrophil-related proteins in serum is shown. r is Pearson correlation. **d)** High LCN2 sub-group consists of patients with histologically diagnosed tunnels, which cluster separately and away from patients without tunnels and low LCN2 levels [213].

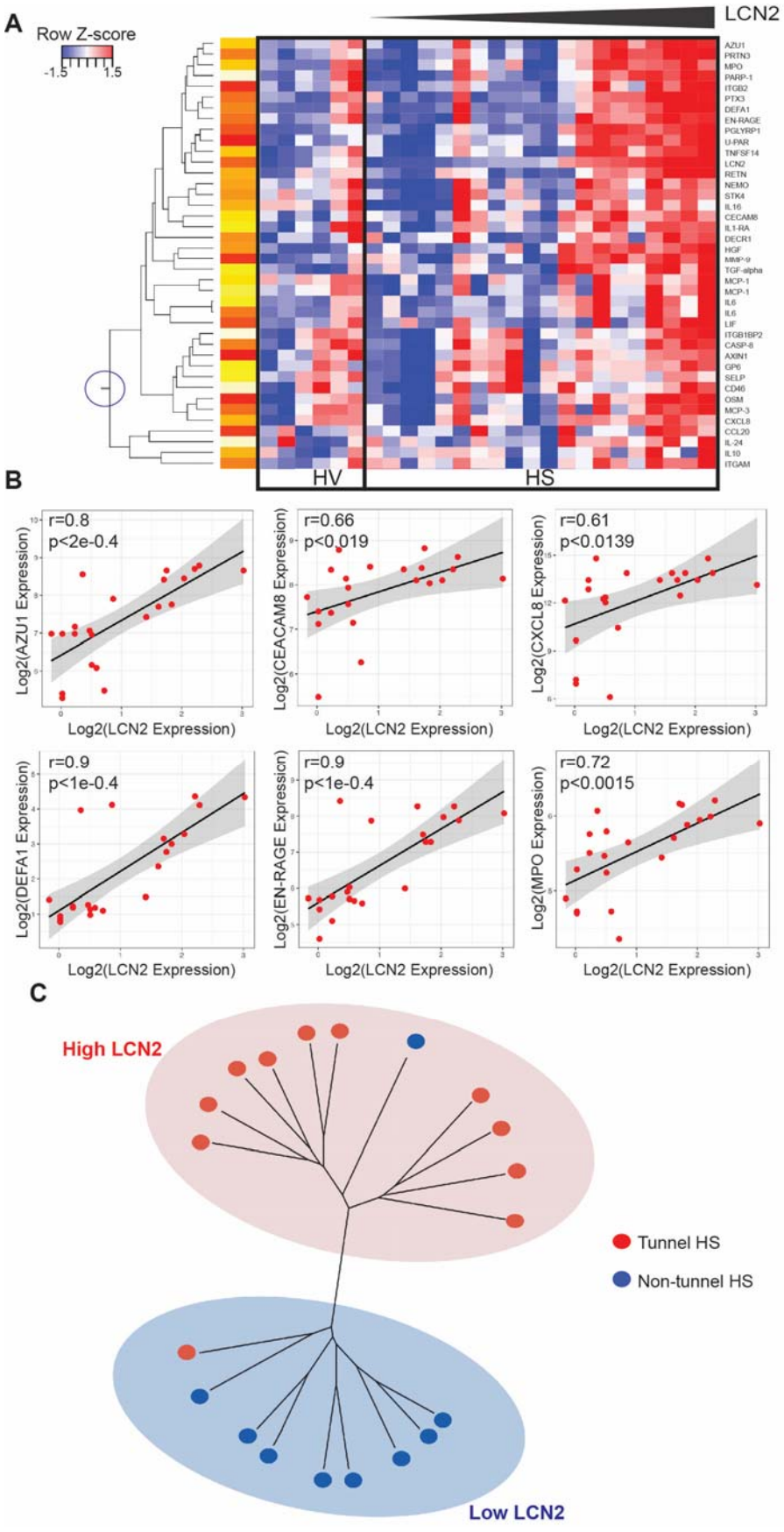
A
Row Z-score
-1.5
1.5
LCN2
AZU1
PRTN3
MPO
PARP-1
ITGB2
PTX3
DEFA1
EN-RAGE
PGLYRP1
U-PAR
TNFSF14
LCN2
RETN
NEMO
STK4
IL16
CEACAM8
IL1-RA
DECR1
HGF
MMP-9
TGF-alpha
MCP-1
MCP-1
IL6
IL6
LIF
ITGB1BP2
CASP-8
AXIN1
GP6
SELP
CD46
OSM
MCP-3
CXCL8
CCL20
IL-24
IL10
ITGAM
HV
HS
B
r=0.8
p<2e-0.4
Log2(AZU1 Expression)
Log2(LCN2 Expression)
r=0.66
p<0.019
Log2(CEACAM8 Expression)
Log2(LCN2 Expression)
r=0.61
p<0.0139
Log2(CXCL8 Expression)
Log2(LCN2 Expression)
r=0.9
p<1e-0.4
Log2(DEFA1 Expression)
Log2(LCN2 Expression)
r=0.9
p<1e-0.4
Log2(EN-RAGE Expresicn)
Log2(LCN2 Expression)
r=0.72
p<0.0015
Log2(MPO Expression)
Log2(LCN2 Expression)
C
High LCN2
Tunnel HS
Non-tunnel HS
Low LCN2

5.2.3 HS patients with tunnels have a different serum proteomic profile compared to patients without tunnels

We then compared DEPs in sera of HS patients with and without histologically confirmed tunnels, with FCH relative to healthy control shown (Figure 34A) and conducted an enrichment analysis of DEPs unique to HS samples with tunnels (relative to healthy controls) using the canonical/KEGG/REACTOME/bioCarta pathways. Serum of HS patients with tunnels had an enrichment of pathways involved in proliferation and signal transduction, inflammation, extracellular matrix remodeling and tissue-development (development biology, axon guidance, pathways in cancer) (Figure 34B). There were 41 unique DEPs in tunnel samples compared to 23 proteins unique to non-tunnel samples, both relative to healthy controls (Figure 34C). There was minimal overlap between tunnel and non-tunnel samples (5 proteins). Smoking status did not influence the serum proteome between patients with and without tunnels; of the 7 differentially expressed proteins between HS smokers and HS nonsmokers, only 1 (SERPINA7) was differentially expressed between tunnel and non-tunnel HS samples.

HS samples with tunnels had a neutrophilic signature (CTSD, IL-17A, IL-17D, LCN2) compared to HS without tunnels. Serum of patients with tunnels had an upregulation of known cardiovascular biomarkers (HGF, ST2, PGLYRP1). Given the neutrophilic signature associated with tunnels, and that pus draining from tunnels is neutrophil-mediated, we asked whether patients with draining or non-draining tunnels had a different proteome profile (Figure 34D). There was a significant difference in levels of neutrophilic-related proteins (IL-17A, LCN2, CXCL8, EN-RAGE, DEFA-1, MMP-9) between HS samples with draining versus nondraining tunnels. In cases where there was no significant difference in protein levels between healthy volunteers and HS, or tunnel versus non-tunnel samples, there was a significant difference in protein levels between draining and non-draining tunnel (EN-RAGE, DEFA1, MMP-9). This suggests that patients with actively draining tunnels have a different serum proteome profile. Furthermore, cardiovascular biomarker ST2 was significantly elevated in patients with draining tunnels, further linking the role of tunnels in HS and the increased risk for cardiovascular co-morbidities (Figure 34D).

Figure 34: HS patients with tunnels have a different serum proteome profile.
A) Enriched biological processes in serum of HS patients with tunnels by canonical/KEGG/Reactome/BioCarta pathways using the XGR tool. Vertical line is FDR=0.05 **B)** Venn Diagram of differentially expressed proteins in HS patients with and without tunnels relative to HV **C)** Olink expression of serum protein levels, shown in Log2(Expression) for neutrophil and cardiovascular-risk related proteins in serum of HS and HV, HS patients with and without tunnels, and HS patients with draining and non-draining tunnels. Each dot represents an individual sample [213].

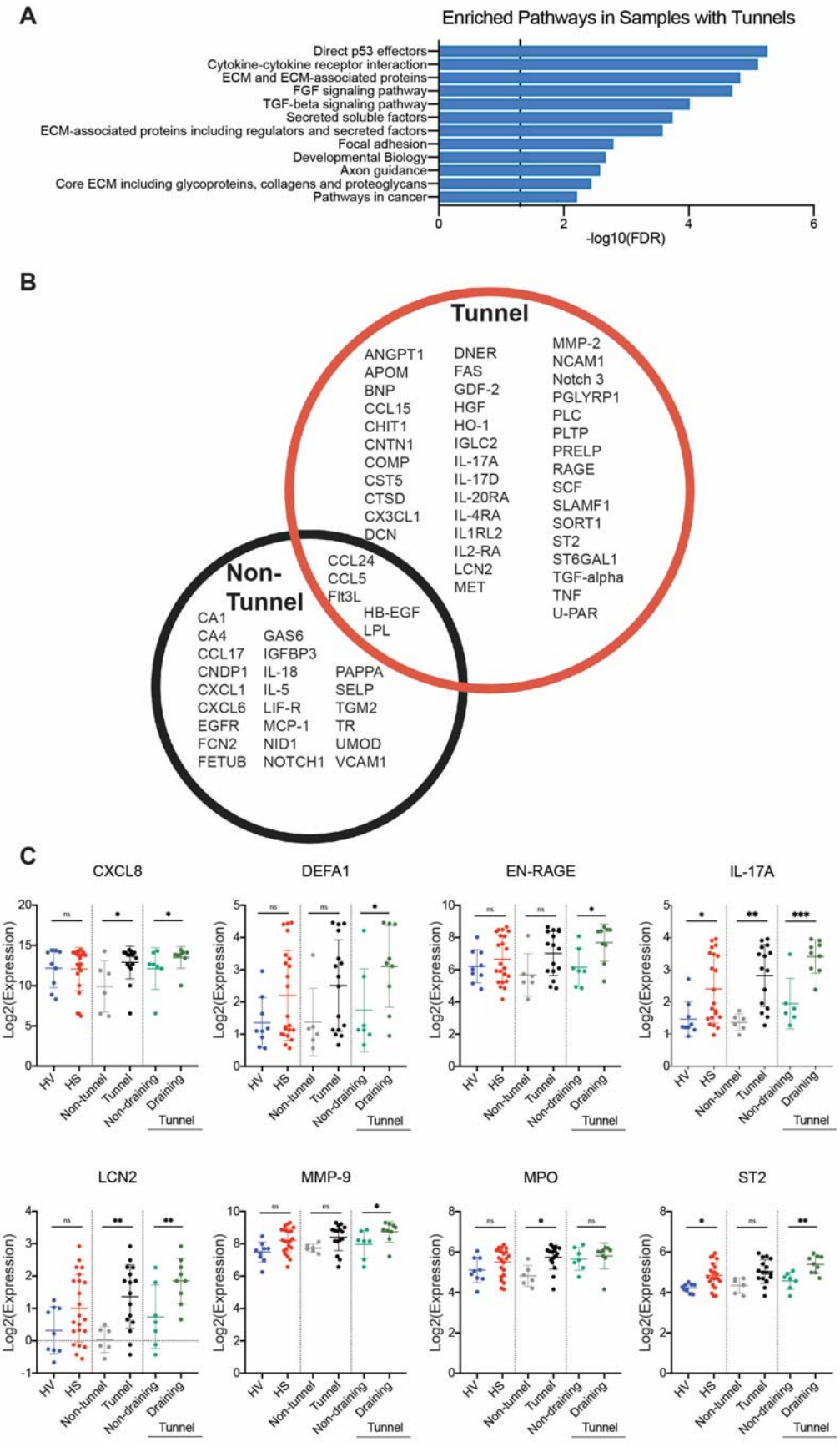
A
Enriched Pathways in Samples with Tunnels
Direct p53 effectors
Cytokine-cytokine receptor interaction
ECM and ECM-associated proteins
FGF signaling pathway
TGF-beta signaling pathway
Secreted soluble factors
ECM-associated proteins including regulators and secreted factors
Focal adhesion
Developmental Biology
Axon guidance
Core ECM including glycoproteins, collagens and proteoglycans
Pathways in cancer
0
2
4
6
-log10(FDR)
B
Tunnel
ANGPT1
APOM
BNP
CCL15
CHIT1
CNTN1
COMP
CST5
CTSD
CX3CL1
DCN
DNER
FAS
GDF-2
HGF
HO-1
IGLC2
IL-17A
IL-17D
IL-20RA
IL-4RA
IL1RL2
IL2-RA
LCN2
MET
MMP-2
NCAM1
Notch 3
PGLYRP1
PLC
PLTP
PRELP
RAGE
SCF
SLAMF1
SORT1
ST2
ST6GAL1
TGF-alpha
TNF
U-PAR
Non-Tunnel
CCL24
CCL5
Flt3L
HB-EGF
LPL
CA1
CA4
CCL17
CNDP1
CXCL1
CXCL6
EGFR
FCN2
FETUB
GAS6
IGFBP3
IL-18
IL-5
LIF-R
MCP-1
NID1
NOTCH1
PAPPA
SELP
TGM2
TR
UMOD
VCAM1
C
CXCL8
DEFA1
EN-RAGE
IL-17A
LCN2
MMP-9
MPO
ST2
Log2(Expression)
HV
HS
Non-tunnel
Tunnel
Non-draining
Draining
Tunnel

5.2.4 Correlation of biomarkers suggests a skin-blood interaction in HS

We also correlated protein expression between serum and skin in HS patients (Figure 35). There was a significant correlation between protein levels in blood and lesional ($r=0.67$, $p<0.01$) and perilesional ($r=0.61$, $p<0.01$) skin. 26 proteins were up-regulated, and 26 proteins were down-regulated in HS lesional skin and blood relative to healthy controls. Among the mutually up-regulated proteins, Th1 cytokines ((CXCL9 ($FCH_{skin}=5.31$, $FCH_{blood}=1.48$), CXCL11 ($FCH_{skin}=3.25$, $FCH_{blood}=1.48$)), IL-12/IL-23 cytokines ((CXLC1 ($FCH_{skin}=14.20$, $FCH_{blood}=1.07$), TNF ($FCH_{skin}=3.61$, $FCH_{blood}=1.26$)), the Th17 cytokine (CCL20 ($FCH_{skin}=6.36$, $FCH_{blood}=1.29$), and HGF ($FCH_{skin}=1.85$, $FCH_{blood}=1.16$) were higher in skin compared to blood ($n=19$). 15 proteins, including IL-8, IL-6, MCP-1, and MMP-1 were upregulated in skin but not in blood, and 25 proteins, including VEGFA, immunoregulatory IL-10, and growth factors TGF-alpha and FGF-21/23/19/5 were upregulated in blood but not in skin.

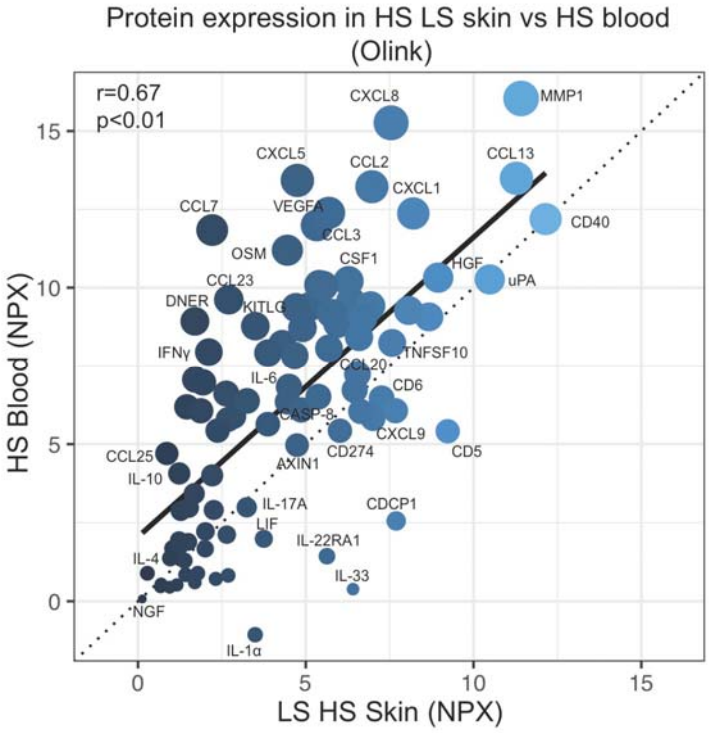

Figure 35: There is a significant correlation of blood-skin biomarkers in HS.
Olink proteomics in HS blood versus lesional skin. r is Pearson correlation.

We examined LS, and healthy-appearing PL and NL skin biopsies as previously described [86] (Figure 36A). We first asked if there was any correlation between HS skin and serum by studying IL-6, which has been previously suggested as a biomarker in HS serum [75]. IL-6 protein level in serum was significantly correlated with IL-6 mRNA in LS (r=0.62, p=0.0096), PL (r=0.56, p=0.0138) and NL (r=0.5, p=0.0261) skin (Figure 36B). We focused this analysis on PL skin biopsies since the overall RNA-quality was better in the PL compared to LS samples, consistent with the increased presence of neutrophils in lesions of LS skin. There was a significant correlation between proteins involved in the interferon axis (CXCL9, CXCL11), known psoriasis-related proteins (PI3/elastin, SELP), B-cell related protein (IGCL2), neutrophil related markers (LCN2, SERPINA5, SLAMF1) and biomarkers of general inflammation (HGF, HO-1) (Figure 36C). Granulocyte colony-stimulating factor (G-CSF/CSF3) is a major hematopoietic cytokine regulating granulopoiesis and is involved in both inducing granulocyte production and release from the bone marrow [166, 216]. Given the strong correlation between neutrophil-related biomarkers in the serum and skin, and the neutrophilic signature associated with HS overall, we asked if CSF3 is a possible driver of increased neutrophil activity is. The mRNA levels of CSF3 were elevated in LS and PL skin of HS patients compared to skin from healthy volunteers. Therefore, we asked if there was a correlation between CFS3 levels in LS skin and neutrophil-related biomarkers in serum (Figure 36D). Indeed, many of the neutrophil-related markers correlated with increased expression of CSF3 mRNA in the skin, suggesting that the active inflammatory lesion may be driving the recruitment of neutrophils and thus increasing the expression of neutrophil-related protein in the serum (Figure 36D).

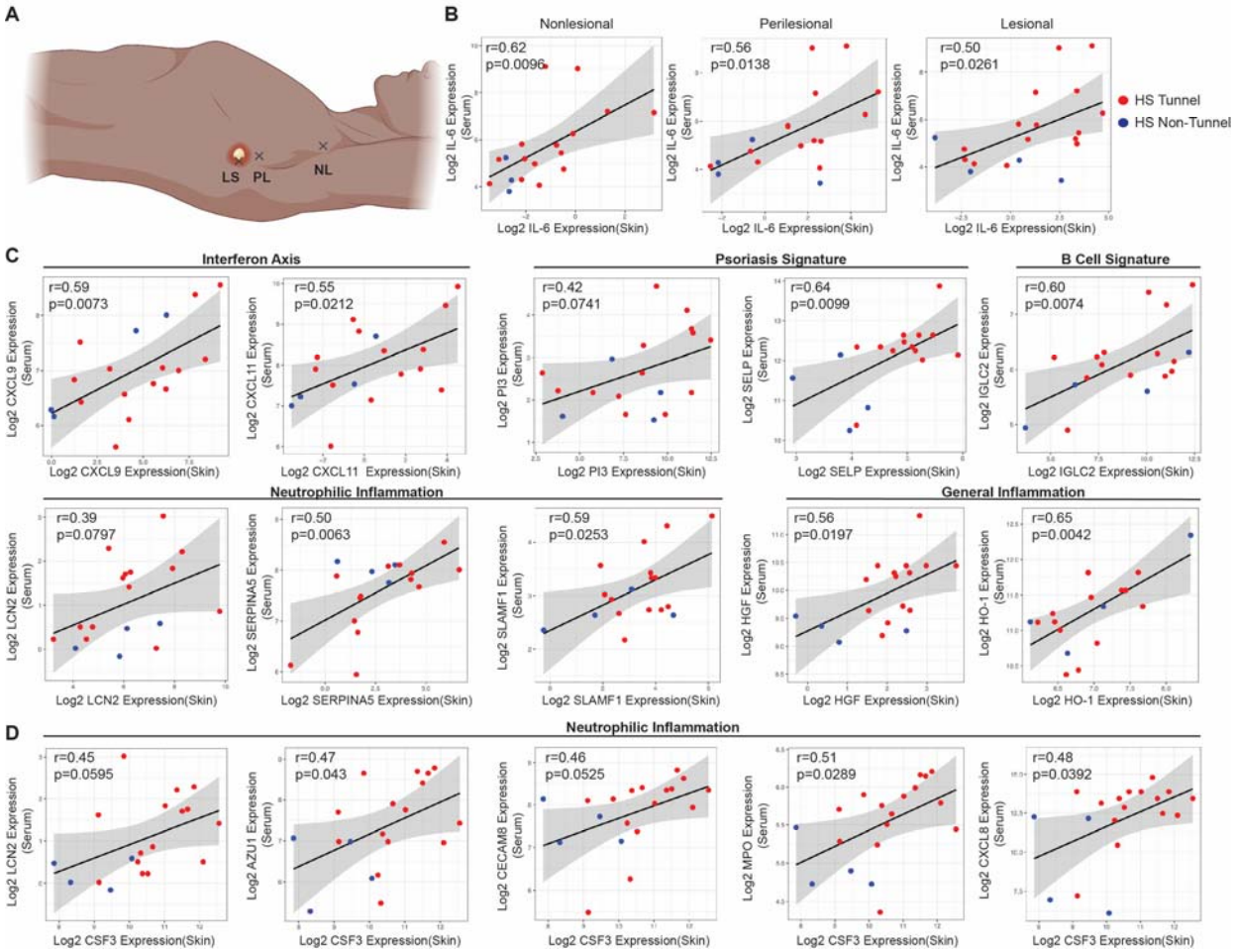

Figure 36: There is a multi-axis serum-skin correlation in HS.
A) LS was biopsied at an edge of an active inflammatory lesion. PL and NL skin biopsies were taken from healthy-appearing skin 2cm and 10cm from the edge of the active inflammatory lesion, respectively, and biopsied on the same anatomical area as the LS biopsy. **B)** Correlation plots of IL-6 protein serum levels and the IL-6 mRNA levels in LS, PL and NL skin; scatterplots are shown with estimated linear regression and 95% confidence interval; r Pearson Correlation. **c)** Serum-skin correlation of serum protein levels (Log2 Olink expression) with their corresponding mRNA levels in PL skin (Log2 mRNA expression) **D)** Serum-skin correlation between mRNA levels of CSF3 in LS skin and levels of neutrophil-related proteins in the serum [213].

5.2.5 Levels of neutrophil-related proteins in the serum correlate with clinical activity

We then asked whether clinical characteristics correlated with LCN2 and IL-17A protein levels in the serum (Figure 37). Given that only advanced HS patients (Hurley Stage II and III) were included in this study, we could not correlate the serum levels of LCN2 and IL-17A with Hurley Staging. However, patients with Hurley Stage III were more likely to present with draining tunnels (p=0.00905) and thus are more likely to have neutrophilic inflammation in the serum, consistent with analysis in Figure 3d. Unlike the IHS4 criteria, Hurley staging does not take into account the presence of nodules, abscesses and number of draining tunnels in a weighted approach. IHS4 scoring, which assigns points to the number of nodules, abscesses and draining tunnels/fistulae, correlated the most with the serum protein levels of neutrophilic LCN2 and IL-17A, suggesting its utility as a tool to quantify disease activity and clinical response in HS. Therefore, our data suggests that the IHS4 score is more representative of disease activity than Hurley staging. Furthermore, IHS4 levels also correlated with other markers of general inflammation (TNF-α, IL-6) and biomarkers of cardiovascular risk (ST2, HGF, TIE2). This may suggest that patients with more severe HS are at an increased risk of cardiovascular disease.

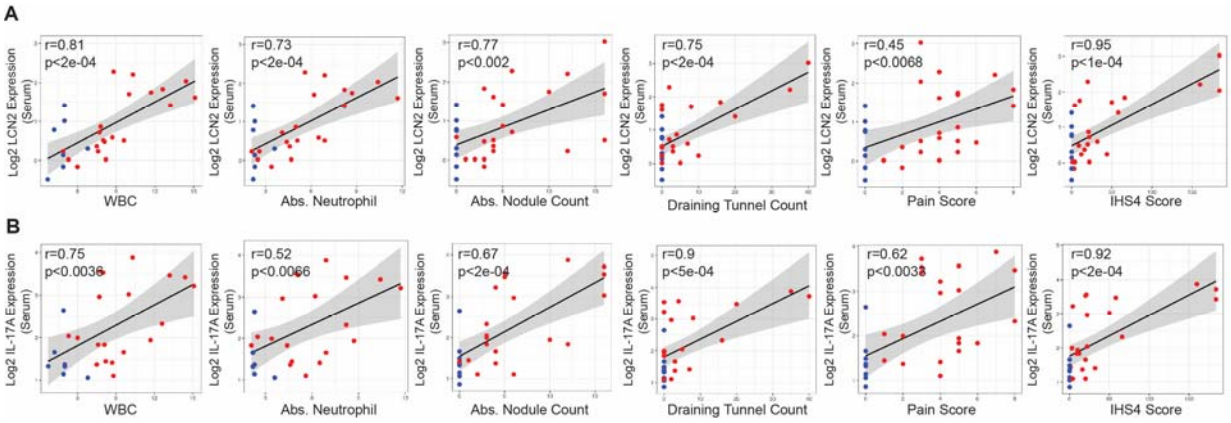

Figure 37: Serum protein correlations with clinical markers and skin disease severity. Correlation of White Blood Cell Count (WBC), Absolute Neutrophil Count (Abs. Neutrophil), Absolute Nodule Count (defined as the sum of nodules and abscesses), Draining Tunnel Count, Pain Score, and IHS4 scores with **A)** LCN2 and **B)** IL-17A protein levels in the serum. Scatterplots are shown with estimated linear regression and 95% confidence interval; r Pearson Correlation. Blue dots represent healthy control samples and red dots are HS samples [213].

5.2.6 Shared versus unique proteomic features in HS and psoriasis

We then profiled 1,536 serum proteins from HS and psoriasis patients and age- and BMI-matched healthy controls using the Olink Explore high-throughput proteomic platform. In order to decrease heterogeneity associated with HS, we chose to focus on HS patients with tunnels. In total, 11 moderate-to-severe psoriasis patients (mean age: 46.9+/-10.9 years), 10 moderate-to-severe HS patients with tunnels (mean age: 36.5+/-14.2 years), and 10 healthy controls (mean age: 39.5+/-19.3 years) were included in this study after signing an institutional review board-approved consent. There were no significant differences in age and BMI between HS patients, psoriasis

patients, and healthy controls Patients with psoriasis had Psoriasis Area and Severity Index/PASI≥12 (mean PASI score 16.3), and HS patients had a mean International Hidradenitis Suppurativa Severity Score System/IHS4 score of 64.5 and dermal tunnels (confirmed by ultrasound examination and histological assessment of biopsies[86]). Patients did not use topical treatment for ≥2 weeks and had >5 half-lives of wash-out period from previous disease modifying therapies.

Table 2: Characteristics of HS and psoriasis patients enrolled in the serum analysis.
BMI, body mass index; HS, hidradenitis suppurativa; IHS4, international hidradenitis suppurativa severity score system; PASI, psoriasis area and severity index; SD, standard deviation.

	Psoriasis (n=10)	**HS (n=11)**	**Controls (n=10)**	**P-value**
Age (y), mean (SD)	39.5 (19.3)	36.5 (14.2)	46.9 (10.3)	0.29
Male sex, n (%)	4 (40)	7 (63.6)	8 (80)	0.31
BMI, mean (SD)	32.6 (9.7)	30.5 (8.4)	29.6 (5.6)	0.7
Clinical severity scores, mean (SD)				NA
PASI	16.3 (3.4)	NA	NA	
IHS4	NA	56.1 (60.8)	NA	

The proteomic profiles were compared using criteria of |FCH|≥1.2 and p-value≤0.05 for differentially expressed proteins (DEPs). Overall, psoriasis had fewer DEPs than HS as compared to healthy controls (Figure 38). Psoriasis had 65 up- and 73 downregulated proteins, whereas HS had 217 up- and 217 downregulated proteins. In a direct comparison of HS to psoriasis, we identified 234 up- and 269 downregulated DEPs. Both HS and psoriasis had 17 upregulated DEPs in common, including IL-6, IL-2RA (innate immunity/T-cell activation-related), CD207/Langerin (a Langerhans cell marker), CD300E (a dendritic cell marker),[217] IL-17A and CCL20 (Th17-related), CXCL10 (Th1/IFNγ-related), and CD177 (neutrophil-related). Shared upregulated proteins also included markers related to increased risk of atherosclerosis (PLA2G2A and CHI3L1). Select serum markers are shown in Figure 2. The top upregulated proteins in psoriasis serum were IL-19, Defensin Beta 4A/4B, and PI3, all Th17-associated proteins (FCH>6.5, p<0.001 for all). Top upregulated proteins in HS serum included innate immunity-related/neutrophil-related CXCL8/IL-8,[218] CCL7, a driver of TNF-related inflammation,[219] and PDLIM7 (FCH>16.5, p<0.001 for all). A *gray* box highlights a cluster of shared upregulated markers (Figure 39). Among these, expression of IL-17A was similar between the diseases. Psoriasis displayed higher expression of IFNγ and CXCL9 (Th1-related), while HS displayed greater upregulations of IL-6 and CSF1 (innate immunity-related), GZMA (T-/natural-killer-cell-related), and CCL20 (Th17-related). Overall, a greater inflammatory tone was present in HS, with notable differences in key cytokines differentiating psoriasis and HS, as highlighted in the *pink* box (Figure 39). Markers of innate immunity (CXCL8/IL-8, TNF and IL-1β), neutrophil activation (PGLYRP1), Th1 (CCL3) and Th17 (LCN2) were all significantly over-expressed in HS relative to psoriasis and controls (p<0.05, Figure 2). Proteins uniquely over-expressed in psoriasis (*green* box, Figure 39) included the Th17-related IL-19, PI3/Elafin and DEFB4A/B, all significantly upregulated versus both HS and controls. While both psoriasis and HS had low expression of Th2-

associated cytokines and chemokines, key Th2-related chemokines (CCL17, CCL22, and CCL27) were significantly over-expressed in psoriasis and/or controls versus HS.

In addition to an increased inflammatory profile, HS sera had a downregulation of immunoregulatory molecules, including significantly lower levels of CD200 and the negative regulator IL-34 relative to healthy controls.[220] CD22, an inhibitory co-receptor of B-cells, was significantly lower in HS relative to psoriasis.[221] HS also presented downregulation of SERPINB1 (a neutrophil protease inhibitor) relative to both controls and psoriasis.[222] Taken together, these data demonstrates that HS is a systemic disease with activation of inflammatory circuits similar to psoriasis. HS has an upregulation of proinflammatory cytokines with downregulation of immunomodulatory proteins.

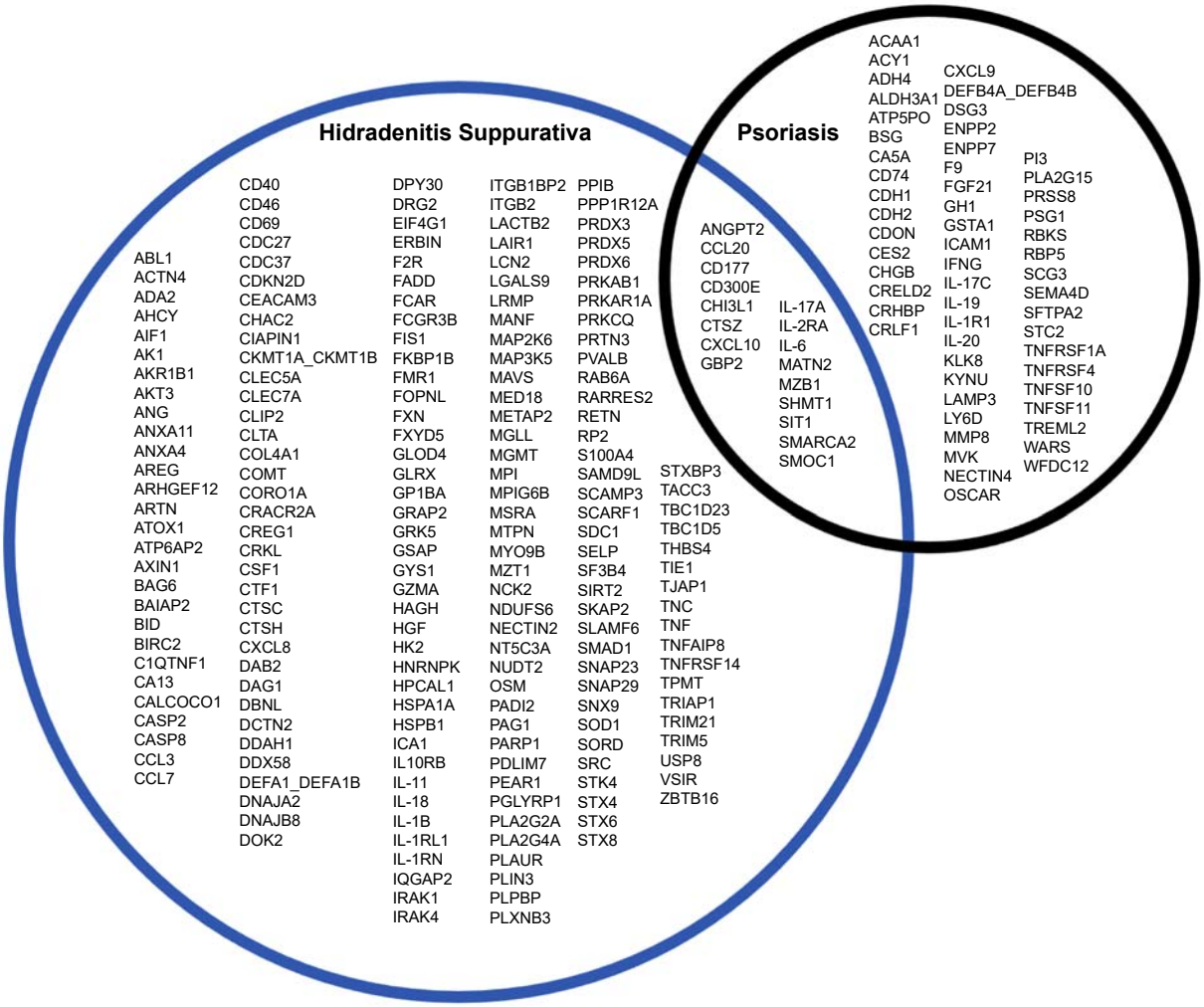

Figure 38: HS serum proteome is more dysregulated than that of psoriasis.
Venn diagram of upregulated DEPs (FCH≥1.2, p≤0.05) in serum of HS and psoriasis patients relative to healthy controls.

5.2.7 Global analysis further defines molecular signature of HS versus psoriasis

To globally assess pathways underlying each disease, we performed canonical pathway analysis using the Ingenuity Pathway Analysis (IPA) tool. The top significantly enriched canonical pathways in psoriasis included HMGB1 signaling (a mediator of inflammation), Th17 activation pathway and IL-17A signaling in airway cells, whereas top pathways related to HS were osteoarthritis pathway, p38 MAPK signaling and role of pattern recognition receptors in recognition of bacteria and viruses.

Figure 39: Comparison of immune regulators in HS and psoriasis serum.
Unsupervised hierarchical clustering heatmap of select DEPs (|FCH|≥1.2, p≤0.05) between psoriasis (PsO), HS and HV. Blue indicates downregulated and red indicates upregulated proteins. Values are FCH; stars represent p-values with * $p<0.05$, ** $p<0.01$, *** $p<0.001$.Red box indicates proteins uniquely upregulated in HS, grey box indicates proteins upregulated in both HS and psoriasis, and green box indicates proteins uniquely upregulated in psoriasis.

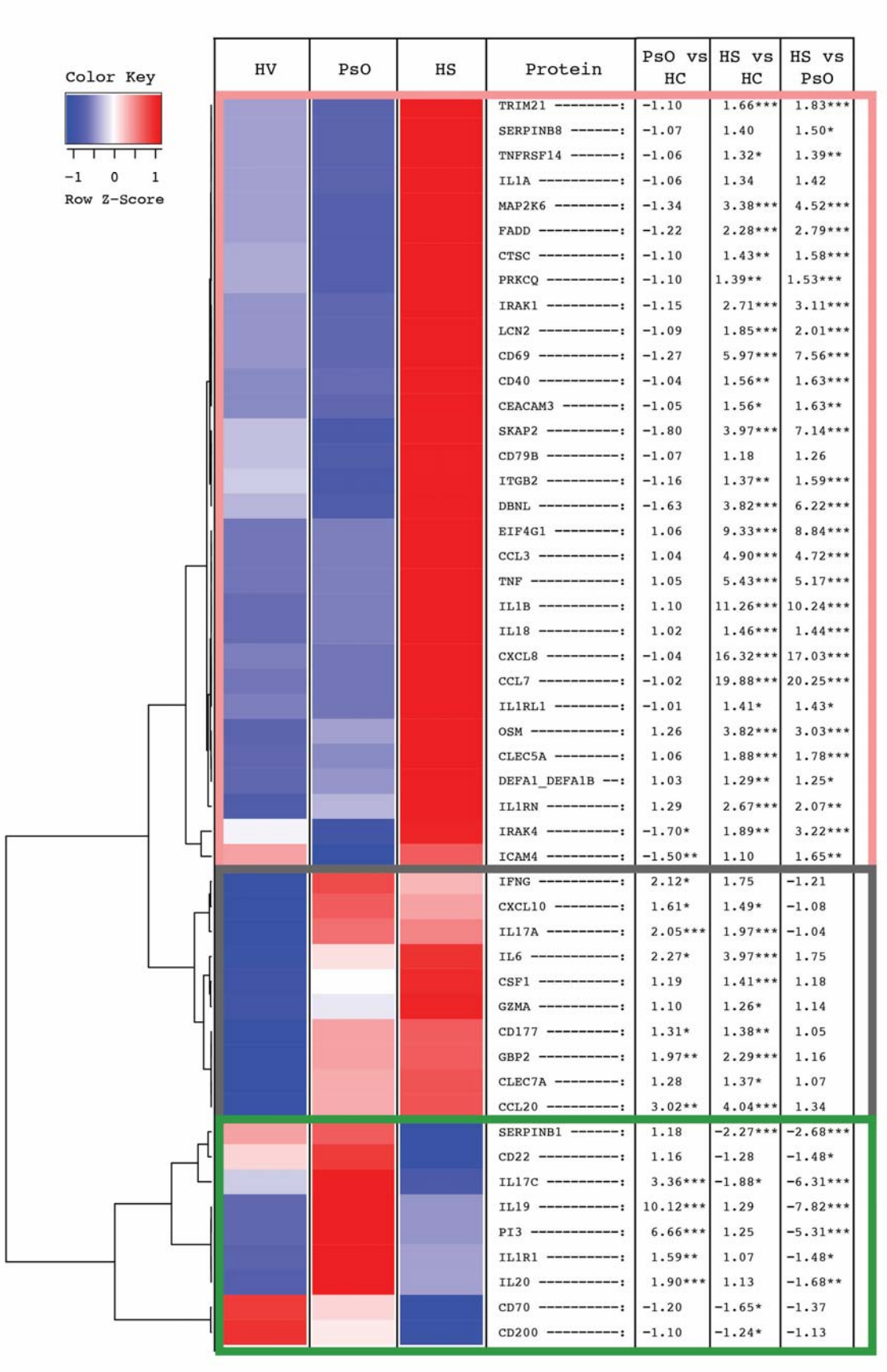

HV	PsO	HS	Protein	PsO vs HC	HS vs HC	HS vs PsO
			TRIM21 --------:	-1.10	1.66***	1.83***
			SERPINB8 ------:	-1.07	1.40	1.50*
			TNFRSF14 ------:	-1.06	1.32*	1.39**
			IL1A ----------:	-1.06	1.34	1.42
			MAP2K6 --------:	-1.34	3.38***	4.52***
			FADD ----------:	-1.22	2.28***	2.79***
			CTSC ----------:	-1.10	1.43**	1.58***
			PRKCQ ---------:	-1.10	1.39**	1.53***
			IRAK1 ---------:	-1.15	2.71***	3.11***
			LCN2 ----------:	-1.09	1.85***	2.01***
			CD69 ----------:	-1.27	5.97***	7.56***
			CD40 ----------:	-1.04	1.56**	1.63***
			CEACAM3 -------:	-1.05	1.56*	1.63**
			SKAP2 ---------:	-1.80	3.97***	7.14***
			CD79B ---------:	-1.07	1.18	1.26
			ITGB2 ---------:	-1.16	1.37**	1.59***
			DBNL ----------:	-1.63	3.82***	6.22***
			EIF4G1 --------:	1.06	9.33***	8.84***
			CCL3 ----------:	1.04	4.90***	4.72***
			TNF -----------:	1.05	5.43***	5.17***
			IL1B ----------:	1.10	11.26***	10.24***
			IL18 ----------:	1.02	1.46***	1.44***
			CXCL8 ---------:	-1.04	16.32***	17.03***
			CCL7 ----------:	-1.02	19.88***	20.25***
			IL1RL1 --------:	-1.01	1.41*	1.43*
			OSM -----------:	1.26	3.82***	3.03***
			CLEC5A --------:	1.06	1.88***	1.78***
			DEFA1_DEFA1B --:	1.03	1.29**	1.25*
			IL1RN ---------:	1.29	2.67***	2.07**
			IRAK4 ---------:	-1.70*	1.89**	3.22***
			ICAM4 ---------:	-1.50**	1.10	1.65**
			IFNG ----------:	2.12*	1.75	-1.21
			CXCL10 --------:	1.61*	1.49*	-1.08
			IL17A ---------:	2.05***	1.97***	-1.04
			IL6 -----------:	2.27*	3.97***	1.75
			CSF1 ----------:	1.19	1.41***	1.18
			GZMA ----------:	1.10	1.26*	1.14
			CD177 ---------:	1.31*	1.38**	1.05
			GBP2 ----------:	1.97**	2.29***	1.16
			CLEC7A --------:	1.28	1.37*	1.07
			CCL20 ---------:	3.02**	4.04***	1.34
			SERPINB1 ------:	1.18	-2.27***	-2.68***
			CD22 ----------:	1.16	-1.28	-1.48*
			IL17C ---------:	3.36***	-1.88*	-6.31***
			IL19 ----------:	10.12***	1.29	-7.82***
			PI3 -----------:	6.66***	1.25	-5.31***
			IL1R1 ---------:	1.59**	1.07	-1.48*
			IL20 ----------:	1.90***	1.13	-1.68**
			CD70 ----------:	-1.20	-1.65*	-1.37
			CD200 ---------:	-1.10	-1.24*	-1.13

Given the differing serum profile of psoriasis and HS, we evaluated which upstream regulators govern the two diseases. We used the IPA upstream regulator analysis tool, which analyzes linkages of the differentially expressed genes or proteins in order to identify upstream regulators, and focused on complex, cytokine, growth factor, and transcriptional regulators. The upstream regulators governing both psoriasis and HS included IFNγ, Oncostatin M/OSM (member of the IL-6 family),[223] lipopolysaccharide/LPS (a potent stimulator of inflammation) and TNF. STAT3 was an upstream regulator unique to psoriasis whereas IL-1β was unique to HS. In a direct comparison of HS versus psoriasis, TNF, followed by IL-1β were the most significant upstream regulators (Figure 40).

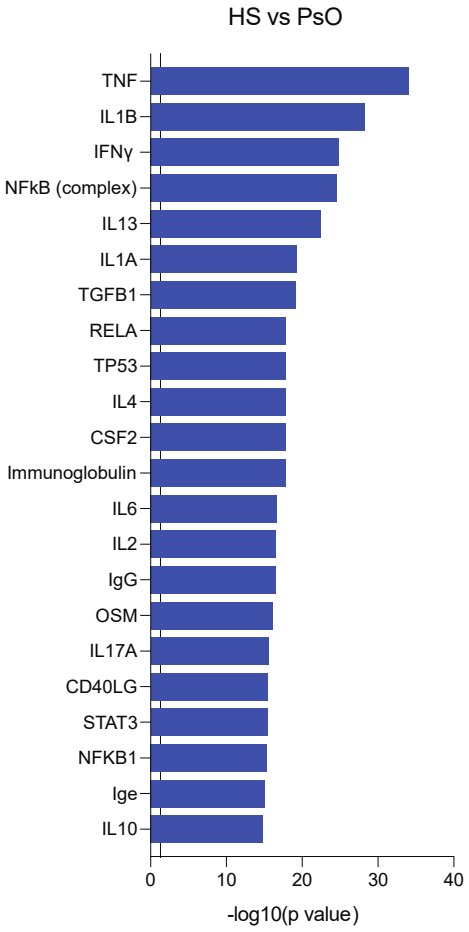

Figure 40: Upstream regulation of HS and psoriasis inflammatory profile.
IPA upstream regulators in HS relative to PsO based. Vertical line denotes threshold of p-value of 0.05.

5.2.8 The proteomic profile of HS serum demonstrates a Th1/Th17/IL-23-skewed systemic inflammation

We then performed an immune-related GSVA pathway analysis and observed significant enrichment of the Th1, Th17, and IL-23/IL-12 pathways, along with weak enrichment of the Th2 pathway across both diseases (Figure 41). Pathways of proteins synergistically or additively induced by TNF and IL-17 were significantly enriched in both diseases (p<0.05), with psoriasis presenting a greater, non-significant enrichment of the synergistically induced subset.[224] On the other hand, HS presented greater enrichment of innate immunity response and positive regulation of immunoglobulin production pathways. To validate our results, we also included known pathways upregulated in HS and psoriasis from previous reports,[225-229] which revealed that both psoriasis and HS display enrichment of the psoriasis pathways.

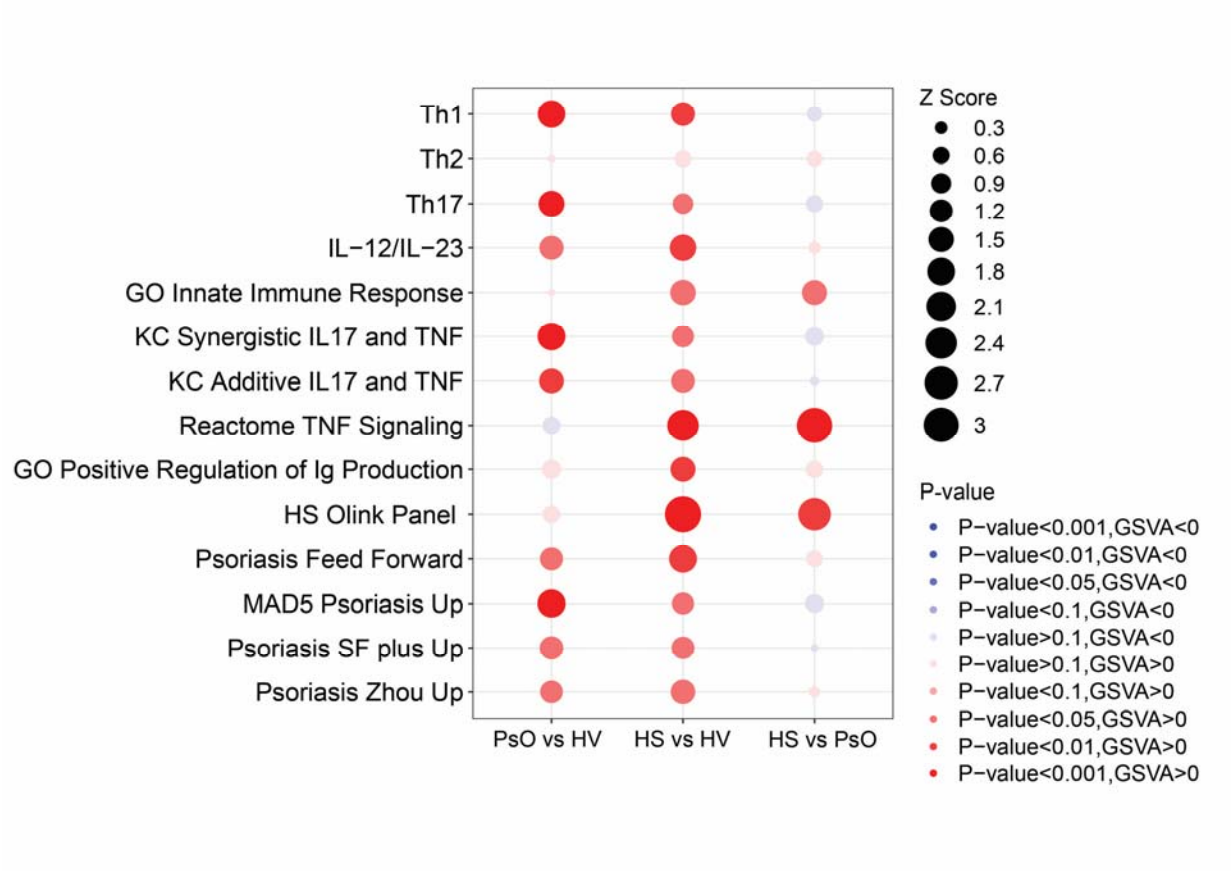

Figure 41: Pathway dysregulation in HS and psoriasis.
Bubble plot depicting GSVA scores in PsO and HS relative to HV, and in HS relative to PsO. The diameter of the bubble is proportional to the Z score. Bubble color represents p-value as defined in the legend on the right.

5.2.9 Disease classification of HS and psoriasis serum

Given the overlap of several inflammatory proteins in the sera of psoriasis and HS patients, we sought to identify a set of biomarkers that would specifically differentiate psoriasis and HS. Associations between upregulated proteins as disease classifiers were analyzed using a previously established logistic model from our laboratory that utilizes a set of biomarkers to distinguish and predict disease state.[230] We focused on Th17-related markers, PI3, an established marker specific to psoriasis,[231] and LCN2, a biomarker associated with HS.[126, 127, 232] Using this predictive algorithm we were able to successfully differentiate psoriasis and HS samples with a specificity and sensitivity of 1 (Figure 42). More specifically, a serum level of PI3 that is equal or greater than 1.42*(level of LCN2)–0.32 indicates that the serum sample belongs to an HS patient with high accuracy. We then asked whether commercially available serum biomarkers can also differentiate disease state for broader use. Indeed, the combination of CXCL8, TNF or IL-6 can successfully differentiate psoriasis and HS.

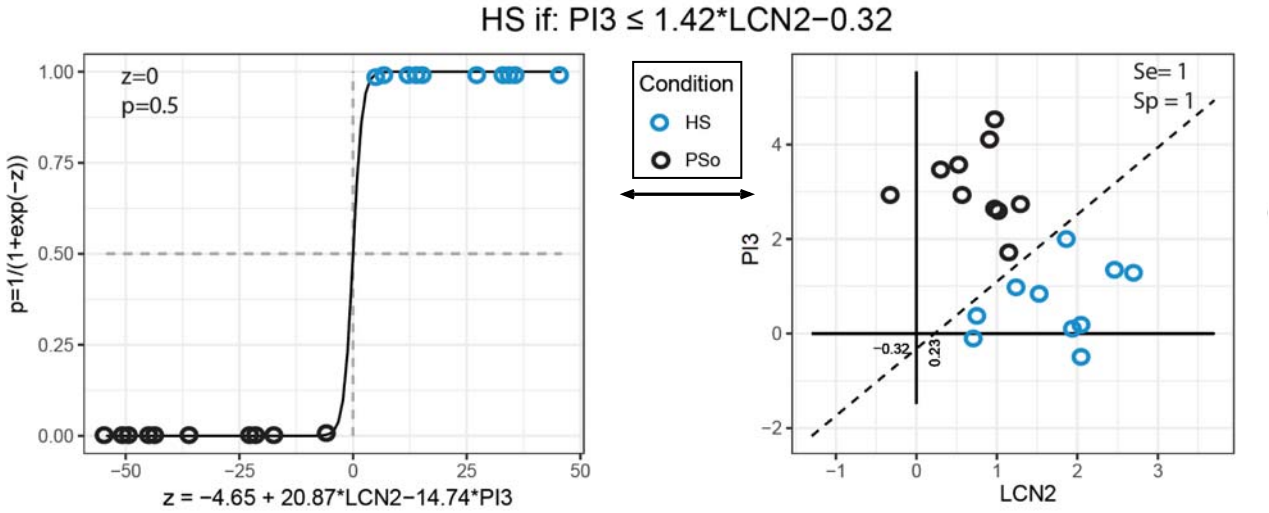

Figure 42: Serum LCN2 and PI3 expression discriminates between HS and psoriasis. Discriminant disease analysis using the predictive logistic model based on serum LCN2 and PI3 biomarkers. Axis are Log(Olink Expression Value) reported in Olink Normalized Protein eXpression (NPX) units.

5.2.10 Immune and cardiovascular biomarkers correlate with IHS4 and PASI scores

We then correlated serum biomarker levels with PASI and ISH4 for psoriasis and HS, respectively, as well as patients' BMI. In summary, 124 proteins correlated with PASI score, and 247 proteins correlated with IHS4 score ($|r|>0.5$, $p\leq0.10$). A total of 22 proteins correlated, either positively or negatively, with both PASI and IHS4 scores. In psoriasis, top markers correlating with severity included corticotropin-releasing hormone (CRH) and PAPPA, markers of early-stage atherosclerosis,[233, 234] previously reported in psoriasis patients ($r>0.7$, $p<0.05$).[233, 235, 236] Other markers positively correlated with psoriasis severity included CD69, a T-cell marker and a key

mediator of psoriasis pathogenesis,[237] granzyme B (GZMB), a natural-killer/T-call marker related with atherosclerosis,[238] IL-17A, IL-17F, IL-19 (Th17-related), CCL23 and CCL13 (Th2-related), the dendritic cell-marker CD300E,[217] and IL-1α, suggested to link immune activation and atherosclerosis ($r \geq 0.55$, $p \leq 0.1$).[239, 240] Top proteins positively correlated with HS clinical severity included tissue growth-factors-related markers, such as growth hormone 1 (GH1), CHRDL2, and TGFα, along with markers related with increased cardiovascular risk (PLA2G2A, CHI3L1, MMP9), TNF, key Th1-related chemokines (CXCL9/CXCL10), and Th17- and Th2-related receptors, IL-17RA and IL-4R, respectively ($r > 0.7$, $p < 0.01$).[241-243] Other positive correlations in HS by our criteria included markers related with innate immunity and cellular activation (LILRA5, IL-6, CD40),[244] the neutrophil-related PGLYRP1, Th1/IFNγ- (IFNγ, IFNγR1), Th17- (LCN2, IL-17F, CEBPB),[150] and Th2- (IL-10, IL-13) related markers ($r > 0.5$, $p \leq 0.10$).

Across both diseases, markers positively correlated with severity scores included IL-17F, CLEC4A and TGFBI, and markers inversely correlated with severity included leptin/LEP, CGREF1,[245] and FLT3LG[246] ($r > |0.4|$, $p \leq 0.10$). Of note, while LEP was robustly correlated with BMI ($r > 0.65$, $p < 0.05$), LEP levels were weakly inversely correlated with severity across both diseases ($r < -0.5$, $p \leq 0.10$).

5.3 Discussion

This work presents a large-scale proteomic analysis of serum from moderate-to-severe HS patients in comparison to healthy controls and psoriasis patients. Consistent with previous reports in skin, we identified elevation of IL-17A in HS serum [42, 97, 98]. We demonstrate systemic neutrophilic inflammation in HS, consistent with elevated absolute neutrophil counts in the blood. Unbiased analysis of samples demonstrated clustering of HS based on high and low LCN2 levels in the serum, which corresponded with histologically confirmed presence or absence of epithelialized dermal tunnels, respectively. This is consistent with neutrophils and keratinocytes (likely from the epithelized tunnels) being the source of LCN2 elevation [58]. There was a significant serum-skin correlation of neutrophilic markers present in perilesional skin, suggesting that there is an ongoing systemic inflammation even in healthy-appearing skin. Consistent with this, smaller-scale studies have shown that there is an upregulation of pro-inflammatory pathways even in healthy-appearing unaffected skin, further giving credence to the concept of HS as a systemic dermatosis [40, 97, 247]. ELISA-based analysis of HS serum has demonstrated dysregulation in pathways involving general inflammation [205], neutrophil activation [58], complement pathway [104] and antibody formation [105]. We identified CSF3 in the skin as a potential regulator of neutrophilic inflammation in the serum. Taken together, our data suggests that HS has significant clinical and molecular heterogeneity, demonstrating that patients with HS tunnels have a different proteomic profile.

HS is a heterogenous disease in its clinical presentation, however, it is unknown if different morphological structures manifest in unique inflammatory signatures in HS skin and serum. We present a large-scale proteomic analysis demonstrating an unbiased clustering of HS disease into distinct subgroups. When subdivided by the presence of tunnels, there was a higher number of DEPs than when examining HS as a whole. HS had fewer DEPs compared to psoriasis and AD, which could reflect a smaller body surface area affected and the compartmentalization of immune response in HS. We demonstrate an interesting association between a morphological structure in the skin (tunnels) and serum biomarkers. Patients with draining tunnels had a significantly higher

levels of neutrophil-related proteins in the serum (IL-17A, MPO, LCN2, CXCL8, EN-RAGE, DEFA1, MMP-9) compared to nondraining tunnels. This is consistent with the pus in draining tunnels being neutrophil mediated. Interestingly, HS patients with tunnels demonstrated enrichment of pathways related to ECM re-modelling and developmental biology. These signatures may explain the development of dermal tunnels and shift the paradigm from tunnels being an end-stage fibrotic feature of the disease to an active inflammatory structure. LCN2 is a protein secreted by granulocytes, neutrophils and keratinocytes. TNF-α is a potent inducer of LCN2 in granulocytes, while TNF-α and IL-17 has been shown to induce LCN2 production in keratinocytes [58]. Consistent with this, patients with tunnels had increased levels of IL-17A and TNF-α in the serum, which provides the direct mechanistic link for the increased levels of LCN2 in patients with tunnels. While some studies have shown that LCN2 is associated with obesity [76, 77, 248] and could provide some cardiometabolic protection [248], a study of psoriasis patients did not find a correlation between BMI and LCN2 levels but did report an elevation of LCN2 in serum psoriasis patients compared to healthy controls [249]. Similarly, we did not find a significant difference in BMI between LCN2-low and LCN2-high patients in our cohort (p=0.34). In our study, LCN2 levels in the serum are correlated with neutrophilic markers and the number of tunnels, suggesting that the strong LCN2 signature associated with the disease activity and the presence of tunnels may supersede any differences related to the BMI. We believe that the elevated LCN2 levels were likely derived from the high inflammatory burden of the disease rather than BMI. This highlights the role of tunnels in disease activity. Patients with draining tunnels had significantly higher levels of ST2 protein compared to those with nondraining tunnels, suggesting that the inflammation extends beyond the skin and can potentially affect the cardiovascular health.

Furthermore, the presence of tunnels influences the time it takes to achieve HiSCR response in the PIONEER 2 study of adalimumab [168, 169]. Our data provides the molecular mechanism for why patients with tunnels have a different disease activity and respond differently to biologic therapy [169]. Differences in biomarkers between tunnels and non-tunnel samples define disease endotypes that could impact therapeutic choices. For example, we found higher levels of TNF in tunnel-positive individuals, and it has been shown that the presence of tunnels increases time to a clinical response to adalimumab [169]. We speculate that the high levels of TNF could require the use of high-dose TNF antibodies that have been shown to be effective in severe cases [66]. Our study provides evidence of how morphological structures could influence the molecular profile of HS patients. Identifying HS subsets (potentially based on the presence or absense of tunnels) can identify not just novel biomakeres specific to each disease subset, but potentially identify effective treatment unique to each HS subgroup.

Our findings demonstrate that the skin may be a driver of the neutrophilic inflammation in serum, as there was a proportional correlation between CSF3 mRNA in the skin and the neutrophil-related proteins in serum. We had previously reported increasing gradient of IL-17 from nonlesional to lesional skin [97]. IL-17 has been shown to stimulate granulopoiesis by inducing G-CSF [162, 163, 250, 251]. It is plausible that IL-17, TNF-α, and IL-6 in HS skin may stimulate G-CSF production by fibroblasts, monocytes and endothelial cells, which in turn stimulates release of neutrophils from the bone marrow[164, 251]. Potentially, G-CSF could affect cutaneous characteristics, as several individual case reports have reported psoriasiform cutaneous eruption in patients receiving G-CSF [252-255].

To our knowledge, this is the largest study integrating the inflammatory cytokines in HS serum and skin using an unbiased panel of bio biomarkers. While one group compared levels of 30 protein between HS skin and blood, they did not find strong skin-blood correlations [174]. We found a correlation between skin mRNA and protein expression, as well as significant correlation between protein levels in HS skin and blood. This suggests elevated mRNAs are being actively translated into protein products in the skin, and that resulting proteins may be released into skin and potentially diffuse into the blood, as has also been proposed for elevated cytokines measured in the blood of psoriasis patients.

Acute and chronic pain contributes significantly to the reduced quality of life in patients with HS [256]. In this study, we explored the correlation between clinical parameters and the levels of neutrophilic proteins in the serum. Of particular interest is the correlation between LCN2 and IL-17A and reported pain levels in HS. The mechanisms of pain levels in HS have not been elucidated. Reports have suggested that neutrophil chemoattractant leukotriene B_4 as well as the migration cascade of neutrophils themselves can lead to hyperalgesia and mechanical hyper nociception [257, 258]. Consistent with this, animal studies have shown that both LCN2 and IL-17A are involved in mechanical hyperalgesia [259, 260]. Our data provides one plausible mechanism for the pain burden in HS.

Interestingly, across our cohort of moderate-to-severe patients, we found that sera from HS patients demonstrated more abnormalities compared to psoriasis. This finding was surprising given the limited involvement of HS lesions in intertriginous areas versus the widespread distribution of psoriatic lesions in psoriasis. A possible explanation is the depth of HS lesions versus psoriasis lesions, with a significant dermal component characterizing HS, especially in patients with active tunnels, as was the case in our HS cohort. Moreover, the higher disease burden in HS may explain the need of greater dosing of psoriasis-approved agents, such as adalimumab and infliximab, in the treatment of HS patients.[66, 261] Congruent with accumulating evidence suggesting an increase in cardiovascular risk and atherosclerosis-related markers in psoriasis and HS patients,[100, 262-264] we found upregulations and positive correlations of atherosclerosis-related circulating proteins with disease severity scores, supporting an atherosclerosis/cardiovascular signature in both diseases. In HS, strong correlations with severity were observed for PLA2G2A, CHI3L1, and MMP9, along with immune markers previously reported to increase cardiovascular risk, including IL-6 and TNF.[241-243, 265] High upregulation of CXCL8/IL-8 in HS may link neutrophil recruitment/activation and increased atherosclerosis risk.[218]

A strength of our study is that we assessed a large panel of known biomarkers in an unbiased approach. Previous studies of HS serum demonstrated elevated levels of IL-17A, TNF-α, LCN2, and IL-6 [58, 75, 128, 266]. The clinical disease heterogeneity in HS complicates the identification of biomarkers of clinical response. All of the patients in our study were either untreated or had undergone a washout period, therefore eliminating these confounders in the analysis. Furthermore, given that changes in proteomic profiles are related to changes in BMI and fat distribution, we utilized BMI-matched healthy controls [267]. Importantly, rather than focusing on known disease-associated cytokines, we sought to determine new disease associated biomarkers through use of a large biomarker panel and a hypothesis free approach.

The limitations of our work include a modest sample size (although comparable to other cohorts studied [58, 205, 207], use of controls that were older than the HS cohort and the relative limitation of the Olink platform where analysis is restricted to pre-grouped biomarker subsets. Future larger-scale studies are warranted to identify how other HS manifestations (abscesses vs nodule, draining vs non draining tunnel) impact serum proteome. This analysis is also limited to moderate and severe HS patients, and it would be desirable to study new on-set or mild HS patients in future studies. If serum biomarkers are also elevated in early-stage disease, these biomarkers may facilitate diagnosis and decrease the 5–14-year diagnostic delay experienced by HS patients [2]. Given the cyclical nature of HS severity, marked by debilitating flare-ups and a remitting course, serum biomarkers become particularly crucial in order to assess disease activity and accurately diagnose, as well as measure therapeutic response.

In conclusion, we demonstrate that HS is a systemic, inflammatory condition associated with neutrophil-rich signature in serum and skin, with a significant serum-skin correlation of neutrophilic activity. We identify two HS subgroups corresponding with LCN2 protein levels in the serum and histologically confirmed presence of tunnels in affected skin. Taken together, our results highlight the need for further biomarker studies in HS that integrate the skin and blood proteome, and associate measured abnormalities with clinical disease activity scores and changes with disease improvement induced by a range of established and evolving therapeutic approaches. We identify a number of new proteins that are dysregulated in HS, and which could contribute to overall disease activity, as well as the complexity of the therapeutic approaches. This may explain the difficulty of treating HS with ‘narrow’ cytokine antagonists, as is highly successful with psoriasis that shows predominantly Th17 pathway activation.

CHAPTER 6:
Characterizing the molecular response to IL-17RA

CHAPTER 6. Characterizing the molecular response to IL-17RA blockade

6.1 Introduction

The identification and development of novel therapeutics is hindered by our relative lack of understanding of the molecular pathogenesis of HS[47]. The morphologic heterogeneity of the disease (which include nodules, abscesses, tunnels and fibrotic regions) as well as a lack of a standardized consensus in assessing the molecular response in therapeutic studies (i.e., which regions to biopsy) add to the challenge of HS research[268]. Furthermore, molecular and cellular biomarkers of disease activity have remained elusive in HS. One study identified a robust decrease in transcriptomic B cell signature in HS lesional biopsies following treatment with adalimumab and a decrease in B cell lymphocyte chemoattractant CXCL13, while another studied identified a reduction in frequency of T-helper (Th) 17 cells [29, 85]. However, other studies of apremilast and ustekinumab did not identify a singular biomarker of treatment response despite clinical efficacy[170, 205].

Recent work demonstrated increases in IL-17A and IL-17C cytokines and increased infiltration of Th17 cells in HS [42, 49, 51, 97, 99, 104, 269]. In light of the evidence for the role of IL-17 signaling in disease pathogenesis, therapeutic targeting of IL-17A in HS has been explored in small cohort studies[63-65, 71]. Given the elevated levels of both IL-17A/C in HS, targeting IL-17 Receptor A (IL-17RA), a shared subunit of the receptor complex, is an attractive therapeutic avenue[123, 270-274]. We have recently conducted a clinical study of brodalumab, a human monoclonal antibody targeting IL-17RA that is FDA approved for moderate-to-severe psoriasis, in HS and reported promising clinical results [203, 275-277].

IL-17 receptor (IL-17R) family consists of five receptor subunit members: IL-17RA-RE[278], and has tissue specific activation of a diverse group of downstream factors including p38, NF-kb, TRAF6, TRAF3, and Act1[279]. The receptor subunits are transmembrane domain containing proteins ranging from 499 to 866 amino acids and form a heteromeric receptor complex. IL-17RA is the largest member of this subunit family[270]. IL-17A/F signal through the IL-17RA/Il-17RC receptor complex, while IL-17C signals through IL-17RA/Il-17RE complex[123, 271-274].

IL-17RA is expressed ubiquitously with higher expression levels in hematopoietic tissues. IL-17RA is found to be expressed across multiple tissues including epithelial cells (including keratinocytes), endothelial cells, peripheral T cells, B cell lineages, fibroblasts, macrophages and DCs[279]. Interestingly, levels of cell surface expression of IL-17RA correlate with strength of signaling, suggesting even partial blockade of IL-17RA can decrease proinflammatory activity of IL-17 signaling[279-281]. Following IL-17A binding, surface expression of IL-17RA decreases, suggesting that IL-17RA may function in limiting signal transduction by receptor-mediated internalization [281, 282].

Targeting IL-17RA in order to block various IL-17 family cytokines is an attractive therapeutic option that has been explored in several inflammatory diseases including psoriasis, psoriatic arthritis, and rheumatoid arthritis [271]. Brodalumab binds to IL17RA and prevents IL-17 from activating the downstream signaling. Brodalumab is an IL-17 receptor antagonist (IL-17RA) that is FDA approved for the treatment of moderate to severe psoriasis [275-277]. In psoriasis, brodalumab leads to a significant clinical response and molecular improvements characterized by

decrease of epidermal thickness and cellular proliferation as well as infiltrating leukocytes[275, 276, 283].

We conducted an open-label pilot cohort study to evaluate safety and tolerability of brodalumab in patients with moderate-to-severe HS and have reported promising therapeutic results (Figure 43). In this chapter, we characterize the molecular impact of IL-17RA antagonism in HS. This is the first study which systematically compares treatment response in lesional and perilesional skin in the setting of an intervention.

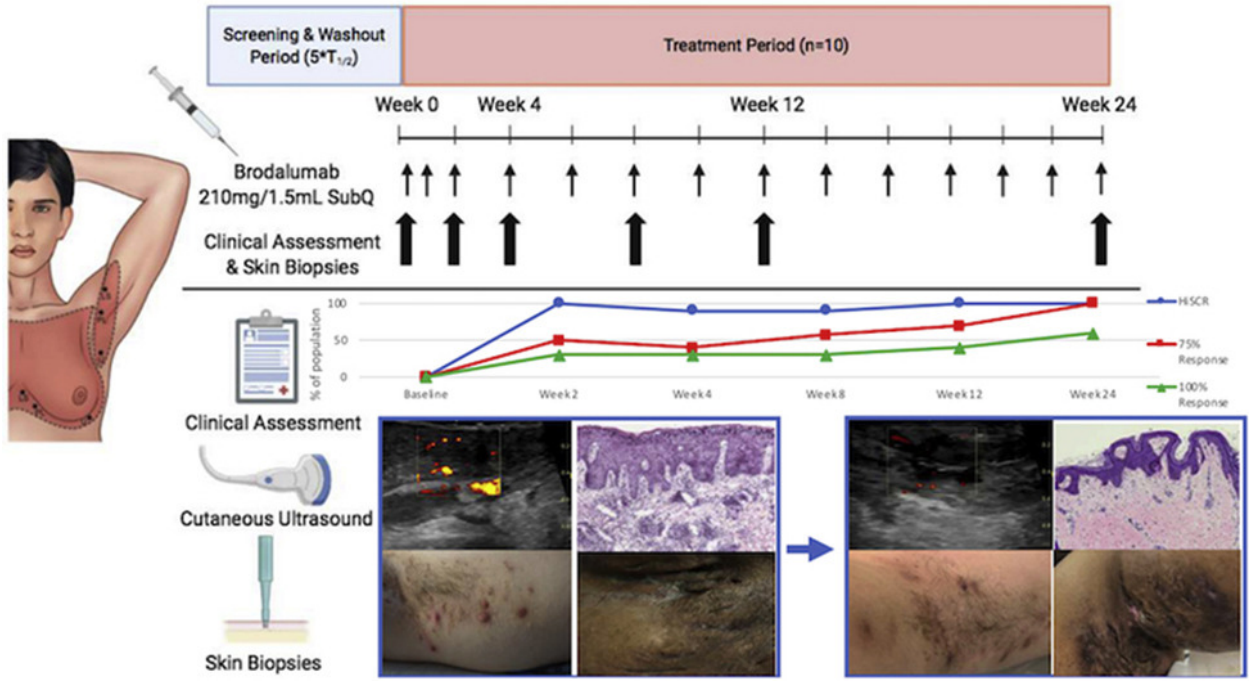

Figure 43: Clinical trial design.
Graphical abstract outlining the open-label clinical trial of brodalumab for the treatment of moderate-to-severe HS [203].

6.2 Results

6.2.1 IL17-RA blockade reduces HS clinical activity

Ten patients completed this study. All patients (100%) achieved HiSCR at week 2 compared with baseline (Fig 1), with 5 of 10 patients achieving a 75% reduction in AN count and 3 of 10 patients achieving a 100% reduction in absolute nodule (AN, sum of nodules and abscesses) count. All 10 patients (100%) had achieved HiSCR at week 12, with 7 of 10 patients achieving a 75% reduction in AN count, and 40% of patients achieving a 100% reduction in AN count (Figure 44). This continued to increase, with 100% patients having a 75% reduction in AN count at week 24 and 40% of patients having a 100% response in AN count. At week 2, 50% patients achieved IHS4 category change, increasing to 80% at week 12, which was maintained until week 24. At week 12, 40% of patients had a 2-category change in IHS4 score that was maintained until week 24.

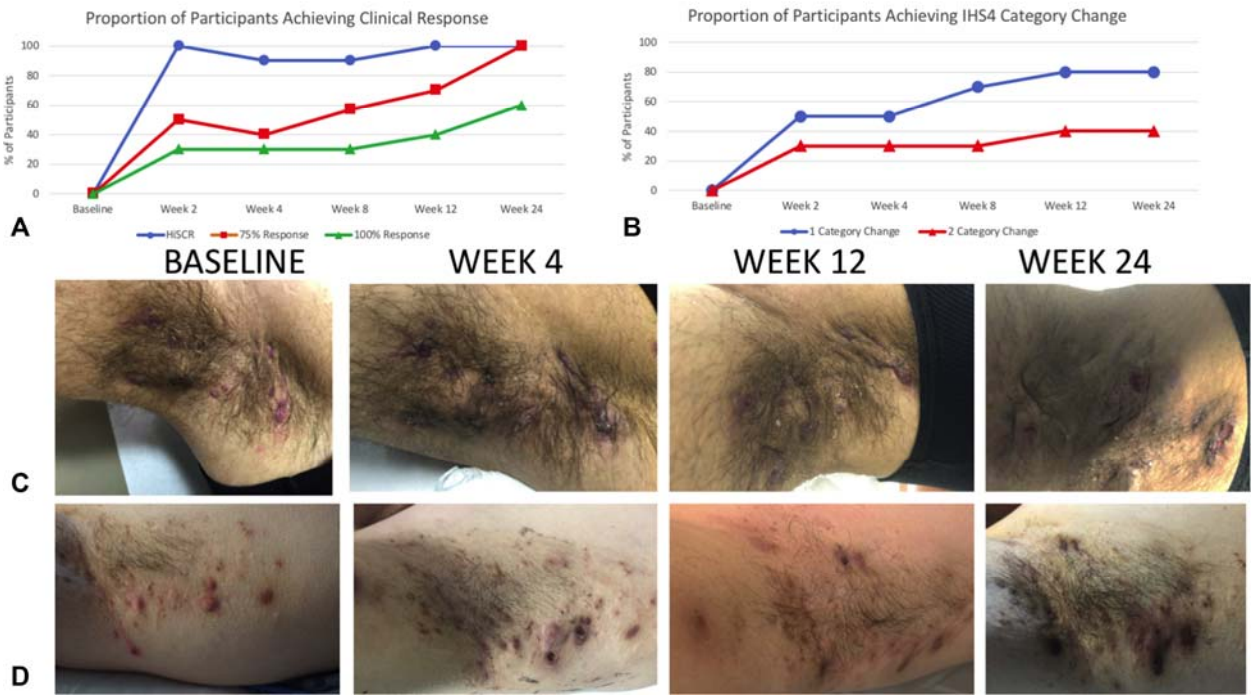

Figure 44: Measures of clinical response to brodalumab therapy in HS.
A) The proportion of patients achieving HiSCR at weeks 12 and 24 was 100%, with 75% reduction in AN counts (red) and 100% reduction in AN counts (green) in 60% and 40% of participants, respectively. **B)** Measurement of clinical outcomes using IHS4 category change shows 80% and 40% of patients achieving 1-category and 2-category change respectively. **C** and **D)**Representative clinical photos show a rapid reduction in the inflammatory nature of nodules at week 4 compared to baseline and continued improvement at week 12. HiSCR was maintained at Week 24 despite external triggers initiating limited flares of disease [203].

Significant decreases in vascularity and inflammation, as measured by cutaneous Doppler ultrasonography, were seen at weeks 4, 12, and 24 compared with baseline in all 10 patients (Figure 45). Doppler signal reductions were particularly apparent in the superficial dermis and surrounding parallel hyperechoic structures of the dermis, indicative of epithelialized tunnels (Fig 45).

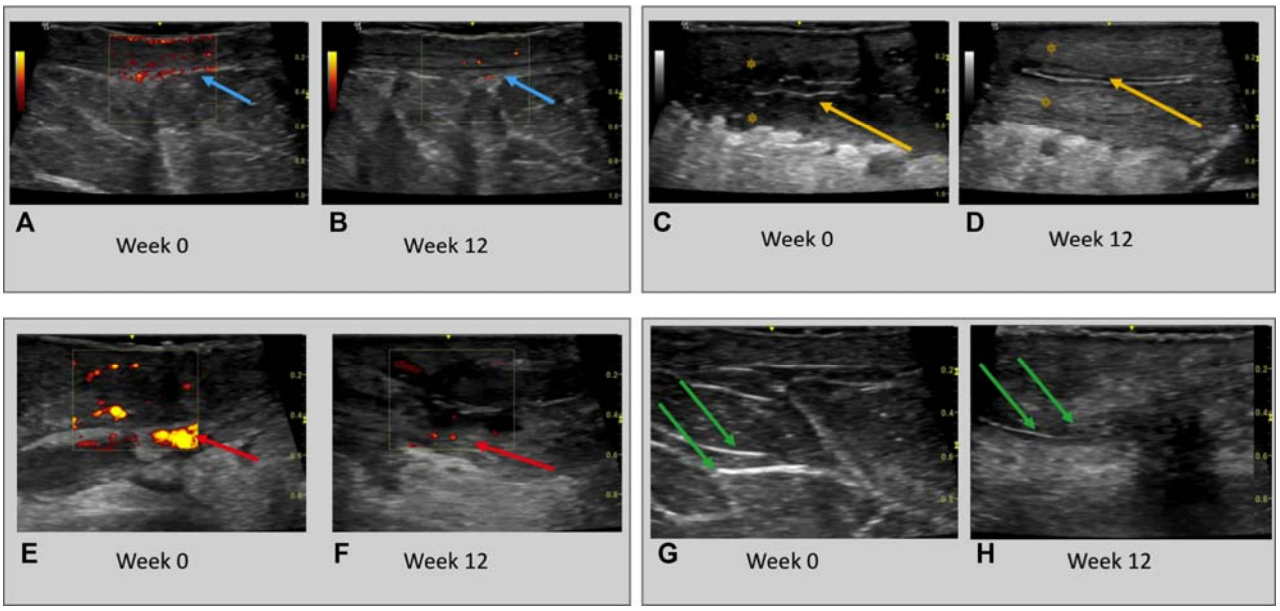

Figure 45: Treatment induces skin changes that are detected by ultrasound examination. Ultrasonographic changes at baseline and after 12 weeks of treatment with brodalumab. Dermal Doppler ultrasonography intensity in lesional dermal tissues at **A)** baseline (blue arrows) is significantly attenuated at **B)** week 12 (blue arrows) of therapy. The diameter of draining tunnels (yellow arrows) and surrounding edema (yellow asterisk) at **C)** baseline is also reduced at **D)** week 12. Similarly, Doppler intensity (red arrows) surrounding **E)** epithelialized dermal tunnels **F)** reduces at week 12 compared with baseline. The diameter and echogenicity of dermal tunnels (green arrows) is also **H)** attenuated at week 12 compared with **G)** baseline[203].

6.2.2 Molecular resolution of HS transcriptome with brodalumab treatment

We investigated brodalumab-induced changes in HS transcriptome (HSTR). RNA-sequencing was performed on whole-tissue skin biopsies and criteria of FCH≥|1.5| and FDR ≤ 0.05 was utilized for differentially expressed genes (DEGs). HS transcriptome was defined as the DEGs between lesional (HSTR-LS) or perilesional (HSTR-PL) skin and healthy appearing nonlesional biopsy skin. HSTR-LS had 923 down- and 913 up-regulated DEGs, whereas HSTR-PL had 819 down- and 835- upregulated DEGs. Lesional and perilesional samples were both highly inflamed at baseline and no DEGs were detected between lesional and perilesional skin (Figure 46A-D). We identified a significant correlation between genes in lesional and perilesional skin ($r=0.94$, $p<1E-04$, Figure 46A). Treatment produced an 88.3% reduction in HSTR-PL compared to 55.1% reduction in HSTR-LS week 12 ($p<0.001$) (Figure 46E-F). The odds ratio of treatment response was 6.11, suggesting that there is a 6 times greater probability of detecting a change in HS transcriptome in perilesional skin compared to lesional skin at week 12.

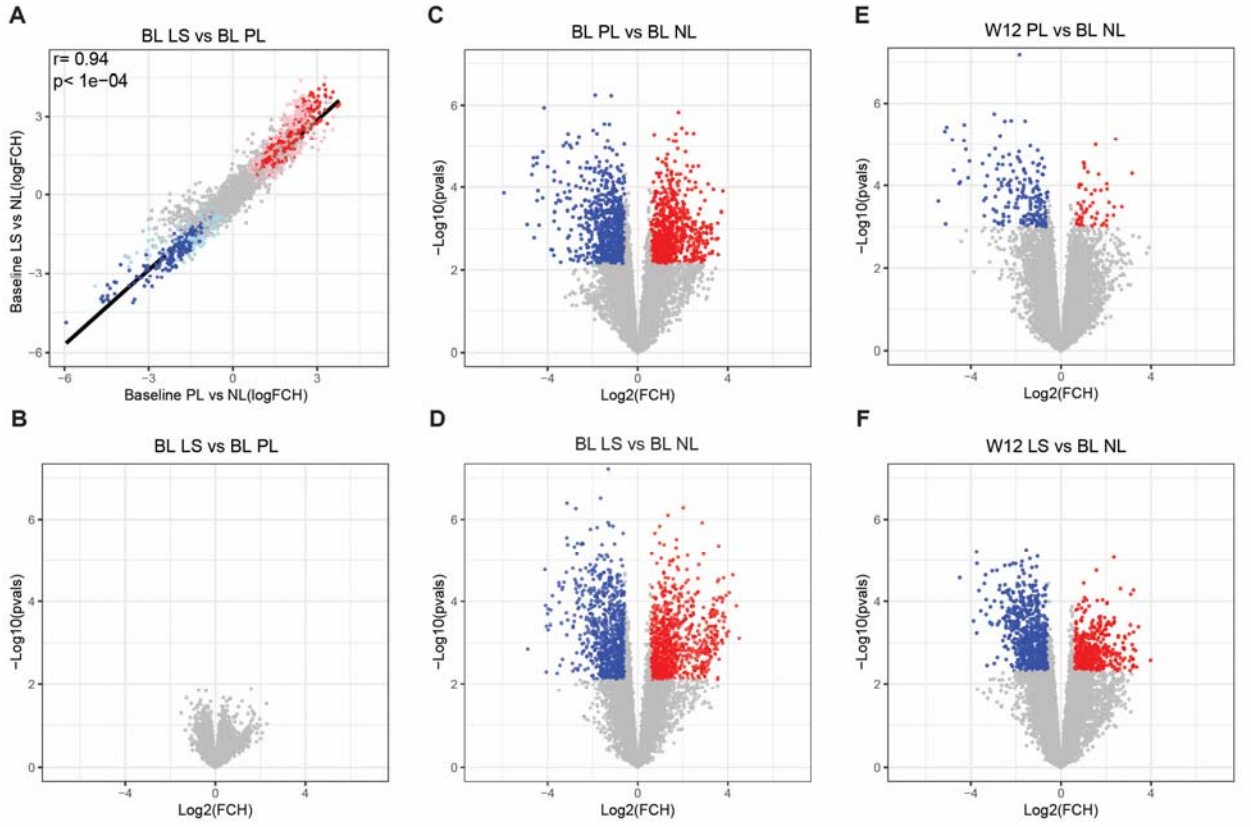

Figure 46: Perilesional skin shares overlapping transcriptomic profile with lesional skin at baseline but exhibits more changes with treatment response.

A) Correlation of DEGs as defined by |FCH| $\geq$ 1.5 and FDR $\leq$ 0.05. Red circles indicate upregulated DEGs while blue circles indicate downregulated DEGs in HS skin. r is Pearson correlation. Grey circles indicate genes that are not differentially expressed. Volcano plot of differentially expressed genes in **B)** LS vs PL skin **C)** PL vs NL and **D)** LS vs NL. Modulation of DEGs by brodalumab at week 12 in **E)** PL and **F)** LS versus baseline NL skin.

Given that treatment response was better detected in HSTR-PL, we focused subsequent analysis on perilesional skin (Figure 47-49). DEGs modulated with treatment included neutrophilic markers (CSF3, CD177), Th1 (CXCL11, STAT4), Th17 (IL21R), Th2 (GATA3) and innate interferon pathway related (IFI16, IL18, MX1, MX2, IFITM3, ISG20) markers as well as B cell chemoattractant CXCL13 (Figure 49). Using gene-set variation analysis (GSVA) we quantified the behavior of previously curated gene-sets and observed decreases in the general inflammatory response and pathways related to psoriasis, Th1, Th17 and IL-12/IL-23 signaling (Figure 48). IL-17 signaling is involved in keratinocyte proliferation, differentiation and feed-forward inflammation in which Th17-derived IL-17A/F can lead to increased production of other inflammatory cytokines including IL-36, CCL20, CXCL chemokines and S100 proteins while keratinocyte derived IL-17C can amplify this signaling by leading to increased secretion of IL-

17A by Th17 cells[29, 53, 201, 272]. We thus asked whether previously defined keratinocyte signaling pathways are also decreased with treatment and observed a reduction of multiple keratinocyte-related axis (Figure 48). Clinically, patients had a reduction in purulent drainage from dermal tunnels[203]. Given that tunnels are involved in neutrophilic inflammation, we asked whether neutrophilic related pathways are also downregulated with brodalumab treatment and observed a significant decrease of neutrophil-related pathways in perilesional skin[99, 269] (Figure 48).

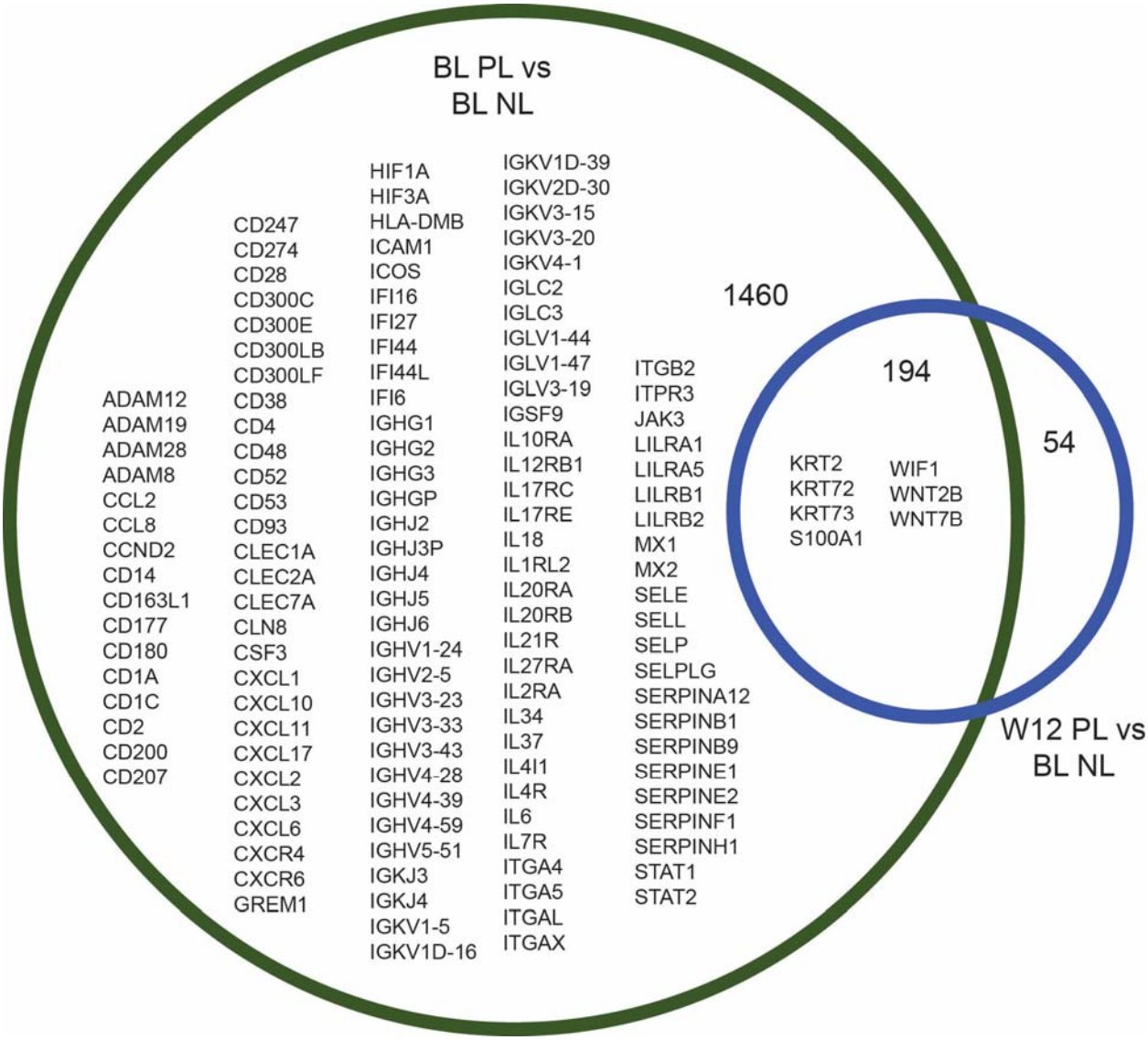

Figure 47: Proteins modulated by treatment at week 12 in perilesional skin.
Select immune-related DEGs in PL skin at baseline versus at week 12, both relative to NL skin at baseline. Numbers designate the total number of DEGs.

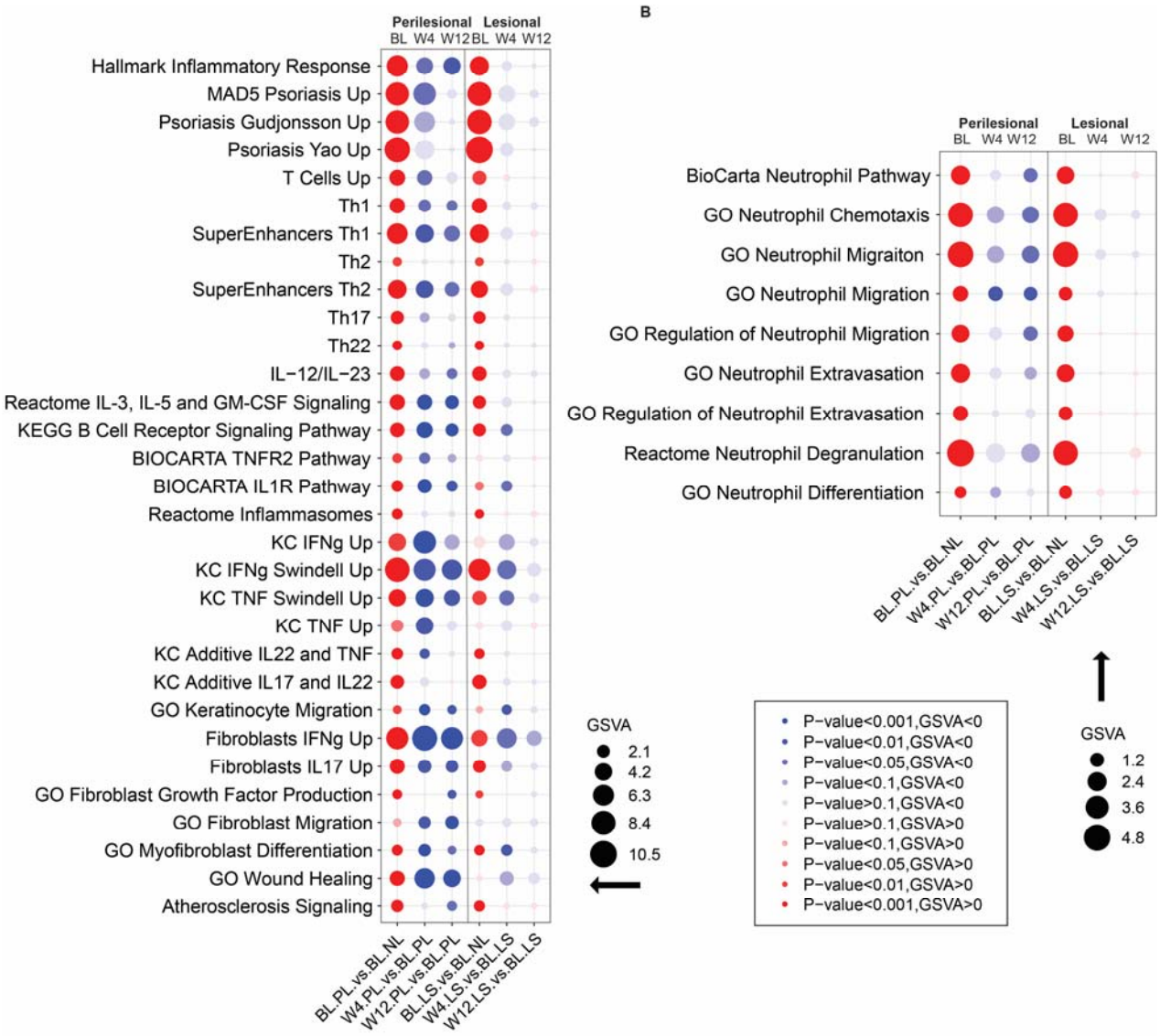

Figure 48: Altered immune pathways in HS skin with treatment.
A) Decrease of overall inflammatory response, known psoriasis pathways and pathways involved in keratinocyte proliferation at week 4 and week 12 following treatment **B)** Decrease of neutrophil-associated pathways following treatment with brodalumab. W=Week.. The size of the bubble diameter is proportional to the GSVA score, and the bubble color indicates significance (P value).

Using uncorrected p values, we detected several downregulated transcripts in perilesional skin at week 12 compared to perilesional baseline skin, with downregulation of several immunoglobulin transcripts and a decreased infiltration of naïve B cells into perilesional skin with treatment (Figure 49).

A

Gene	FCH	P Value
IGHV2-26	**-5.53**	**0.0161**
IL6	**-5.03**	**0.0058**
IGHV1-24	**-4.92**	**0.0235**
CSF3	-4.9	0.0614
IGHG1	-3.8	0.0507
IGKV3-20	**-3.78**	**0.0393**
LILRA5	**-3.77**	**0.0253**
IGKV2D-24	**-3.76**	**0.0422**
IGKV1-12	-3.7	0.0503
IGKV1-39	-3.47	0.0583
TREM1	-3.46	0.0505
IGKV3-15	-3.32	0.0534
IGLV1-44	-3.28	0.0741
IGHG4	-3.21	0.193
IGLV3-19	-3.11	0.105
IGHV4-31	-3.09	0.13
PTX3	**-3.09**	**0.013**
IGHV2-5	-3.07	0.0978
IGHV4-59	-3.04	0.0812
CD177	-3.02	0.096
IGHV3-53	-3	0.108
IGHV3-11	-2.98	0.0957
TGM2	**-2.98**	**0.00417**
GREM1	**-2.97**	**0.00034**
IGKV3D-20	-2.95	0.0841
PRG4	-2.95	0.0687
IGHV3-49	-2.94	0.132
IGKV6D-21	-2.93	0.139
IGLL5	-2.91	0.129
IGLV2-14	-2.91	0.0871
IGHG3	-2.89	0.169
IGKV4-1	-2.88	0.0643
IGHJ2	-2.87	0.0717
IGHV3-73	-2.85	0.159
IGLV2-23	-2.84	0.111

B

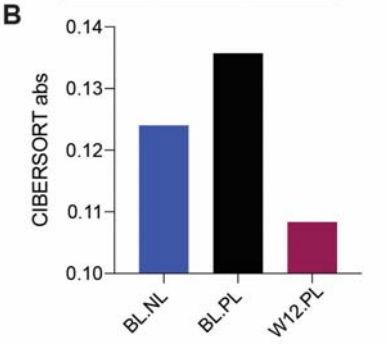

Figure 49: Perilesional skin has a decrease of immunoglobulin-related genes.
A) The top downregulated genes based on FCH at week 12 in PL skin compared to baseline PL skin. Genes in bold are those with a p value ≤0.05 **B)** CIBERSORT fraction of infiltration of naïve B cells into HS skin at BL and Week 12.

6.2.3 Treatment response is better appreciated in perilesional skin

Treatment improvement measures the extent to which posttreatment perilesional and lesional skin transcripts approach baseline nonlesional levels, wherein 100% improvement corresponds to baseline nonlesional level of transcripts in posttreatment perilesional and lesional skin. We thus calculated the improvement for pathways modulated with treatment[53]. There was modest improvement from baseline at Week 4 (Figure 50). No significant differences between improvement in perilesional and lesional skin were observed. We note that at week 4, there were no DEGs in perilesional or lesional skin compared to nonlesional skin at baseline.

At week 12, there was a significantly higher improvement observed in perilesional compared to lesional skin (Figure 51). Given that perilesional and lesional skin had no DEGs at baseline, this data further suggests that a better treatment response is observed in perilesional skin. There was a gradual increase of improvement between from week 4 to week 12 in multiple pathways in perilesional skin, including neutrophil-related pathways (neutrophil chemotaxis, neutrophil migration, degranulation), psoriasis related pathways and pathways related to atherosclerosis signaling (Figure 52).

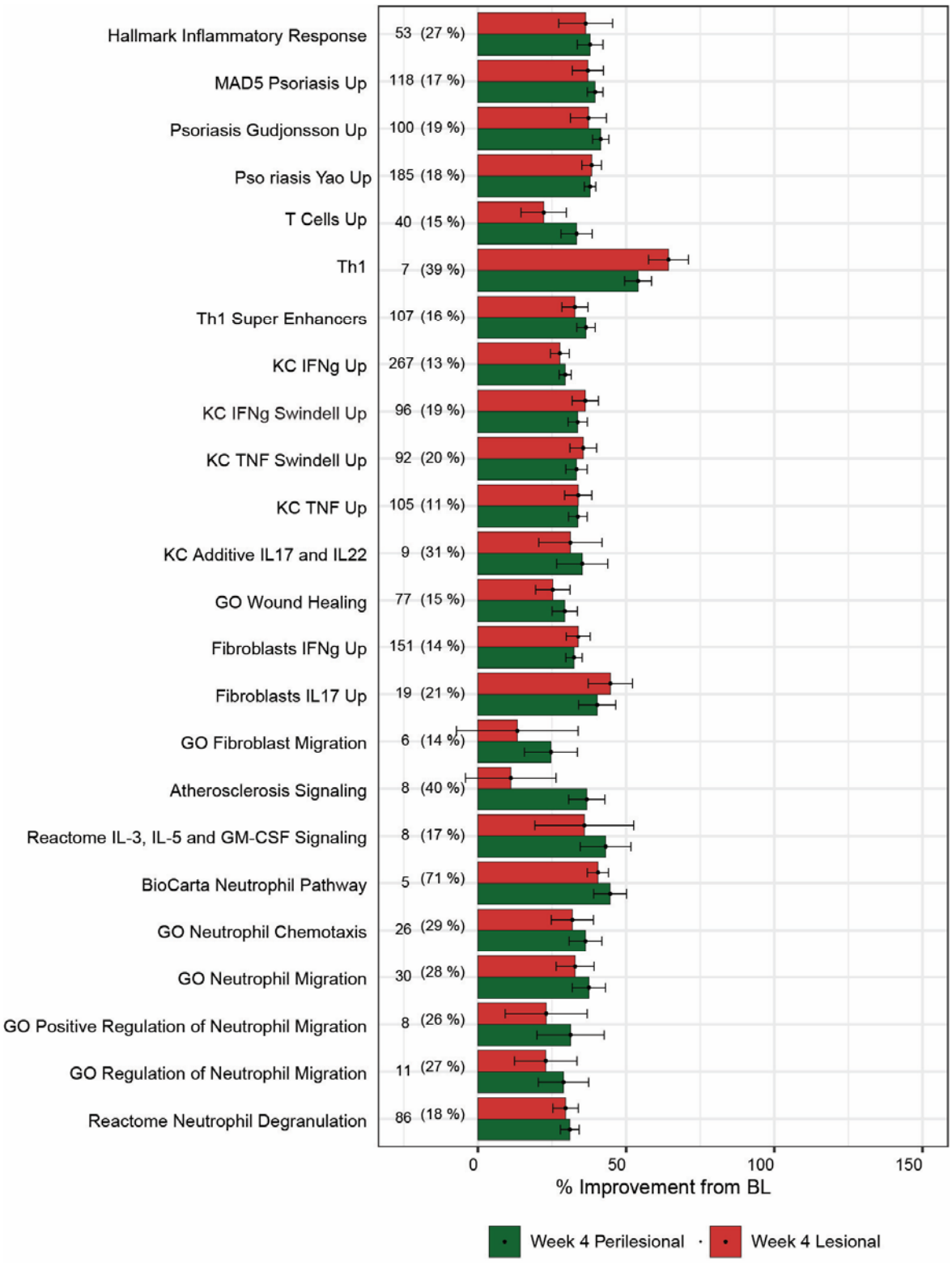

Figure 50: Comparing treatment response at week 4.
Means of percentage improvement week 4 between PL and LS skin. n/N=number of genes HS transcriptome/number of genes in the pathway gene set.

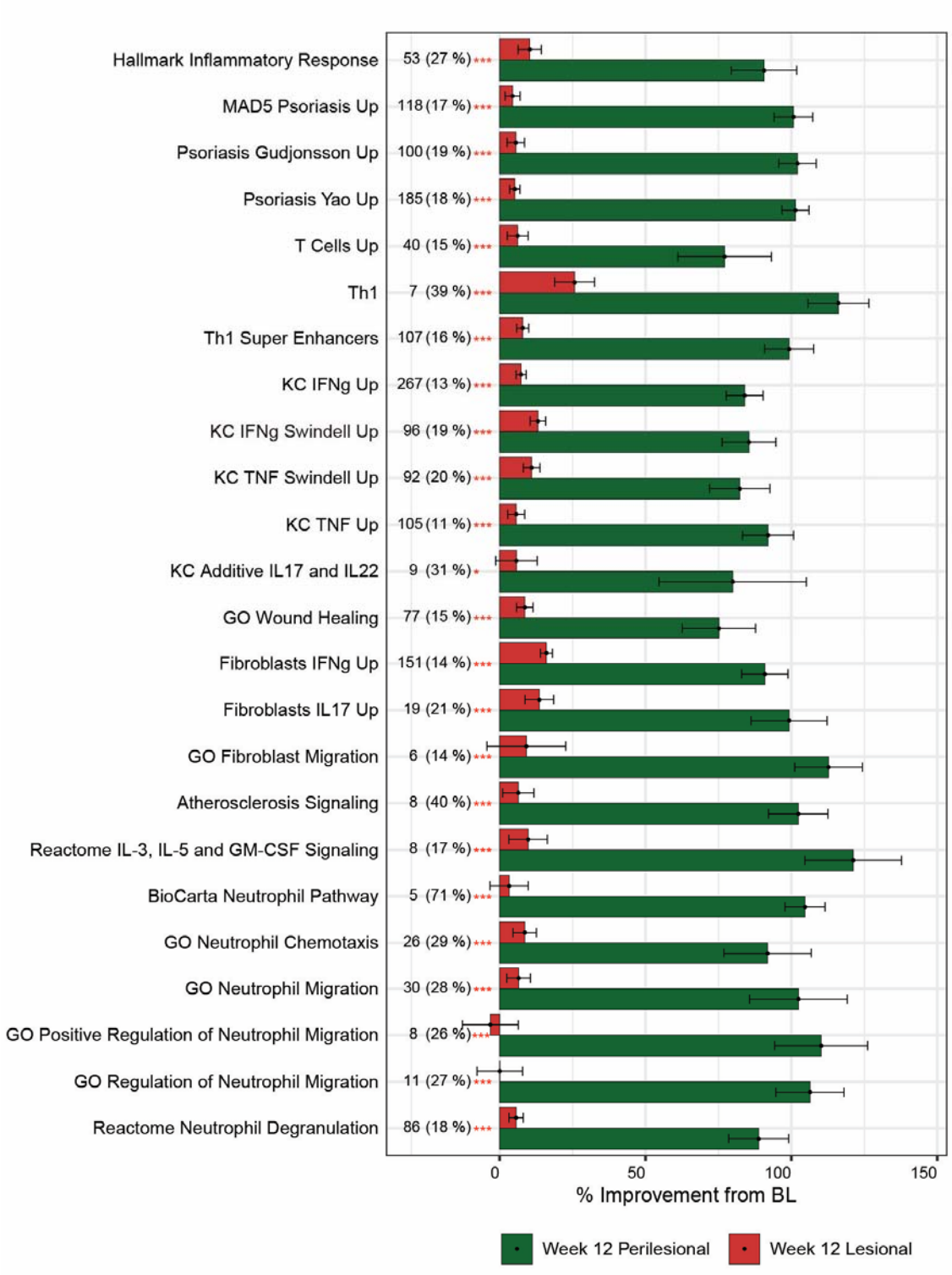

Figure 51: Treatment response at week 12.
Means of percentage improvement at week 12 between perilesional and lesional skin. n/N=number of genes HS transcriptome/number of genes in the pathway gene set, the red stars denote significance of improvement between the two sample types.

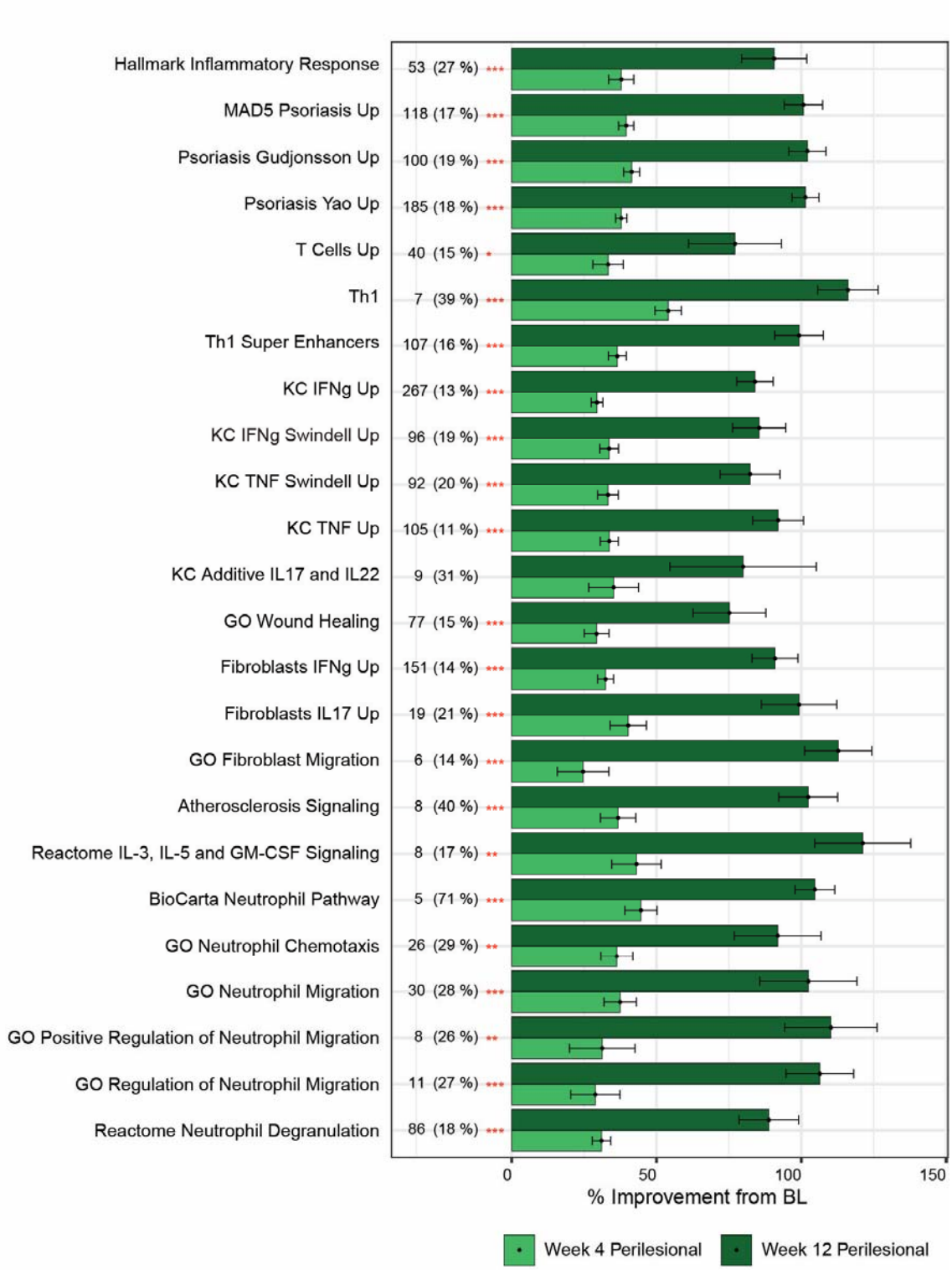

Figure 52: Treatment response at week 4 and 12.
Means of percentage improvement in perilesional skin between week 4 and week 12. n/N=number of genes HS transcriptome/number of genes in the pathway gene set, the red stars denote significance of improvement between the two sample types.

6.2.4 Treatment with brodalumab leads to decreased inflammatory infiltration in the skin

We then assessed the histopathologic changes following brodalumab treatment. Consistent with our previous investigations, we did not find a significant difference between histological properties of lesional and perilesional skin at baseline (manuscript under review). We observed a reduction in epidermal thickness in both lesional and perilesional skin at week 4 and week 12. There was a significant reduction of CD3 and CD11c infiltrates compared to baseline in both perilesional and lesional skin. Epidermal infiltration of CD11c observed in lesional skin at baseline was resolved with treatment (Figure 53).

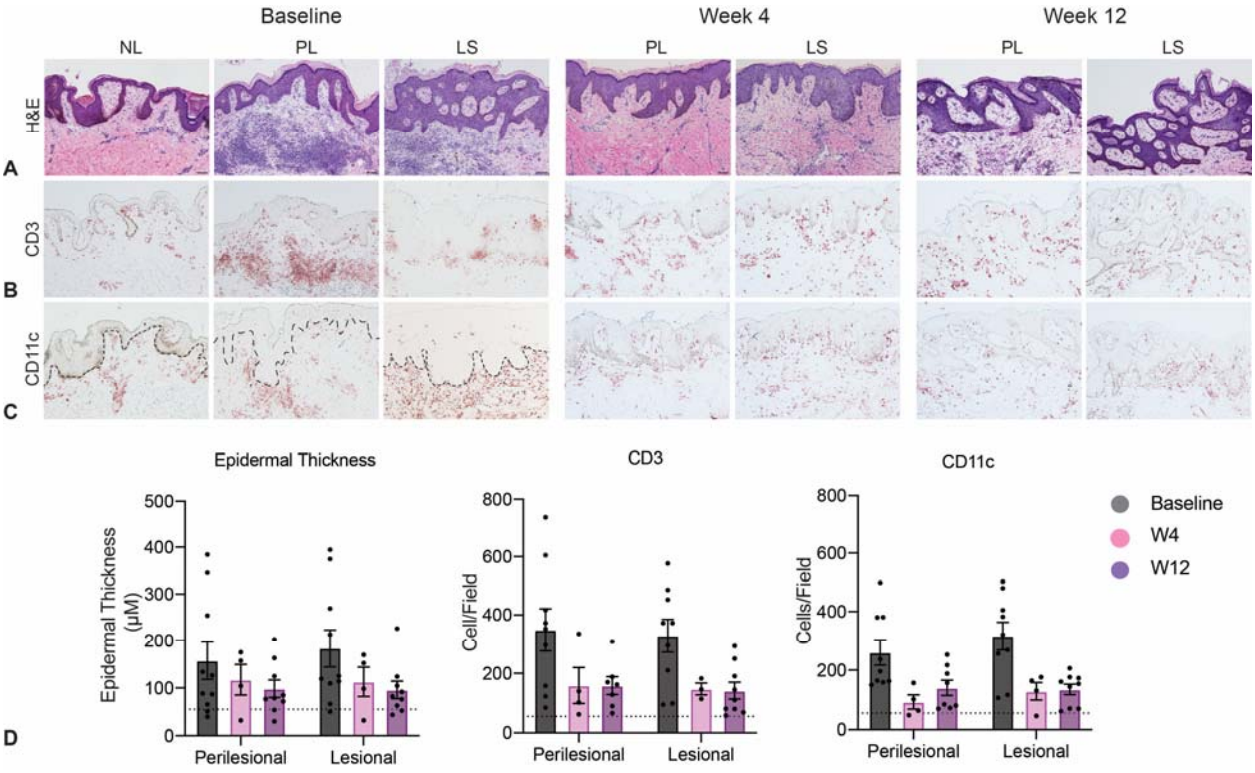

Figure 53: Brodalumab decreased inflammatory infiltration in HS skin.
A) H&E stain demonstrates a mild reduction in epidermal thickness in lesional skin. There is also comparable reduction of **B)** T cell marker CD3 infiltration in both perilesional and lesional skin. **C)** myeloid cell marker CD11c Scale bar = 100 μM. **D)** Quantification of total inflammatory infiltration across the patient cohort. Dashed line represents infiltrate quantification of nonlesional skin at baseline. Error bars show SEM. Stars denote significance with * $p \leq 0.05$ ** $p \leq 0.01$ *** $p \leq 0.001$.

6.2.5 Brodalumab treatment yields a decrease of granulocyte-related pathways in serum

Using Olink high throughput proteomics, we assessed 368 inflammation-, cardiovascular- and cardiometabolic-related biomarkers in serum. Pathway analysis of all downregulated proteins at both week 4 and week 12 showed an enrichment of downregulated pathways related to TNF response, neutrophil chemotaxis (granulocyte chemotaxis, neutrophil migration, granulocyte migration) and general inflammatory response (myeloid leukocyte migration, leukocyte chemotaxis, inflammatory response) (Figure 54A). Differentially expressed proteins (DEPs) in the serum were defined using a criteria of FCH≥|1.5| and $p \leq 0.05$. At week 4, HS serum had 5 down- (CASP-8, macrophage inflammatory protein 1 CCL3/MIP-1α, IL8, ITGB1BP2, monocyte-chemotactic protein 3 MCP3/CCL7) and 3 up-regulated (IL-17A, IL-17C, IL-17RA) DEPs, and at week 12 there were 2 down (FABP2, TNF)- and 4 up-regulated DEPs (FGF-21, IL-17A, IL6, PRSS2), both relative to baseline (Figure 55B).

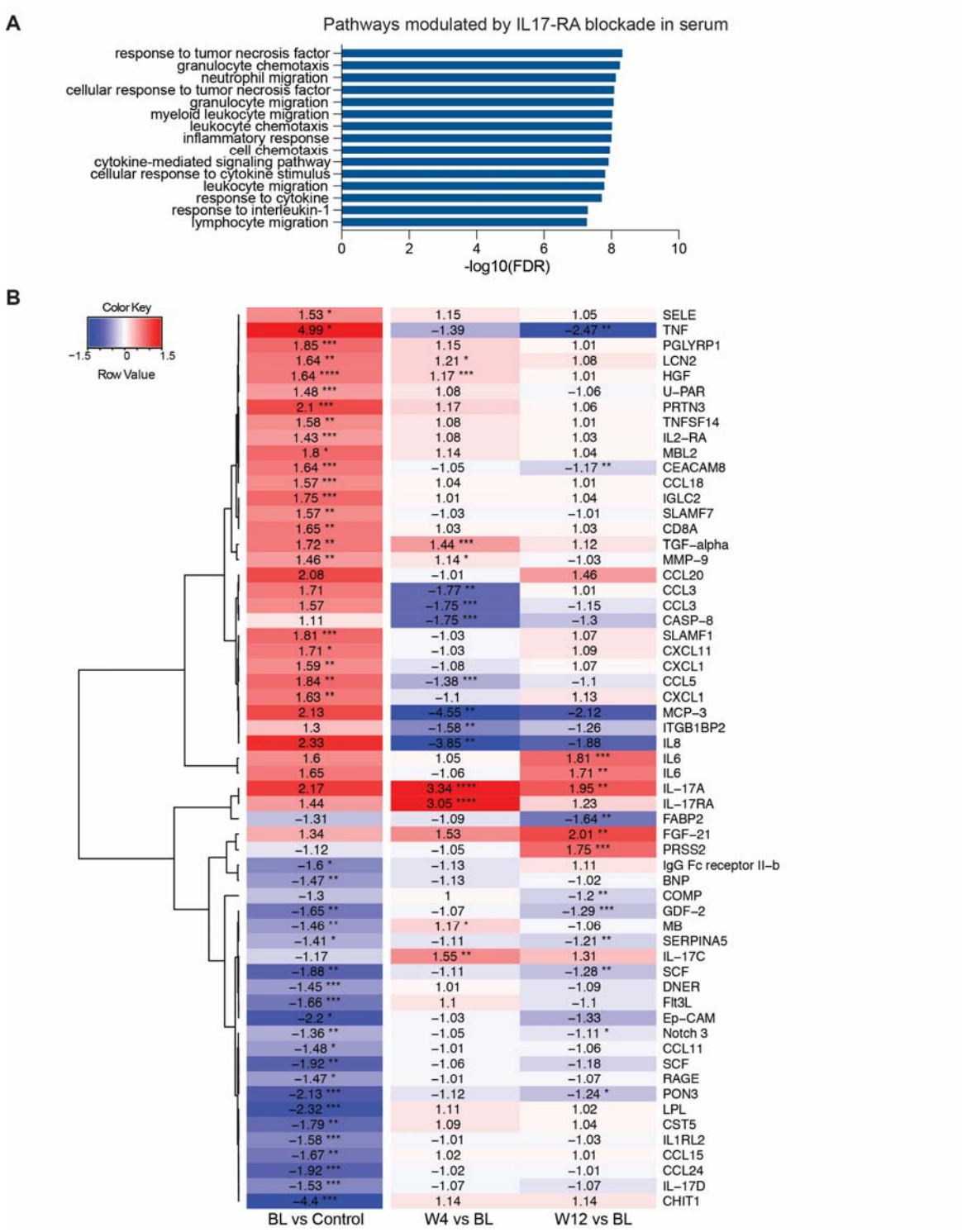

Figure 54: Assessment of pathways modulated in serum by brodalumab treatment. Enrichment analysis of all proteins downregulated in serum with treatment at week 4 and 12 based on PANTHER-Slim GO biological processes. **B)** Heatmap of all differentially expressed proteins (FCH≥1.5, p≤0.05) at Week (W) 4 and 12. Stars denote significance with * $p \leq 0.05$ ** $p \leq 0.01$ *** $p \leq 0.001$.

6.2.6 Higher expression of LCN2 in skin and IL-17A in serum correlates with greater decrease of inflammatory cytokines in skin with treatment

The heterogeneous nature of HS presents a challenge to therapeutic management. We therefore asked whether we could use a biomarker to stratify patients that may have a better molecular response to treatment. Given the decrease of neutrophilic signatures in both skin and blood following treatment with brodalumab, we focused on neutrophil-associated biomarkers. Neutrophil gelatinase-associated lipocalin (LCN2) is expressed in neutrophils, and can be used to identify a more inflamed and neutrophilic subtype in skin and serum (manuscript under review) [213]. Consistent with this, patients with higher LCN2 levels in lesional skin at baseline had a greater decrease of inflammatory markers implicated in HS pathogenesis (IL1B, IL36G, LCN2, TNF) in perilesional skin at Week 12 (Figure 6A). IL-17A is an inducer of LCN2 [284-286]. Since IL-17A serum concentration are commonly measured as evidenced by its commercial use, we asked whether we could use baseline IL-17A expression to identify patients that will have a greater molecular response in the skin. Patients with higher IL-17A expression in serum also had a greater decrease in inflammatory cytokines in perilesional skin at week 12 (Figure 6B). Taken together, these data suggest that patients with high baseline expression of neutrophil-related LCN2 in the skin and IL-17A in the serum may have a greater molecular response to brodalumab therapy.

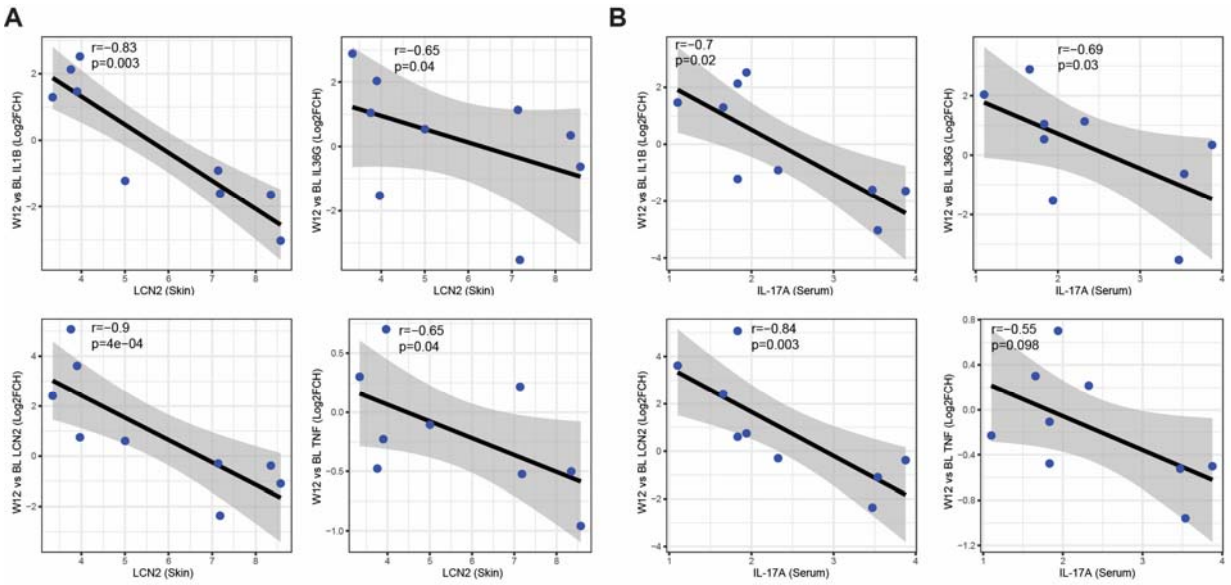

Figure 55: Correlation of potential markers with molecular disease activity at week 12. **A)** Expression of LCN2 levels in lesional skin and **B)** expression level of IL-17A in serum correlates with a decrease of inflammatory markers at Week (W) 12 in perilesional skin. r is Spearman correlation. X axis is log2(Expression).

6.2.7 IL-17RA blockade with brodalumab decreases tunnel size and drainage

Treatment with IL-17RA antagonist brodalumab at a dose of 210mg/1.5mL subcutaneously every 2-weeks has been demonstrated to ameliorate the clinical manifestations of disease [203]. The impact of biologic therapy on HS tunnels has not been studied. We asked whether tunnels can be modulated therapeutically. Throughout this trial, Doppler ultrasonography of HS skin was performed at Baseline, Week 4, Week 12 and Week 24. We analyzed the tunnel size and inflammation (as measured by Doppler intensity) prior and following treatment with brodalumab. In the baseline reading, a wide lumen of the tunnel (white arrow) and major Doppler signal is evident within the deep dermal tunnels but not the epidermis (Figure 56A). Following treatment, the tunnel wall thickness as well as the tunnel diameter was significantly decreased following treatment ($p<0.001$) (Figure 56B-C). There was also less power Doppler intensity following treatment, suggesting that tunnels displayed less inflammation with IL17-RA blockade ($p<0.001$) (Figure 56D).

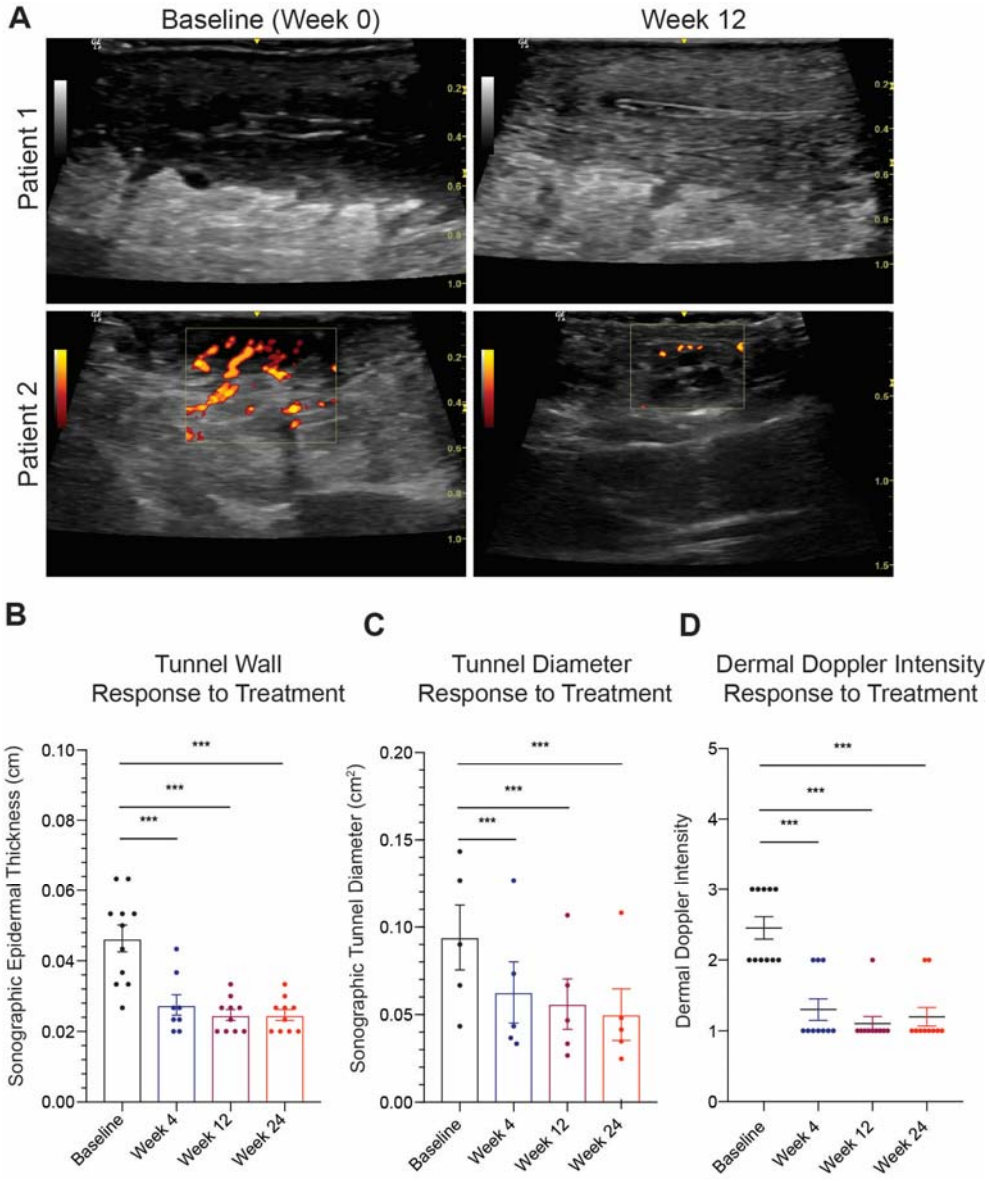

Figure 56: Tunnels are therapeutically targetable.
A) Tunnels in HS dermis express IL-17 family cytokines. **B)** Doppler Ultrasonography representing reduction in tunnel diameter and doppler intensity following 12 weeks of treatment with IL-17 receptor antagonist. **C)** There is a significant decrease in tunnel wall **D)** tunnel diameter and **E)** dermal doppler intensity following treatment with IL-17 receptor antagonist. Decrease in tunnel inflammation is seen as early as 4 weeks. Results are the mean ± SEM, FCH is shown. *p<0.05, **p<0.01, ***p<0.001[99].

6.3 Discussion

A pathogenic role for IL-17 and Th17 T-cells is suggested by preliminary studies conducted with secukinumab and brodalumab, which demonstrated clinical improvements [63-65, 71, 186, 203, 271]. IL-17 effects on epithelial cells in epidermis and tunnels may be particularly important in HS as there are marked upregulation of products including IL-17C, CXCL8/IL-8 and IL-36 isoforms that are produced in IL-17 activated epithelial cells [42, 99, 148, 151, 152, 168]. However, in the context of the disease that displays connective tissue pathology and significant B cell infiltration, IL-17 may also have important effects on these cell types[101, 102, 182, 287-292]. Consistent with this, we identify several pathways significantly modulated by brodalumab in HS including overall decrease of inflammatory response and psoriasis-related pathways. In addition to decreased neutrophil pathways in the skin, we also observed a reduction in granulocyte and neutrophil chemotaxis and migration pathways in the serum with treatment. Dermal IL-17 can recruit neutrophil migration towards affected areas[293]. Consistent with this, IL-17 pathway antagonists have been shown to be effective in patients with generalized pustular psoriasis, a disease that is also dominated by neutrophilic inflammation[101].

Recent work has reported the attenuation of a B cell response following anti-TNF therapy [101, 102]. Involvement of B cells, plasma cells and fibroblasts only recently became acknowledged as potentially important in HS pathogensis[47, 101, 102, 107, 182]. Our data demonstrates a decrease in infiltration of naïve B cells following treatment with brodalumab. The multitude of pathways modulated by IL-17RA blockade suggests that IL-17A may be a critical node in the multidimensional axis underlying HS pathogenesis. Furthermore, previous mechanistic studies of skin and/or serum following treatment with apremilast, infliximab and ustekinumab in HS were not able to identify a significant singular biomarker of treatment response [115, 170, 205, 294]. Beyond interaction of IL-17 pathway with innate cytokines, inflammation in HS may also be contributed by B cells and complement activated cascades, making the identification of cohesive treatment biomarkers more difficult than it is in psoriasis which is driven a singular inflammatory axis. As such, research looking at pathways rather than individual gene/protein biomarkers may be useful. In our study we found treatment response biomarkers that satisfied individual p value thresholds but did not meet the specified FDR threshold. However, many individual markers are interrelated by inflammatory response pathways that are well understood from other diseases. Thus, the pathway approach that we took has more power to determine disease associated or treatment associated changes in inflammation.

Further work is needed to determine whether innate cytokines interact with IL17 to produce a feed forward inflammatory pathway as is the case in psoriasis, or whether these are independent inflammatory pathways that may be dominant in different subset of patients, leading to the question of whether targeted treatment based on HS subtypes may be needed in HS. In our cohort, patients with high LCN2 in lesional skin had greater decreases in neutrophil-related cytokines (IL36G, IL1B) following treatment, suggesting that brodalumab likely targets the neutrophil-related component of HS in this HS subtype. Future larger scale studies are needed to link these observations with outcomes but reduction in the overall inflammation in skin would be expected to lead to a decreased clinical burden.

The decision of which site to biopsy is critical for assessment of molecular response in therapeutic trials. Biopsying a target nodule may hasten its resolution unrelated to the use of a

therapeutic agent[170]. Additionally, due to the cyclical nature of HS, the regression to the mean phenomenon must be considered at an individual level [170, 230, 295]. At a given time, a lesion may spontaneously improve, and thus biopsying the index or the lesional site may also produce a false positive treatment result. Our biopsy methods are based on proposed lesional definitions and are the only suggested biopsy guidelines for therapeutic trials in HS. Biopsy of perilesional skin which displays molecular and cellular pathology comparable to the main inflammatory lesion, may be preferable and the results of this study show that larger treatment responses can be measured in sequential biopsies of the larger area of perilesional skin.

The limitations of this study include a small cohort size and the lack of a placebo-controlled group. Another limitation is that kinetics of IL-17RA saturation by brodalumab have not been established and it is possible that our posttreatment biopsies were performed at a timepoint when IL-17 receptor saturation was incomplete as patients tended to have an increase of clinical symptoms towards the end of a two-week treatment cycle, which is when biopsies were collected. Receptor mediated clearance of brodalumab in HS might be increased due to the high neutrophil production and relatively short lifespan of neutrophils, as neutrophils express high levels of IL-17RA[203]. Furthermore, the decision to biopsy active inflammatory nodules during brodalumab treatment may have limited the ability to define change as active lesions regressed at other sites.

Treatment with brodalumab modulates several pathways consistent with multi-axis disease pathogenesis. Our data demonstrates that neutrophil-related biomarkers can be used to identify patients that may have a better molecular response to Brodalumab. Furthermore, this study demonstrates that perilesional skin may be used to assess molecular response in therapeutic trials of HS. Given that perilesional skin is roughly ten times the area of a lesional nodule, this allows for a greater area for biopsying without the concern of a biopsy hasting resolution of an active inflammatory nodule.

CHAPTER 7:
General Discussion

CHAPTER 7. General Discussion

7.1 Overview

Despite the reported prevalence 0.03-8%, the heavy burden on the quality of life and an increased risk of all-cause mortality, HS remains a poorly understood and greatly understudied disease [1-3, 5]. As of 2018 there have been only 17 clinical trials specific to HS, with only one approved biologic therapy - a stark comparison to other chronic skin diseases with hundreds of reported trials in psoriasis and AD [296]. This highlights the dire need for translational studies into disease pathogenesis that will lead to the development of novel biomarkers and therapeutic targets in HS.

The accepted pathogenic model of HS is shifting away from the idea of a primary follicular occlusion event to a model of complex interplay of several inflammatory axes and an aberrant immune response driving disease pathogenesis. Unlike other systemic inflammatory skin diseases, HS has a strong dermal involvement marked by inflammatory infiltration and immunologically active epithelialized tunnels [99]. Until recently, there has been no standardized approach to study HS skin [86]. This was particularly limiting in the setting of HS as a superficial biopsy may miss dermal inflammation and tunnels, while lack of site matched biopsies may overestimate the inflammatory contributions in the setting of topographical variation of IL-17-associated mediators.

7.2 Dermal tunnels are active contributors to disease pathogenesis

HS tunnels, also known as sinus tracts, are associated with more advanced disease[30, 38]. This concept is incorporated by all three major HS staging systems, and most underscored by the IHS4 scale, which assigns a 4x weighted score to the presence of a tunnel compared to an inflammatory nodule[28]. However, whether HS tunnels are immunologically active has not been studied in detail. One study identified the presence of active biofilms, suggesting that sinus tracts may serve as anoxic cavities creating an excellent environment for bacterial growth[196]. This was further supported by increased expression of IL-8, IL-16, VEGF, IL-1β in the gelatinous material in HS tunnels as well as MMPs and TNF-positive cells [189, 297]. These studies first introduced the idea that these cytokines could lead to the recruitment of neutrophils, T cells and macrophages into the tunnel's epithelium. However, whether the tunnel epithelium itself is immunologically active, or is a merely anatomic feature caused by tissue destruction that serves as a conduit for drainage has been unanswered by previous research. Furthermore, it was unknown whether tunnel epithelium produces these pro-inflammatory cytokines or if they are a byproduct of the immune response to the bacterial biofilm.

Our work is the first to perform an in-depth characterization of tunnel epithelia. We show that tunnels are immunologically active contributors to disease pathogenesis. The IL-17 axis has been implicated in both HS and psoriasis, and our work expands on this by demonstrating that a similar feed-forward mechanism is observed within the tunnel epithelium (Figure 57) [53]. The response of keratinocytes to IL-17 is self-amplifying, and leads to the development of epidermal hyperplasia, recruitment of immune cells and overproduction of IL-17 induced keratinocyte-derived molecular products including S100A7 and LCN2, both of which are elevated in HS patients and even more so in patients with tunnels. The CXCL1 and CXCL8 gradient likely drives transepithelial neutrophil recruitment and the feed-forward inflammatory loop, and also contributes to the development of IPGM observed in HS (Figure 57). This has direct relevance to

therapeutic strategies. Studies have shown that patients with dermal tunnels require a longer time to achieve a clinical response with adalimumab [169, 204]. In this context, our work suggests that either higher-dose (as seen with high-dose infliximab treatment) or combination therapies are needed for patients with tunnels due to the increased inflammation generated by both the epidermal and tunnel epithelia [66, 99]. Currently, biologics are reserved for patients whose disease did not respond to alternative therapies such as antibiotics [298-302]. Given that the tunnels are active contributors to disease and are therapeutically targetable, this raises the question of whether biologics which target cytokines identified in the tunnel epithelium (including IL-17 family cytokines) may be useful in earlier stages of disease in order to prevent tunnel growth and subsequent disease progression that is at least partially contributed to by the amplification of cytokines within the tunnel epithelia.

Mechanisms underlying tunnel formation remain poorly understood. One study suggested that keratinocyte outgrowth from the follicular outer root sheath may contribute to tunnel formation[182]. Given that tunnel deroofing leads recurrence in 14.5% of cases, regenerative properties of tunnel epithelia must be considered[303]. We observed an increase of growth factors (including HGF, which is a known inducer of epithelial cell migration) and wound healing pathways in our skin transcriptomic and serum proteomic data[130, 132]. Whether these factors contribute to tunnel formation and recurrence following deroofing (likely due to potential regenerative properties associated with the epithelia) must be explored.

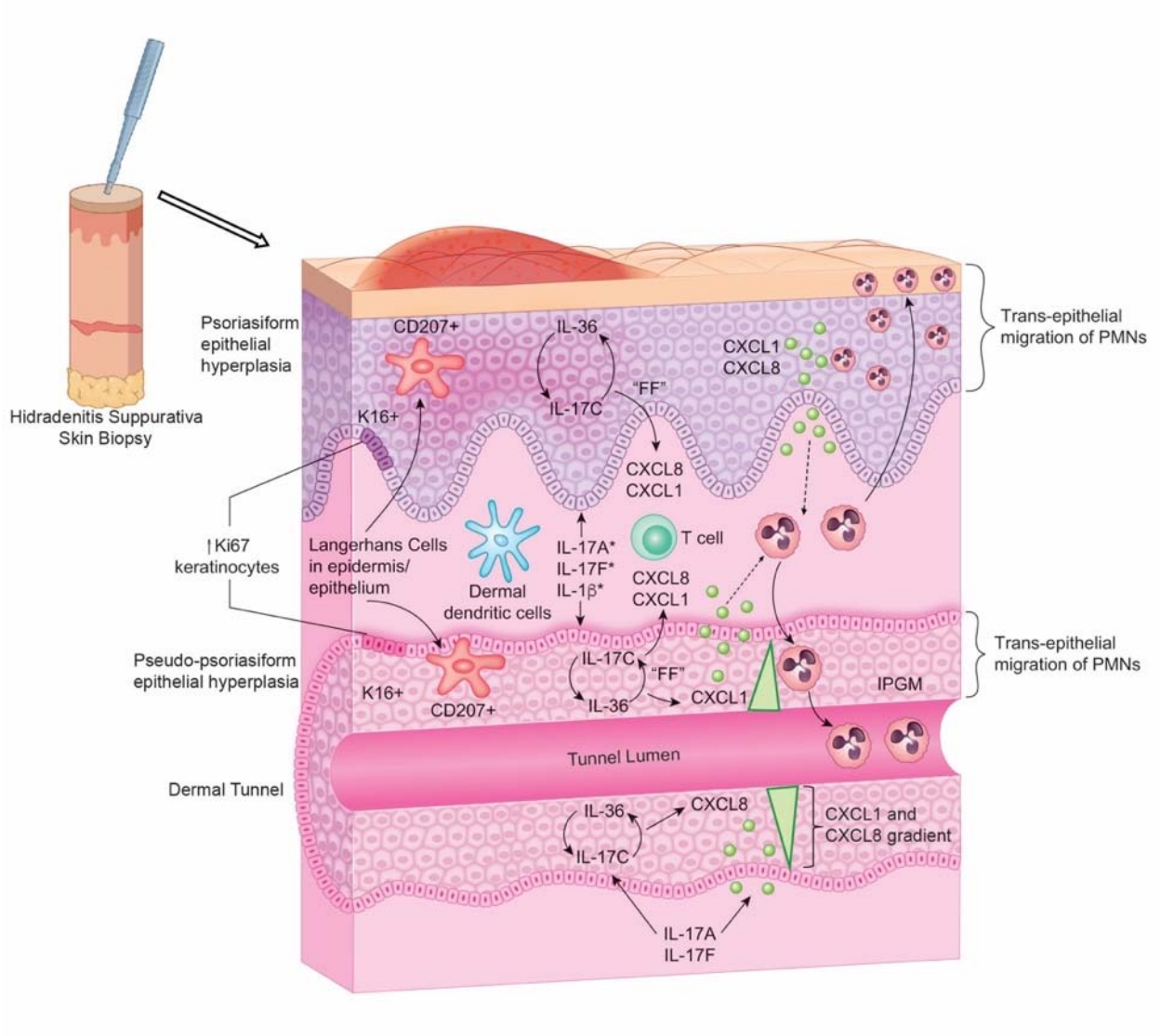

Figure 57: Model of inflammation in HS dermal tunnels and epidermis.
Dermal tunnels in HS are epithelial structures that likely drive recruitment and infiltration of neutrophils through the production of CXCL1 and CXCL8 chemokines, which is further amplified by IL-17 [99].

7.3 Stratification of HS into a neutrophil-rich tunnel-high endotype and implications for targeted therapy

Precision medicine in the context of phenotypes, endotypes and genotypes has been best studied in allergic disease and AD. Disease phenotype can be classified based on visible manifestations including age of onset, lesion type, and inflammatory subset. However, disease phenotypes are often fluid and subject to change over time, and do not give insight into the pathogenic mechanism[304, 305]. As such, the field of AD has shifted towards defining disease endotypes, in which the pathogenic mechanism underlying the visible phenotype becomes the center of therapeutic targeting [306 307].

Our data argues for the presence of a neutrophil-rich, tunnel-positive endotype in HS. There are multiple layers of evidence that suggest a neutrophil-high HS subtype (and potentially endotype). Resting neutrophils can be primed by several cytokines and chemokines including TNF, G-CSF, CXCL8/IL-8 and IFNγ, all of which are elevated in HS skin and blood. We identify LCN2 as a biomarker associated with neutrophil-high subtype. LCN2 is a secreted protein found in neutrophil secondary granules and is also expressed by granulocytes and keratinocytes in HS [308, 309]. LCN2 can stimulate neutrophils to produce proinflammatory cytokines including IL-6, CXCL8/IL-8, TNF, all of which are elevated in HS [286]. TNF can then induce LCN2 expression in keratinocytes. Together, this creates a feed-forward loop where LCN2 promotes downstream secretion of proinflammatory cytokines which in turn can stimulate further LCN2 expression. Our work and others have reported positive correlations between LCN2 and disease severity (as measured by Sartorius score and IHS4) and the number of body areas affected by HS [58]. We expand on this finding by demonstrating that patients with high LCN2 levels in the serum have histologically confirmed deep dermal tunnels, further highlighting the blood-skin interaction and tunnels as a contributor to inflammatory burden.

Evidence has shown that LCN2 promotes neutrophil recruitment through induction of granulocyte colony-stimulating factor (G-CSF/CSF3) during acute and chronic mycobacterial pulmonary infections[310]. CSF3 is a major cytokine regulator of neutrophils which stimulates production of neutrophils in bone marrow as well as neutrophil mobilization in the circulation [311]. Consistent with the elevated LCN2 levels in HS skin, our work and a previous study identified an elevation of CSF3 in HS skin and blood, respectively [167]. Similar to LCN2, IL-17 (which is also elevated in HS skin) can induce production of CSF3 by keratinocytes and fibroblasts [167]. Taken together, our data argues for a model wherein increased production of CSF3 by fibroblasts and keratinocytes (including tunnel keratinocytes) in the skin contributes to ongoing inflammation within lesional skin, neutrophil production/recruitment, as well as tissue destruction [167]. CSF3 in the blood can contribute to neutrophil production and release at bone marrow. Neutrophils may then be recruited to lesional skin by increased CXCL1 and CXCL8 produced by epidermis and tunnel epithelial (Figure 58). In addition, other (non-chemokine) inflammatory factors that attract neutrophils including complement fragments (complement C3a and C5a), leukotriene (LTB4), and matrix metalloproteinases (MMPs) are also elevated in HS [41, 44, 311, 312].

Our work identified several targetable molecules in the LCN2 high HS endotype including Janus Kinase (JAK)-3[313]. Inflammatory signaling pathways rely on JAK3 signal transducers and activators of transcript (STAT) pathway for signaling[314]. Cytokines that signal through JAK3 include IL-2, IL-4, IL-7, IL-9, and IL-15, and some of these have been elevated in our transcriptomic data. Inhibition of JAK3 may provide therapeutic benefit, as cytokines that signal through this transducer broadly support T cell activation and survival. These cytokines also signal through receptors that utilize JAK1 as a co-signaling molecule. JAK1/2 inhibitor baricitinib and JAK1/3 inhibitor tofacitinib have shown efficacy in dermatologic diseases including psoriasis[315, 316]. There is preliminary evidence for the role of JAK inhibition in HS, with a small case series demonstrating efficacy of tofacitinib in patients who did not respond to infliximab[317].

Taken together, our data suggests that the neutrophil-rich tunnel-positive subtype of HS may be an endotype that is driven by the LCN2 -CSF3-neutrophil signaling axis (Figure 58). Our clinical study provides the first evidence for the utility of such HS stratification in the context of

treatment response. Because we are largely limited by our patient size in this clinical study (n=10), a lack of placebo-controlled arm and no long-term outcome data, we focused on molecular change rather than correlation with clinical response. Our data demonstrates that patients with high expression of LCN2 in the skin and IL-17A in the serum have a greater reduction of known HS mediators in the skin at week 12. The reduction of these inflammatory mediators is likely also responsible for the decreased clinical activity we observed during the trial. Further large-scale clinical trials are necessary to assess whether patients with this HS endotype respond better to IL-17 blockade.

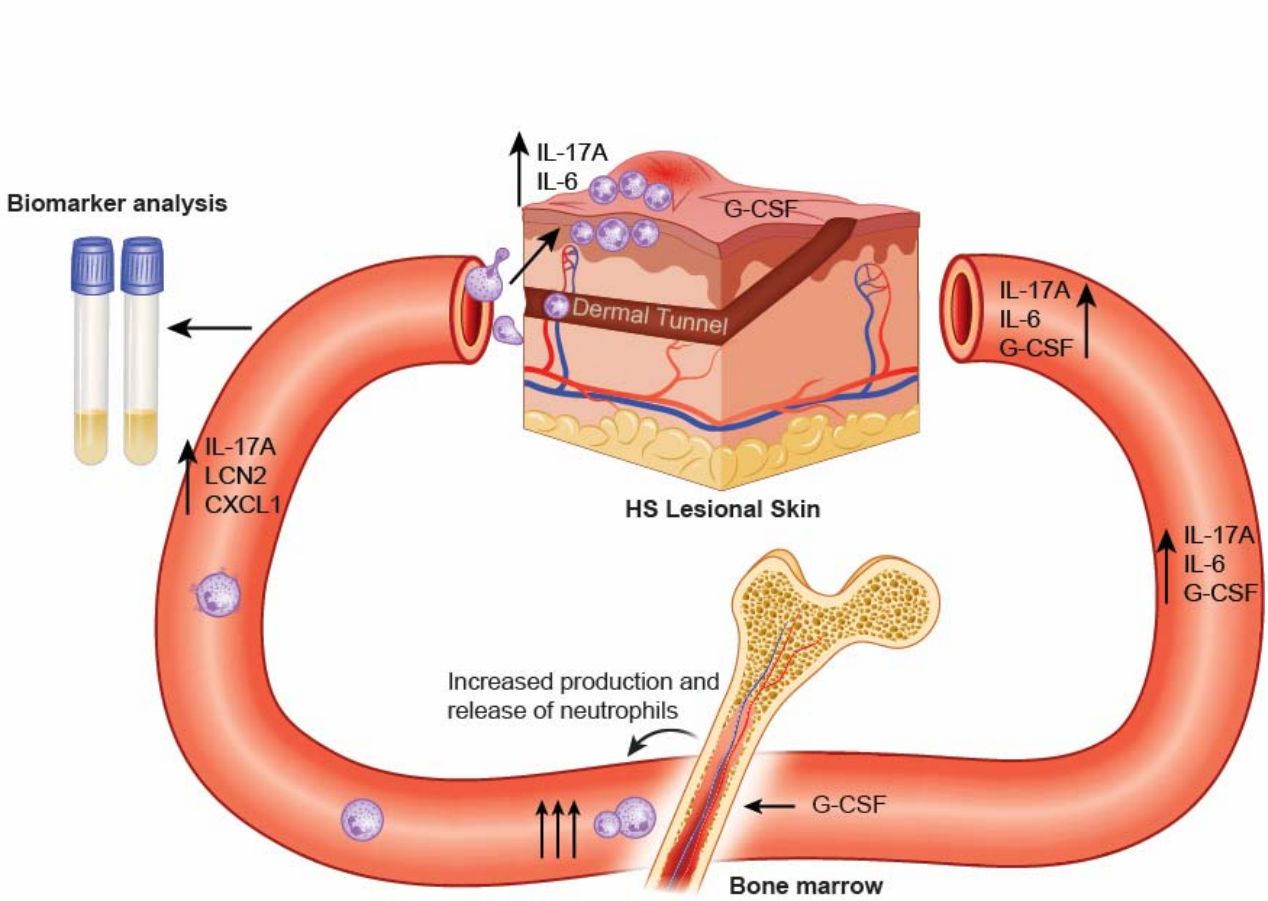

Figure 58: Crosstalk between HS skin and blood.
HS nodules produce IL-17A and G-CSF. G-CSF may travel to the blood and act on the bone marrow to promote increased production and release of neutrophils, which are then recruited back into HS lesions[213].

7.4 Perilesional and lesional skin share overlapping features

HS lesional skin is characterized by a large and cellularly-diverse immune infiltration. Whether this infiltration extends to the surrounding perilesional skin has remained inconclusive. There are preliminary reports suggesting that perilesional and lesional skin may be similar with studies reporting elevated level of IL-17A and IL1β mRNA even in healthy-appearing perilesional skin [41,42]. Our detailed transcriptomic, proteomic and histological profiling demonstrated that there were no statistically significant differences between mRNA and protein expression between perilesional and lesional skin. Consistent with our works, others have reported increased levels of

inflammatory mRNA even healthy appearing nonlesional HS skin [42]. This suggests that there is a low-grade immune response occurring globally in HS skin.

Whether perilesional skin represents 'pre-lesional' areas that are developing inflammation prior to the development of visible nodules or is instead a spillover of lesional inflammation remains unknown. Histological and molecular profiling of early-stage (Hurley Stage 1) disease is necessary in order to address the question of whether the inflammation in perilesional and nonlesional skin is a spill-over of disease or precedes (and is an active) contributor of the development of visible nodules and abscesses. If nonlesional and perilesional skin is inflamed even prior to the development of widespread visible lesions, this would suggest that the underlying low-grade inflammation precedes the development of visible lesions, which based on the presented evidence seems likely.

7.5 HS is associated with systemic inflammation

While previous epidemiological studies have suggested a link between HS and systemic metabolic disorder, whether these factors contribute to a proinflammatory state as observed in psoriasis, atopic dermatitis, arthritis, rheumatoid arthritis and atherosclerosis has not been well defined[206, 207, 318-320].The inflammatory milieu in HS skin is characterized by several cytokines that are also pro-atherosclerotic, including IL-1, IL-6, IL-8, IL-17A and TNF. Previous studies have identified elevation of these cytokines in HS serum or plasma, however, whether these cytokines readily exchange with the circulation has been undescribed.

We identified greater dysregulation of several proteins involved in atherosclerotic signatures even in a direct comparison to BMI-matched healthy controls and psoriasis patients further suggesting that the increased risk of cardiovascular disease in HS patients is due to the underlying inflammation rather than present co-morbidities. To further strengthen this point, we identified strong correlations of known markers associated with cardiovascular risk (CHI3L1, PLA2G2A, MMP9 and others) and disease severity (as measured by IHS4). We also observed a strong Th1 signature in both HS skin and serum. Th1 cells have been identified in atherosclerotic plaques and may lead to plaque instability as well as recruitment of other cytokines into the plaques[321]. Interestingly, these signatures were decreased with brodalumab treatment suggesting that treatment of disease activity may be beneficial to patients' long-term cardiovascular risk. We also found a strong skin-blood association suggesting likely diffusion of cytokines between skin and blood. Further studies are necessary to assess whether there is increased permeability of HS vessels allowing for increased communication between skin and blood.

Our data argues that the increased risk of cardiovascular-associated disease in HS may be attributed to HS-induced global immune activation in addition to the known contribution of co-existing comorbidities. Several guidelines have been put forward in recent years suggesting that psoriasis is a cardiovascular-enhancing condition, highlighting the need for increased screening and earlier engagement with primary care doctors/cardiologists [322, 323]. Given the inflammation observed in HS skin and blood, the increase of several pro-atherosclerotic and cardiovascular-risk factors, the role of this inflammation as the causal and underlying factors of cardiovascular events in HS must be explored. Furthermore, long-term outcomes studies are necessary to address whether targeting inflammation in HS reduces long-term cardiovascular risk. Our work with brodalumab provides the direct evidence that modulation of these inflammatory pathways has an

impact on both the skin and blood. Outcome studies are necessary to address whether HS treatment and subsequent decrease of overall inflammation lowers the risk of cardiovascular development.

7.6 Conclusions

In this work, we characterized HS pathogenesis with a particular focus on elucidating the neutrophil- and tunnel-rich disease endotype. We demonstrate that epithelized dermal tunnels are active contributors to disease pathogenesis and are therapeutically targetable. We also demonstrate that HS perilesional skin is similarly inflamed as lesional skin, which has direct impact on the design of future clinical trials. Taken together, the findings of this thesis set the basis for exploring targeted therapies specific to disease endotypes, which will translate to better treatment for patients suffering from this burdensome disease.

CHAPTER 8:
Materials and Methods

CHAPTER 8. Materials and Methods

8.1 Study subject recruitment

Subjects were enrolled under two protocols approved by the Rockefeller University's Institutional Review Board. Written informed consent was obtained from all subjects and the study was performed according to the Declaration of Helsinki Principles. All subjects underwent a rigorous screening, which included medical history, physical examination and complete blood count and chemistries. Study inclusion criteria for HS patients was confirmed diagnosis of HS by the study dermatologist (J.W.F.) in adults (≥18 years of age). Exclusion criteria included a history of Human Immunodeficiency Virus (HIV), Tuberculosis or Inflammatory Bowel Disease, active Hepatitis B or C infection and Pregnancy/Breastfeeding. Patients were required to have a negative test result for HIV, Hepatitis B virus surface antigen, Hepatitis C virus antibody, tuberculosis (measured by QuantiFERON Gold) and pregnancy. Patients had to undergo a washout period of ≥5 half-lives from disease modifying therapies including systemic antibiotics, immunosuppressants or biologics prior to enrollment in the study.

A total of ten patients completed the open-label single center pilot cohort study (clinicaltrials.gov identifier: NCT03960268). On-study patients were administered 210mg/1.5mL subcutaneous injection of Brodalumab (Siliq, Valeant Pharmaceuticals/Ortho Dermatologics). The loading dose involved two weekly injections (Week 0, Week 1) followed by one dose every 2 weeks until the study endpoint (12 weeks). Clinical assessments, blood work (routine hematologic values including hemoglobin, leukocyte and platelet count, and blood collection for biomarker analysis) as well as punch skin biopsies were taken at intervals. HS severity was assessed by the attending dermatologist at baseline, and each visit. Additional patients were enrolled as part of a natural progression of disease study where no treatment was administered. Samples (blood and biopsies) were collected from these patients according to the above guidelines. For both studies, assessment of HS severity was undertaken using several methods including: HiSCR, IHS4, as well as patient- and physician-measured visual analogue scales (VSA) of pain, itch and global severity [26, 28]. Quality of life measurement was assessed by the Dermatology Life Quality Index[324]. Age, BMI or site-matched healthy controls were also enrolled in the study.

Psoriasis lesional and nonlesional tissue for IHC and RT-PCR was from deidentified residual samples of plaque-type psoriasis vulgaris from previous studies in our laboratory, from which clinical characteristics are not available. A psoriasis area severity index (PASI) ≥ 12 (moderate-severe psoriasis vulgaris with ≥10% body surface area involvement) was required for study enrollment.

8.2 Ultrasound-guided biopsies

Cutaneous sonographical assessment of skin and biopsy sites was performed using a multi-frequency linear GE LOGIQ probe (10-22 MHz, GE Healthcare) by the attending dermatologist (J.W.F.). Ultrasound measurements were performed in triplicates, and average values were used for calculations. Power doppler intensity was assessed using semiquantitative method with 1 being no or minimal focal intensity and 3 indicating diffuse high intensity. Dermal tunnel measurement was calculated using the maximum transverse dimension. Skin punch biopsies of 6mm in diameter were obtained under ultrasound guidance from lesional, perilesional and nonlesional skin of HS

patients, and site-matched skin from healthy control volunteers [86]. All samples were de-identified prior to molecular characterization.

8.3 Immunohistochemistry

Frozen slides with skin sections were allowed to air dry for 10 minutes. Slides were fixed in cold acetone for 3 minutes, and then were allowed to air dry again for 5 minutes. Slides were washed for 5 minutes in 1xPBS (0.1M, pH 7.5), and blocked in 10% blocking serum corresponding to the species the primary antibody was produced in. Slides were then fixed in primary antibody diluted in 1% blocking serum overnight at 4°C. The following day, slides were washed in PBS and incubated in biotinylated secondary antibody (1:200 dilution) for 30 minutes at room temperature (RT) (Vector Laboratories, Burlingame, CA). Endogenous peroxidase was quenched with 0.3% H_2O_2. Slides were washed in PBS, and then incubated for 40 minutes in Vectastain Elite ABC (Vector Laboratories, Burlingame, CA) for 40 minutes at RT. Signal was developed with chromogen 3-amino-9ethylcarbazole (AEC, Sigma-Aldrich, Burlington, MA). Antibodies used for immunohistochemistry are listed in Table 3.

Epidermal thickness and cellular infiltration (positive cells per mm) were counted using ImageJ software (V1.42; National Institute of Health, Bethesda, MD).

8.4 Immunofluorescence

Frozen skin sections were dried at RT, fixed with acetone, blocked and incubated with primary antibody overnight as described above. Sections were then co-stained with a second primary antibody overnight and developed using the appropriate secondary antibody. Slides were imaged using appropriate filters of a Zeiss Axioplan 2 wide-filed fluorescence microscope (Thornwood, NY). We thank the Bio-Imaging Resource Center at the Rockefeller University for the resources and guidance. Antibodies used for immunofluorescence are listed in Table 3.

Table 3: List of antibodies used for immunohistochemistry and immunofluorescence

Name	Company	Catalogue #	Dilution
Syndecan1	Abcam	ab181789	[1:10,000]
BDCA1	Miltenyi Biotech	AD5-8E7	[1:20]-[1:100]
c-Kit	Invitrogen	ma5-12944	[1:100]
CD11c	BD Pharmingen	550375	[1:100]
CD177	LSBio	LS-B1953-50	[1:200]
CD20	Abcam	ab9475	[1:10]
CD3	BD Biosciences	SK7	[1:100]
CXCL1	Abcam	ab86436	[1:500]
CXCL8	LSBio	c8048	[1:100]
Filaggrin	Abnova	MAB3538	[1:100]
IL-17C	LS Bio	LS-C406475	[1:300]
Keratin 16	LSBio	LS-B14481	[1:500]-[1:1000]
Ki-67	Sta. Cruz	sc-101861	[1:25]
Laminin	Santa Cruz	sc-130542	[1:10,000]
Langerin	BD Pharmingen	564789	[1:500]
Lipocalin-2	Abcam	ab23477	[1:50]
Loricrin	Abcam	ab24722	[1:1000]
Melan A	Novacastra	cl-l-melan	[1:40]
Neutrophil Elastase	NP57	DAKO	[1:200]
S100A7	Abcam	47C1068	[1:1000]
Trichohyalin	Abcam	ab58755	[1:10]

8.5 Isolation of peripheral blood mononuclear cells

Blood was diluted 1:1 in PBS, and Ficoll was added (4:3 diluted PBS/Blood: Ficoll) by slowly underlaying the blood. The mixture was centrifuged at 400g for 20 minutes. Peripheral blood mononuclear cell (PBMC) layer (cloudy interphase) was collected, washed in PBS, and centrifuged at 100g for 10 minutes. Pellet was collected and stored at -80°C until processing.

8.6 Peripheral blood activation

For intracellular cytokine staining assays, blood was resuspended 1:1 in RPMI media (Thermofisher Scientific, Waltham, MA). Cells were activated using 25ng/ml phorbol myristate acetate (PMA) and 2µg/ml ionomycin, and 10µg/mL Brefeldin A (all from Sigma Aldrich, St.

Louis, MO) for 4 hours in the 5% CO_2 incubator at 37°C. Unactivated controls were treated with Brefeldin A only, and also incubated at 37°C for 4 hour. 50mM EDTA was added, blood was vortexed and incubated at RT for 15 minutes to stop activation. Blood was then incubated with FACS lysing solution at RT in the dark for 10 minutes. Cells were washed with 1x PBS. Pellet was collected and stored -80°C.

8.7 Flow cytometry

Cells were stained in the appropriate antibody cocktail for 20 minutes at 4°C in staining buffer (1% FBS in PBS), washed and fixed in 4% paraformaldehyde for 20 minutes on ice. Appropriate isotypes and un-activated controls were used.

8.8 Serum preparation

Blood was collected in speckle top tubes and centrifuged at 400g for 10 minutes. Serum was collected and stored at -80°C.

8.9 Mesoscale analysis

Meso Scale Discovery (MSD, Rockville, MD) cytokine assay was used to measure target protein levels in the serum. Individual assays were performed according to the manufacturer's instructions. In brief, serum was diluted, and incubated on the plate at RT for 2 hours. The plate was washed, and 1X detection antibody solution was applied at RT for 2 hours. The plate was washed and read.

8.10 Protein extraction from frozen skin biopsy sections

Skin samples were frozen in Optimal Cutting Temperature compound (OCT, Thermofisher Scientific, Waltham, MA). 15µM sections were cut on the cryostat and placed into prechilled low-binding Eppendorf tube in buffer (RIPA, phenylmethylsulfonyl fluoride (PMSF, Thermo fisher Scientific, Waltham, MA) and cOmplete Protease inhibitor (Roche, San Francisco, CA)). Hand hold tissue grinder homogenizer was used to homogenize the samples on ice for one minute. The sample was then incubated on a rotating wheel at 4°C for 30 minutes, and centrifuged at 15 minutes at 10,000 rpm at 4°C. The supernatant was then stored at -80°C.

8.11 Olink panel

Samples were analyzed using the proteomic Olink Proseek multiplex assay (Uppsala, Sweden). 10 µl of serum and 10ng of tissue were used for proximity extension assay which uses a real-time polymerase chain reaction to detect oligonucleotide-labeled antibody probe pairs to individual targets, as previously described [325, 326]. Samples were assessed using the Olink Inflammation (92 analytes), Cardiovascular II (92 analytes) and Cardiovascular III (92 analytes) and Cardiometabolic panel (92 analytes), or the novel Explore 1,536 analyte panel. Only the samples that met the quality control and had detectable protein expression were included in the analysis.

8.12 RNA extraction

RNA from biopsies was isolated with miRNeasy Mini kit (Qiagen, Hilden, Germany). DNA was removed using on-column DNase digestion (RNase-free DNase Set, Qiagen Hilden, Germany). The total amount of RNA extracted was assessed using Nanodrop 1000

spectrophotometer (Thermo fisher Scientific, Waltham, MA). Prior to RNA-sequencing, quality of the RNA was assessed using the Agilent Bioanalyzer 2100 (Agilent Technologies, Palo Alto, CA).

8.13 Real time PCR

A total of 10ng of RNA was used per reaction. 4x TaqMan Fast Virus 1-Step Mastermix was prepared according to the manufacturer's instruction (Thermo fisher Scientific, Waltham, MA). RNA was reverse transcribed at 50°C for 5 minutes, inactivated/denatured at 95°C for 20 seconds and amplified for 40 cycles at alternating between 95°C for 15 seconds and 60°C for 60 seconds. 200ng of RNA was used for the Taqman gene expression array cards which are listed in Table 4 (Thermo fisher Scientific, Waltham, MA).

Table 4: List of primers.

Assay ID	Gene Symbol	Species
Hs00171074_m1	CCL17	Human
Hs00171149_m1	CCL19	Human
Hs00355476_m1	CCL20	Human
Hs00171076_m1	CCL21	Human
Hs00171146_m1	CCL26	Human
Hs04187715_m1	CCL8	Human
Hs00360669_m1	CD177	Human
Hs01047413_g1	CD19	Human
Hs00998488_m1	CD22	Human
Hs99999901_s1	18s rRNA	Human
Hs01120071_m1	CD38	Human
Hs00998119_m1	CD79A	Human
Hs01567026_m1	CD86	Human
Hs00175480_m1	CTLA4	Human
Hs00236937_m1	CXCL1	Human
Hs00757930_m1	CXCL13	Human
Hs00601975_m1	CXCL2	Human
Hs00171061_m1	CXCL3	Human
Hs00174103_m1	CXCL8	Human
Hs00171065_m1	CXCL9	Human
Hs00823638_m1	DEFB4A	Human
Hs01057148_m1	EBI3	Human
Hs01085834_m1	FOXP3	Human

Hs00738432_g1	CSF3	Human
Hs00929873_m1	CSF2	Human
Hs00989184_m1	GZMA	Human
Hs00188051_m1	GZMB	Human
Hs99999902_m1	RPLP0	Human
Hs00157950_m1	HLA-DOB	Human
Hs00359999_m1	ICOS	Human
Hs00961622_m1	IL10	Human
Hs01073447_m1	IL12A	Human
Hs01011518_m1	IL12B	Human
Hs00174379_m1	IL13	Human
Hs01003716_m1	IL15	Human
Hs00913644_m1	IL16	Human
Hs00174383_m1	IL17A	Human
Hs00975262_m1	IL17B	Human
Hs00171163_m1	IL17C	Human
Hs01028648_m1	IL17F	Human
Hs01038788_m1	IL18	Human
Hs00604657_m1	IL19	Human
Hs00174092_m1	IL1A	Human
Hs01555410_m1	IL1B	Human
Hs00174114_m1	IL2	Human
Hs00218888_m1	IL20	Human
Hs00222310_m1	IL21R	Human
Hs01574154_m1	IL22	Human
Hs00372324_m1	IL23A	Human
Hs01114274_m1	IL24	Human
Hs03044841_m1	IL25	Human
Hs00218189_m1	IL26	Human
Hs00377366_m1	IL27	Human
Hs01098710_m1	IL31	Human
Hs00992441_m1	IL32	Human
Hs04931857_m1	IL33	Human
Hs00205367_m1	IL36A	Human
Hs00758166_m1	IL36B	Human
Hs00219742_m1	IL36G	Human

Hs01104220_g1	IL36RN	Human
Hs00367201_m1	IL37	Human
Hs00544661_m1	IL1F10	Human
Hs00174122_m1	IL4	Human
Hs00174131_m1	IL6	Human
Hs00174125_m1	IL9	Human
Hs01101168_g1	ILK	Human
Hs01075529_m1	NOS2	Human
Hs00178427_m1	LCK	Human
Hs01008571_m1	LCN2	Human
Hs06633590_s1	LTA	Human
Hs00242739_m1	LTB	Human
Hs00914334_m1	LTF	Human
Hs00236988_g1	MIF	Human
Hs00899658_m1	MMP1	Human
Hs00968305_m1	MMP3	Human
Hs00236952_m1	ELANE	Human
Hs00292281_m1	PRKCQ-AS1	Human
Hs00942835_g1	S100A12	Human
Hs01923188_u1	S100A7	Human
Hs00752780_s1	S100A7A	Human
Hs00374264_g1	S100A8	Human
Hs00610058_m1	S100A9	Human
Hs01691258_g1	SERPINB4	Human
Hs01086000_m1	TGFB3	Human
Hs00174128_m1	TNF	Human
Hs00963364_m1	TNFRSF13B	Human
Hs00171292_m1	TNFRSF17	Human
Hs00937195_g1	TNFRSF4	Human
Hs00165362_m1	NCF1	Human
Hs01891184_s1	CXCR2	Human
Hs99999149_s1	CCR5	Human
Hs00934033_m1	CD69	Human
Hs00376160_m1	JCHAIN	Human

8.14 RNA-sequencing and analysis

Transcriptome-wide sequencing was performed using the NovaSeq 6000 (Illumina, San Diego, California). Only samples that passed quality control were included in the RNA-seq analysis. Libraries were constructed with TruSeq RNA Sample Prep Kit (Illumina, San Diego, California). Libraries were sequenced in pair-end mode to generate 100bp reads. Raw reads were aligned to the human genome build GRCH37 with STAR v2.4.2 aligner and then summarized to gene level counts using features of Ensembl (release 70) gene model with featureCount. Differential expression was estimated with DESeq2, and vst was used to log2 transform the normalized counts.

8.15 Laser capture microdissection

Samples were mounted onto metal frame slides (Molecular Machines and Industries, Haslett, MI). One section was stained with H&E for reference. Laser capture microdissection (LCM) was performed using the CellCut system (Molecular Machines and Industries, Haslett, MI). Reticular dermis, basal epidermis and suprabasal (spinous, granular, cornified layers) epidermis as well as dermal tunnels were isolated using LCM. Cap tubes (Molecular Machines and Industries, Haslet, MI) were used to capture tissue. Tissue was frozen and stored at -80°C until processing.

8.16 Enrichment analysis

Enrichment analysis was performed using the eXploring Genomic Relations Tool using the Gene Ontology terms [327]. Canonical pathways and upstream regulators were identified using the Ingenuity Pathway Analysis (Qiagen).

8.17 Statistical analysis

Statistical analysis was performed in R (R-project.org, R foundation, Vienna, Austria) using publicly available Bioconductor packages (www.bioconductor.org). Gene expression profiles were modeled with using mixed-effect models of disease status (HS vs healthy) as fixed factors and random effect for each patient using the R *limma* framework [328]. Multiple hypotheses testing was adjusted using the Benjamini-Hochberg procedure. Fold-changes (FCH) for comparisons were estimated, and hypothesis testing was conducted under the general framework for linear models in *limma* package. Unsupervised clustering of healthy control volunteer, nonlesional, perilesional and lesional means were conducted using Euclidean distance and the average agglomeration criteria. Krueger laboratory and previously published pathways were quantified using a gene-set variation analysis (GSVA) z-score [329] [121, 122].

Undetected RT-PCR values were estimated as 20% of the minimum across all of the samples for each gene. Comparison between samples was performed using least squared means of log2-transformed hARP normalized expression values. P values for t-tests were adjusted for multiple hypothesis testing using the Benjamini-Hochberg procedure. Total counts of IHC markers and means of each group were analyzed using least squared means.

CHAPTER 9:
References

CHAPTER 9. References

Parts of this thesis are based on published work. Permission to use the work in this thesis has been obtained from the publisher.

1) Frew JW, Navrazhina K, Byrd AS, et al. Defining lesional, perilesional and unaffected skin in hidradenitis suppurativa: proposed recommendations for clinical trials and translational research studies. Br J Dermatol. 2019;181(6):1339-1341.

2) Navrazhina K, Frew JW, Krueger JG. Interleukin 17C is elevated in lesional tissue of hidradenitis suppurativa. Br J Dermatol. 2020;182(4):1045-1047.

3) Frew JW, Navrazhina K, Grand D, et al. The effect of subcutaneous brodalumab on clinical disease activity in hidradenitis suppurativa: An open-label cohort study. J Am Acad Dermatol. 2020;83(5):1341-1348.

4) Grand D, Frew JW, Navrazhina K, Krueger JG. Doppler ultrasound-based noninvasive biomarkers in hidradenitis suppurativa: evaluation of analytical and clinical validity. Br J Dermatol. Published online ahead of print June 29, 2020.

5) Navrazhina K, Frew JW, Krueger JG. Interleukin 17C is elevated in lesional tissue of hidradenitis suppurativa. Br J Dermatol. 2020;182(4):1045-1047.

6) Navrazhina K*, Frew JW*, Gilleaudeau P, Sullivan-Whalen M, Garcet S, Krueger JG. Epithelialized tunnels are a source of inflammation in hidradenitis suppurativa. J Allergy Clin Immunol. Published online February 3, 2021. *equal contribution

7) Navrazhina K, Garcet S, Gonzalez J, Grand D, Frew JW, Krueger JG. In-depth analysis of the hidradenitis suppurativa serum proteome identifies distinct inflammatory subtypes. J Invest Dermatol. Published online March 22, 2021.

References:

1. Sabat R, Jemec GBE, Matusiak Ł, Kimball AB, Prens E, Wolk K. Hidradenitis suppurativa. Nat Rev Dis Primers 2020; 6:18.
2. Jemec GB, Kimball AB. Hidradenitis suppurativa: Epidemiology and scope of the problem. J Am Acad Dermatol 2015; 73:S4-7.
3. Jemec GB, Heidenheim M, Nielsen NH. The prevalence of hidradenitis suppurativa and its potential precursor lesions. J Am Acad Dermatol 1996; 35:191-4.
4. Deckers IE, van der Zee HH, Boer J, Prens EP. Correlation of early-onset hidradenitis suppurativa with stronger genetic susceptibility and more widespread involvement. J Am Acad Dermatol 2015; 72:485-8.
5. Egeberg A, Gislason GH, Hansen PR. Risk of Major Adverse Cardiovascular Events and All-Cause Mortality in Patients With Hidradenitis Suppurativa. JAMA Dermatol 2016; 152:429-34.
6. Alavi A, Anooshirvani N, Kim WB, Coutts P, Sibbald RG. Quality-of-life impairment in patients with hidradenitis suppurativa: a Canadian study. Am J Clin Dermatol 2015; 16:61-5.
7. Matusiak Ł, Bieniek A, Szepietowski JC. Hidradenitis suppurativa markedly decreases quality of life and professional activity. J Am Acad Dermatol 2010; 62:706-8, 8.e1.
8. Mac Mahon J, Kirthi S, Byrne N, O'Grady C, Tobin AM. An Update on Health-Related Quality of Life and Patient-Reported Outcomes in Hidradenitis Suppurativa. Patient Relat Outcome Meas 2020; 11:21-6.
9. Theut Riis P, Thorlacius L, Knudsen List E, Jemec GBE. A pilot study of unemployment in patients with hidradenitis suppurativa in Denmark. Br J Dermatol 2017; 176:1083-5.

10. von der Werth JM, Williams HC. The natural history of hidradenitis suppurativa. J Eur Acad Dermatol Venereol 2000; 14:389-92.
11. Ingram JR. The Genetics of Hidradenitis Suppurativa. Dermatol Clin 2016; 34:23-8.
12. Frew JW, Vekic DA, Woods J, Cains GD. A systematic review and critical evaluation of reported pathogenic sequence variants in hidradenitis suppurativa. Br J Dermatol 2017; 177:987-98.
13. Lowell S, Jones P, Le Roux I, Dunne J, Watt FM. Stimulation of human epidermal differentiation by delta-notch signalling at the boundaries of stem-cell clusters. Curr Biol 2000; 10:491-500.
14. Orvain C, Lin YL, Jean-Louis F, Hocini H, Hersant B, Bennasser Y, et al. Hair follicle stem cell replication stress drives IFI16/STING-dependent inflammation in hidradenitis suppurativa. J Clin Invest 2020; 130:3777-90.
15. Sabat R, Jemec GBE, Matusiak L, Kimball AB, Prens E, Wolk K. Hidradenitis suppurativa. Nat Rev Dis Primers 2020; 6:18.
16. Platzer C, Meisel C, Vogt K, Platzer M, Volk HD. Up-regulation of monocytic IL-10 by tumor necrosis factor-alpha and cAMP elevating drugs. Int Immunol 1995; 7:517-23.
17. Platzer C, Fritsch E, Elsner T, Lehmann MH, Volk HD, Prösch S. Cyclic adenosine monophosphate-responsive elements are involved in the transcriptional activation of the human IL-10 gene in monocytic cells. Eur J Immunol 1999; 29:3098-104.
18. Wittebole X, Hahm S, Coyle SM, Kumar A, Calvano SE, Lowry SF. Nicotine exposure alters in vivo human responses to endotoxin. Clin Exp Immunol 2007; 147:28-34.
19. Vazquez BG, Alikhan A, Weaver AL, Wetter DA, Davis MD. Incidence of hidradenitis suppurativa and associated factors: a population-based study of Olmsted County, Minnesota. J Invest Dermatol 2013; 133:97-103.
20. Revuz JE, Canoui-Poitrine F, Wolkenstein P, Viallette C, Gabison G, Pouget F, et al. Prevalence and factors associated with hidradenitis suppurativa: results from two case-control studies. J Am Acad Dermatol 2008; 59:596-601.
21. Sabat R, Chanwangpong A, Schneider-Burrus S, Metternich D, Kokolakis G, Kurek A, et al. Increased prevalence of metabolic syndrome in patients with acne inversa. PLoS One 2012; 7:e31810.
22. Mikkelsen PR, Dufour DN, Zarchi K, Jemec GB. Recurrence rate and patient satisfaction of CO2 laser evaporation of lesions in patients with hidradenitis suppurativa: a retrospective study. Dermatol Surg 2015; 41:255-60.
23. Gauntner TD. Hormonal, stem cell and Notch signalling as possible mechanisms of disease in hidradenitis suppurativa: a systems-level transcriptomic analysis. Br J Dermatol 2019; 180:203-4.
24. Schrader AM, Deckers IE, van der Zee HH, Boer J, Prens EP. Hidradenitis suppurativa: a retrospective study of 846 Dutch patients to identify factors associated with disease severity. J Am Acad Dermatol 2014; 71:460-7.
25. Sartorius K, Emtestam L, Jemec GB, Lapins J. Objective scoring of hidradenitis suppurativa reflecting the role of tobacco smoking and obesity. Br J Dermatol 2009; 161:831-9.
26. Kimball AB, Sobell JM, Zouboulis CC, Gu Y, Williams DA, Sundaram M, et al. HiSCR (Hidradenitis Suppurativa Clinical Response): a novel clinical endpoint to evaluate therapeutic outcomes in patients with hidradenitis suppurativa from the placebo-

controlled portion of a phase 2 adalimumab study. J Eur Acad Dermatol Venereol 2016; 30:989-94.
27. Hessam S, Scholl L, Sand M, Schmitz L, Reitenbach S, Bechara FG. A Novel Severity Assessment Scoring System for Hidradenitis Suppurativa. JAMA Dermatol 2018; 154:330-5.
28. Zouboulis CC, Tzellos T, Kyrgidis A, Jemec GBE, Bechara FG, Giamarellos-Bourboulis EJ, et al. Development and validation of the International Hidradenitis Suppurativa Severity Score System (IHS4), a novel dynamic scoring system to assess HS severity. Br J Dermatol 2017; 177:1401-9.
29. Fletcher JM, Moran B, Petrasca A, Smith CM. IL-17 in inflammatory skin diseases psoriasis and hidradenitis suppurativa. Clin Exp Immunol 2020; 201:121-34.
30. Gill L, Williams M, Hamzavi I. Update on hidradenitis suppurativa: connecting the tracts. F1000Prime Rep 2014; 6:112.
31. Saunte DML, Jemec GBE. Hidradenitis Suppurativa: Advances in Diagnosis and Treatment. Jama 2017; 318:2019-32.
32. Kimball AB, Okun MM, Williams DA, Gottlieb AB, Papp KA, Zouboulis CC, et al. Two Phase 3 Trials of Adalimumab for Hidradenitis Suppurativa. N Engl J Med 2016; 375:422-34.
33. Yu CC, Cook MG. Hidradenitis suppurativa: a disease of follicular epithelium, rather than apocrine glands. Br J Dermatol 1990; 122:763-9.
34. Attanoos RL, Appleton MA, Douglas-Jones AG. The pathogenesis of hidradenitis suppurativa: a closer look at apocrine and apoeccrine glands. Br J Dermatol 1995; 133:254-8.
35. Boer J, Weltevreden EF. Hidradenitis suppurativa or acne inversa. A clinicopathological study of early lesions. Br J Dermatol 1996; 135:721-5.
36. Jemec GB, Hansen U. Histology of hidradenitis suppurativa. J Am Acad Dermatol 1996; 34:994-9.
37. von Laffert M, Helmbold P, Wohlrab J, Fiedler E, Stadie V, Marsch WC. Hidradenitis suppurativa (acne inversa): early inflammatory events at terminal follicles and at interfollicular epidermis. Exp Dermatol 2010; 19:533-7.
38. Wolk K, Join-Lambert O, Sabat R. Aetiology and pathogenesis of hidradenitis suppurativa. Br J Dermatol 2020; 183:999-1010.
39. Kokolakis G, Wolk K, Schneider-Burrus S, Kalus S, Barbus S, Gomis-Kleindienst S, et al. Delayed Diagnosis of Hidradenitis Suppurativa and Its Effect on Patients and Healthcare System. Dermatology 2020:1-10.
40. van der Zee HH, de Ruiter L, van den Broecke DG, Dik WA, Laman JD, Prens EP. Elevated levels of tumour necrosis factor (TNF)-α, interleukin (IL)-1β and IL-10 in hidradenitis suppurativa skin: a rationale for targeting TNF-α and IL-1β. Br J Dermatol 2011; 164:1292-8.
41. Witte-Handel E, Wolk K, Tsaousi A, Irmer ML, Mossner R, Shomroni O, et al. The IL-1 Pathway Is Hyperactive in Hidradenitis Suppurativa and Contributes to Skin Infiltration and Destruction. J Invest Dermatol 2019; 139:1294-305.
42. Kelly G, Hughes R, McGarry T, van den Born M, Adamzik K, Fitzgerald R, et al. Dysregulated cytokine expression in lesional and nonlesional skin in hidradenitis suppurativa. Br J Dermatol 2015; 173:1431-9.

43. Hunger RE, Surovy AM, Hassan AS, Braathen LR, Yawalkar N. Toll-like receptor 2 is highly expressed in lesions of acne inversa and colocalizes with C-type lectin receptor. Br J Dermatol 2008; 158:691-7.
44. Penno CA, Jäger P, Laguerre C, Hasler F, Hofmann A, Gass SK, et al. Lipidomics Profiling of Hidradenitis Suppurativa Skin Lesions Reveals Lipoxygenase Pathway Dysregulation and Accumulation of Proinflammatory Leukotriene B4. J Invest Dermatol 2020; 140:2421-32.e10.
45. Frew JW, Hawkes JE, Krueger JG. A systematic review and critical evaluation of inflammatory cytokine associations in hidradenitis suppurativa. F1000Res 2018; 7:1930.
46. Frew JW, Hawkes JE, Krueger JG. A systematic review and critical evaluation of immunohistochemical associations in hidradenitis suppurativa. F1000Research 2018; 7.
47. Frew JW, Marzano AV, Wolk K, Join-Lambert O, Alavi A, Lowes MA, et al. A Systematic Review of Promising Therapeutic Targets in Hidradenitis Suppurativa: A Critical Evaluation of Mechanistic and Clinical Relevance. J Invest Dermatol 2020.
48. Wolk K, Warszawska K, Hoeflich C, Witte E, Schneider-Burrus S, Witte K, et al. Deficiency of IL-22 contributes to a chronic inflammatory disease: pathogenetic mechanisms in acne inversa. J Immunol 2011; 186:1228-39.
49. Hotz C, Boniotto M, Guguin A, Surenaud M, Jean-Louis F, Tisserand P, et al. Intrinsic Defect in Keratinocyte Function Leads to Inflammation in Hidradenitis Suppurativa. J Invest Dermatol 2016; 136:1768-80.
50. Schroder K, Hertzog PJ, Ravasi T, Hume DA. Interferon-gamma: an overview of signals, mechanisms and functions. J Leukoc Biol 2004; 75:163-89.
51. Schlapbach C, Hanni T, Yawalkar N, Hunger RE. Expression of the IL-23/Th17 pathway in lesions of hidradenitis suppurativa. J Am Acad Dermatol 2011; 65:790-8.
52. Abusleme L, Moutsopoulos NM. IL-17: overview and role in oral immunity and microbiome. Oral Dis 2017; 23:854-65.
53. Krueger JG, Wharton KA, Jr., Schlitt T, Suprun M, Torene RI, Jiang X, et al. IL-17A inhibition by secukinumab induces early clinical, histopathologic, and molecular resolution of psoriasis. J Allergy Clin Immunol 2019; 144:750-63.
54. Gay D, Ghinatti G, Guerrero-Juarez CF, Ferrer RA, Ferri F, Lim CH, et al. Phagocytosis of Wnt inhibitor SFRP4 by late wound macrophages drives chronic Wnt activity for fibrotic skin healing. Sci Adv 2020; 6:eaay3704.
55. Papayannopoulos V. Neutrophil extracellular traps in immunity and disease. Nat Rev Immunol 2018; 18:134-47.
56. Byrd AS, Carmona-Rivera C, O'Neil LJ, Carlucci PM, Cisar C, Rosenberg AZ, et al. Neutrophil extracellular traps, B cells, and type I interferons contribute to immune dysregulation in hidradenitis suppurativa. Sci Transl Med 2019; 11.
57. Wolk K, Frambach Y, Jacobi A, Wilsmann-Theis D, Phillipp S, Witte-Händel E, et al. Increased levels of lipocalin 2 in palmoplantar pustular psoriasis. J Dermatol Sci 2018; 90:68-74.
58. Wolk K, Wenzel J, Tsaousi A, Witte-Handel E, Babel N, Zelenak C, et al. Lipocalin-2 is expressed by activated granulocytes and keratinocytes in affected skin and reflects disease activity in acne inversa/hidradenitis suppurativa. Br J Dermatol 2017; 177:1385-93.
59. Kovacs M, Podda M. Guselkumab in the treatment of severe hidradenitis suppurativa. J Eur Acad Dermatol Venereol 2019; 33:e140-e1.

60. Kearney N, Byrne N, Kirby B, Hughes R. Successful use of guselkumab in the treatment of severe hidradenitis suppurativa. Clin Exp Dermatol 2020; 45:618-9.
61. Montero-Vilchez T, Martinez-Lopez A, Salvador-Rodriguez L, Arias-Santiago S, Molina-Leyva A. The use of guselkumab 100 mg every 4 weeks on patients with hidradenitis suppurativa and a literature review. Dermatol Ther 2020; 33:e13456.
62. Frew JW, Navrazhina K, Grand D, Sullivan-Whalen M, Gilleaudeau P, Garcet S, et al. The effect of subcutaneous brodalumab on clinical disease activity in hidradenitis suppurativa: An open-label cohort study. J Am Acad Dermatol 2020; 83:1341-8.
63. Reguiaï Z, Fougerousse AC, Maccari F, Bécherel PA. Effectiveness of secukinumab in hidradenitis suppurativa: an open study (20 cases). J Eur Acad Dermatol Venereol 2020; 34:e750-e1.
64. Casseres RG, Prussick L, Zancanaro P, Rothstein B, Joshipura D, Saraiya A, et al. Secukinumab in the treatment of moderate to severe hidradenitis suppurativa: Results of an open-label trial. J Am Acad Dermatol 2020; 82:1524-6.
65. Prussick L, Rothstein B, Joshipura D, Saraiya A, Turkowski Y, Abdat R, et al. Open-label, investigator-initiated, single-site exploratory trial evaluating secukinumab, an anti-interleukin-17A monoclonal antibody, for patients with moderate-to-severe hidradenitis suppurativa. Br J Dermatol 2019; 181:609-11.
66. Ghias MH, Johnston AD, Kutner AJ, Micheletti RG, Hosgood HD, Cohen SR. High-dose, high-frequency infliximab: A novel treatment paradigm for hidradenitis suppurativa. J Am Acad Dermatol 2020; 82:1094-101.
67. Prens LM, Bouwman K, Aarts P, Arends S, van Straalen KR, Dudink K, et al. Drug survival of Adalimumab and Infliximab in Hidradenitis Suppurativa Patients: A Daily Practice Cohort Study. Br J Dermatol 2021.
68. Frew JW, Marzano AV, Wolk K, Join-Lambert O, Alavi A, Lowes MA, et al. A Systematic Review of Promising Therapeutic Targets in Hidradenitis Suppurativa: A Critical Evaluation of Mechanistic and Clinical Relevance. J Invest Dermatol 2021; 141:316-24.e2.
69. Tzanetakou V, Kanni T, Giatrakou S, Katoulis A, Papadavid E, Netea MG, et al. Safety and Efficacy of Anakinra in Severe Hidradenitis Suppurativa: A Randomized Clinical Trial. JAMA Dermatol 2016; 152:52-9.
70. Leslie KS, Tripathi SV, Nguyen TV, Pauli M, Rosenblum MD. An open-label study of anakinra for the treatment of moderate to severe hidradenitis suppurativa. J Am Acad Dermatol 2014; 70:243-51.
71. Ribero S, Ramondetta A, Fabbrocini G, Bettoli V, Potenza C, Chiricozzi A, et al. Effectiveness of Secukinumab in the treatment of moderate-severe hidradenitis suppurativa: results from an Italian multicentric retrospective study in a real-life setting. J Eur Acad Dermatol Venereol 2021.
72. Rosales Santillan M, Morss PC, Porter ML, Kimball AB. Biologic therapies for the treatment of hidradenitis suppurativa. Expert Opin Biol Ther 2020; 20:621-33.
73. van der Zee HH, de Winter K, van der Woude CJ, Prens EP. The prevalence of hidradenitis suppurativa in 1093 patients with inflammatory bowel disease. Br J Dermatol 2014; 171:673-5.
74. Reddy S, Strunk A, Garg A. Comparative Overall Comorbidity Burden Among Patients With Hidradenitis Suppurativa. JAMA Dermatol 2019; 155:797-802.

75. Jimenez-Gallo D, de la Varga-Martinez R, Ossorio-Garcia L, Albarran-Planelles C, Rodriguez C, Linares-Barrios M. The Clinical Significance of Increased Serum Proinflammatory Cytokines, C-Reactive Protein, and Erythrocyte Sedimentation Rate in Patients with Hidradenitis Suppurativa. Mediators Inflamm 2017; 2017:2450401.
76. Wang Y, Lam KS, Kraegen EW, Sweeney G, Zhang J, Tso AW, et al. Lipocalin-2 is an inflammatory marker closely associated with obesity, insulin resistance, and hyperglycemia in humans. Clin Chem 2007; 53:34-41.
77. Koiou E, Tziomalos K, Katsikis I, Kandaraki EA, Kalaitzakis E, Delkos D, et al. Weight loss significantly reduces serum lipocalin-2 levels in overweight and obese women with polycystic ovary syndrome. Gynecol Endocrinol 2012; 28:20-4.
78. Zomer HD, Trentin AG. Skin wound healing in humans and mice: Challenges in translational research. J Dermatol Sci 2018; 90:3-12.
79. Mestas J, Hughes CC. Of mice and not men: differences between mouse and human immunology. J Immunol 2004; 172:2731-8.
80. Jenei A, Dajnoki Z, Medgyesi B, Gaspar K, Beke G, Kinyo A, et al. Apocrine Gland-Rich Skin Has a Non-Inflammatory IL-17-Related Immune Milieu, that Turns to Inflammatory IL-17-Mediated Disease in Hidradenitis Suppurativa. J Invest Dermatol 2019; 139:964-8.
81. Dajnoki Z, Béke G, Kapitány A, Mócsai G, Gáspár K, Rühl R, et al. Sebaceous Gland-Rich Skin Is Characterized by TSLP Expression and Distinct Immune Surveillance Which Is Disturbed in Rosacea. J Invest Dermatol 2017; 137:1114-25.
82. Béke G, Dajnoki Z, Kapitány A, Gáspár K, Medgyesi B, Póliska S, et al. Immunotopographical Differences of Human Skin. Front Immunol 2018; 9:424.
83. Sangiuliano B, Pérez NM, Moreira DF, Belizário JE. Cell death-associated molecular-pattern molecules: inflammatory signaling and control. Mediators Inflamm 2014; 2014:821043.
84. Gong T, Liu L, Jiang W, Zhou R. DAMP-sensing receptors in sterile inflammation and inflammatory diseases. Nat Rev Immunol 2020; 20:95-112.
85. Moran B, Sweeney CM, Hughes R, Malara A, Kirthi S, Tobin AM, et al. Hidradenitis Suppurativa Is Characterized by Dysregulation of the Th17:Treg Cell Axis, Which Is Corrected by Anti-TNF Therapy. J Invest Dermatol 2017; 137:2389-95.
86. Frew JW, Navrazhina K, Byrd AS, Garg A, Ingram JR, Kirby JS, et al. Defining lesional, perilesional and unaffected skin in hidradenitis suppurativa: proposed recommendations for clinical trials and translational research studies. Br J Dermatol 2019; 181:1339-41.
87. Gupta AK, Turnbull DH, Harasiewicz KA, Shum DT, Watteel GN, Foster FS, et al. The use of high-frequency ultrasound as a method of assessing the severity of a plaque of psoriasis. Arch Dermatol 1996; 132:658-62.
88. Lis-Święty A, Janicka I, Skrzypek-Salamon A, Brzezińska-Wcisło L. A systematic review of tools for determining activity of localized scleroderma in paediatric and adult patients. J Eur Acad Dermatol Venereol 2017; 31:30-7.
89. Wortsman X, Jemec GB. Real-time compound imaging ultrasound of hidradenitis suppurativa. Dermatol Surg 2007; 33:1340-2.
90. Wortsman X, Moreno C, Soto R, Arellano J, Pezo C, Wortsman J. Ultrasound in-depth characterization and staging of hidradenitis suppurativa. Dermatol Surg 2013; 39:1835-42.

91. Wortsman X, Rodriguez C, Lobos C, Eguiguren G, Molina MT. Ultrasound Diagnosis and Staging in Pediatric Hidradenitis Suppurativa. Pediatr Dermatol 2016; 33:e260-4.
92. Wortsman X, Castro A, Figueroa A. Color Doppler ultrasound assessment of morphology and types of fistulous tracts in hidradenitis suppurativa (HS). J Am Acad Dermatol 2016; 75:760-7.
93. Grand D, Frew JW, Navrazhina K, Krueger JG. Doppler Ultrasound-Based Non-Invasive Biomarkers in Hidradenitis Suppurativa: Evaluation of Analytical and Clinical Validity. Br J Dermatol 2020.
94. el Gammal S, Pieck C, Auer T, Kaspar K, Hoffmann K, Altmeyer P, et al. [100 MHz ultrasound of psoriasis vulgaris plaque]. Ultraschall Med 1998; 19:270-4.
95. Vossen A, van der Zee HH, Prens EP. Hidradenitis Suppurativa: A Systematic Review Integrating Inflammatory Pathways Into a Cohesive Pathogenic Model. Front Immunol 2018; 9:2965.
96. van der Zee HH, de Ruiter L, Boer J, van den Broecke DG, den Hollander JC, Laman JD, et al. Alterations in leucocyte subsets and histomorphology in normal-appearing perilesional skin and early and chronic hidradenitis suppurativa lesions. Br J Dermatol 2012; 166:98-106.
97. Navrazhina K, Frew JW, Krueger JG. Interleukin 17C is elevated in lesional tissue of hidradenitis suppurativa. Br J Dermatol 2020; 182:1045-7.
98. Lima AL, Karl I, Giner T, Poppe H, Schmidt M, Presser D, et al. Keratinocytes and neutrophils are important sources of proinflammatory molecules in hidradenitis suppurativa. Br J Dermatol 2016; 174:514-21.
99. Navrazhina K, Frew JW, Gilleaudeau P, Sullivan-Whalen M, Garcet S, Krueger JG. Epithelialized Tunnels are a Source of Inflammation in Hidradenitis Suppurativa. J Allergy Clin Immunol 2021.
100. Zouboulis CC, Nogueira da Costa A, Makrantonaki E, Hou XX, Almansouri D, Dudley JT, et al. Alterations in innate immunity and epithelial cell differentiation are the molecular pillars of hidradenitis suppurativa. J Eur Acad Dermatol Venereol 2020; 34:846-61.
101. Gudjonsson JE, Tsoi LC, Ma F, Billi AC, van Straalen KR, Vossen AR, et al. Contribution of plasma cells and B-cells to hidradenitis suppurativa pathogenesis. JCI Insight 2020.
102. Lowe MM, Naik HB, Clancy S, Pauli M, Smith KM, Bi Y, et al. Immunopathogenesis of hidradenitis suppurativa and response to anti-TNFα therapy. JCI Insight 2020.
103. Musilova J, Moran B, Sweeney CM, Malara A, Zaborowski A, Hughes R, et al. Enrichment of Plasma Cells in the Peripheral Blood and Skin of Patients with Hidradenitis Suppurativa. J Invest Dermatol 2020; 140:1091-4.e2.
104. Hoffman LK, Tomalin LE, Schultz G, Howell MD, Anandasabapathy N, Alavi A, et al. Integrating the skin and blood transcriptomes and serum proteome in hidradenitis suppurativa reveals complement dysregulation and a plasma cell signature. PLoS One 2018; 13:e0203672.
105. Assan F, Gottlieb J, Tubach F, Lebbah S, Guigue N, Hickman G, et al. Anti-Saccharomyces cerevisiae IgG and IgA antibodies are associated with systemic inflammation and advanced disease in hidradenitis suppurativa. J Allergy Clin Immunol 2020; 146:452-5.e5.

106. Ghias MH, Hyde MJ, Tomalin LE, Morgan BP, Alavi A, Lowes MA, et al. Role of the Complement Pathway in Inflammatory Skin Diseases: A Focus on Hidradenitis Suppurativa. J Invest Dermatol 2020; 140:531-6.e1.
107. Grand D, Navrazhina K, Frew JW. Integrating complement into the molecular pathogenesis of Hidradenitis Suppurativa. Exp Dermatol 2020; 29:86-92.
108. Kanni T, Zenker O, Habel M, Riedemann N, Giamarellos-Bourboulis EJ. Complement activation in hidradenitis suppurativa: a new pathway of pathogenesis? Br J Dermatol 2018; 179:413-9.
109. Schlapbach C, Hänni T, Yawalkar N, Hunger RE. Expression of the IL-23/Th17 pathway in lesions of hidradenitis suppurativa. J Am Acad Dermatol 2011; 65:790-8.
110. van der Zee HH, Laman JD, de Ruiter L, Dik WA, Prens EP. Adalimumab (antitumour necrosis factor-α) treatment of hidradenitis suppurativa ameliorates skin inflammation: an in situ and ex vivo study. Br J Dermatol 2012; 166:298-305.
111. Banerjee A, McNish S, Shanmugam VK. Interferon-gamma (IFN-γ) is Elevated in Wound Exudate from Hidradenitis Suppurativa. Immunol Invest 2017; 46:149-58.
112. Zouboulis CC, Okun MM, Prens EP, Gniadecki R, Foley PA, Lynde C, et al. Long-term adalimumab efficacy in patients with moderate-to-severe hidradenitis suppurativa/acne inversa: 3-year results of a phase 3 open-label extension study. J Am Acad Dermatol 2019; 80:60-9.e2.
113. Blok JL, Li K, Brodmerkel C, Jonkman MF, Horváth B. Gene expression profiling of skin and blood in hidradenitis suppurativa. Br J Dermatol 2016; 174:1392-4.
114. Del Duca E, Pavel AB, Dubin C, Song T, Wallace EB, Peng X, et al. Major Differences in Expression of Inflammatory Pathways in Skin from Different Body Sites of Healthy Individuals. J Invest Dermatol 2019; 139:2228-32.e10.
115. Lowe MM, Naik HB, Clancy S, Pauli M, Smith KM, Bi Y, et al. Immunopathogenesis of hidradenitis suppurativa and response to anti-TNF-α therapy. JCI Insight 2020; 5.
116. Daxhelet M, Suppa M, White J, Benhadou F, Thorlacius LR, Jemec GBE, et al. Proposed Definitions of Typical Lesions in Hidradenitis Suppurativa. Dermatology 2020; 236:431-8.
117. Aran D, Hu Z, Butte AJ. xCell: digitally portraying the tissue cellular heterogeneity landscape. Genome Biol 2017; 18:220.
118. Glickman JW, Dubin C, Renert-Yuval Y, Dahabreh D, Kimmel GW, Auyeung K, et al. Cross-sectional study of blood biomarkers of patients with moderate to severe alopecia areata reveals systemic immune and cardiovascular biomarker dysregulation. J Am Acad Dermatol 2020.
119. Sanyal RD, Pavel AB, Glickman J, Chan TC, Zheng X, Zhang N, et al. Atopic dermatitis in African American patients is T(H)2/T(H)22-skewed with T(H)1/T(H)17 attenuation. Ann Allergy Asthma Immunol 2019; 122:99-110.e6.
120. Shouval DS, Biswas A, Goettel JA, McCann K, Conaway E, Redhu NS, et al. Interleukin-10 receptor signaling in innate immune cells regulates mucosal immune tolerance and anti-inflammatory macrophage function. Immunity 2014; 40:706-19.
121. Visvanathan S, Baum P, Vinisko R, Schmid R, Flack M, Lalovic B, et al. Psoriatic skin molecular and histopathologic profiles after treatment with risankizumab versus ustekinumab. J Allergy Clin Immunol 2019; 143:2158-69.

122. Brodmerkel C, Li K, Garcet S, Hayden K, Chiricozzi A, Novitskaya I, et al. Modulation of inflammatory gene transcripts in psoriasis vulgaris: Differences between ustekinumab and etanercept. J Allergy Clin Immunol 2019; 143:1965-9.
123. Ramirez-Carrozzi V, Sambandam A, Luis E, Lin Z, Jeet S, Lesch J, et al. IL-17C regulates the innate immune function of epithelial cells in an autocrine manner. Nat Immunol 2011; 12:1159-66.
124. Guttman-Yassky E, Krueger JG. IL-17C: A Unique Epithelial Cytokine with Potential for Targeting across the Spectrum of Atopic Dermatitis and Psoriasis. J Invest Dermatol 2018; 138:1467-9.
125. Hawkes JE, Chan TC, Krueger JG. Psoriasis pathogenesis and the development of novel targeted immune therapies. J Allergy Clin Immunol 2017; 140:645-53.
126. Chassaing B, Srinivasan G, Delgado MA, Young AN, Gewirtz AT, Vijay-Kumar M. Fecal lipocalin 2, a sensitive and broadly dynamic non-invasive biomarker for intestinal inflammation. PLoS One 2012; 7:e44328.
127. Thorsvik S, Damås JK, Granlund AV, Flo TH, Bergh K, Østvik AE, et al. Fecal neutrophil gelatinase-associated lipocalin as a biomarker for inflammatory bowel disease. J Gastroenterol Hepatol 2017; 32:128-35.
128. Matusiak Ł, Szczęch J, Bieniek A, Nowicka-Suszko D, Szepietowski JC. Increased interleukin (IL)-17 serum levels in patients with hidradenitis suppurativa: Implications for treatment with anti-IL-17 agents. J Am Acad Dermatol 2017; 76:670-5.
129. Couper KN, Blount DG, Riley EM. IL-10: the master regulator of immunity to infection. J Immunol 2008; 180:5771-7.
130. Lee YR, Yamazaki M, Mitsui S, Tsuboi R, Ogawa H. Hepatocyte growth factor (HGF) activator expressed in hair follicles is involved in in vitro HGF-dependent hair follicle elongation. J Dermatol Sci 2001; 25:156-63.
131. Li JF, Duan HF, Wu CT, Zhang DJ, Deng Y, Yin HL, et al. HGF accelerates wound healing by promoting the dedifferentiation of epidermal cells through β1-integrin/ILK pathway. Biomed Res Int 2013; 2013:470418.
132. Spix JK, Chay EY, Block ER, Klarlund JK. Hepatocyte growth factor induces epithelial cell motility through transactivation of the epidermal growth factor receptor. Exp Cell Res 2007; 313:3319-25.
133. Metzemaekers M, Gouwy M, Proost P. Neutrophil chemoattractant receptors in health and disease: double-edged swords. Cell Mol Immunol 2020; 17:433-50.
134. Ikeda-Miyagawa Y, Kobayashi K, Yamanaka H, Okubo M, Wang S, Dai Y, et al. Peripherally increased artemin is a key regulator of TRPA1/V1 expression in primary afferent neurons. Mol Pain 2015; 11:8.
135. Elitt CM, McIlwrath SL, Lawson JJ, Malin SA, Molliver DC, Cornuet PK, et al. Artemin overexpression in skin enhances expression of TRPV1 and TRPA1 in cutaneous sensory neurons and leads to behavioral sensitivity to heat and cold. J Neurosci 2006; 26:8578-87.
136. Quarcoo D, Fischer TC, Peckenschneider N, Groneberg DA, Welker P. High abundances of neurotrophin 3 in atopic dermatitis mast cell. J Occup Med Toxicol 2009; 4:8.
137. Kennedy AJ, Wellmer A, Facer P, Saldanha G, Kopelman P, Lindsay RM, et al. Neurotrophin-3 is increased in skin in human diabetic neuropathy. J Neurol Neurosurg Psychiatry 1998; 65:393-5.

138. Teixeira AL, Gama CS, Rocha NP, Teixeira MM. Revisiting the Role of Eotaxin-1/CCL11 in Psychiatric Disorders. Front Psychiatry 2018; 9:241.
139. Deshmane SL, Kremlev S, Amini S, Sawaya BE. Monocyte chemoattractant protein-1 (MCP-1): an overview. J Interferon Cytokine Res 2009; 29:313-26.
140. Orta-Mascaró M, Consuegra-Fernández M, Carreras E, Roncagalli R, Carreras-Sureda A, Alvarez P, et al. CD6 modulates thymocyte selection and peripheral T cell homeostasis. J Exp Med 2016; 213:1387-97.
141. Donohue PJ, Richards CM, Brown SA, Hanscom HN, Buschman J, Thangada S, et al. TWEAK is an endothelial cell growth and chemotactic factor that also potentiates FGF-2 and VEGF-A mitogenic activity. Arterioscler Thromb Vasc Biol 2003; 23:594-600.
142. Tamada K, Shimozaki K, Chapoval AI, Zhai Y, Su J, Chen SF, et al. LIGHT, a TNF-like molecule, costimulates T cell proliferation and is required for dendritic cell-mediated allogeneic T cell response. J Immunol 2000; 164:4105-10.
143. Burkly LC. TWEAK/Fn14 axis: the current paradigm of tissue injury-inducible function in the midst of complexities. Semin Immunol 2014; 26:229-36.
144. Poindexter NJ, Williams RR, Powis G, Jen E, Caudle AS, Chada S, et al. IL-24 is expressed during wound repair and inhibits TGFalpha-induced migration and proliferation of keratinocytes. Exp Dermatol 2010; 19:714-22.
145. Jin SH, Choi D, Chun YJ, Noh M. Keratinocyte-derived IL-24 plays a role in the positive feedback regulation of epidermal inflammation in response to environmental and endogenous toxic stressors. Toxicol Appl Pharmacol 2014; 280:199-206.
146. Chiricozzi A, Suárez-Fariñas M, Fuentes-Duculan J, Cueto I, Li K, Tian S, et al. Increased expression of interleukin-17 pathway genes in nonlesional skin of moderate-to-severe psoriasis vulgaris. Br J Dermatol 2016; 174:136-45.
147. Keermann M, Kõks S, Reimann E, Prans E, Abram K, Kingo K. Transcriptional landscape of psoriasis identifies the involvement of IL36 and IL36RN. BMC Genomics 2015; 16:322.
148. Marzano AV, Damiani G, Ceccherini I, Berti E, Gattorno M, Cugno M. Autoinflammation in pyoderma gangrenosum and its syndromic form (pyoderma gangrenosum, acne and suppurative hidradenitis). Br J Dermatol 2017; 176:1588-98.
149. Johnston A, Xing X, Wolterink L, Barnes DH, Yin Z, Reingold L, et al. IL-1 and IL-36 are dominant cytokines in generalized pustular psoriasis. J Allergy Clin Immunol 2017; 140:109-20.
150. Chiricozzi A, Nograles KE, Johnson-Huang LM, Fuentes-Duculan J, Cardinale I, Bonifacio KM, et al. IL-17 induces an expanded range of downstream genes in reconstituted human epidermis model. PLoS One 2014; 9:e90284.
151. Di Caprio R, Balato A, Caiazzo G, Lembo S, Raimondo A, Fabbrocini G, et al. IL-36 cytokines are increased in acne and hidradenitis suppurativa. Arch Dermatol Res 2017; 309:673-8.
152. Thomi R, Kakeda M, Yawalkar N, Schlapbach C, Hunger RE. Increased expression of the interleukin-36 cytokines in lesions of hidradenitis suppurativa. J Eur Acad Dermatol Venereol 2017; 31:2091-6.
153. Carrier Y, Ma HL, Ramon HE, Napierata L, Small C, O'Toole M, et al. Inter-regulation of Th17 cytokines and the IL-36 cytokines in vitro and in vivo: implications in psoriasis pathogenesis. J Invest Dermatol 2011; 131:2428-37.

154. Mahil SK, Catapano M, Di Meglio P, Dand N, Ahlfors H, Carr IM, et al. An analysis of IL-36 signature genes and individuals with IL1RL2 knockout mutations validates IL-36 as a psoriasis therapeutic target. Sci Transl Med 2017; 9.
155. Catapano M, Vergnano M, Romano M, Mahil SK, Choon SE, Burden AD, et al. IL-36 Promotes Systemic IFN-I Responses in Severe Forms of Psoriasis. J Invest Dermatol 2020; 140:816-26.e3.
156. Nograles KE, Zaba LC, Guttman-Yassky E, Fuentes-Duculan J, Suárez-Fariñas M, Cardinale I, et al. Th17 cytokines interleukin (IL)-17 and IL-22 modulate distinct inflammatory and keratinocyte-response pathways. Br J Dermatol 2008; 159:1092-102.
157. Albanesi C, Cavani A, Girolomoni G. IL-17 is produced by nickel-specific T lymphocytes and regulates ICAM-1 expression and chemokine production in human keratinocytes: synergistic or antagonist effects with IFN-gamma and TNF-alpha. J Immunol 1999; 162:494-502.
158. von Laffert M, Stadie V, Wohlrab J, Marsch WC. Hidradenitis suppurativa/acne inversa: bilocated epithelial hyperplasia with very different sequelae. Br J Dermatol 2011; 164:367-71.
159. Witte E, Kokolakis G, Witte K, Philipp S, Doecke WD, Babel N, et al. IL-19 is a component of the pathogenetic IL-23/IL-17 cascade in psoriasis. J Invest Dermatol 2014; 134:2757-67.
160. Homey B, Dieu-Nosjean MC, Wiesenborn A, Massacrier C, Pin JJ, Oldham E, et al. Up-regulation of macrophage inflammatory protein-3 alpha/CCL20 and CC chemokine receptor 6 in psoriasis. J Immunol 2000; 164:6621-32.
161. Kim TG, Jee H, Fuentes-Duculan J, Wu WH, Byamba D, Kim DS, et al. Dermal clusters of mature dendritic cells and T cells are associated with the CCL20/CCR6 chemokine system in chronic psoriasis. J Invest Dermatol 2014; 134:1462-5.
162. Schwarzenberger P, Huang W, Ye P, Oliver P, Manuel M, Zhang Z, et al. Requirement of endogenous stem cell factor and granulocyte-colony-stimulating factor for IL-17-mediated granulopoiesis. J Immunol 2000; 164:4783-9.
163. Schwarzenberger P, La Russa V, Miller A, Ye P, Huang W, Zieske A, et al. IL-17 stimulates granulopoiesis in mice: use of an alternate, novel gene therapy-derived method for in vivo evaluation of cytokines. J Immunol 1998; 161:6383-9.
164. Kaushansky K. Lineage-specific hematopoietic growth factors. N Engl J Med 2006; 354:2034-45.
165. Mei J, Liu Y, Dai N, Hoffmann C, Hudock KM, Zhang P, et al. Cxcr2 and Cxcl5 regulate the IL-17/G-CSF axis and neutrophil homeostasis in mice. J Clin Invest 2012; 122:974-86.
166. Semerad CL, Liu F, Gregory AD, Stumpf K, Link DC. G-CSF is an essential regulator of neutrophil trafficking from the bone marrow to the blood. Immunity 2002; 17:413-23.
167. Wolk K, Brembach TC, Šimaitė D, Bartnik E, Cucinotta S, Pokrywka A, et al. Activity and components of the granulocyte colony-stimulating factor pathway in hidradenitis suppurativa. Br J Dermatol 2021.
168. Frew JW, Jiang CS, Singh N, Grand D, Navrazhina K, Vaughan R, et al. Clinical response rates, placebo response rates, and significantly associated covariates are dependent on choice of outcome measure in hidradenitis suppurativa: A post hoc analysis of PIONEER 1 and 2 individual patient data. J Am Acad Dermatol 2019.

169. Frew JW, Jiang CS, Singh N, Grand D, Navrazhina K, Vaughan R, et al. Dermal Tunnels Influence Time to Clinical Response and Family History Influences Time to Loss of Clinical Response in Hidradenitis Suppurativa Patients Treated with Adalimumab. Clin Exp Dermatol 2020.
170. Vossen A, van der Zee HH, Davelaar N, Mus AMC, van Doorn MBA, Prens EP. Apremilast for moderate hidradenitis suppurativa: no significant change in lesional skin inflammatory biomarkers. J Eur Acad Dermatol Venereol 2019; 33:761-5.
171. He H, Olesen CM, Pavel AB, Clausen ML, Wu J, Estrada Y, et al. Tape-Strip Proteomic Profiling of Atopic Dermatitis on Dupilumab Identifies Minimally Invasive Biomarkers. Front Immunol 2020; 11:1768.
172. Pavel AB, Zhou L, Diaz A, Ungar B, Dan J, He H, et al. The proteomic skin profile of moderate-to-severe atopic dermatitis patients shows an inflammatory signature. J Am Acad Dermatol 2020; 82:690-9.
173. Witte-Händel E, Wolk K, Tsaousi A, Irmer ML, Mößner R, Shomroni O, et al. The IL-1 Pathway Is Hyperactive in Hidradenitis Suppurativa and Contributes to Skin Infiltration and Destruction. J Invest Dermatol 2019; 139:1294-305.
174. Vossen A, van der Zee HH, Tsoi LC, Xing X, Devalaraja M, Gudjonsson JE, et al. Novel cytokine and chemokine markers of hidradenitis suppurativa reflect chronic inflammation and itch. Allergy 2019; 74:631-4.
175. Murota H, Izumi M, Abd El-Latif MI, Nishioka M, Terao M, Tani M, et al. Artemin causes hypersensitivity to warm sensation, mimicking warmth-provoked pruritus in atopic dermatitis. J Allergy Clin Immunol 2012; 130:671-82.e4.
176. Albers KM, Zhang XL, Diges CM, Schwartz ES, Yang CI, Davis BM, et al. Artemin growth factor increases nicotinic cholinergic receptor subunit expression and activity in nociceptive sensory neurons. Mol Pain 2014; 10:31.
177. Krajewski PK, Matusiak Ł, von Stebut E, Schultheis M, Kirschner U, Nikolakis G, et al. Pain in Hidradenitis Suppurativa: A Cross-sectional Study of 1,795 Patients. Acta Derm Venereol 2021; 101:adv00364.
178. Matusiak Ł, Szczęch J, Kaaz K, Lelonek E, Szepietowski JC. Clinical Characteristics of Pruritus and Pain in Patients with Hidradenitis Suppurativa. Acta Derm Venereol 2018; 98:191-4.
179. Nakamura T, Nishizawa T, Hagiya M, Seki T, Shimonishi M, Sugimura A, et al. Molecular cloning and expression of human hepatocyte growth factor. Nature 1989; 342:440-3.
180. Phan LM, Fuentes-Mattei E, Wu W, Velazquez-Torres G, Sircar K, Wood CG, et al. Hepatocyte Growth Factor/cMET Pathway Activation Enhances Cancer Hallmarks in Adrenocortical Carcinoma. Cancer Res 2015; 75:4131-42.
181. Grand D, Frew JW, Navrazhina K, Krueger JG. Doppler ultrasound-based noninvasive biomarkers in hidradenitis suppurativa: evaluation of analytical and clinical validity. Br J Dermatol 2020.
182. Frew JW, Navrazhina K, Marohn M, Lu PC, Krueger JG. Contribution of fibroblasts to tunnel formation and inflammation in hidradenitis suppurativa/ acne inversa. Exp Dermatol 2019; 28:886-91.
183. Ofenloch RF. Health-related quality of life in hidradenitis suppurativa. Br J Dermatol 2017; 176:861-2.

184. Vanlaerhoven A, Ardon CB, van Straalen KR, Vossen A, Prens EP, van der Zee HH. Hurley III Hidradenitis Suppurativa Has an Aggressive Disease Course. Dermatology 2018; 234:232-3.
185. Goldburg SR, Strober BE, Payette MJ. Part I. Hidradenitis Suppurativa: Epidemiology, clinical presentation, and pathogenesis. J Am Acad Dermatol 2019.
186. Goldburg SR, Strober BE, Payette MJ. Part 2. Current and emerging treatments for hidradenitis suppurativa. J Am Acad Dermatol 2019.
187. Kurzen H, Jung EG, Hartschuh W, Moll I, Franke WW, Moll R. Forms of epithelial differentiation of draining sinus in acne inversa (hidradenitis suppurativa). Br J Dermatol 1999; 141:231-9.
188. Margesson LJ, Danby FW. Hidradenitis suppurativa. Best Pract Res Clin Obstet Gynaecol 2014; 28:1013-27.
189. Kidacki M, Cong Z, Flamm A, Helm K, Danby FW, Nelson AM. 'Invasive proliferative gelatinous mass' of hidradenitis suppurativa contains distinct inflammatory components. Br J Dermatol 2019; 181:192-3.
190. Juneau RA, Pang B, Weimer KE, Armbruster CE, Swords WE. Nontypeable Haemophilus influenzae initiates formation of neutrophil extracellular traps. Infect Immun 2011; 79:431-8.
191. Berends ET, Horswill AR, Haste NM, Monestier M, Nizet V, von Kockritz-Blickwede M. Nuclease expression by Staphylococcus aureus facilitates escape from neutrophil extracellular traps. J Innate Immun 2010; 2:576-86.
192. Byrd AS, O'Brien XM, Johnson CM, Lavigne LM, Reichner JS. An extracellular matrix-based mechanism of rapid neutrophil extracellular trap formation in response to Candida albicans. J Immunol 2013; 190:4136-48.
193. Korn T, Bettelli E, Oukka M, Kuchroo VK. IL-17 and Th17 Cells. Annu Rev Immunol 2009; 27:485-517.
194. Kolls JK, Linden A. Interleukin-17 family members and inflammation. Immunity 2004; 21:467-76.
195. Di Cesare A, Di Meglio P, Nestle FO. The IL-23/Th17 axis in the immunopathogenesis of psoriasis. J Invest Dermatol 2009; 129:1339-50.
196. Ring HC, Bay L, Nilsson M, Kallenbach K, Miller IM, Saunte DM, et al. Bacterial biofilm in chronic lesions of hidradenitis suppurativa. Br J Dermatol 2017; 176:993-1000.
197. Folgueras AR, Guo X, Pasolli HA, Stokes N, Polak L, Zheng D, et al. Architectural niche organization by LHX2 is linked to hair follicle stem cell function. Cell Stem Cell 2013; 13:314-27.
198. Kadaja M, Keyes BE, Lin M, Pasolli HA, Genander M, Polak L, et al. SOX9: a stem cell transcriptional regulator of secreted niche signaling factors. Genes Dev 2014; 28:328-41.
199. Ge Y, Gomez NC, Adam RC, Nikolova M, Yang H, Verma A, et al. Stem Cell Lineage Infidelity Drives Wound Repair and Cancer. Cell 2017; 169:636-50.e14.
200. Coates M, Mariottoni P, Corcoran DL, Kirshner HF, Jaleel T, Brown DA, et al. The skin transcriptome in hidradenitis suppurativa uncovers an antimicrobial and sweat gland gene signature which has distinct overlap with wounded skin. PLoS One 2019; 14:e0216249.
201. Hawkes JE, Yan BY, Chan TC, Krueger JG. Discovery of the IL-23/IL-17 Signaling Pathway and the Treatment of Psoriasis. J Immunol 2018; 201:1605-13.

202. Frew JW, Piguet V. Ex Vivo Models and Interpretation of Mechanistic Studies in Hidradenitis Suppurativa. J Invest Dermatol 2020; 140:1323-6.
203. Frew JW, Navrazhina K, Grand D, Sullivan-Whalen M, Gilleaudeau P, Garcet S, et al. The effect of subcutaneous brodalumab on clinical disease activity in hidradenitis suppurativa: An open-label cohort study. J Am Acad Dermatol 2020.
204. Frew JW, Jiang CS, Singh N, Grand D, Navrazhina K, Vaughan R, et al. Clinical response rates, placebo response rates, and significantly associated covariates are dependent on choice of outcome measure in hidradenitis suppurativa: A post hoc analysis of PIONEER 1 and 2 individual patient data. J Am Acad Dermatol 2020; 82:1150-7.
205. Blok JL, Li K, Brodmerkel C, Horvátovich P, Jonkman MF, Horváth B. Ustekinumab in hidradenitis suppurativa: clinical results and a search for potential biomarkers in serum. Br J Dermatol 2016; 174:839-46.
206. Brunner PM, Suárez-Fariñas M, He H, Malik K, Wen HC, Gonzalez J, et al. The atopic dermatitis blood signature is characterized by increases in inflammatory and cardiovascular risk proteins. Sci Rep 2017; 7:8707.
207. Brunner PM, He H, Pavel AB, Czarnowicki T, Lefferdink R, Erickson T, et al. The blood proteomic signature of early-onset pediatric atopic dermatitis shows systemic inflammation and is distinct from adult long-standing disease. J Am Acad Dermatol 2019; 81:510-9.
208. Kim J, Tomalin L, Lee J, Fitz LJ, Berstein G, Correa-da Rosa J, et al. Reduction of Inflammatory and Cardiovascular Proteins in the Blood of Patients with Psoriasis: Differential Responses between Tofacitinib and Etanercept after 4 Weeks of Treatment. J Invest Dermatol 2018; 138:273-81.
209. Bell EJ, Decker PA, Tsai MY, Pankow JS, Hanson NQ, Wassel CL, et al. Hepatocyte growth factor is associated with progression of atherosclerosis: The Multi-Ethnic Study of Atherosclerosis (MESA). Atherosclerosis 2018; 272:162-7.
210. Villacorta H, Maisel AS. Soluble ST2 Testing: A Promising Biomarker in the Management of Heart Failure. Arq Bras Cardiol 2016; 106:145-52.
211. Reddy S, Strunk A, Jemec GBE, Garg A. Incidence of Myocardial Infarction and Cerebrovascular Accident in Patients With Hidradenitis Suppurativa. JAMA Dermatol 2020; 156:65-71.
212. Miller IM, Ellervik C, Vinding GR, Zarchi K, Ibler KS, Knudsen KM, et al. Association of metabolic syndrome and hidradenitis suppurativa. JAMA Dermatol 2014; 150:1273-80.
213. Navrazhina K, Garcet S, Gonzalez J, Grand D, Frew JW, Krueger JG. In-Depth Analysis of the Hidradenitis Suppurativa Serum Proteome Identifies Distinct Inflammatory Subtypes. J Invest Dermatol 2021.
214. Mi H, Muruganujan A, Huang X, Ebert D, Mills C, Guo X, et al. Protocol Update for large-scale genome and gene function analysis with the PANTHER classification system (v.14.0). Nat Protoc 2019; 14:703-21.
215. Schroll A, Eller K, Feistritzer C, Nairz M, Sonnweber T, Moser PA, et al. Lipocalin-2 ameliorates granulocyte functionality. Eur J Immunol 2012; 42:3346-57.
216. Furze RC, Rankin SM. Neutrophil mobilization and clearance in the bone marrow. Immunology 2008; 125:281-8.

217. Clark GJ, Jamriska L, Rao M, Hart DN. Monocytes immunoselected via the novel monocyte specific molecule, CD300e, differentiate into active migratory dendritic cells. J Immunother 2007; 30:303-11.
218. An Z, Li J, Yu J, Wang X, Gao H, Zhang W, et al. Neutrophil extracellular traps induced by IL-8 aggravate atherosclerosis via activation NF-kappaB signaling in macrophages. Cell Cycle 2019; 18:2928-38.
219. Brunner PM, Glitzner E, Reininger B, Klein I, Stary G, Mildner M, et al. CCL7 contributes to the TNF-alpha-dependent inflammation of lesional psoriatic skin. Exp Dermatol 2015; 24:522-8.
220. Halmos VT, Kozma D, Mihalik P, Kurko E. [Alcohol-induced hypoglycemia (author's transl)]. Dtsch Z Verdau Stoffwechselkr 1979; 39:219-26.
221. Yasumatsu R, Altiok O, Benarafa C, Yasumatsu C, Bingol-Karakoc G, Remold-O'Donnell E, et al. SERPINB1 upregulation is associated with in vivo complex formation with neutrophil elastase and cathepsin G in a baboon model of bronchopulmonary dysplasia. Am J Physiol Lung Cell Mol Physiol 2006; 291:L619-27.
222. Gong D, Farley K, White M, Hartshorn KL, Benarafa C, Remold-O'Donnell E. Critical role of serpinB1 in regulating inflammatory responses in pulmonary influenza infection. J Infect Dis 2011; 204:592-600.
223. Dey G, Radhakrishnan A, Syed N, Thomas JK, Nadig A, Srikumar K, et al. Signaling network of Oncostatin M pathway. J Cell Commun Signal 2013; 7:103-8.
224. Chiricozzi A, Guttman-Yassky E, Suarez-Farinas M, Nograles KE, Tian S, Cardinale I, et al. Integrative responses to IL-17 and TNF-alpha in human keratinocytes account for key inflammatory pathogenic circuits in psoriasis. J Invest Dermatol 2011; 131:677-87.
225. Kim J, Bissonnette R, Lee J, Correa da Rosa J, Suarez-Farinas M, Lowes MA, et al. The Spectrum of Mild to Severe Psoriasis Vulgaris Is Defined by a Common Activation of IL-17 Pathway Genes, but with Key Differences in Immune Regulatory Genes. J Invest Dermatol 2016; 136:2173-82.
226. Tian S, Krueger JG, Li K, Jabbari A, Brodmerkel C, Lowes MA, et al. Meta-analysis derived (MAD) transcriptome of psoriasis defines the "core" pathogenesis of disease. PLoS One 2012; 7:e44274.
227. Suarez-Farinas M, Lowes MA, Zaba LC, Krueger JG. Evaluation of the psoriasis transcriptome across different studies by gene set enrichment analysis (GSEA). PLoS One 2010; 5:e10247.
228. Zhou X, Krueger JG, Kao MC, Lee E, Du F, Menter A, et al. Novel mechanisms of T-cell and dendritic cell activation revealed by profiling of psoriasis on the 63,100-element oligonucleotide array. Physiol Genomics 2003; 13:69-78.
229. Navrazhina K GS, Gonzalez J, Grand D, Frew JW, Krueger JG. In-Depth Analysis of the Hidradenitis Suppurativa Serum Proteome Identifies Distinct Inflammatory Subtypes. J Invest Dermatol 2021; Online ahead of print.
230. Garcet S, Nograles K, Correa da Rosa J, Schafer PH, Krueger JG. Synergistic cytokine effects as apremilast response predictors in patients with psoriasis. J Allergy Clin Immunol 2018; 142:1010-3.e6.
231. Oestreicher JL, Walters IB, Kikuchi T, Gilleaudeau P, Surette J, Schwertschlag U, et al. Molecular classification of psoriasis disease-associated genes through pharmacogenomic expression profiling. Pharmacogenomics J 2001; 1:272-87.

232. Egeberg A, Jemec GBE, Kimball AB, Bachelez H, Gislason GH, Thyssen JP, et al. Prevalence and Risk of Inflammatory Bowel Disease in Patients with Hidradenitis Suppurativa. J Invest Dermatol 2017; 137:1060-4.
233. Polat M, Bugdayci G, Sahin A, Kaya H, Sezer T, Ozturk S. Can pregnancy-associated plasma protein-A be a marker for the assessment of atherosclerosis risk in patients with chronic plaque psoriasis? Postepy Dermatol Alergol 2016; 33:340-4.
234. Cho W, Kang JL, Park YM. Corticotropin-Releasing Hormone (CRH) Promotes Macrophage Foam Cell Formation via Reduced Expression of ATP Binding Cassette Transporter-1 (ABCA1). PLoS One 2015; 10:e0130587.
235. Vasiadi M, Therianou A, Sideri K, Smyrnioti M, Sismanopoulos N, Delivanis DA, et al. Increased serum CRH levels with decreased skin CRHR-1 gene expression in psoriasis and atopic dermatitis. J Allergy Clin Immunol 2012; 129:1410-3.
236. Cemil BC, Canpolat F, Yilmazer D, Eskioglu F, Alper M. The association of PASI scores with CRH-R1 expression in patients with psoriasis. Arch Dermatol Res 2012; 304:127-32.
237. Cibrian D, Saiz ML, de la Fuente H, Sanchez-Diaz R, Moreno-Gonzalo O, Jorge I, et al. CD69 controls the uptake of L-tryptophan through LAT1-CD98 and AhR-dependent secretion of IL-22 in psoriasis. Nat Immunol 2016; 17:985-96.
238. Joehanes R, Ying S, Huan T, Johnson AD, Raghavachari N, Wang R, et al. Gene expression signatures of coronary heart disease. Arterioscler Thromb Vasc Biol 2013; 33:1418-26.
239. Bou-Dargham MJ, Khamis ZI, Cognetta AB, Sang QA. The Role of Interleukin-1 in Inflammatory and Malignant Human Skin Diseases and the Rationale for Targeting Interleukin-1 Alpha. Med Res Rev 2017; 37:180-216.
240. Burzynski LC, Humphry M, Pyrillou K, Wiggins KA, Chan JNE, Figg N, et al. The Coagulation and Immune Systems Are Directly Linked through the Activation of Interleukin-1alpha by Thrombin. Immunity 2019; 50:1033-42 e6.
241. Wootton PT, Drenos F, Cooper JA, Thompson SR, Stephens JW, Hurt-Camejo E, et al. Tagging-SNP haplotype analysis of the secretory PLA2IIa gene PLA2G2A shows strong association with serum levels of sPLA2IIa: results from the UDACS study. Hum Mol Genet 2006; 15:355-61.
242. Ridker PM, Chasman DI, Rose L, Loscalzo J, Elias JA. Plasma levels of the proinflammatory chitin-binding glycoprotein YKL-40, variation in the chitinase 3-like 1 gene (CHI3L1), and incident cardiovascular events. J Am Heart Assoc 2014; 3:e000897.
243. Valdembri D, Regano D, Maione F, Giraudo E, Serini G. Class 3 semaphorins in cardiovascular development. Cell Adh Migr 2016; 10:641-51.
244. Mitchell A, Rentero C, Endoh Y, Hsu K, Gaus K, Geczy C, et al. LILRA5 is expressed by synovial tissue macrophages in rheumatoid arthritis, selectively induces pro-inflammatory cytokines and IL-10 and is regulated by TNF-alpha, IL-10 and IFN-gamma. Eur J Immunol 2008; 38:3459-73.
245. Dolcino M, Cozzani E, Riva S, Parodi A, Tinazzi E, Lunardi C, et al. Gene expression profiling in dermatitis herpetiformis skin lesions. Clin Dev Immunol 2012; 2012:198956.
246. Hannum C, Culpepper J, Campbell D, McClanahan T, Zurawski S, Bazan JF, et al. Ligand for FLT3/FLK2 receptor tyrosine kinase regulates growth of haematopoietic stem cells and is encoded by variant RNAs. Nature 1994; 368:643-8.

247. Sanchez J, Le Jan S, Muller C, François C, Renard Y, Durlach A, et al. Matrix remodelling and MMP expression/activation are associated with hidradenitis suppurativa skin inflammation. Exp Dermatol 2019; 28:593-600.
248. Mosialou I, Shikhel S, Luo N, Petropoulou PI, Panitsas K, Bisikirska B, et al. Lipocalin-2 counteracts metabolic dysregulation in obesity and diabetes. J Exp Med 2020; 217.
249. Kamata M, Tada Y, Tatsuta A, Kawashima T, Shibata S, Mitsui H, et al. Serum lipocalin-2 levels are increased in patients with psoriasis. Clin Exp Dermatol 2012; 37:296-9.
250. Hirai Y, Iyoda M, Shibata T, Kuno Y, Kawaguchi M, Hizawa N, et al. IL-17A stimulates granulocyte colony-stimulating factor production via ERK1/2 but not p38 or JNK in human renal proximal tubular epithelial cells. Am J Physiol Renal Physiol 2012; 302:F244-50.
251. Xu S, Cao X. Interleukin-17 and its expanding biological functions. Cell Mol Immunol 2010; 7:164-74.
252. Cho SG, Park YM, Moon H, Kim KM, Bae SS, Kim GB, et al. Psoriasiform eruption triggered by recombinant granulocyte-macrophage colony stimulating factor (rGM-CSF) and exacerbated by granulocyte colony stimulating factor (rG-CSF) in a patient with breast cancer. J Korean Med Sci 1998; 13:685-8.
253. Kavanaugh A. Flare of psoriasis and psoriatic arthritis following treatment with granulocyte colony-stimulating factor. Am J Med 1996; 101:567-8.
254. Mössner R, Beckmann I, Hallermann C, Neumann C, Reich K. Granulocyte colony-stimulating-factor-induced psoriasiform dermatitis resembles psoriasis with regard to abnormal cytokine expression and epidermal activation. Exp Dermatol 2004; 13:340-6.
255. Jang MS, Park JB, Kim JH, Yang MH, Lee KH, Han SH, et al. Granulocyte Colony-Stimulating Factor-Induced Psoriasiform Dermatitis Improved by Narrowband Ultraviolet B. Ann Dermatol 2017; 29:232-3.
256. Savage KT, Singh V, Patel ZS, Yannuzzi CA, McKenzie-Brown AM, Lowes MA, et al. Pain management in hidradenitis suppurativa and a proposed treatment algorithm. J Am Acad Dermatol 2020.
257. Levine JD, Lau W, Kwiat G, Goetzl EJ. Leukotriene B4 produces hyperalgesia that is dependent on polymorphonuclear leukocytes. Science 1984; 225:743-5.
258. Cunha TM, Verri WA, Jr., Schivo IR, Napimoga MH, Parada CA, Poole S, et al. Crucial role of neutrophils in the development of mechanical inflammatory hypernociception. J Leukoc Biol 2008; 83:824-32.
259. Jeon S, Jha MK, Ock J, Seo J, Jin M, Cho H, et al. Role of lipocalin-2-chemokine axis in the development of neuropathic pain following peripheral nerve injury. J Biol Chem 2013; 288:24116-27.
260. Ebbinghaus M, Natura G, Segond von Banchet G, Hensellek S, Böttcher M, Hoffmann B, et al. Interleukin-17A is involved in mechanical hyperalgesia but not in the severity of murine antigen-induced arthritis. Sci Rep 2017; 7:10334.
261. Kimball AB, Kerdel F, Adams D, Mrowietz U, Gelfand JM, Gniadecki R, et al. Adalimumab for the treatment of moderate to severe Hidradenitis suppurativa: a parallel randomized trial. Ann Intern Med 2012; 157:846-55.
262. Lockshin B, Balagula Y, Merola JF. Interleukin 17, inflammation, and cardiovascular risk in patients with psoriasis. J Am Acad Dermatol 2018; 79:345-52.

263. Skroza N, Mambrin A, Proietti I, Balduzzi V, Bernardini N, Marchesiello A, et al. Evaluation of Cardiovascular Risk in Hidradenitis Suppurativa Patients Using Heart Rate Variability (HRV) Analysis. Cardiovasc Ther 2020; 2020:1321782.
264. Elnabawi YA, Garshick MS, Tawil M, Barrett TJ, Fisher EA, Lo Sicco K, et al. CCL20 in Psoriasis: A Potential Biomarker of Disease Severity, Inflammation, and Impaired Vascular Health. J Am Acad Dermatol 2020.
265. Abeywardena MY, Leifert WR, Warnes KE, Varghese JN, Head RJ. Cardiovascular biology of interleukin-6. Curr Pharm Des 2009; 15:1809-21.
266. Matusiak L, Bieniek A, Szepietowski JC. Increased serum tumour necrosis factor-alpha in hidradenitis suppurativa patients: is there a basis for treatment with anti-tumour necrosis factor-alpha agents? Acta Derm Venereol 2009; 89:601-3.
267. Lind L, Figarska S, Sundström J, Fall T, Ärnlöv J, Ingelsson E. Changes in Proteomic Profiles are Related to Changes in BMI and Fat Distribution During 10 Years of Aging. Obesity (Silver Spring) 2020; 28:178-86.
268. Frew JW, Lowes MA, Goldfarb N, Butt M, Piguet V, O'Brien E, et al. Global Harmonization of Morphological Definitions in Hidradenitis Suppurativa for a Proposed Glossary. JAMA Dermatol 2021.
269. Navrazhina K, Garcet, S, Gonzalez, J, Grand, D, Frew, JW, Krueger, JG. In-Depth Analysis of the Hidradenitis Suppurativa Serum Proteome Identifies Distinct Inflammatory Subtypes. Journal of Investigative Dermatology 2021.
270. Hymowitz SG, Filvaroff EH, Yin JP, Lee J, Cai L, Risser P, et al. IL-17s adopt a cystine knot fold: structure and activity of a novel cytokine, IL-17F, and implications for receptor binding. Embo j 2001; 20:5332-41.
271. Nirula A, Nilsen J, Klekotka P, Kricorian G, Erondu N, Towne JE, et al. Effect of IL-17 receptor A blockade with brodalumab in inflammatory diseases. Rheumatology (Oxford) 2016; 55:ii43-ii55.
272. Chang SH, Reynolds JM, Pappu BP, Chen G, Martinez GJ, Dong C. Interleukin-17C promotes Th17 cell responses and autoimmune disease via interleukin-17 receptor E. Immunity 2011; 35:611-21.
273. Wright JF, Bennett F, Li B, Brooks J, Luxenberg DP, Whitters MJ, et al. The human IL-17F/IL-17A heterodimeric cytokine signals through the IL-17RA/IL-17RC receptor complex. J Immunol 2008; 181:2799-805.
274. Kuestner RE, Taft DW, Haran A, Brandt CS, Brender T, Lum K, et al. Identification of the IL-17 receptor related molecule IL-17RC as the receptor for IL-17F. J Immunol 2007; 179:5462-73.
275. Papp KA, Leonardi C, Menter A, Ortonne JP, Krueger JG, Kricorian G, et al. Brodalumab, an anti-interleukin-17-receptor antibody for psoriasis. N Engl J Med 2012; 366:1181-9.
276. Russell CB, Rand H, Bigler J, Kerkof K, Timour M, Bautista E, et al. Gene expression profiles normalized in psoriatic skin by treatment with brodalumab, a human anti-IL-17 receptor monoclonal antibody. J Immunol 2014; 192:3828-36.
277. Papp KA, Reich K, Paul C, Blauvelt A, Baran W, Bolduc C, et al. A prospective phase III, randomized, double-blind, placebo-controlled study of brodalumab in patients with moderate-to-severe plaque psoriasis. Br J Dermatol 2016; 175:273-86.
278. Aggarwal S, Gurney AL. IL-17: prototype member of an emerging cytokine family. J Leukoc Biol 2002; 71:1-8.

279. Gaffen SL. Structure and signalling in the IL-17 receptor family. Nat Rev Immunol 2009; 9:556-67.
280. Shen F, Hu Z, Goswami J, Gaffen SL. Identification of common transcriptional regulatory elements in interleukin-17 target genes. J Biol Chem 2006; 281:24138-48.
281. Maitra A, Shen F, Hanel W, Mossman K, Tocker J, Swart D, et al. Distinct functional motifs within the IL-17 receptor regulate signal transduction and target gene expression. Proc Natl Acad Sci U S A 2007; 104:7506-11.
282. Lindemann MJ, Hu Z, Benczik M, Liu KD, Gaffen SL. Differential regulation of the IL-17 receptor by gammac cytokines: inhibitory signaling by the phosphatidylinositol 3-kinase pathway. J Biol Chem 2008; 283:14100-8.
283. Lebwohl M, Strober B, Menter A, Gordon K, Weglowska J, Puig L, et al. Phase 3 Studies Comparing Brodalumab with Ustekinumab in Psoriasis. N Engl J Med 2015; 373:1318-28.
284. Ferreira MC, Whibley N, Mamo AJ, Siebenlist U, Chan YR, Gaffen SL. Interleukin-17-induced protein lipocalin 2 is dispensable for immunity to oral candidiasis. Infect Immun 2014; 82:1030-5.
285. Stallhofer J, Friedrich M, Konrad-Zerna A, Wetzke M, Lohse P, Glas J, et al. Lipocalin-2 Is a Disease Activity Marker in Inflammatory Bowel Disease Regulated by IL-17A, IL-22, and TNF-α and Modulated by IL23R Genotype Status. Inflamm Bowel Dis 2015; 21:2327-40.
286. Shao S, Cao T, Jin L, Li B, Fang H, Zhang J, et al. Increased Lipocalin-2 Contributes to the Pathogenesis of Psoriasis by Modulating Neutrophil Chemotaxis and Cytokine Secretion. J Invest Dermatol 2016; 136:1418-28.
287. Algood HM, Allen SS, Washington MK, Peek RM, Jr., Miller GG, Cover TL. Regulation of gastric B cell recruitment is dependent on IL-17 receptor A signaling in a model of chronic bacterial infection. J Immunol 2009; 183:5837-46.
288. Halwani R, Al-Kufaidy R, Vazquez-Tello A, Pureza MA, BaHammam AS, Al-Jahdali H, et al. IL-17 Enhances Chemotaxis of Primary Human B Cells during Asthma. PLoS One 2014; 9:e114604.
289. Wang X, Chan CC, Yang M, Deng J, Poon VK, Leung VH, et al. A critical role of IL-17 in modulating the B-cell response during H5N1 influenza virus infection. Cell Mol Immunol 2011; 8:462-8.
290. Schirmer C, Klein C, von Bergen M, Simon JC, Saalbach A. Human fibroblasts support the expansion of IL-17-producing T cells via up-regulation of IL-23 production by dendritic cells. Blood 2010; 116:1715-25.
291. Kehlen A, Thiele K, Riemann D, Langner J. Expression, modulation and signalling of IL-17 receptor in fibroblast-like synoviocytes of patients with rheumatoid arthritis. Clin Exp Immunol 2002; 127:539-46.
292. Park MJ, Moon SJ, Lee EJ, Jung KA, Kim EK, Kim DS, et al. IL-1-IL-17 Signaling Axis Contributes to Fibrosis and Inflammation in Two Different Murine Models of Systemic Sclerosis. Front Immunol 2018; 9:1611.
293. Griffin GK, Newton G, Tarrio ML, Bu DX, Maganto-Garcia E, Azcutia V, et al. IL-17 and TNF-α sustain neutrophil recruitment during inflammation through synergistic effects on endothelial activation. J Immunol 2012; 188:6287-99.

294. Montaudié H, Seitz-Polski B, Cornille A, Benzaken S, Lacour JP, Passeron T. Interleukin 6 and high-sensitivity C-reactive protein are potential predictive markers of response to infliximab in hidradenitis suppurativa. J Am Acad Dermatol 2017; 76:156-8.
295. Barnett AG, van der Pols JC, Dobson AJ. Regression to the mean: what it is and how to deal with it. Int J Epidemiol 2005; 34:215-20.
296. Naik HB, Lowes MA. A Call to Accelerate Hidradenitis Suppurativa Research and Improve Care-Moving Beyond Burden. JAMA Dermatol 2019.
297. Mozeika E, Pilmane M, Nurnberg BM, Jemec GB. Tumour necrosis factor-alpha and matrix metalloproteinase-2 are expressed strongly in hidradenitis suppurativa. Acta Derm Venereol 2013; 93:301-4.
298. Ingram JR, Collier F, Brown D, Burton T, Burton J, Chin MF, et al. British Association of Dermatologists guidelines for the management of hidradenitis suppurativa (acne inversa) 2018. Br J Dermatol 2019; 180:1009-17.
299. Alikhan A, Sayed C, Alavi A, Alhusayen R, Brassard A, Burkhart C, et al. North American clinical management guidelines for hidradenitis suppurativa: A publication from the United States and Canadian Hidradenitis Suppurativa Foundations: Part II: Topical, intralesional, and systemic medical management. J Am Acad Dermatol 2019; 81:91-101.
300. Alavi A, Lynde C, Alhusayen R, Bourcier M, Delorme I, George R, et al. Approach to the Management of Patients With Hidradenitis Suppurativa: A Consensus Document. J Cutan Med Surg 2017; 21:513-24.
301. Gulliver W, Zouboulis CC, Prens E, Jemec GB, Tzellos T. Evidence-based approach to the treatment of hidradenitis suppurativa/acne inversa, based on the European guidelines for hidradenitis suppurativa. Rev Endocr Metab Disord 2016; 17:343-51.
302. Thomi R, Schlapbach C, Yawalkar N, Simon D, Yerly D, Hunger RE. Elevated levels of the antimicrobial peptide LL-37 in hidradenitis suppurativa are associated with a Th1/Th17 immune response. Exp Dermatol 2018; 27:172-7.
303. Saylor DK, Brownstone ND, Naik HB. Office-Based Surgical Intervention for Hidradenitis Suppurativa (HS): A Focused Review for Dermatologists. Dermatol Ther (Heidelb) 2020; 10:529-49.
304. Agache I, Akdis C, Jutel M, Virchow JC. Untangling asthma phenotypes and endotypes. Allergy 2012; 67:835-46.
305. Al-Samri MT, Benedetti A, Préfontaine D, Olivenstein R, Lemière C, Nair P, et al. Variability of sputum inflammatory cells in asthmatic patients receiving corticosteroid therapy: A prospective study using multiple samples. J Allergy Clin Immunol 2010; 125:1161-3.e4.
306. Agache I, Akdis CA. Precision medicine and phenotypes, endotypes, genotypes, regiotypes, and theratypes of allergic diseases. J Clin Invest 2019; 129:1493-503.
307. Czarnowicki T, He H, Krueger JG, Guttman-Yassky E. Atopic dermatitis endotypes and implications for targeted therapeutics. J Allergy Clin Immunol 2019; 143:1-11.
308. Dahl SL, Woodworth JS, Lerche CJ, Cramer EP, Nielsen PR, Moser C, et al. Lipocalin-2 Functions as Inhibitor of Innate Resistance to Mycobacterium tuberculosis. Front Immunol 2018; 9:2717.
309. Wolk K, Wenzel J, Tsaousi A, Witte-Händel E, Babel N, Zelenak C, et al. Lipocalin-2 is expressed by activated granulocytes and keratinocytes in affected skin and reflects

disease activity in acne inversa/hidradenitis suppurativa. Br J Dermatol 2017; 177:1385-93.
310. Guglani L, Gopal R, Rangel-Moreno J, Junecko BF, Lin Y, Berger T, et al. Lipocalin 2 regulates inflammation during pulmonary mycobacterial infections. PLoS One 2012; 7:e50052.
311. Panopoulos AD, Watowich SS. Granulocyte colony-stimulating factor: molecular mechanisms of action during steady state and 'emergency' hematopoiesis. Cytokine 2008; 42:277-88.
312. Tsaousi A, Witte E, Witte K, Röwert-Huber HJ, Volk HD, Sterry W, et al. MMP8 Is Increased in Lesions and Blood of Acne Inversa Patients: A Potential Link to Skin Destruction and Metabolic Alterations. Mediators Inflamm 2016; 2016:4097574.
313. Narla S, Azzam M, Townsend S, Vellaichamy G, Marzano AV, Alavi A, et al. Identifying key components and therapeutic targets of the immune system in hidradenitis suppurativa with an emphasis on neutrophils. Br J Dermatol 2020.
314. Alves de Medeiros AK, Speeckaert R, Desmet E, Van Gele M, De Schepper S, Lambert J. JAK3 as an Emerging Target for Topical Treatment of Inflammatory Skin Diseases. PLoS One 2016; 11:e0164080.
315. Feldman SR, Thaçi D, Gooderham M, Augustin M, de la Cruz C, Mallbris L, et al. Tofacitinib improves pruritus and health-related quality of life up to 52 weeks: Results from 2 randomized phase III trials in patients with moderate to severe plaque psoriasis. J Am Acad Dermatol 2016; 75:1162-70.e3.
316. Papp KA, Menter MA, Raman M, Disch D, Schlichting DE, Gaich C, et al. A randomized phase 2b trial of baricitinib, an oral Janus kinase (JAK) 1/JAK2 inhibitor, in patients with moderate-to-severe psoriasis. Br J Dermatol 2016; 174:1266-76.
317. Savage KT, Santillan MR, Flood KS, Charrow A, Porter ML, Kimball AB. Tofacitinib shows benefit in conjunction with other therapies in recalcitrant hidradenitis suppurativa patients. JAAD Case Rep 2020; 6:99-102.
318. Jensen P, Skov L. Psoriasis and Obesity. Dermatology 2016; 232:633-9.
319. Romano S, Salustri E, Ruscitti P, Carubbi F, Penco M, Giacomelli R. Cardiovascular and Metabolic Comorbidities in Rheumatoid Arthritis. Curr Rheumatol Rep 2018; 20:81.
320. Raggi P, Genest J, Giles JT, Rayner KJ, Dwivedi G, Beanlands RS, et al. Role of inflammation in the pathogenesis of atherosclerosis and therapeutic interventions. Atherosclerosis 2018; 276:98-108.
321. Armstrong AW, Voyles SV, Armstrong EJ, Fuller EN, Rutledge JC. A tale of two plaques: convergent mechanisms of T-cell-mediated inflammation in psoriasis and atherosclerosis. Exp Dermatol 2011; 20:544-9.
322. Menter A, Strober BE, Kaplan DH, Kivelevitch D, Prater EF, Stoff B, et al. Joint AAD-NPF guidelines of care for the management and treatment of psoriasis with biologics. J Am Acad Dermatol 2019; 80:1029-72.
323. Arnett DK, Blumenthal RS, Albert MA, Buroker AB, Goldberger ZD, Hahn EJ, et al. 2019 ACC/AHA Guideline on the Primary Prevention of Cardiovascular Disease: Executive Summary: A Report of the American College of Cardiology/American Heart Association Task Force on Clinical Practice Guidelines. J Am Coll Cardiol 2019; 74:1376-414.
324. Finlay AY, Khan GK. Dermatology Life Quality Index (DLQI)--a simple practical measure for routine clinical use. Clin Exp Dermatol 1994; 19:210-6.

325. Assarsson E, Lundberg M, Holmquist G, Björkesten J, Thorsen SB, Ekman D, et al. Homogenous 96-plex PEA immunoassay exhibiting high sensitivity, specificity, and excellent scalability. PLoS One 2014; 9:e95192.
326. Bettoli V, Join-Lambert O, Nassif A. Antibiotic Treatment of Hidradenitis Suppurativa. Dermatol Clin 2016; 34:81-9.
327. The Gene Ontology Resource: 20 years and still GOing strong. Nucleic Acids Res 2019; 47:D330-d8.
328. Smyth GK. Linear models and empirical bayes methods for assessing differential expression in microarray experiments. Stat Appl Genet Mol Biol 2004; 3:Article3.
329. Hänzelmann S, Castelo R, Guinney J. GSVA: gene set variation analysis for microarray and RNA-seq data. BMC Bioinformatics 2013; 14:7.